REPORT NO. FAA-RD-75-125

ADA028765

V/STOL AIRCRAFT NOISE PREDICTION
(JET PROPULSORS)

N.N. REDDY
D.F. BLAKNEY
J.G. TIBBETS
J.S. GIBSON

12

DDC
RECEIVED
APR 15 1976
C

JUNE 1975

FINAL REPORT

Document is available to the public through the National Technical Information Service, Springfield, Virginia 22161.

Prepared for

U.S. DEPARTMENT OF TRANSPORTATION
FEDERAL AVIATION ADMINISTRATION
Systems Research & Development Service
Washington, D.C. 20590

COPY AVAILABLE TO DDC DOES NOT PERMIT FULLY LEGIBLE PRODUCTION

NOTICE

This document is disseminated under the sponsorship of the Department of Transportation in the interest of information exchange. The United States Government assumes no liability for its contents or use thereof.

Technical Report Documentation Page

1. Report No. FAA-RD-75-125	2. Government Accession No.	3. Recipient's Catalog No.
4. Title and Subtitle V/STOL Aircraft Noise Prediction (Jet Propulsors)		5. Report Date June 1975
		6. Performing Organization Code 327p.
7. Author(s) N. N. Reddy, D. F. Blakney, J. G. Tibbets, J. S. Gibson		8. Performing Organization Report No. LG75ER0054
9. Performing Organization Name and Address Lockheed-Georgia Company Marietta, Georgia		10. Work Unit No. (TRAIS)
		11. Contract or Grant No. DOT-FA72WA-3099
12. Sponsoring Agency Name and Address Department of Transportation Federal Aviation Administration Systems Research and Development Service Washington, D. C. 20590		13. Type of Report and Period Covered Final Report June 1974 - June 1975
		14. Sponsoring Agency Code

15. Supplementary Notes

This report supersedes the earlier report No. FAA-RD-73-145; August 1973.

16. Abstract

A computer program is presented for predicting the noise levels of V/STOL aircraft with jet-propulsive-lift systems. Using the equations developed in Part I of this report the noise levels may also be estimated with hand calculations. Vectored thrust, externally blown flap, upper surface blown flap, internally blown flap, and augmentor wing are the propulsive-lift concepts considered. Semi-empirical equations are derived using the test results and theories for the following aircraft noise sources: internal engine, jet, excess (core engine), high-lift system, airframe, and auxiliary power unit. The computer program predicts the perceived noise levels and tone corrected perceived noise levels for V/STOL aircraft at any specified sideline distance for known geometrical and operational parameters. This report supersedes the earlier report No. FAA-RD-73-145, August 1973.

17. Key Words Aircraft noise prediction, acoustics, V/STOL noise, noise control, aerodynamic noise.	18. Distribution Statement Document is available to the public through the N.T.I.S., Springfield Virginia 22151

19. Security Classif. (of this report)	20. Security Classif. (of this page)	21. No. of Pages	22. Price
Unclassified	Unclassified	309	

Form DOT F 1700.7 (8-72)

METRIC CONVERSION FACTORS

Approximate Conversions to Metric Measures

Symbol	When You Know	Multiply by	To Find	Symbol
		LENGTH		
in	inches	*2.5	centimeters	cm
ft	feet	30	centimeters	cm
yd	yards	0.9	meters	m
mi	miles	1.6	kilometers	km
		AREA		
in^2	square inches	6.5	square centimeters	cm^2
ft^2	square feet	0.09	square meters	m^2
yd^2	square yards	0.8	square meters	m^2
mi^2	square miles	2.6	square kilometers	km^2
	acres	0.4	hectares	ha
		MASS (weight)		
oz	ounces	28	grams	g
lb	pounds	0.45	kilograms	kg
	short tons (2000 lb)	0.9	tonnes	t
		VOLUME		
tsp	teaspoons	5	milliliters	ml
Tbsp	tablespoons	15	milliliters	ml
fl oz	fluid ounces	30	milliliters	ml
c	cups	0.24	liters	l
pt	pints	0.47	liters	l
qt	quarts	0.95	liters	l
gal	gallons	3.8	liters	l
ft^3	cubic feet	0.03	cubic meters	m^3
yd^3	cubic yards	0.76	cubic meters	m^3
		TEMPERATURE (exact)		
°F	Fahrenheit temperature	5/9 (after subtracting 32)	Celsius temperature	°C

*1 in = 2.54 (exactly). For other exact conversions and more detailed tables, see NBS Misc. Publ. 286, Units of Weights and Measures, Price $2.25, SD Catalog No. C13.10:286.

Approximate Conversions from Metric Measures

Symbol	When You Know	Multiply by	To Find	Symbol
		LENGTH		
mm	millimeters	0.04	inches	in
cm	centimeters	0.4	inches	in
m	meters	3.3	feet	ft
m	meters	1.1	yards	yd
km	kilometers	0.6	miles	mi
		AREA		
cm^2	square centimeters	0.16	square inches	in^2
m^2	square meters	1.2	square yards	yd^2
km^2	square kilometers	0.4	square miles	mi^2
ha	hectares (10,000 m^2)	2.5	acres	
		MASS (weight)		
g	grams	0.035	ounces	oz
kg	kilograms	2.2	pounds	lb
t	tonnes (1000 kg)	1.1	short tons	
		VOLUME		
ml	milliliters	0.03	fluid ounces	fl oz
l	liters	2.1	pints	pt
l	liters	1.06	quarts	qt
l	liters	0.26	gallons	gal
m^3	cubic meters	35	cubic feet	ft^3
m^3	cubic meters	1.3	cubic yards	yd^3
		TEMPERATURE (exact)		
°C	Celsius temperature	9/5 (then add 32)	Fahrenheit temperature	°F

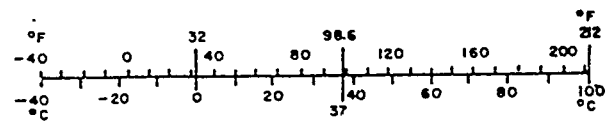

PREFACE

The overall objectives of this study are to identify the noise sources unique to V/STOL aircraft with jet-propulsive-lift systems and to develop a computer program to predict far-field noise levels. Several investigations are being conducted continuously by industry and government agencies to improve the noise prediction and suppression methods of various components of aircraft noise. The development of this program used available aeroacoustic theories and test data such that appropriate and effective modeling could be achieved. Wherever the data bank is limited, reasonable assumptions are made.

This report supersedes the previous report, "V/STOL Noise Prediction and Reduction" (No. FAA-RD-73-145), developed under the same contract (No. DOT-FA72WA-3099). In order to make this report useful for a large segment of aeroacoustics engineers and scientists, it is written in two parts. The first part provides the descriptions of jet-propulsive-lift systems of V/STOL aircraft, the analyses of noise source characteristics, and the derivation of the equations to predict aircraft noise levels. The second part describes the computer program and its use to predict the noise levels of V/STOL aircraft using operational and geometrical parameters.

TABLE OF CONTENTS

	Page
SUMMARY AND CONCLUSIONS	1
INTRODUCTION	7
REFERENCES	9
PART I - ANALYSIS AND DISCUSSION OF NOISE CHARACTERISTICS	
Table of Contents	1-i
List of Figures	1-iii
List of Symbols	1-v
1. Description of Powered Lift Systems	1-1
2. Noise Source Components	1-7
3. Noise Prediction Method	1-49
References	1-75
PART II - DESCRIPTION AND USE OF COMPUTER PROGRAM	
Table of Contents	2-i
List of Figures	2-iii
4. Noise Prediction Program Description	2-1
5. Machine Requirements	2-130
6. Diagnostics	2-131
APPENDICES	
A. Sample Cases	A-1
B. Computer Program Listing	A-8
C. Baseline Aircraft Noise Predictions	A-56
D. Hand-Calculation Procedure	A-85

SUMMARY AND CONCLUSIONS

The primary objective of this investigation is the formulation and development of a unified program to predict far-field noise from jet-powered V/STOL aircraft of the type which utilize propulsive-lift systems. A substantial part of this report is the study conducted under phases 5 through 8 of Contract DOT-FA72WA-3099. The investigation conducted under phases 1 through 4 and reported in August 1973 (Reference 1) is also updated and revised to reflect the advancement in the definition and understanding of noise generation and propagation of jet-powered V/STOL aircraft. Thus, this report supersedes the previous report of August 1973.

The following six jet-propulsive-lift systems are consudered:

- Vectored Thrust
- Externally Blown Flap
- Upper Surface Blowing Flap
- Internally Blown Flap
- Augmentor Wing
- Hybrid System

These concepts appear to have the potential for development of environmentally acceptable STOL aircraft. A brief description of each integrated propulsive system is presented, including geometry and flow field.

Noise source categories for the aircraft types identified in this investigation are: internally generated engine, jet mixing, lift augmentation system, and non-propulsive systems. State-of-the-art theoretical developments and experimental data were utilized in evaluating the characteristics of noise sources and establishing the relative significance of each source.

Experimental data of various components of propulsive-lift system noise were extensively used in developing the analytical procedures for aircraft noise prediction. In areas where neither theoretical nor experimental data were available, engineering judgement and intuitive knowledge were used. In addition to the generation and propagation characteristics of noise sources,

atmospheric attenuation, effect of aircraft motion, ground reflection effects, extra ground attenuation, shielding of sound by aircraft components, and noise reduction techniques were considered in developing the noise prediction model.

A computer program was developed, based on the analytical model, to compute the contribution of each noise source generated at the aircraft and propagated towards an observer on the ground. One-third octave band spectra, overall sound pressure levels (OASPL), perceived noise levels (PNL), and tone-corrected perceived noise levels (PNLT) can be computed for each source and for the total aircraft. Computations can be made for a fixed position of the aircraft over a defined (variable) flight profile, either for a specified observer location or for various observer locations along any sideline. The program also has a capability of selecting the maximum noise levels along a sideline for a given aircraft position and repeats the procedure for various aircraft positions to identify the location of observer and aircraft where the absolute maximum noise occurs. These features are considerable improvements over the original program which only could predict noise levels at a given point. A simplified logic diagram used in developing the computer program is given in Figure 1.

Part 1 of this report describes the analysis of radiated sound from V/STOL aircraft. The various noise sources and acoustic effects identified with jet propelled V/STOL aircraft are:

- Internally Generated Engine Noise
  - compressor/fan
  - turbine
  - excess engine
- Jet Noise
  - mixed flow jet exhaust
  - co-axial flow
- Lift Augmentation Noise
  - impingement
  - wall jet
  - trailing edge

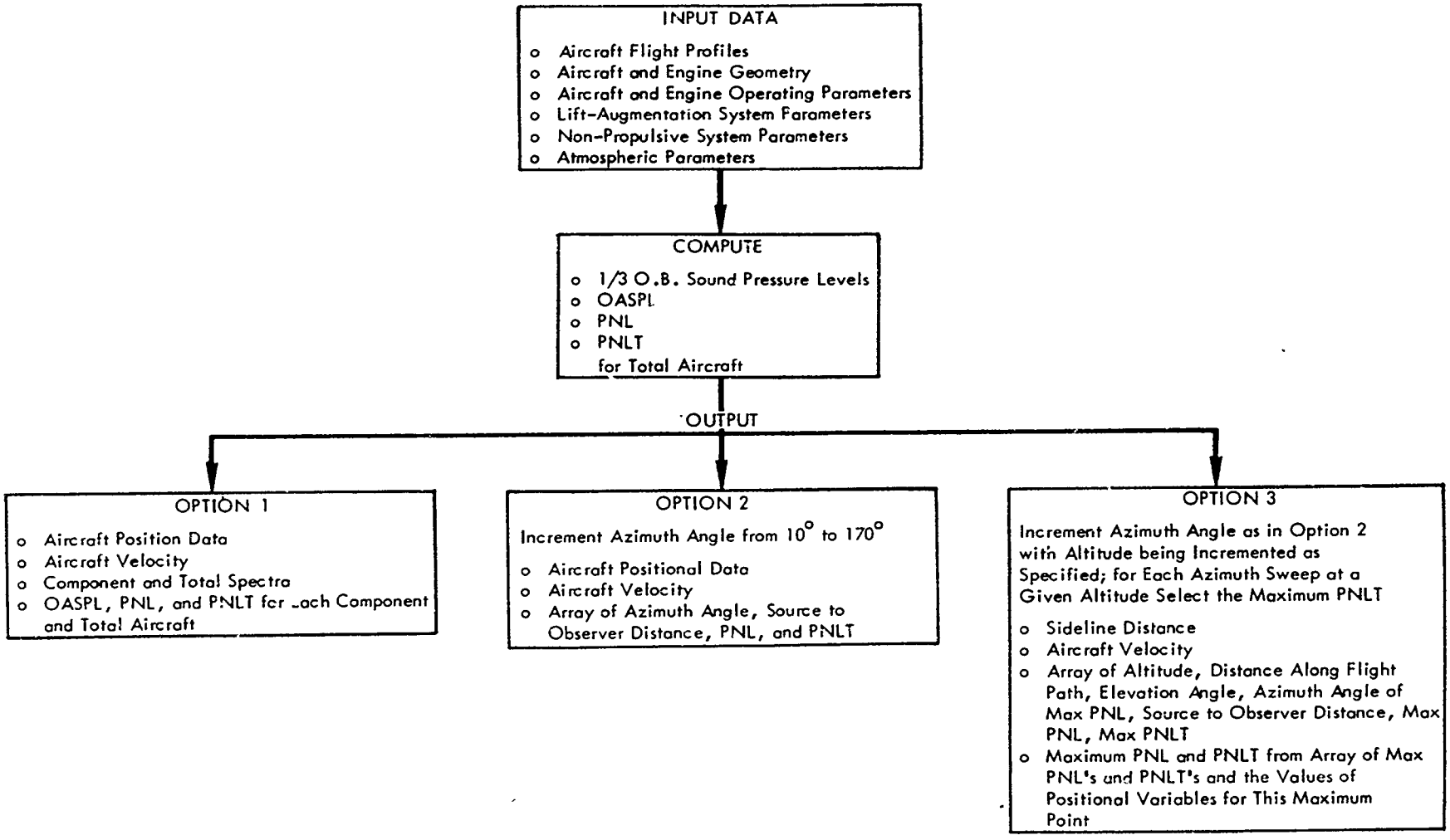

Figure 1. Logic of V/STOL Noise Prediction program

- trailing edge wake
- augmentor wing

- Non-Propulsive Noise
  - airframe
  - auxiliary power unit

- Propagation and Flight Effects
  - effect of aircraft motion
  - ground reflection
  - extra ground attentuation
  - shielding by aircraft components

- Noise Reduction Features

The development of methodology and sources of information used are discussed in this part of the report.

Part II presents the computer program and its use for prediciton of V/STOL aircraft noise for any aircraft position over a defined flight profile.

The program consists of a main control program and 22 subroutines. The noise from each source defined for V/STOL aircraft is predicted by a separate subroutine. The following subroutines have been developed to predict the radiated noise from 12 different sources:

(1) AERO - airframe aerodynamic noise
(2) FAN - single stage fan noise
(3) TURBNE - engine turbine noise
(4) JET- jet mixing noise
(5) EXCESS - excess engine noise (core)
(6) AUGWNG - noise of complete augmentor wing high lift system
(7) WNGJET - jet mixing noise from wing slot nozzle
(8) IMPING - noise from impingement of jet flow on wing flap surface
(9) WALJET - noise from jet flow over wing/flap surface
(10) WAKE - noise from trailing edge wake

(11) TRAIL - trailing edge noise

(12) APU - noise from auxiliary power unit (PNL only)

In addition, the following 10 other subroutines calculate the propagation effects, noise reduction, and interpolation functions:

(1) EGA - effect of extra ground attenuation

(2) GRE - effect of ground reflection

(3) SHIELD - effect of wing shielding

(4) FWDSPD - effect of aircraft forward motion

(5) DOPLER - Doppler frequency shift due to motion of the source

(6) REDUCE - noise reduction features

(7) PNLREV - perceived noise level (PNL) calculations from a 1/3 octave band spectrum

(8) TONE - tone corrections to PNL from a 1/3 octave band spectrum

(9) GIRC - table interpolation routine for single independent variable tables

(10) DTAB2 - table interpolation routine for tables with two independent variables.

The main program (STOLPROG) and the 22 subroutines form a unified noise prediction tool for V/STOL aircraft. However, experience indicates that as new concepts of propulsive systems and noise suppression are developed, new noise sources appear and the characteristics of the sources may change. Therefore, the noise prediction program must be continually modified to reflect the changes in noise source characteristics. In addition, several acoustic technology items are still under development. For example there is not yet a full understanding of forward speed effects and several research contracts on this subject are currently underway in the industry. Likewise, acoustic feedback phenomena and the noise generation by orderly structure of turbulence and core engine noise are yet to be completely understood. These are only a few examples of new and emerging technology. The novelty of this program is that as the state of the art advances in understanding of any particular noise generating and propagating mechanism, or as additional experimental evidence becomes available, the analytical model and the computer program may be modified by updating only the affected modules.

This program may also be used to predict the noise levels for reduced takeoff and landing (RTOL) aircraft, since the integrated propulsive-lift systems are similar to those of V/STOL aircraft.

INTRODUCTION

It is anticipated that V/STOL aircraft will play a major role in meeting the short-haul transportation requirements in the 1980's. This will include aircraft operations at existing large airports, smaller regional airports, and probably from new downtown V/STOL ports[2] as illustrated in Figure 2. These V/STOL aircraft will have much shorter ground runs and will climb out of the airport and make landing approaches at steeper angles. Terminal area operations, in the case of regional or downtown airports, may cause increases in noise exposure for adjacent urban areas and also possibly for suburban areas under the low altitude cruise path. In addition to operations, the other primary difference between conventional and V/STOL aircraft is in the manner the engines are integrated into the airframe. The integrated propulsive lift system provides more lift, higher thrust-to-weight ratios, and shorter take-off and landing distances than conventional turbofan transport aircraft[3,4].

Figure 2. Proposed Jet-Powered STOL Operation

A great deal of effort has already been, and continues to be, devoted to the development of new V/STOL aircraft configurations and to understand their noise characteristics. During the past few years, substantial amounts of static model tests, and limited model tests with forward speed, have been conducted on various propulsive-lift system concepts to define noise characteristics and estimate community noise levels. Some experimental investigations have also been conducted to explore possible noise reduction features. The resulting test data have been utilized to establish scaling laws and to estimate aircraft noise levels on the ground during take-off and landing operations.

Since there were no unified noise prediction standards available for this class of aircraft, the current program was undertaken which utilized available test and analytical data to evolve a noise prediction procedure. A preliminary version of the prediction procedures[1] was released in 1973. The present report, which includes the analyses of much new technical material, updates the original version into a more accurate and usable form.

This report is written in two separate parts. The first part describes the analyses of noise generation mechanisms, radiated sound fields, and the methodology for prediction of full-scale far-field noise levels. The second part consists of the description and uses of the noise prediction computer program.

REFERENCES

1. Guinn, W. A.; Blakney, D. F.; and Gibson, J. S.: "V/STOL Noise Prediction and Reduction," FAA-RD-73-145, Aug. 1973.

2. Hubbard, H. H.; Chestnutt, D.; and Maglieri, D. J.: "Noise Control Technology for Jet-Powered STOL Vehicles," ICAS Paper No. 72-50, The Eighth Congress of International Council of the Aeronautical Sciences, Sept. 1972.

3. "Aircraft Engine Noise Reduction," Conference at NASA Lewis Research Center, Cleveland, Ohio, May 16-17, 1972, NASA SP-311.

4. "STOL Technology," Conference at NASA Lewis Research Center, Cleveland Ohio, October 17-19, 1972, NASA SP-320.

PRECEDING PAGE BLANK-NOT FILMED

PART I

ANALYSIS AND DISCUSSION OF NOISE CHARACTERISTICS

by

N. N. Reddy

This is a two-part report. The first part consists of Sections 1 - 3, describing the analyses and analytical model for prediction of V/STOL noise. The second part consists of Sections 4 - 6, describing the development and use of the V/STOL noise prediction program.

PRECEDING PAGE BLANK NOT FILMED

TABLE OF CONTENTS

	Page
LIST OF FIGURES	1-iii
LIST OF SYMBOLS	1-v
1. DESCRIPTION OF POWERED-LIFT SYSTEMS	1-1
1.1 Vectored Thrust (V.T.)	1-1
1.2 Externally Blown Flap (EBF)	1-1
1-3 Upper Surface Blowing Flap (USB)	1-1
1-4 Internally Blown Flap (IBF)	1-5
1.4.1 IBF/BLC	1-5
1.4.2 IBF/Jet Flap	1-5
1.5 Augmentor Wing (AW)	1-5
1.5.1 Two-Stream Engine	1-6
1.5.2 Three-Stream Engine	1-6
1.6 Hybrid System	1-6
2. NOISE-SOURCE COMPONENTS	1-7
2.1 Internally Generated Engine Noise	1-7
2.1.1 Compressor/Fan Noise	1-7
2.1.2 Turbine Noise	1-10
2.1.3 Excess Engine (Core and Tailpipe) Noise	1-15
2.2 Jet Noise	1-15
2.2.1 Mixed Flow Jet Exhaust	1-18
2.2.2 Co-axial Nozzle	1-21
2.3 Lift-Augmentation System Noise	1-22
2.3.1 Impingement Noise	1-22
2.3.2 Wall Jet Noise	1-29
2.3.3 Trailing Edge Noise	1-31
2.3.4 Trailing Edge Wake Noise	1-39
2.3.5 Augmentor Wing Noise	1-42
2.4 Non-propulsive Noise	1-45
2.4.1 Aircraft Noise	1-45
2.4.2 Auxiliary Power Unit	1-46

TABLE OF CONTENTS (Continued)

Page

3. NOISE PREDICTION METHOD 1-49

3.1 Radiated Sound from the Aircraft 1-49

3.2 Effect of Aircraft Motion 1-52

3.2.1 Effect of Source Motion (Doppler Frequency Shift) . . . 1-53

3.2.2 Effect of Aircraft Motion on Acoustic Energy 1-55

3.3 Ground Reflection Procedure 1-58

3.4 Extra Ground Attenuation (EGA) 1-65

3.5 Shielding of Sound by the Aircraft Components 1-65

3.6 Noise Reduction Features 1-68

3.6.1 Internally Generated Engine Noise 1-70

3.6.2 Jet Mixing Noise 1-70

3.6.3 Lift Augmentation Noise 1-70

REFERENCES 1-75

LIST OF FIGURES

Figure	Title	Page
1-1	Powered-Lift Concepts (3 pages)	1-2
1-2	Basic Engine Noise Sources	1-8
1-3	Directivity Pattern of Fan Noise	1-11
1-4	Spectral Distribution of Fan Noise	1-12
1-5	Directivity for Turbine Noise	1-14
1-6	Spectral Distribution for Turbine Noise	1-16
1-7	Spectral Distribution of Excess Noise	1-17
1-8	Spectral Distribution of Jet Noise	1-19
1-9	Frequency Shift Parameter for Co-axial Jets	1-23
1-10	Noise Sources of Power-Lift System	1-24
1-11	Directivity of Impingement Noise	1-28
1-12	Spectral Distribution of Impingement Noise	1-30
1-13	Directivity of Wall Jet Noise	1-31
1-14	Spectral Distribution of Wall Jet Noise	1-33
1-15	Spectral Distribution of Trailing Edge Noise	1-36
1-16	Velocity at Trailing Edge	1-38
1-17	Sound Intensity Distribution in the Flap Wake	1-40
1-18	Flap wake Noise Directivity	1-41
1-19	Directivity of AW Noise	1-43
1-20	Spectral Distribution of AW Noise	1-44
1-21	Spectral Distribution of Airframe Noise	1-47
1-22	Flight Path Geometry	1-50
1-23	Atmospheric Absorption Coefficient	1-51
1-24	Doppler Frequency Shift	1-54

LIST OF FIGURES (Continued)

Figure	Title	Page
1-25	Effect of Aircraft Motion on Jet Noise	1-57
1-26	Effect of Aircraft Motion on EBF System Noise	1-59
1-27	Effect of Aircraft Motion on Vectored Thrust Noise	1-60
1-28	Ground Reflections	1-61
1-29	Interference Frequencies (Ground Reflections)	1-64
1-30	Extra Ground Attenuation	1-66
1-31	Geometry for Wing/Flap	1-69
1-32	Noise Reduction Due to Trailing Edge Blowing for EBF	1-72
1-33	Noise Reduction for Augmentor Wing	1-74

LIST OF SYMBOLS

A_1	area of primary jet nozzle, ft^2
A_2	area of secondary jet nozzle, ft^2
A_I	impingement area
A_N	area of the jet nozzle (mixed flow), ft^2
A_T	turbine stage exit area, ft^2
AR	aspect ratio of the wing
b	width of the wall jet, ft.
c_a	ambient speed of sound, ft/sec.
c_{ISA}	speed of sound in international standard atmosphere, ft/sec.
C_n	effective nozzle discharge coefficient
D	diameter of circular nozzle (mixed flow), ft.
D_1	diameter of circular nozzle or height of slot nozzle, ft.
D_2	diameter of circular nozzle or width of slot nozzle, ft.
d_i	impingement diameter, ft.
D_e	equivalent circular nozzle diameter, ft.
D_h	hydraulic diameter of the nozzle, ft.
DI	directivity index
f	frequency, Hz
Δf	frequency band width (Hz)
h	gap height for plug nozzles, ft. or height of the nozzle for slot nozzle, ft.
h_I	impingement height, ft.
I	sound intensity, watts/square meter
K	constant
ℓ	length of the wall jet, ft.
M_a	Mach number of aircraft

M_J	jet Mach number
m	number of noise sources
N_i	ground reflection index
N_F	Fresnel number
OASPL	overall sound pressure level, dB (ref. 2×10^{-4} dynes/cm^2)
$OASPL_{bc}$	OASPL for core jet alone, dB
PNL	perceived noise level, dB
PR	pressure ratio
R	distance between the sound source and observer, ft.
R_c	radius of curvature of wing/flap, ft.
R_L	flow run length, ft.
r_D	direct sound ray length
r_R	total reflected sound ray length
S	Strouhal number
SHP	maximum shaft horsepower of APU unit
T	temperature, °R
T_a	ambient temperature, °R
T_J	jet exhaust temperature, °R
ΔT	change in temperature, °R
t	maximum thickness of wing, ft.
T_1	temperature of primary jet exhaust
T_2	temperature of secondary jet exhaust
V_{rel}	relative velocity, ft/sec.
V_J	jet exit velocity, ft/sec.
V_1	velocity of primary jet, ft/sec.
V_2	velocity of secondary jet, ft/sec.
V_{ip}	impingement velocity, ft/sec.

1. DESCRIPTION OF POWERED-LIFT SYSTEMS

In recent years several concepts have been evolved to provide the propulsive lift required for short take-off and landing operations. The six integrated powered-lift systems outlined below offer good development potential for V/S/RTOL aircraft.

1.1 VECTORED THRUST (VT)

For the vectored thrust concept, lift augmentation is obtained by changing the engine vector. This is accomplished by deflecting the flow from the exhaust nozzle downward as shown in Figure 1-1a. To minimize flow turning losses, turning vanes are often used in a swivel nozzle. The flow through the turning vanes generates additional turbulence and noise which is a function of the flow velocity at the vanes. Beyond the general dependence on velocity, there is no theoretical or empirical formulation available to estimate the noise as a function of parameters such as velocity, turning vane dimensions, number of vanes, or the angle with which the flow turns for this additional vane-generated noise.

1.2 EXTERNALLY BLOWN FLAP (EBF)

The externally blown flap concept refers to a configuration with the engine below the wing and the engine exhaust directed toward a slotted-flap arrangement as shown in Figure 1-1b. This configuration is also known as "Externally Blown Flap/Lower Surface Blowing (EBF/LSB)" and "Under-the-Wing Externally Blown Flap (UTW)." The lift augmentation is obtained by the flap-deflected flow and the associated wing supercirculation. The flow-surface interaction and the modification of the flow by the introduction of the wing/flap in the flow are the additional noise-source mechanisms of this high-lift system.

1.3 UPPER SURFACE BLOWING CONCEPT (USB)

In the case of the upper surface blowing concept (Figure 1-1c), the engine is located over the wing, and the exhaust is discharged on the upper wing surface and is turned downward over the deflected flap by the Coanda principle. This configuration is also known as "Externally Blown Flap/Upper Surface Blowing

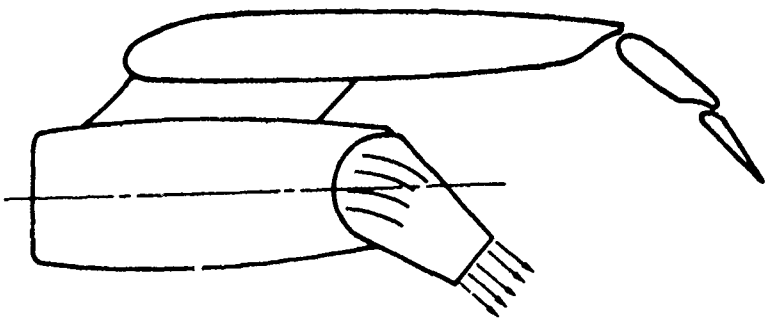

(a) Vectored Thrust (VT)

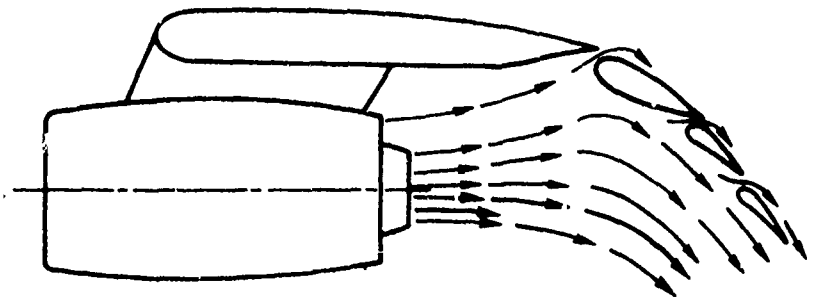

(b) Externally Blown Flap (EBF)

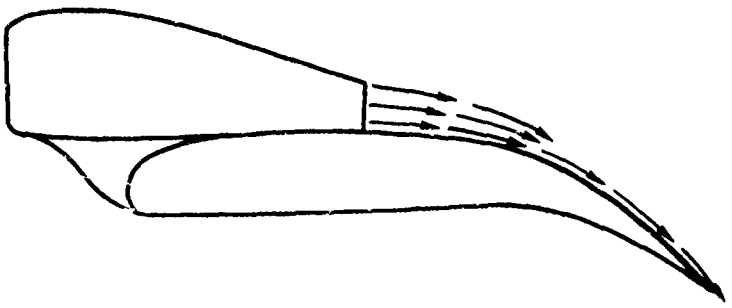

(c) Upper Surface Blown Flap (USB)

Figure 1-1. Powered-Lift Concepts

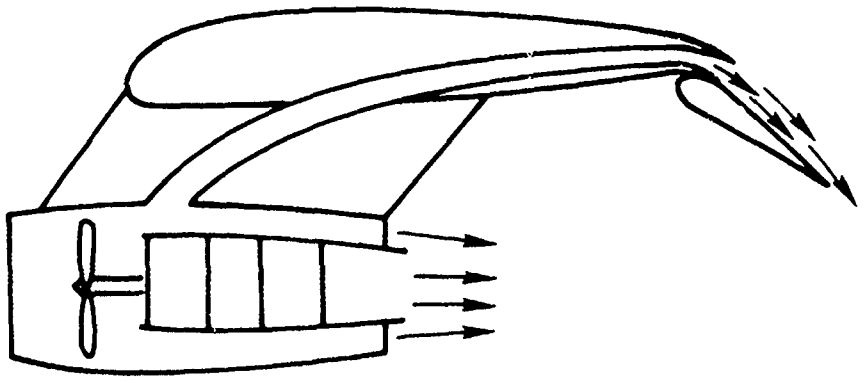

(d) Internally Blown Flap/Boundary Layer Control (IBF/BLC)

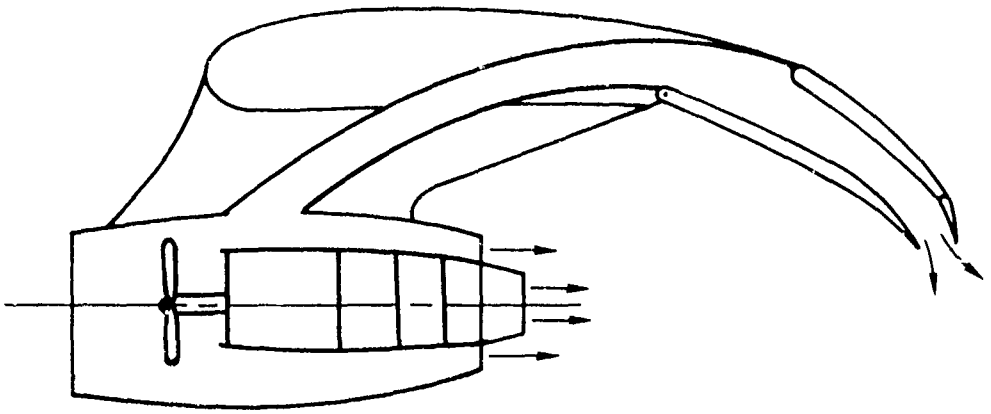

(e) Internally Blown Flap/Jet Flap (IBF/JF)

Figure 1-1. (Continued)

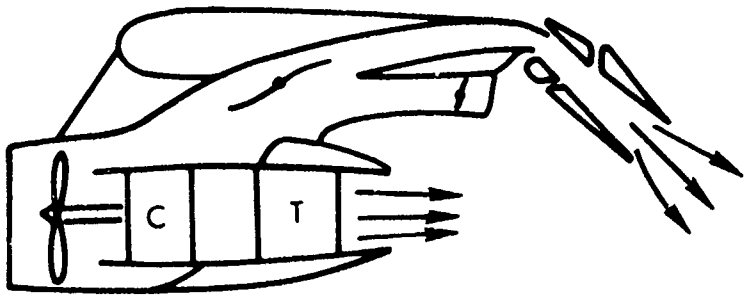

(f) Augmentor Wing (AW)

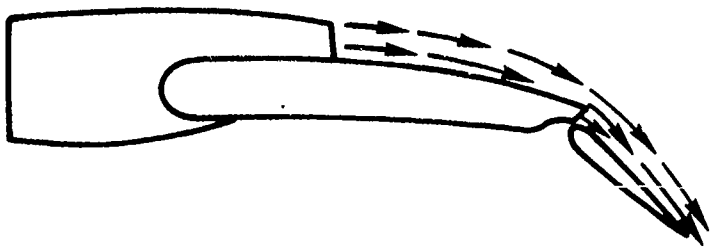

(g) Hybrid (USB with IBF)

Figure 1-1. (Concluded)

(EBF/USB)" or "Over-the-Wing Blown Flap (OTW)" configuration. As in the case of the EBF concept, the lift augmentation is obtained by the combination of flow deflection and wing supercirculation. The modified flow and the flow-wing/flap interaction are the major additional noise mechanisms. The propagation characteristics of the engine and jet noise change due to the unique location of the engine exhaust on the wing/flap surfaces, creating shielding and diffraction.

1.4 INTERNALLY BLOWN FLAP (IBF)

The IBF concept illustrated in Figures 1-1d and 1-1e uses flow from the power plant and ducts it internally to generally high-aspect-ratio slot nozzles on the wing/flap upper surface or trailing edge. This concept may be further subdivided as either boundary layer control (BLC) or jet flap (JF), depending on the amount of flow and how it is used to promote lift augmentation. The additional noise of the IBF powered-lift concept results from the interaction of the flow from the slot nozzles with the wing and flap surfaces.

1.4.1 IBF/BLC

The amount of flow from the wing and/or flap knee nozzle is relatively small and is used essentially to prevent separation of the local boundary layer. There is no lift from flow deflection, and lift augmentation is primarily caused by the improved aerodynamic performance of the flaps during take-off and landing.

1.4.2 IBF/Jet Flap

A substantial amount of mass flow from the power plant is used to blow on the wing/flap surface and, possibly, from the flap trailing edge. Lift augmentation, in this case, is obtained by flap-deflected flow and jet-induced supercirculation, as well as the improved aerodynamic performance of the flaps.

1.5 AUGMENTOR WING (AW)

In the case of the augmentor wing concept, turbofan exhaust air is ducted first into the wing and then out of a wing nozzle system into a flap augmentor

shroud system as shown in Figure 1-1f. The additional lift during take-off and landing is obtained by the augmented and deflected jet stream, the boundary-layer control provided by the induced air, and the supercirculation produced by the flap efflux. Because of the ducting size limitations, these systems are generally operated at high nozzle pressure ratios (on the order of 2.5). Therefore, high noise levels can be generated from this type of lift augmentation and care must be exercised in configuration design to maximize shielding and to provide acoustic liners in the walls of the augmentor (flap) shroud. The AW system can be further classified depending on the type of engine used.

1.5.1 Two-Stream Engine

The engine in this case is typically a low-bypass-ratio turbofan having a fan pressure ratio between 2.5 and 3.5. There are only two exhaust systems: the fan exhaust (which is ducted in its entirety to the augmentor flap), and the hot core jet exhaust (which may be discharged through a conventional or a vectorial nozzle).

1.5.2 Three-Stream Engine

In this case, there are two streams of fan exhaust in addition to hot core jet: a high-pressure exhaust with pressure ratio of between 2.5 and 3.0 which supplies the augmentor, and a low-pressure fan exhaust with pressure ratio of between 1.3 to 1.5 which is discharged through a conventional nozzle. As before, the turbine exhaust may or may not be vectored. O'Keefe and Kelly[1-1] indicate that the three-stream engine aircraft is slightly heavier and noisier than the two-stream version.

1.6 HYBRID SYSTEM

Theoretically, this is a combination of any two of the above-mentioned concepts. Practically, however, there is one combination which has been studied in some depth, and which has been shown to offer good potential. This is the USB/IBF concept, which is shown schematically in Figure 1-1g. Reference 1-2 describes one such concept where the secondary blowing is a flap knee. Searle[1-3] has presented some of the acoustic test results for this Hybrid configuration.

2. NOISE-SOURCE COMPONENTS

Sound from a V/STOL aircraft is radiated from different aeroacoustic source components. To evaluate the sound source mechanisms from which the dominant noise radiates, it is necessary to estimate the noise levels from each source. This also would aid in devising any viable noise control techniques and in changing the operational parameters to reduce aircraft noise. The sources are identified and their contributions to the radiated noise are predicted using the available theories and experimental data. In the current incomplete development of the state of the art, engineering judgement with physical reasoning is used in formulating the prediction model.

2.1 INTERNALLY GENERATED ENGINE NOISE

The noise generated within the engine by the fan, compressor, turbine, combustion, and other mechanisms is propagated through the inlet and exhaust of the jet, as shown in Figure 1-2. Although the noise-generating mechanism itself may not be unique to the V/STOL aircraft, the propagation characteristics are different and depend on the location of the engine and the exhaust relative to the airframe. Some of the sources which have been investigated experimentally or analytically are discussed below.

2.1.1 Compressor/Fan Noise

Two types of noise are generated by the rotating blades inside the ducts: (a) broad band, and (b) discrete-tone noise. In addition to these two types, a combination-tone noise is also generated by unsteady airflow past the rotors and stators of the several fan or compressor stages. The mechanism is generally thought of as comprising the following unstead-flow phenomena:

(1) Vortex shedding from the stator blades.

(2) Lift fluctuations resulting from the inflow turbulence

(3) Turbulent boundary layer on the rotor and stator blades.

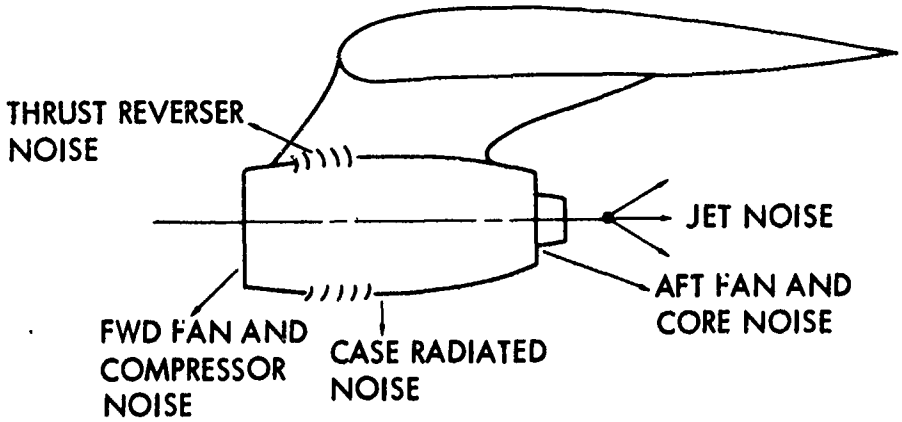

Figure 1-2. Basic Engine Noise Sources

The discrete-tone noise is generated at the frequency corresponding to the integer multiples of the fundamental blade passage frequency radiated from the fans and compressors. It appears that the dominant tone noise for fans with inlet guide vanes is produced by the blade chop through the wakes from the inlet guide vanes. It would thus be expected that, for the fans without IGV's, the magnitude of the sound generated is of lower level, even though the mechanism is the same as blade chop through the inflow turbulence.

In addition, the interaction between rotor and exit guide vanes (EGV) produces noise in a way similar to the IGV-rotor interaction. Experimental data indicate that the significant parameter to be considered in rotor-EGV noise is the blade/vane number ratio.

As a rotor tip speed goes to supersonic velocity, a shock would be formed on each rotor blade, and these shock waves propagate upstream and radiate as a system of Mach waves out of the inlet duct. These would appear in the far field as a series of tones at multiples of the blade passage frequency. However, the experimental results indicate that the energy is redistributed into the frequencies other than tone frequencies. Since the resulting noise spectrum contains all harmonics of the rotational speed, it is known as *combination-tone noise (buzz-saw)*, consisting of a series of tones, each with the same order of magnitude and separated by a fixed frequency. The presence of inlet guide vanes attenuates the Mach wave system, and hence the combination tone noise is insignificant compared with the blade-passage frequency or jet noise.

There are several theoretical methods to predict fan noise. But due to some of the uncertainties of the generating mechanisms and the complexities of propagation through the inhomogeneities within the inlet and exhaust ducts, there is no single unified method.

Recently Burdsall and Urban[1-4] have developed a prediction procedure for the fan/compressor noise using experimental data which requires detailed geometrical and operational parameters. The results apply primarily for single-stage, guide-vaneless fan/compressors. The other application features are: design rotor tip speed, between 1100 and 1600 ft. per second; fan pressure ratio,

between 1.35 and 1.6; fan diameter, from 30 to 100 inches; and fan gap/chord ratios between 0.5 and 1.1. However, for advanced design, the details of a new engine are seldom available and may vary from one engine to the other. Also, since the detailed development of fan/compressor noise prediction method is beyond the scope of this study, a simplified prediction procedure developed and used in the previous report is adapted. The expression is derived from the data in reference 1-5 where it is given for the maximum 500-foot-altitude noise level (PNL) as a function of weight flow and fan pressure ratio as:

$$PNL = 10 \log_{10} W + 20 \log_{10} (PR^{.286} - 1) + K, \qquad (1)$$

where K = 100 for single stage, and
K = 105 for two-stage fan
W = weight flow through the fan (pounds weight/sec)
PR = fan pressure ratio.

If it is assumed that the radiated OASPL of the fan/compressor has the same relation as above except for the constant, then,

$$OASPL = 10 \log_{10} W + 20 \log_{10} [PR^{.286} - 1] - 20 \log_{10} R + K. \qquad (2)$$

The directivity of the noise is assumed to be the same as that given in Reference 1-4, which is illustrated in Figure 1-3. The nondimensional spectral distribution given in Figure 1-4, derived from the experimental data is used for the noise prediction. The constant, k, in equation (2) is derived, to give the same PNL as given in equation (1), to be 127.

2.1.2 Turbine Noise

Turbine noise can become a floor for the engine noise, when the fan/compressor and the jet noise are reduced either by treatment of the inlet and exhaust fan ducts and/or by the use of high-bypass-ratio jet engines. Thus, in recent years, the need to predict turbine noise has been realized. The fundamental mechanisms of noise generation in a turbine are similar to those of compressors/fans. However, the test results of far-field noise from a turbine indicate that a typical turbine noise spectrum consists of high-frequency

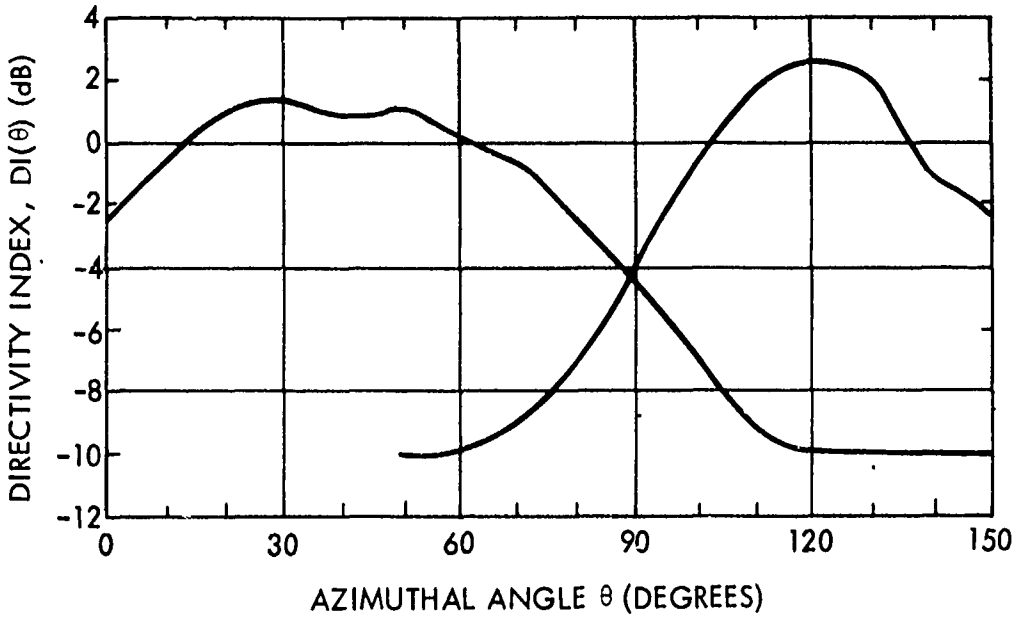

Figure 1-3. Directivity of Fan/Compressor Noise

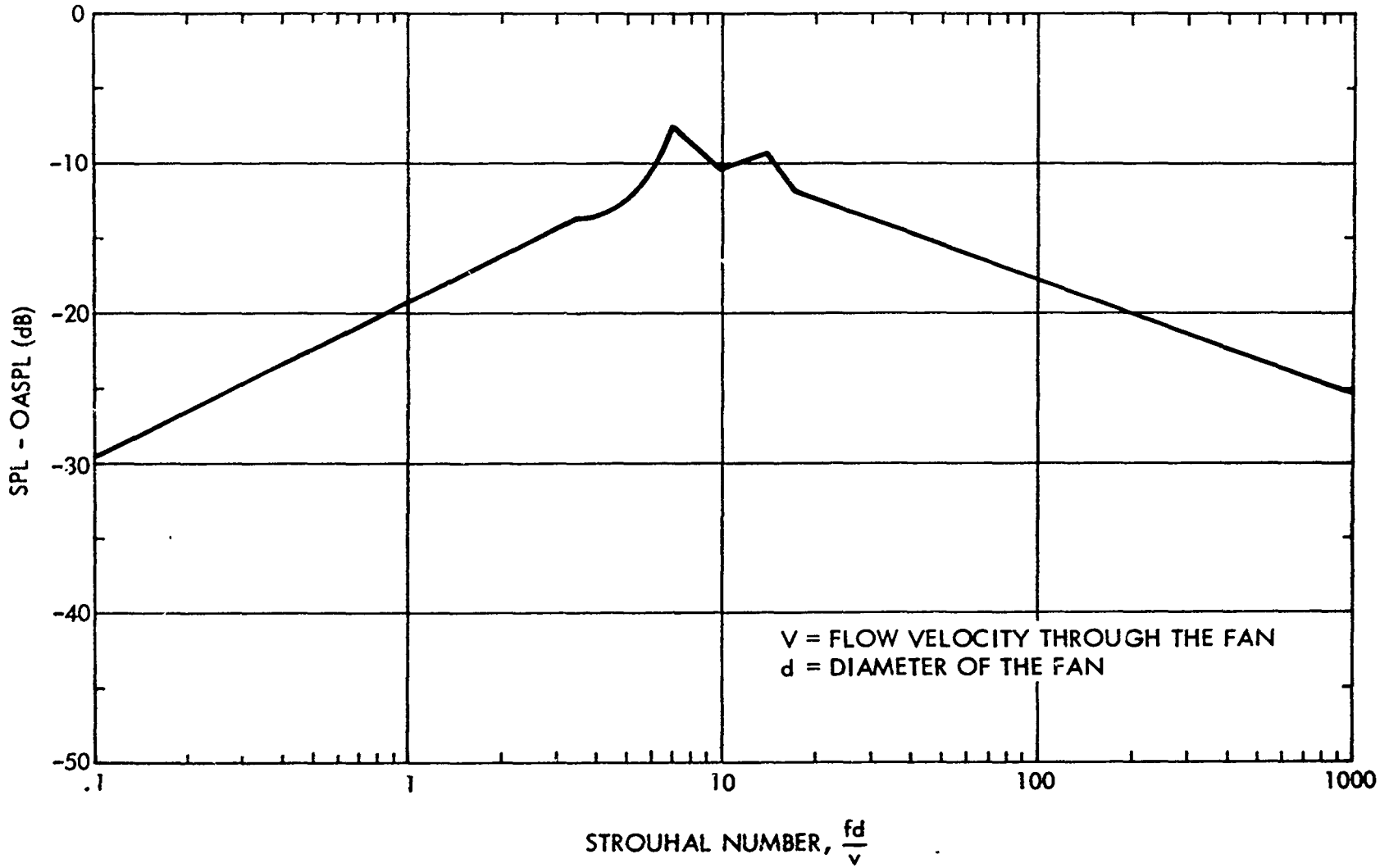

Figure 1-4. Spectral Distribution of Fan Noise

tones (corresponding to the turbine blade passing frequencies) superimposed on a broadband noise. Turbine noise is generally dominant in the aft quadrant and peaks between 110° and 120° from the inlet.

Kazin and Matta[1-6] have developed a semi-empirical relation to predict the turbine noise. This method uses theoretical developments of noise-generation mechanisms similar to that of fan and compressor, and a large body of test data. This method requires knowledge of the stage pressure ratios, the blade tip speeds, the turbine stage exit area, and the spacing between the blade rows. From these results, the following equation for the OASPL at $\theta = 90°$ is derived.

$$\text{OASPL} = 8.75 \log_{10} \left(\frac{\Delta T}{T}\right)_{\text{stage}} + 20 \log_{10} \left(\frac{V_{rel}}{C_a}\right) + 10 \log_{10} \frac{A_T}{R^2} + 138.9, \quad (3)$$

where

$$\left(\frac{\Delta T}{T}\right) = 1 - \left(\frac{1}{PR}\right)^{\frac{-1}{\gamma}} = \frac{\text{Ideal work extraction}}{\text{Inlet Enthalpy}}$$

PR = total-to-static pressure ratio of all the stages

V_{rel} = relative tip speed at the inlet of the first stage

$= \sqrt{V_{Rel}^2 + V_{Axial\ Flow}^2}$, ft/sec.

C_a = speed of sound, ft/sec.

A_T = turbine stage exit area, ft^2

γ = ratio of specific heats, 1.4

R = distance from the jet exit to the observer, ft.

It is assumed that the peak OASPL occurs at $\theta = 120°$ from the inlet. The directivity pattern given in Reference 1-6 is used to compute the OASPL at any given direction. This directivity $DI(\theta)$ is derived empirically from the test results and is shown in Figure 1-5. The OASPL at any given angle is given by,

$$\text{OASPL}\ (\theta) = \text{OASPL}_{\theta = 90°} + DI\ (\theta)\ .$$

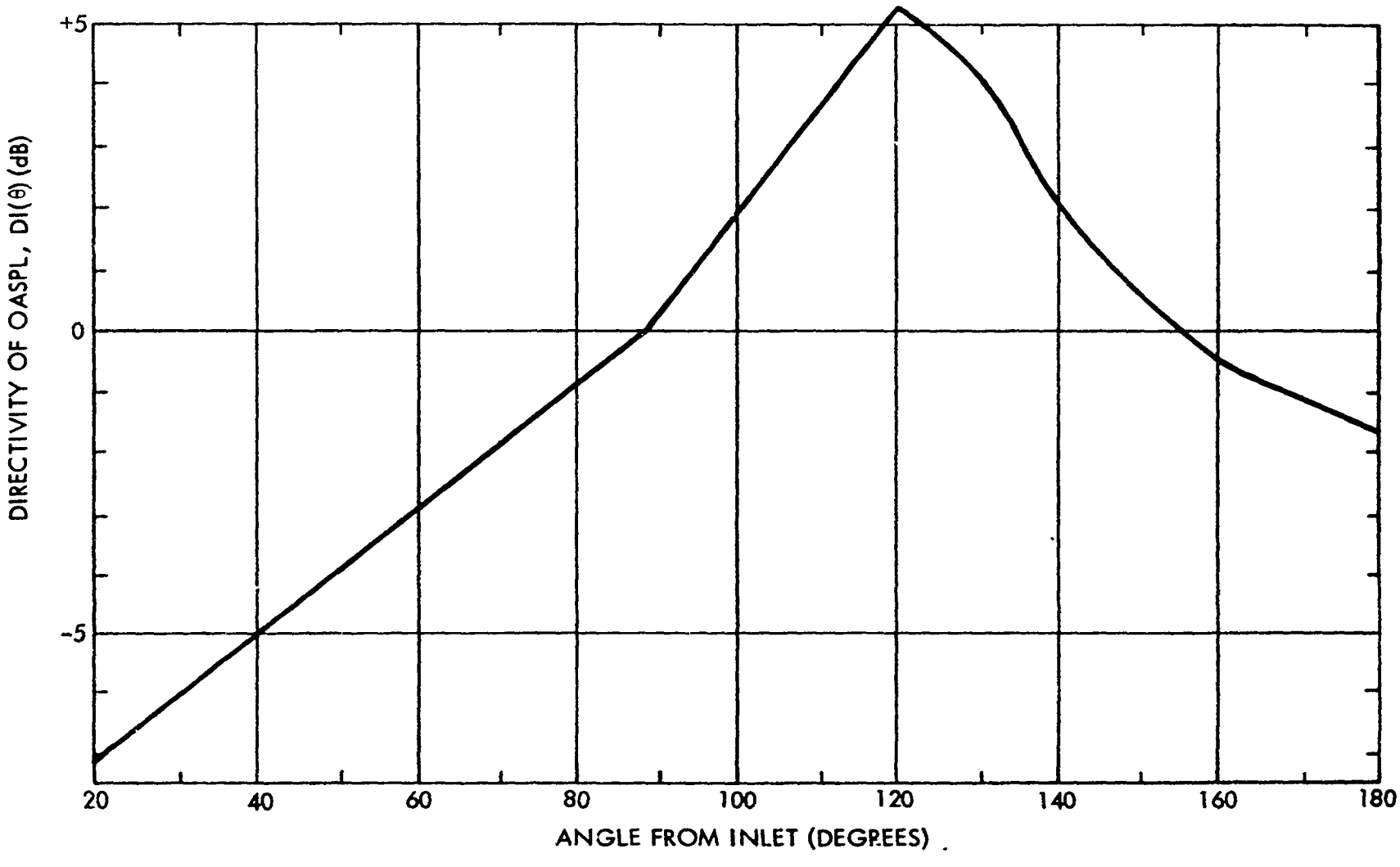

Figure 1-5. Directivity for Turbine Noise

The one-third octave band spectral distribution is presented in Figure 1-6, as a function of the percentage of the engine thrust. Turbine noise prediction could be improved and needs further study on the effect of various parameters influencing the far-field noise.

2.1.3 Excess Engine (Core and Tailpipe Noise

Test results of jet noise studies[1-7] indicate that the sound intensity in the low-velocity range does not necessarily follow velocity raised to the power 8. In general, this velocity exponent is less than 8; the actual value depends on the factor such as the type of noise generated upstream of the nozzle exit, and the turbulence level of the flow before it leaves the nozzle exit. In the case of real engines, the internal noise may consist of combustion, turbine, and obstruction noise. In addition to these internal noise sources, the turbulent flow interfering with the nozzle exit plane generates noise, which may behave like that from dipole sources. This additional noise of the jet at low jet velocities is termed "excess noise" which includes the noise generated by combustion, flow interaction with the obstructions in the tailpipe, and the interaction of turbulence with the nozzle lip.

Crighton[1-8] has considered the monopole (fluctuating mass) and dipole fluctuating thrust) as sources located at the nozzle exit plane and derived the following expressions for the radiated sound:

$$\mathrm{OASPL} = 60 \log_{10} V_J + 10 \log_{10} \frac{A_N}{R} + 20 \log_{10} \varepsilon$$

$$+ 10 \log_{10} [(1 - \cos (180 - \theta)] + K \qquad (4)$$

where $K = 20$. The peak frequency of the excess noise occurs at a nondimensional frequency, fD/V_J, corresponding to 0.3. The one-third octave spectral shape shown in Figure 1-7 is derived somewhat arbitrarily at this point.

2.2 JET NOISE

At the present time, there is no single satisfactory jet noise prediction method. Extensive theoretical and experimental investigations are currently being conducted at Lockheed-Georgia Company[1-9, 1-10] to develop a unified jet

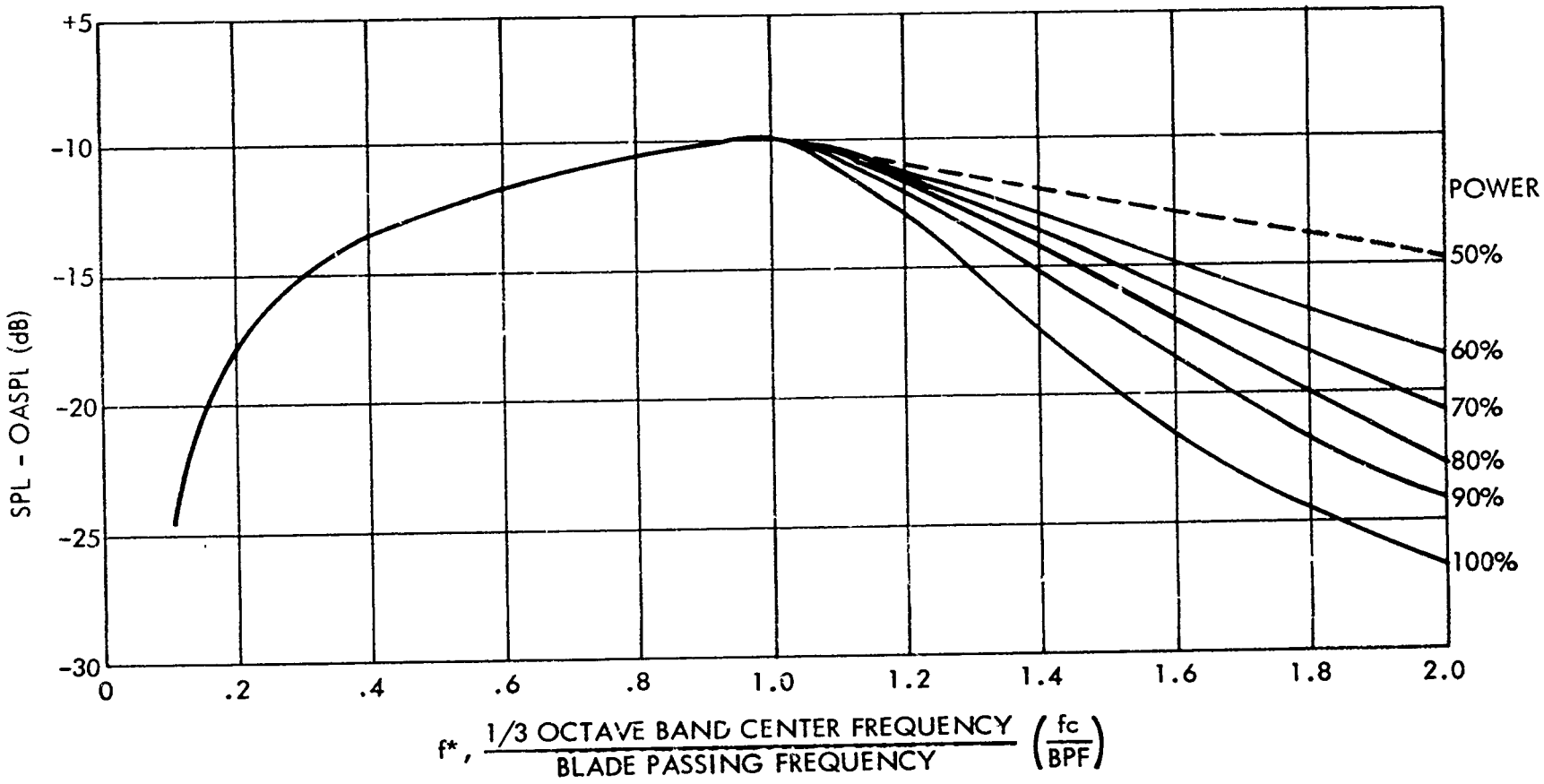

Figure 1-6. Spectral Distribution of Turbine Noise

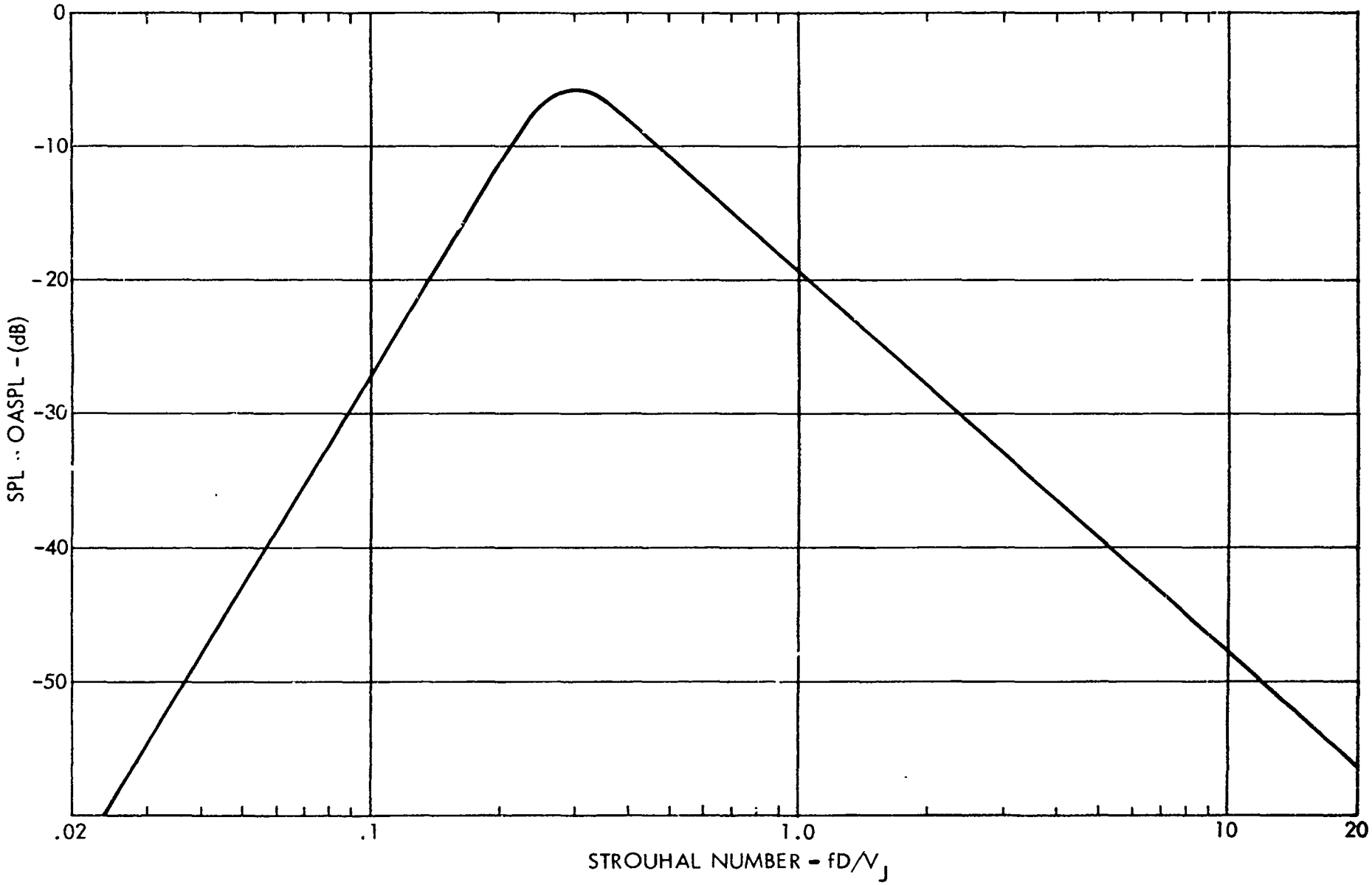

Figure 1-7. Spectral Distribution of Excess Noise

noise-prediction model. This model accounts for the temperature changes, aircraft motion and from low subsonic to supersonic jet Mach numbers. As soon as the results of this work are available, they can be incorporated into this prediction program without much effort.

The program presently uses a method developed recently by Stone[1-11] for NASA's Aircraft Noise Prediction office, which is a semi-empirical relation based on the test results of model jet flows and Lighthill's theory. This method is adapted to suit the computer program and to be consistent with the prediction procedure for the other noise sources of V/STOL aircraft. The jet noise prediction is only for subsonic velocities with a single mixed-flow exhaust from circular, plug, and slot nozzles, and separate flow exhaust from co-annular nozzles. Since the effect of forward speed is included separately in this report, the relative velocity effect is left out in the following equations.

2.2.1 Mixed Flow Jet Exhaust

Circular Nozzles - The overall sound pressure levels (OASPL) at 90° from the inlet is given by:

$$\mathrm{OASPL}_{\theta=90^\circ} = 10 \log_{10} \frac{A_N}{R^2} + 20 \log_{10} \left(\frac{\rho_a}{\rho_{ISA}}\right) - 40 \log_{10} \frac{C_a}{C_{ISA}}$$

$$+ 10 \left[\frac{3 \left(\frac{V_J}{C_a}\right)^{3.5}}{0.6 + \left(\frac{V_J}{C_a}\right)^{3.5}} - 1 \right] \log_{10} \frac{\rho_j}{\rho_a} + 75 \log_{10} \left(\frac{V_J}{C_a}\right)$$

$$- 10 \log_{10} \left[1 + 0.01 \left(\frac{V_J}{C_a}\right)^{4.5} \right] + K, \qquad (5)$$

where subscripts a and ISA refer to ambient conditions and international standard atmospheric conditions, respectively.

The source convection and refraction through flow shear layer affect the directivity of the radiated noise as a function of angle from the inlet. From the experimental results and the theoretical description of the convection and refraction effects, the spectral distribution given in Figure 1-8 is

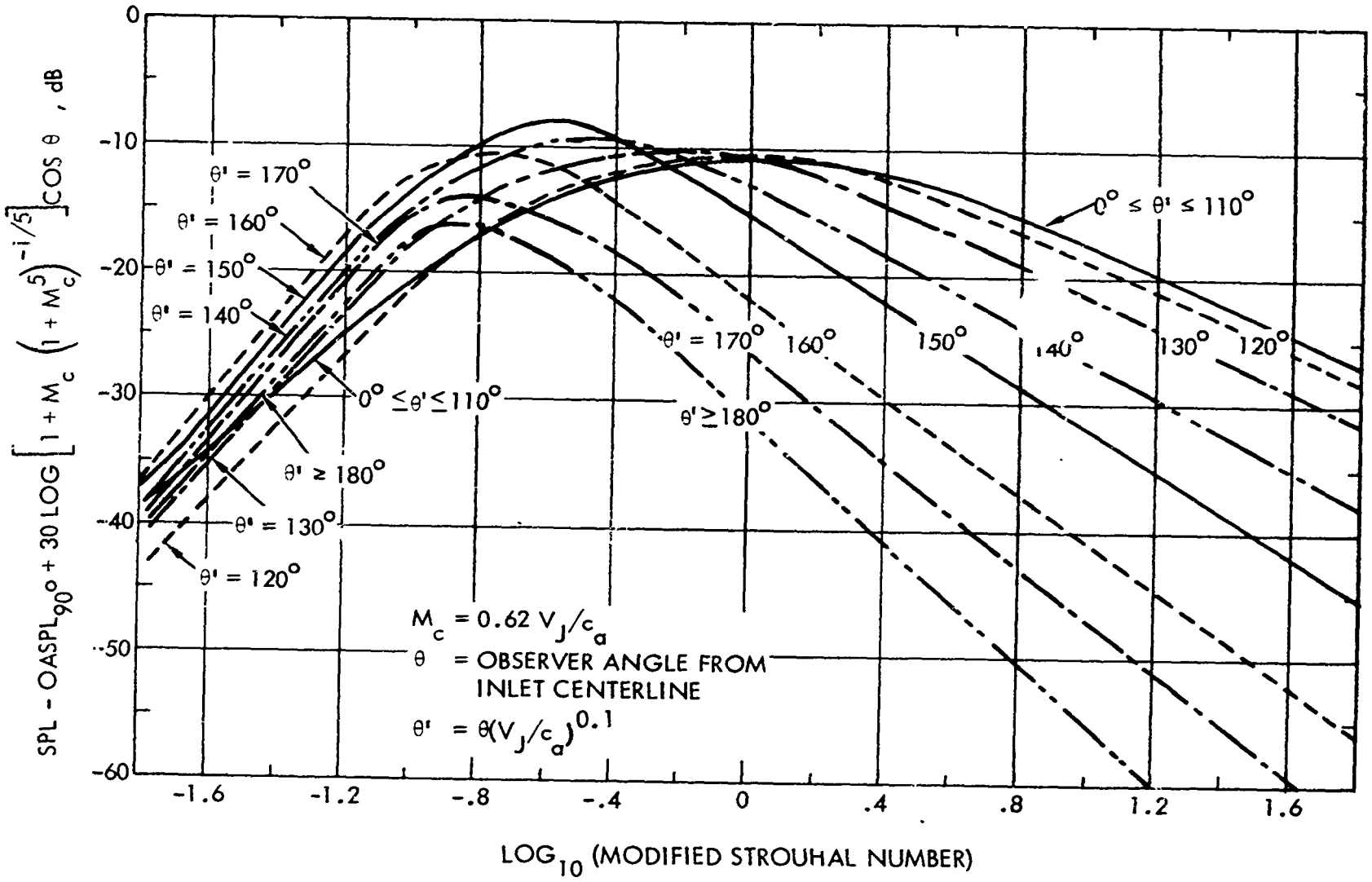

Figure 1-8. Spectral Distribution of Jet Noise

derived for different angles. The nondimensional frequency parameter is given as,

$$S = \frac{fD}{V_J} \left(\frac{T_J}{T_a}\right)^{0.4} (1 + \cos\theta') \tag{6}$$

where $\theta' = \theta(V_J/C_a)^{0.1}$.

<u>Plug Nozzles</u> - The OASPL for plug nozzles at $\theta = 90°$ is given as,

$$OASPL_{\theta=90°} = 10 \log_{10} \left(\frac{A}{R^2}\right) + 20 \log_{10} \left(\frac{\rho_a}{\rho_{ISA}}\right) + 40 \log_{10} \left(\frac{C_a}{C_{ISA}}\right)$$

$$+ 10 \left[\frac{3 \left(\frac{V_J}{C_a}\right)^{3.5}}{0.6 + \left(\frac{V_J}{C_a}\right)^{3.5}} - 1 \right] \log_{10} \left(\frac{\rho_j}{\rho_a}\right) + 75 \log_{10} \left(\frac{V_J}{C_a}\right)$$

$$- 10 \log_{10} \left[1 + 0.1 \left(\frac{V_J}{C_a}\right)^{4.5} \right] + 3 \log_{10} \left(0.01 + \frac{2h}{D}\right) + K, \tag{7}$$

where h = gap height

D = circular nozzle diameter at nozzle exit plane.

The directivity and spectra are assumed to be the same as for a circular nozzle, except that the nondimensional frequency parameter is redefined to include the effect of the plug as,

$$S = \frac{fDe \left(\frac{D_h}{D_e}\right)^{0.4} \left(\frac{T_J}{T_a}\right)^{0.4} (1 + \cos\theta')}{V_J}, \tag{8}$$

where D_h = hydraulic diameter of the nozzle

D_e = equivalent circular nozzle diameter.

Slot Nozzles - For the slot nozzle of aspect ratio (width-to-height ratio) less than about 10, the OASPL, directivity, and the spectra are predicted in the same way as for a circular nozzle. However, the modified nondimensional frequency parameter derived for a plug nozzle as in equation (8) is used.

2.2.2 Co-axial Nozzles

The experimental data and theoretical formulations to predict noise from co-axial jets are sparse. The following empirical relation is derived for jet noise as a function of area ratio, velocity ratio, and temperature ratio with core jet as reference:

$$\mathrm{OASPL} - \mathrm{OASPL}_c \Big|_{\theta=90^\circ} = 5 \log_{10}\left(\frac{T_1}{T_2}\right) + 10 \log_{10} \left\{ \left(1 - \frac{V_2}{V_1}\right)^m + 1.2 \frac{\left[1 + \frac{A_2 V_2^2}{A_1 V_1^2}\right]^4}{\left[1 + \frac{A_2}{A_1}\right]^3} \right\}, \tag{9}$$

where OASPL_c is the OASPL for core jet alone and is given by the equation for circular nozzle (equation 5) or plug nozzle (equation 7).

The exponent m is given by,

$$m = 1.1 \frac{A_2}{A_1} \qquad \text{for } \frac{A_2}{A_1} < 29.7$$

$$m = 6.0 \qquad \text{for } \frac{A_2}{A_2} \geq 29.7 .$$

The directivity and spectra are assumed to be the same as for a circular nozzle with the modification of Strouhal number given as,

$$S = \frac{S_1}{1 - F(S)\,\frac{T_2}{T_1}},$$

where S_1 is the Strouhal number of core jet alone as given in equation (6) and

F(s) is given in Figure 1-9.

2.3 LIFT-AUGMENTATION SYSTEM NOISE

The noise generation and propagation of the lift-augmentation of various jet-powered-lift systems is discussed. The common noise source mechanisms for all the configurations except augmentor wing and vectored thrust are: impingement, wall jet, trailing edge, and trailing-edge wake. In the case of vectored thrust, noise generated by the flow over the turning vanes is the only noise source in addition to the basic jet engine. However, the increased flow turbulence and the change in the jet flow direction do change the characteristics of the jet noise. The noise mechanism of the augmentor wing propulsive-lift system is too complicated to allow for further separation of the noise sources. The sources of various propulsive lift systems are shown in Figure 1-10.

2.3.1 Impingement Noise

Experimental observations indicate that the radiated sound of a jet flow is increased substantially when a rigid surface is introduced into the flow. One of the mechanisms of this additional noise is the impingement of the turbulent flow on a surface. The impingement region is defined as the region in the vicinity of the geometrical stagnation point on the surface, where the similarity of the flow cannot be established. This noise is a function of the flow characteristics (turbulence and mean flow) and the geometry of the rigid surface such as angle of inclination to the flow direction and the dimensions.

Since the physics of the generating mechanism of impingement noise is not completely understood at the present time, a theory cannot be developed. However, the experimental results[1-12, 1-13] indicate that the impingement noise is primarily due to the Reynolds' stresses (quadrupole sources) modified by the presence of the rigid surface. It is suggested in reference 1-12 that

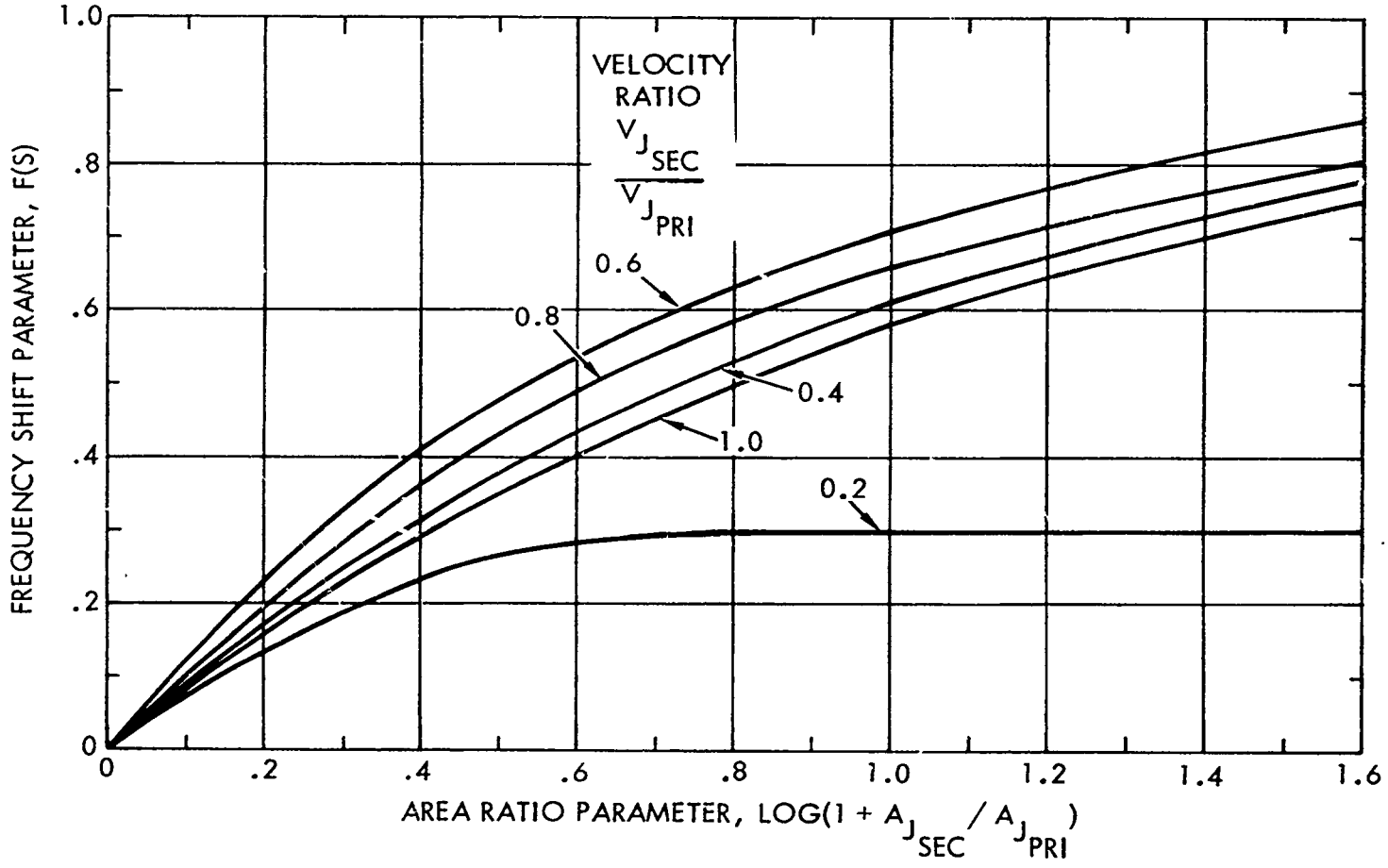

Figure 1-9. Frequency Shift Parameter for Coaxial Jets

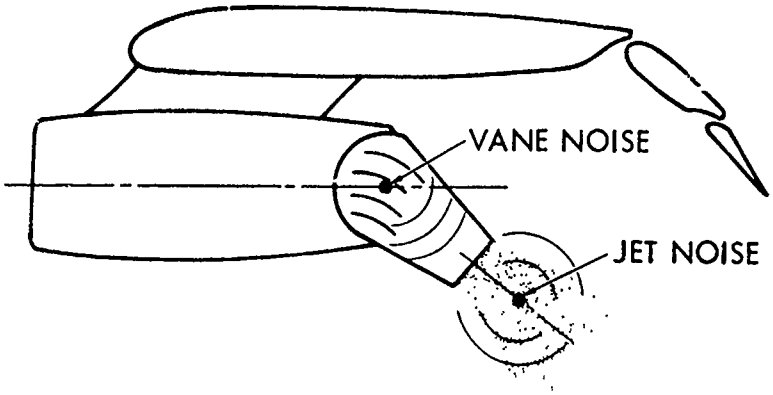

(a) Vectored Thrust

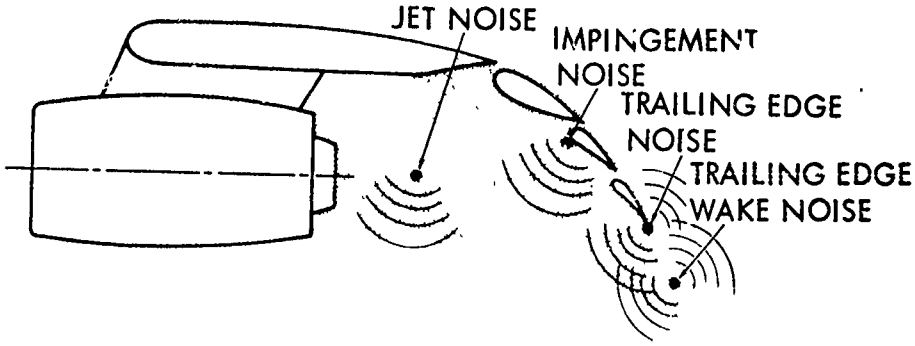

(b) Externally Blown Flap

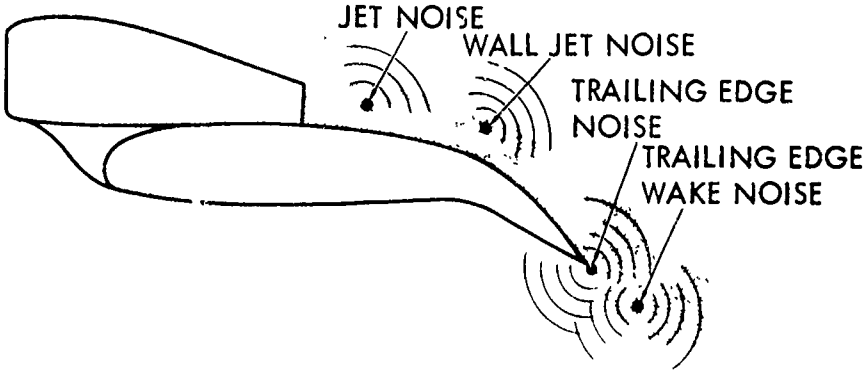

(c) Upper Surface Blown Flap Configuration

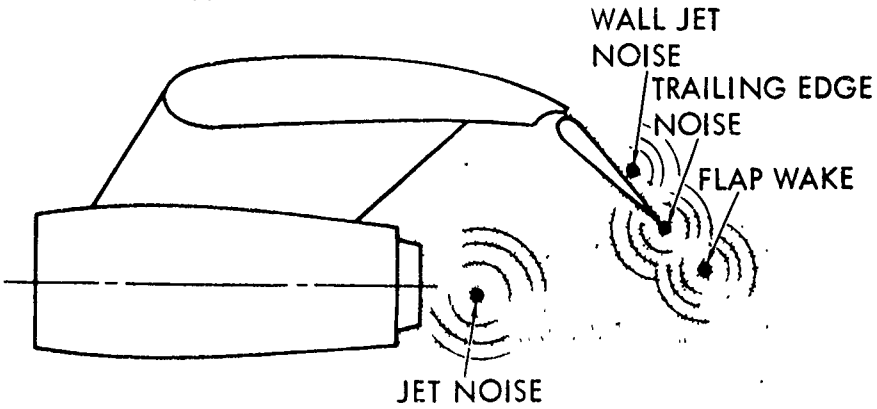

(d) Internally Blown Flap/Boundary Layer Control

Figure 1-10. Noise Sources of Powered - Lift Systems

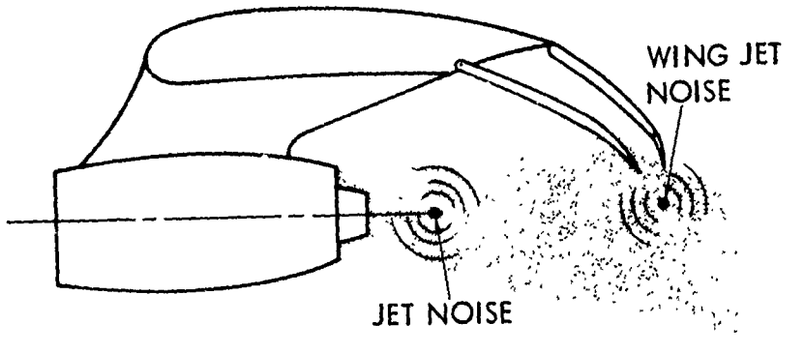

(e) Internally Blown Flap/Jet Flap

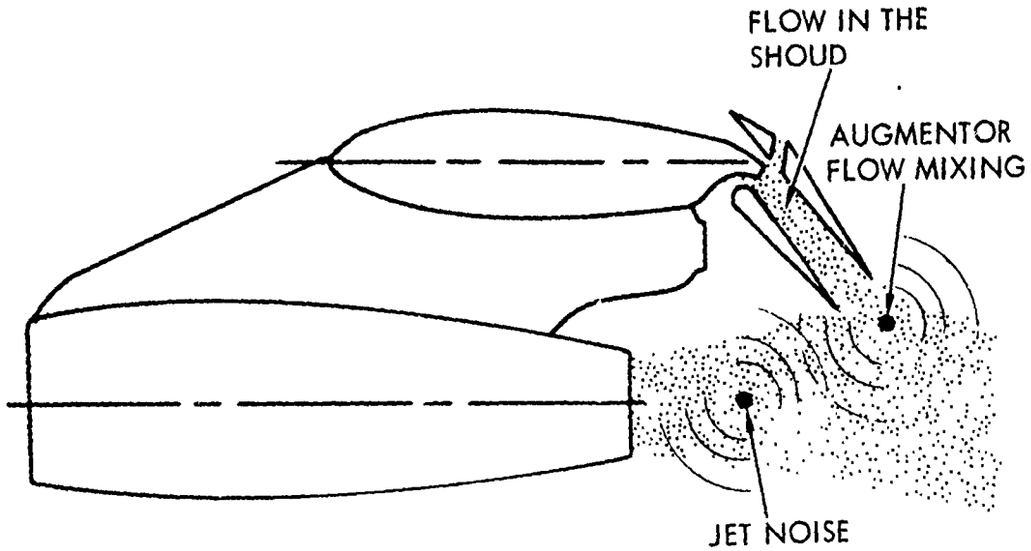

(f) Augmentor Wing

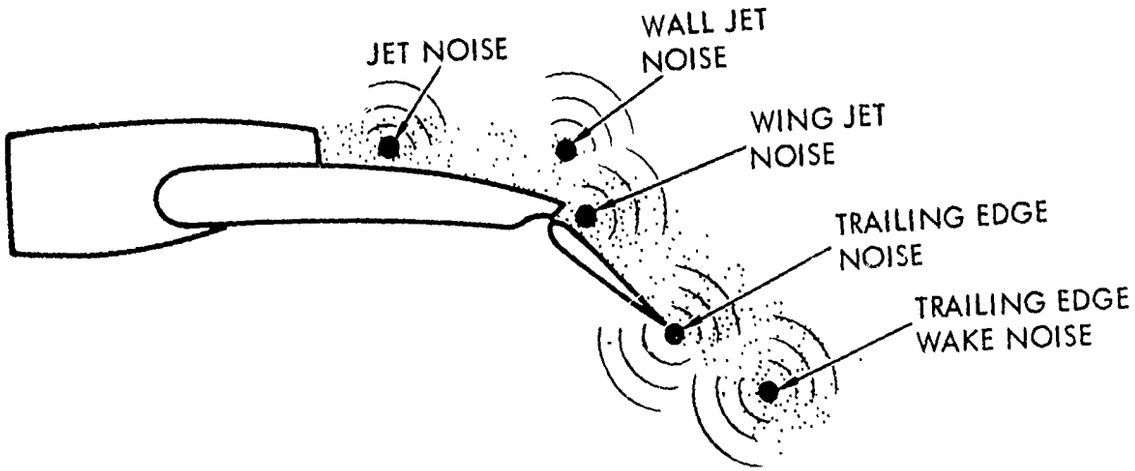

(g) Hybrid (Combination of USB and IBF)

Figure 1-10. (Concluded)

the impingement area and the impingement velocity are the correlation parameters to be used in predicting the far-field noise from impingement. The impingement area is somewhat arbitrarily defined at this time as the area within 50% of the peak impingement velocity in the plane of the rigid surface. The peak impingement velocity is defined as the maximum velocity in the plane of the rigid surface in the absence of the surface. Therefore, the equation for the overall sound intensity is given as:

$$I \sim \frac{\rho_a Ai}{c_a^5} V_{ip}^8 \sin^2\alpha$$

where Ai is the impingement area

V_{ip} is the impingement velocity

α is the angle between the jet axis and the surface.

To predict the impingement noise of high-lift systems, α is the angle between the jet axis and wing/flap surface at the geometrical impingement point. (In the typical EBF, the mean flap angle is considered to be α.)

Assuming ρ_a and c_a are constant, the expression for OASPL may be derived as:

$$(OASPL)_{\theta=90^\circ} = 10 \log_{10} \frac{Ai \sin^2\alpha}{R^2} + 80 \log_{10} V_{ip} + K. \qquad (10)$$

The impingement velocity is estimated by the empirical relation, derived from the experimental results of reference 1-14 as,

$$\frac{V_{ip}}{V_J} = \left[1 + \left(\frac{0.15\, X_I}{C_n\, D_e \sqrt{1+M_J}}\right)^a\right]^{-1/a}$$

where $a = 4\,[1 + 8/3\,(D_e/D_h - 1)]^{-1}$

X_I = distance between the nozzle exit plane and the rigid surface (wing/flap) along the jet axis

D_e = equivalent circular nozzle diameter with the same exit area of the nozzle $= 2\sqrt{A/\pi}$

D_h = hydraulic diameter for slot and multi-lobed nozzles
$= D_e$ for circular and coaxial nozzles

C_n = effective nozzle coefficient (assumed to be unity)

M_J = jet Mach number.

The impingement area is given as,

$A_i = l_s h_i$ for slot nozzle

$= \pi d_i^2/4$ for axisymmetrical nozzles

l_s = nozzle width (for slot nozzles)

h_i and d_i = width and diameter measured in the impingement plane for 50% of the peak impingement velocity for slot and circular nozzle, respectively.

The dimensions h_i or d_i are estimated from the empirical relations given by Bradbury[1-15] as:

$$\frac{h_i}{h} = 0.109\,\frac{x_i}{h}\,\frac{1}{1 + \frac{0.55}{\sqrt{\mu(\mu-1)}}\sqrt{\frac{x_i}{h}}} \quad \text{for slot nozzle,} \tag{12}$$

$$\frac{d_i}{D_e} = 0.89\,\frac{x_i}{D_e}\,\frac{1}{\left[1 + \frac{0.27}{\mu(\mu-1)}\cdot\frac{x_i}{D_e}\right]^{\frac{1}{2}}} \quad \text{for circular nozzle,} \tag{13}$$

where μ = jet velocity/free-stream velocity.

<u>Directivity</u> - The directivity of OASPL is derived from the experimental data of reference 1-13 and is presented in Figure 1-11. Figure 1-11a gives the directivity index $DI(\theta,\alpha)$ to be added to the OASPL predicted from equation (10) as a function of θ and α. (See the insert in Figure 1-11 for the definition of θ and α.) The directivity in ϕ-plane is assumed to be as $A(\theta+\alpha)\cos\phi$,

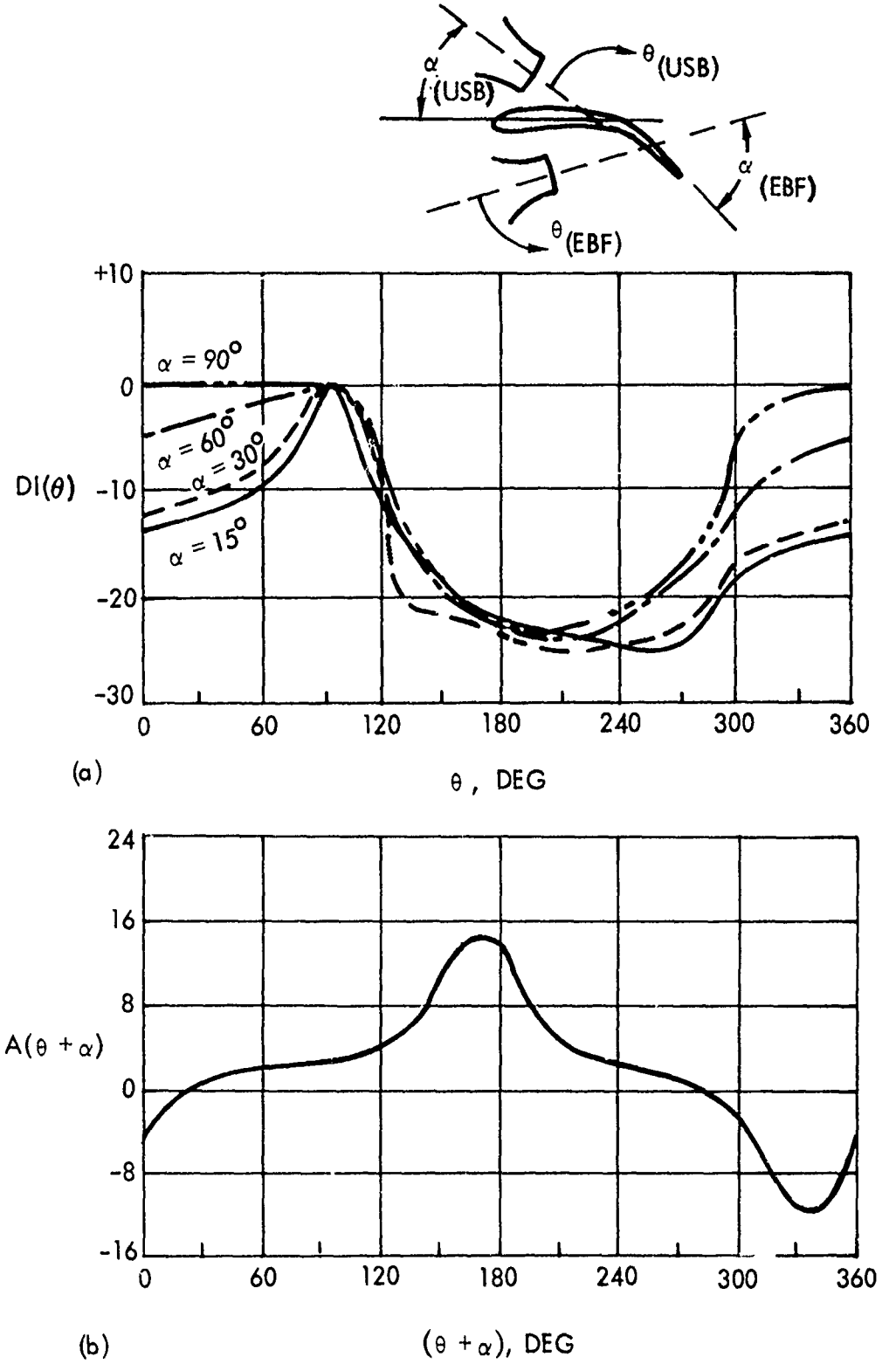

Figure 1-11. Directivity of Impingement Noise

where A $(\theta + \alpha)$ is derived from the experimental data and given in Figure 1-11b; $\phi = 90^\circ$ corresponds to the fly-over plane.

Spectral Distribution - There is neither theoretical explanation nor enough experimental data available to estimate the spectral distribution of impingement noise as a function of directivity. In this report the nondimensional spectral distribution derived from the experimental data of reference (15) is used and assumed to be independent of direction. Nondimensional frequency $fDi/V_{ip} \sin^{\frac{1}{2}}$ appears to correlate well with the experimental data. The nondimensional spectral distribution based on one-third octave frequency shown in Figure 1-12 is used in the prediction model.

2.3.2 Wall Jet Noise

In the USB and IBF cases the wall jet is formed immediately after the impingement and/or attachment of the jet flow on the wing/flap surface. But, in the typical EBF configuration, the impingement location, and for IBF/JF, the wing nozzle location are very close to the trailing edge. Therefore, a developed wall jet does not exist for these configurations.

As the free boundary region of the wall jet (away from the surface) generates the noise by the process of mixing with the ambient air, the mechanism is similar to fluctuating stresses (quadrupole sources). Close to the surface (inner layer), the large mean shear produces a high turbulence intensity. The noise-generation mechanism in the inner layer is associated with the induced fluctuating pressures on the surface and, therefore, is from fluctuating forces (dipole type). Even though the turbulence intensity is large, the volume of the inner layer is very small compared with that of the free boundary region. Therefore, in wall-jet noise prediction, the noise generated in the inner layer region is neglected except at the trailing edge (which is discussed in subsection 4.3.3).

Reddy and Brown[1-16] and Reddy[1-17] have discussed the noise mechanism of a wall jet with reference to USB. The acoustic intensity generated in the wall jet region of USB and IBF can be written as:

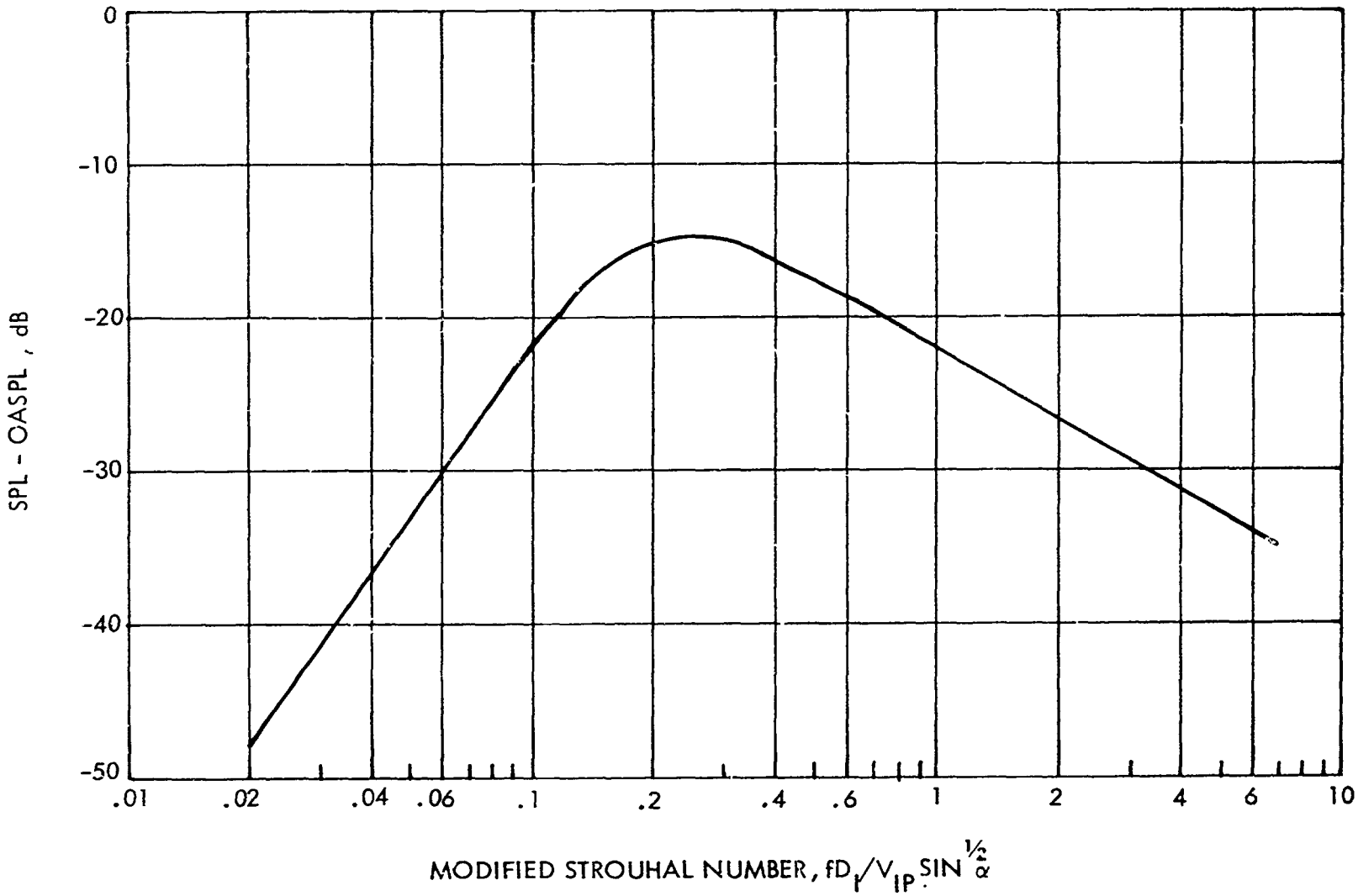

Figure 1-12. Spectral Distribution of Impingement Noise

$$I \sim \frac{\rho_a}{C_a^5} (b\ell) V_m^8$$

where b, ℓ = the width and length of wall jet, respectively

V_m = maximum velocity in the wall jet.

Assuming that ρ_a and C_a are constant, the wall-jet noise at an angle $\theta = 90°$ is given by:

$$OASPL_{\theta=90°} = 10 \log_{10}(\frac{b\ell}{R^2}) + 80 \log_{10} V_m + K \qquad (14)$$

where K = 105.

Directivity and Spectra - The directivity of OASPL is derived, based on the knowledge that most of the sound radiates perpendicular to the surface. Since no experimental data are available to indicate the directivity of the wall-jet noise alone, the directivity given in Figure 1-13 is derived somewhat arbitrarily and accounts for the diffracted sound field for a finite or a semi-infinite surface.

The spectral distribution is assumed to depend on the thickness of the wall jet, δ, and the maximum velocity. Therefore, the nondimensional frequency (Strouhal number) may be written as:

$$S = \frac{f\delta}{V_m} .$$

The peak Strouhal number is assumed to be 1.0, and the one-third octave spectral distribution is shown in Figure 1-14.

2.3.3 Trailing-Edge Noise

The test results of EBF and USB lead many people to assume that trailing-edge noise is a dominant source of the high lift system. Hayden[1-18] formulated an analytical expression for the trailing-edge noise as the dipole sources generated by the fluctuating momentum imparting from the surface at the trailing edge to the unbounded free field. He showed that the radiated sound intensity

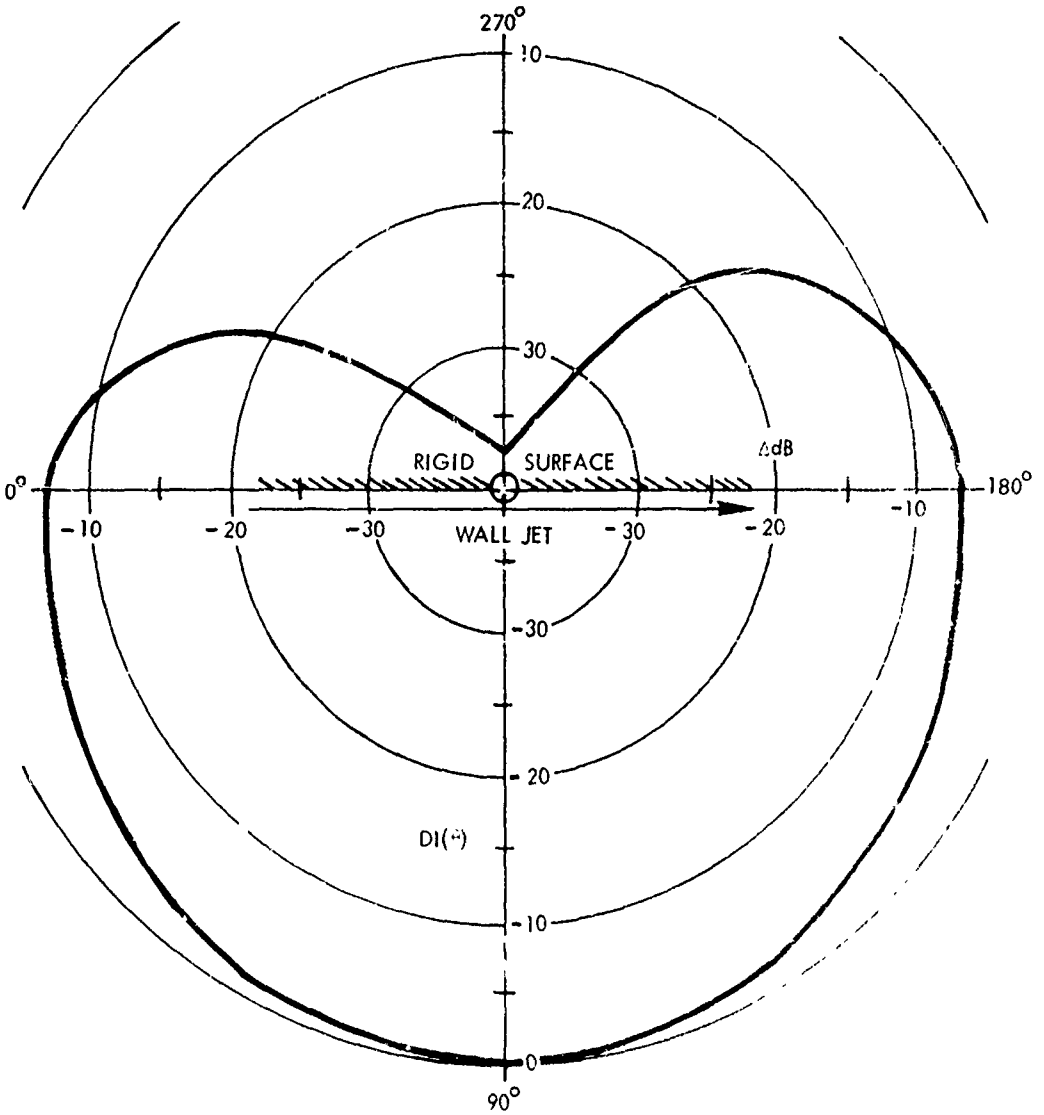

Figure 1-13. Directivity of Wall Jet Noise

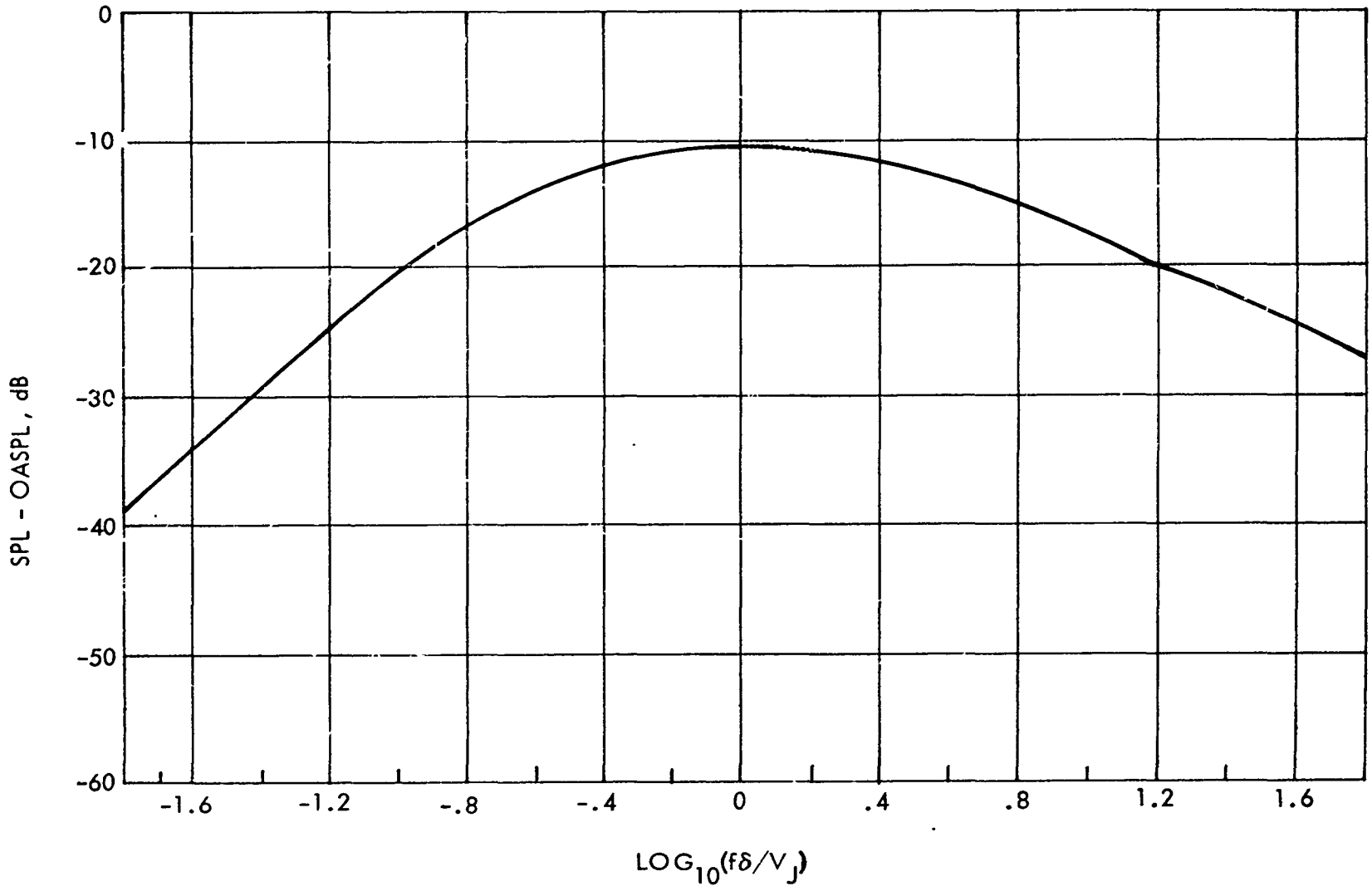

Figure 1-14. Spectral Distribution of Wall Jet Noise

varies as a typical velocity raised to the power 6. Grosche[1-19] from his experimental investigation concluded that the dominant part of the total sound energy of the jet flow over a finite plate is generated from the region close to the trailing edge. His results indicate that the sound intensity varies as the velocity raised to power 5. The jet flow leaving the trailing edge mixes with the ambient air and generates very high turbulence intensities near the trailing edge. Ffowcs-Williams and Hall[1-20] have studied the effect of fluctuating stresses (quadrupole sources) near the scattering edge of a semi-infinite rigid plane. They found for the eddies near the edge ($2kr \ll 1$, where k is the wave number, and r is the distance between the edge and the turbulent eddies), the far-field sound intensity varies as the typical velocity raised to the power 5.

Powell[1-21] argued, for the case of turbulent flow over a rigid surface reaching the edges and beyond, that there is a possible flow around the edge; therefore, a true dipole radiation should emanate from the edge of the plate. The radiated sound power of this "edge noise" varies as the 6th power of typical velocity.

From these theoretical developments and the experimental results, it is reasonable to assume that the trailing edge noise is an important noise source of USB, EBF, and IBF configurations. The magnitude and the spectral distribution of this noise source depends on the turbulence intensity interfering with the edge, the spectral characteristics of the turbulence generated near the trailing edge, and the mean velocity gradient. At the present time, it is not possible to separate these effects and formulate the radiated noise of the trailing edge accurately as a function of operational and geometrical variables. Therefore, the trailing-edge noise is estimated assuming that the pertinent parameters are peak velocity, width, and the thickness of the flow at the trailing edge. The radiated sound intensity of the trailing-edge noise may be written as:

$$I \sim \frac{\rho_a}{C_a^2} V_t^5 (W \cdot \delta_e)$$

where V_{te} = maximum velocity at the trailing edge

W = width of the jet at the trailing edge

δ_{te} = jet thickness at the trailing edge.

Assuming the density and speed of sound to be constant, the equation for OASPL may be written as:

$$OASPL_{\theta=90^\circ} = 50 \log_{10} V_{te} + 10 \log_{10} \left(\frac{W\delta_{te}}{R^2}\right) + K \tag{15}$$

where K = 4.

Directivity and Spectra - From the experimental results the directivity of OASPL is derived to be:

$$DI(\theta,\phi) = 10 \log_{10} \left\{\cos^2 \left(\frac{\theta + \delta_f}{2}\right) \cdot \frac{1}{2} (1 + \sin\phi)\right\} \tag{16}$$

where θ is the angle from the inlet axis

δ_f is the flap angle

ϕ = elevation angle ($\phi = 90^\circ$ flyover location).

The nondimensional spectral distribution is assumed to depend on the velocity and the jet thickness at the trailing edge and may be written as:

$$S = \frac{f\delta_{te}}{V_{te}}.$$

The nondimensional spectral distribution of the trailing-edge noise obtained from the experiments of reference 1-17 is used in prediction. These are presented in Figure 1-15.

Evaluation of the Flow Characteristics at the Trailing Edge - Yu, Reddy, and Whitesides[1-22] measured the flow characteristics for a simplified configuration of EBF. Since they are the only experimental data available, these results are generalized to estimate the velocity, flow width, and flow thickness at the trailing edge of the EBF. Flow width is defined as width along the trailing edge between 50% of the maximum velocity. Wall-jet thickness is defined as the dimension between the trailing edge and 50% of the maximum velocity. The width and thickness, respectively, are given by

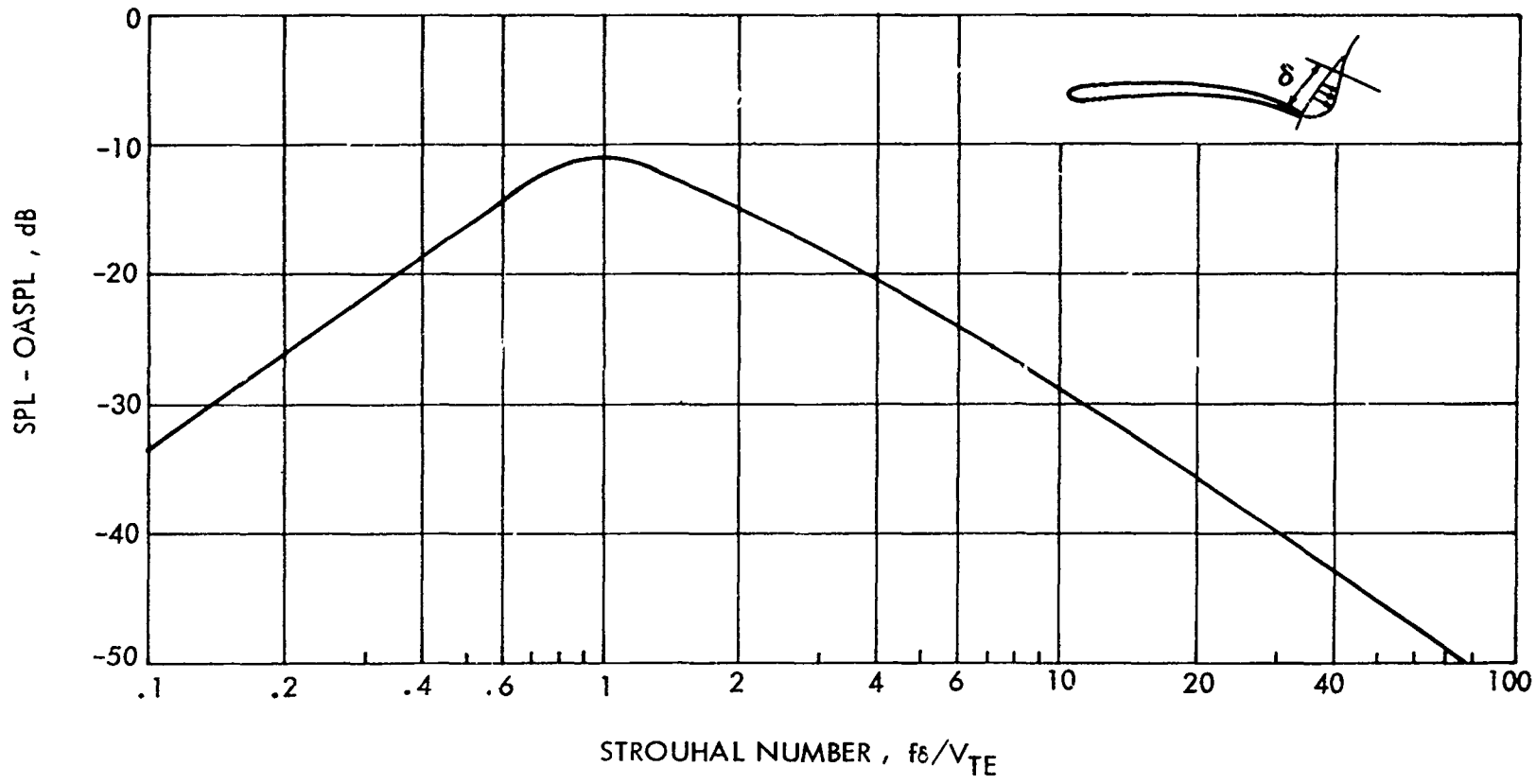

Figure 1-15. Spectral Distribution of Trailing Edge Noise

$$\frac{W}{D_1} = 0.33 \frac{X'}{D_1} + 1.5$$

$$\frac{\delta_{te}}{D_2} = 0.42 \left(\frac{X'}{D_2}\right)^{-0.75} \qquad \text{for } \frac{X'}{D_2} \geq 0.5$$

$$\frac{\delta_{te}}{D_2} = 0.5 \qquad \text{for } \frac{X'}{D_2} < 0.5,$$

where x' is the length between the trailing edge and the geometrical impingement point (intersection of jet axis and the wing/flap surface)

D_1 is the diameter of a circular nozzle or width of a slot nozzle.

D_2 is the diameter of a circular nozzle or height of a slot nozzle.

The maximum velocity at the trailing edge is estimated from the empirical curve shown in Figure 1-16.

In the case of USB and IBF, there is no systematic experimental data available to predict the jet spreading as a function of the geometrical properties of the wing/flap. Therefore the jet width at any axial distance x from the nozzle exit is assumed to be the same as the width of the nozzle. The jet thickness δ_{te} is derived from the experimental data of reference 19 as,

$$\frac{\delta_{te}}{h} = 0.5 \left(\frac{R_L}{h}\right)^{0.5} + 8 \left(\frac{h}{R_c}\right)^2 + 0.2 \left(\frac{R_c\ \theta_c}{h}\right) \tag{17}$$

where R_L = flow run length (distance between the nozzle exit and flap trailing edge

R_c = radius of curvature of the flap

θ_c = flap angle (radians).

In a typical USB configuration, the trailing edge velocity is same as the jet velocity. However, if the flap length is unusually large, then the actual trailing-edge velocity should be computed. In this formulation, it is also

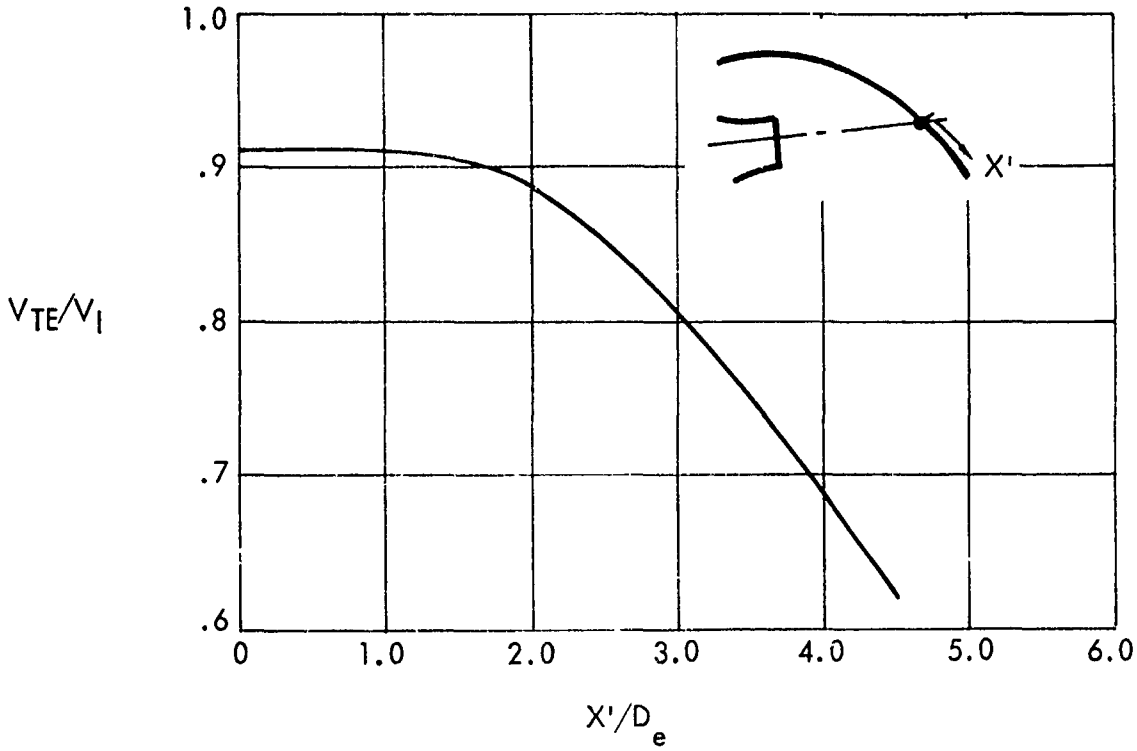

Figure 1-16. Velocity at Trailing Edge

assumed that a slot nozzle is used for the case of USB. However, when a nozzle of other than rectangular shape is used, it is necessary to establish the equivalent width and height of the slot nozzle.

2.3.4 Trailing-Edge Wake Noise

The flow after leaving the trailing edge (trailing-edge wake) possesses characteristics similar to those of a free jet. The mean-flow profiles in this region are nonsymmetrical with greater shear closer to the surface/edge than the region away from the surface as shown in reference 1-16. Even though the noise-generating mechanism is basically the fluctuating stresses (quadrupole sources), the propagating characteristics do change due to the change in the velocity gradients. The source strength distribution in the flap wake taken from reference 1-23 are shown in Figure 1-17. It should be noted that the only mixing noise (in the wake) away from the edge is estimated. The interaction of turbulence near the trailing edge with the edge is accounted for in the trailing-edge noise. Since there are not enough experimental data available to account for the convection and refraction effects of the wake noise, a simple empirical relation is used to estimate the wake noise:

$$\text{OASPL} = 80 \log_{10} V_{te} + 10 \log_{10} \left(\frac{W\delta_{te}}{R^2}\right) + K . \tag{18}$$

The velocity, width, and thickness of the wall jet at the trailing edge are evaluated as described for the trailing edge noise.

Directivity and Spectra - The directivity is derived somewhat arbitrarily, using some of the jet noise experimental data and is given in Figure 1-18.

The spectral distribution is assumed to be the same as jet noise with the jet thickness at the trailing edge as a controlling variable. The nondimensional frequency is given as:

$$S = \frac{f\delta_{te}}{V_{te}} .$$

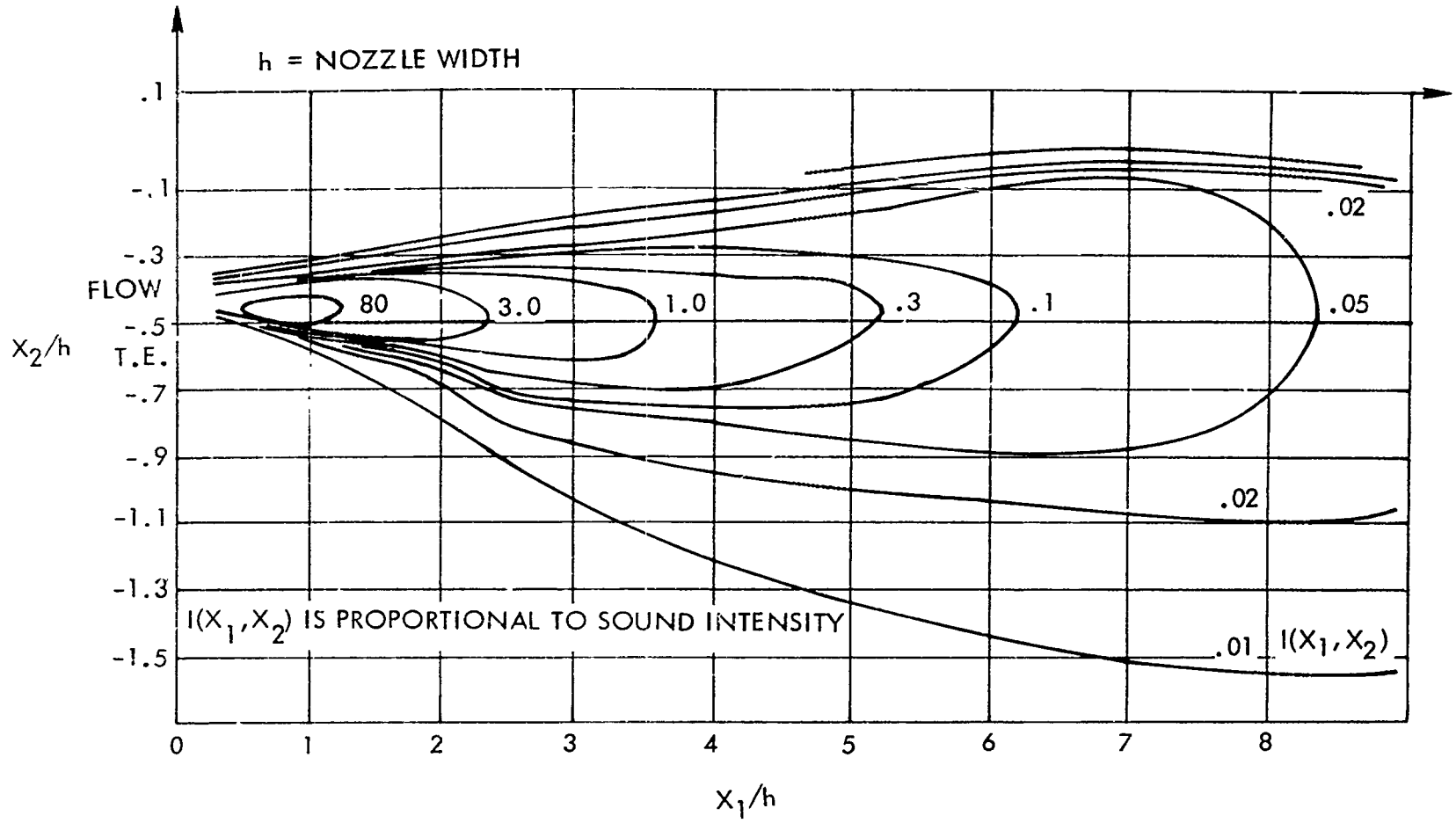

Figure 1-17. Sound Intensity Distribution in the Flap Wake

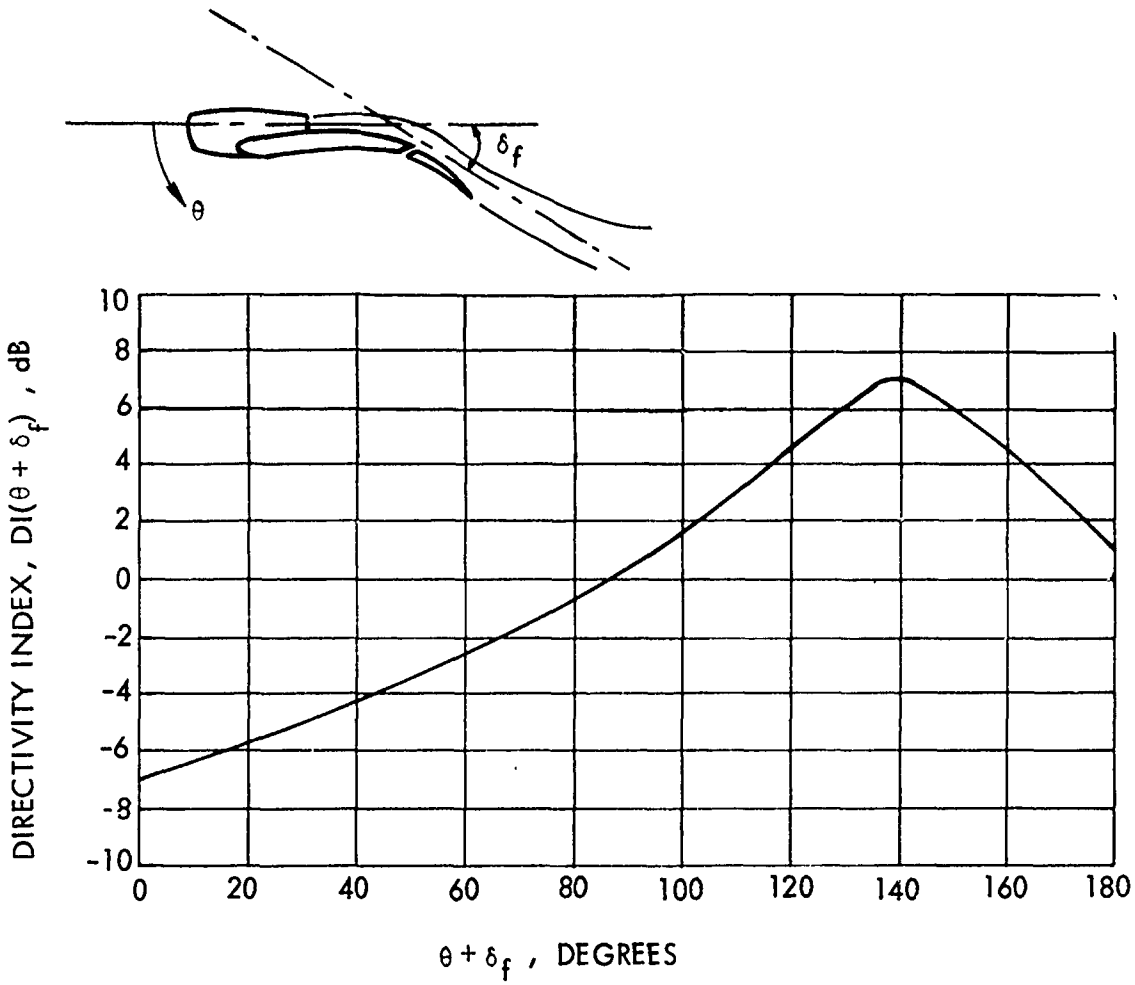

Figure 1-18. Wake Noise Directivity

2.3.5 Augmentor Wing Noise

Since the noise-generating mechanism of the augmentor flap high-lift system is complex, it is not meaningful to divide sources further. The experimental data are used to predict the noise of the augmentor flap of a baseline configuration, which is defined as a slot nozzle with a hard wall flap and a shroud as shown in Figure 1-1e. Dorsch *et al*[1-24] and Gibson[1-25] have conducted some experiments to study the noise characteristics of AW using a slot nozzle and a hard wall flap and shroud. These experimental data are used to develop a noise prediction model. The peak OASPL is given by:

$$OASPL_{peak} = 60 \log_{10} V_J + 10 \log_{10} \frac{A_N}{R^2} - 5 \log_{10} \frac{L_F}{h} + K . \qquad (19)$$

where V_J = velocity of the jet (in the wing)

A_N = area of the wing nozzle

L_F = length of the flap.

The peak OASPL occurs at azimuthal angle, θ peak = $[180° - (\delta_f + 45°)]$. The directivity is established as given in Figure 1-19a with reference to θ_{peak} using the experimental data. The directivity as a function of elevation angle (from fly-over plane to sideline plane) is also empirically derived and given in Figure 1-19b.

Assuming the spectral distribution of radiated sound to be independent of the azimuthal and elevation angle, spectral distribution based on one-third octave band is shown in Figure 1-20. The Strouhal number is based on the hydraulic diameter of the nozzle and the jet velocity.

Reference 1-1 gives the test data for the augmentor wing using multi-element nozzles and treated flap and shroud. These data are incorporated in the AW noise-reduction features.

2.4 NON-PROPULSIVE NOISE

Airframe aerodynamic noise and auxiliary power unit noise, called "non-propulsive" sources, are discussed below.

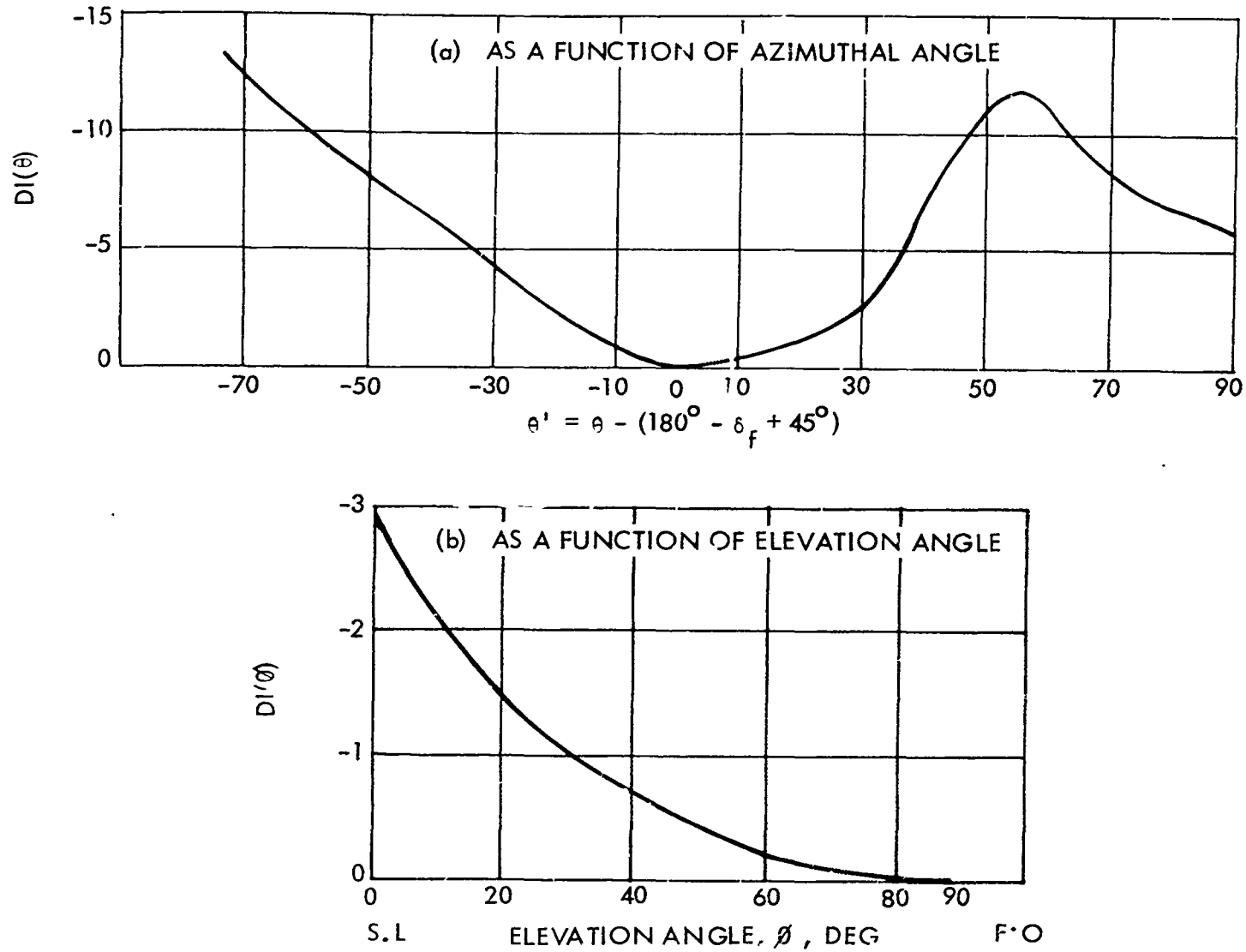

Figure 1-19. Directivity of AW Noise

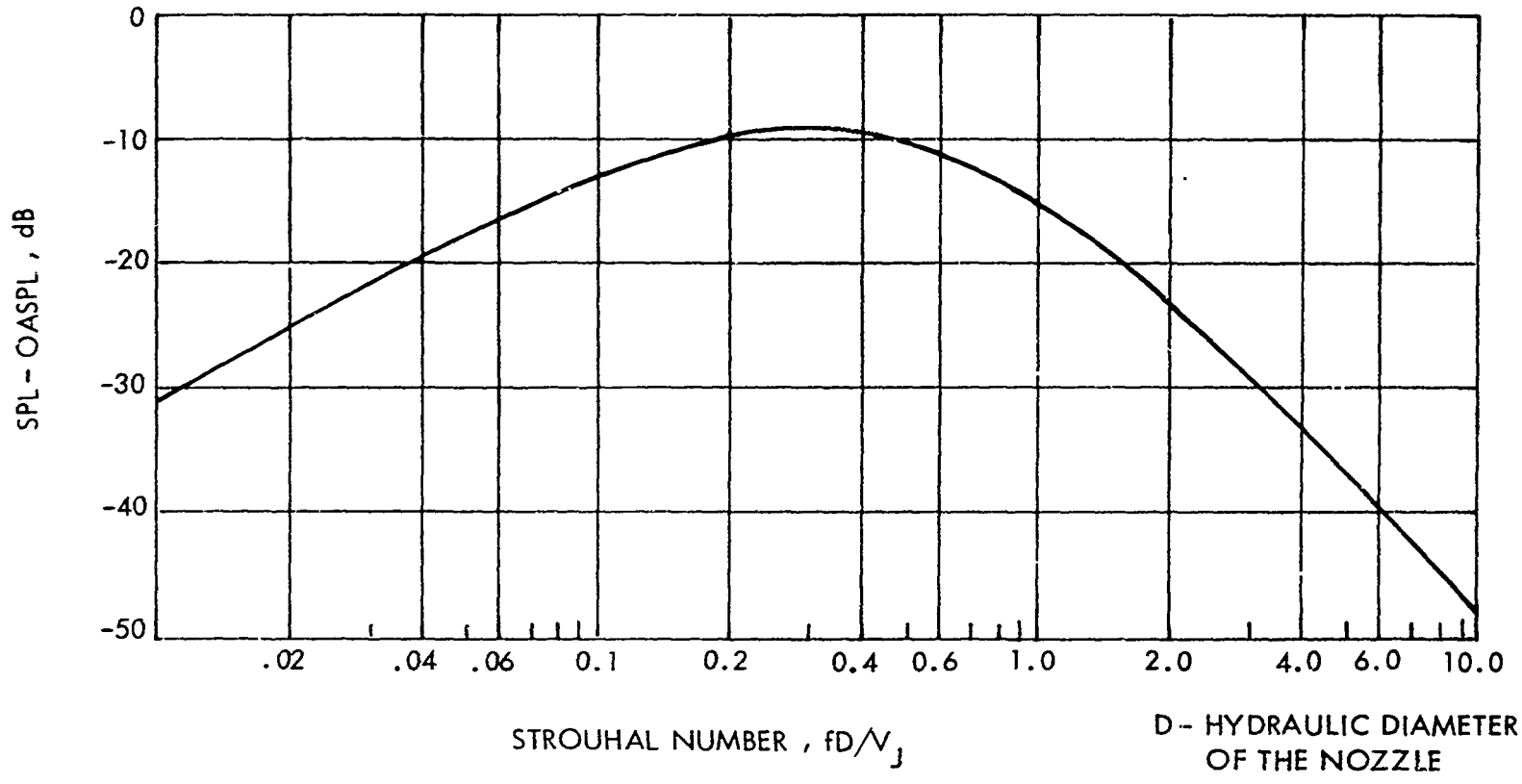

Figure 1-20. Spectral Distribution of AW Noise

2.4.1 Airframe Noise

Airframe noise is defined as the noise generated by the motion of the aircraft through the air. This excludes the noise produced by the propulsive system and other power generating units such as auxiliary power units. In recent years, there were several test programs conducted by Healy[1-26, 1-27], Gibson[1-28, 1-29], and Smith *et al*[1-30] to measure the airframe noise of different size aircrafts. Healy, in reference 1-26, derived the expression for the OASPL of an aircraft using the measured data for four aircrafts with two engines and a glider as:

$$OASPL = 10 \log_{10} \left[\frac{S_i}{R^2} \cdot \frac{V_a^6 \cdot S_W}{(AR)^4} \right] + 28.0 .$$

In deriving this expression, the following assumptions were made:

(1) The exponents of velocity and AR are integers.

(2) The noise generation mechanism is pure dipole.

(3) The measurements are conducted in far field (compact source assumption).

Hardin[1-31] developed an empirical relation using the published and unpublished test data of several commercial, military, and executive aircrafts of all sizes. Linear regression analysis was applied for 53 measurements to obtain the relation:

$$OASPL_{(Flyover)} = 10 \log_{10} \left[\frac{V_a^{4.93} \cdot S_W^{0.72}}{R^{1.62} \cdot (AR)^{2.06}} \right] + 32.56 . \qquad (20)$$

This analysis shows that the sound does not decrease according to the far-field spherical divergence law ($1/R^2$). This has probably occurred because some of the measurements used in the analysis are not really of the far-field type. The velocity index is close to 5, which may be due to the combination of sources with different velocity indices. The primary difference between these two equations is the exponent of aspect ratio, AR. There is no theoretical justification to prefer one over the other.

Revell[1-32, 1-33] attempted to derive an expression relating the radiated noise to the steady-state lift and drag. Hardin *et al*[1-31] also attempted to estimate the noise levels by computing the noise generated by each component, but the state of the art does not permit airframe noise prediction by the component method with any confidence.

The empirical relation developed by Healy or Hardin *et al* should be used to predict the noise levels. Since the relation developed by Hardin is more scientific and used more data than Healy's, the following equation which is a modification of equation (20) is used:

$$\text{OASPL} = 10 \log_{10} \frac{\sin^2\phi}{R^2} \cdot \frac{V^5 \cdot S_W}{(AR)^2} \cdot \frac{1}{(1-M_a)^4} + 7.0 . \qquad (21)$$

The nondimensional spectra based on one-third octave band is given in Figure 1-21, where

$f_{max} = 1.3\ V_a/t(1 - M_a \cos\phi)$ and

t = maximum thickness of the wing

M_a = aircraft Mach number

ϕ = elevation angle

S_W = wing area.

2.4.2 Auxiliary Power Unit Noise

The noise generated by the auxiliary power unit (APU) has several components (such as compressor, turbine, and exhaust). In general, when the aircraft is in operation with the propulsive system working, the noise generated by the APU is not significant. However, when the aircraft is stationary and the APU is in operation, this noise source could be important.

APU noise is estimated using the near-field noise test data from references 1-34 and 1-35 using the maximum shaft horsepower or the maximum bleed air in pounds per minute as:

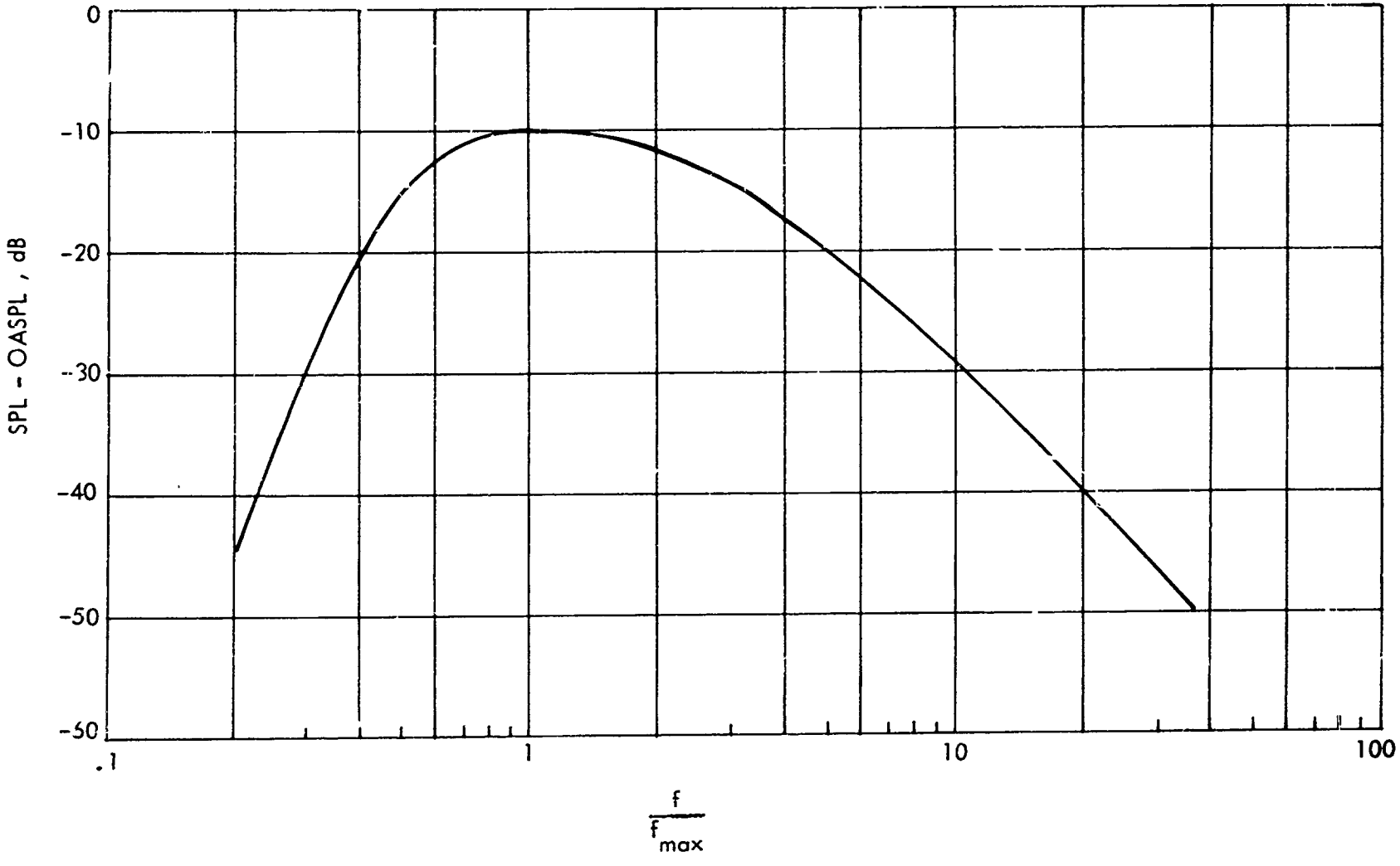

Figure 1-21. Spectral Distribution for Airframe Noise

$$PNL = 0.11\ W_B - 20 \log R + 103$$

or (22)

$$PNL = 0.106\ SHP - 20 \log R + 106$$

where W_B = maximum bleed air in lbs/min

SHP = maximum shaft horsepower.

3. NOISE PREDICTION METHOD

The noise prediction method developed here is for jet propelled V/STOL aircraft configurations. The geometry of the aircraft flight path with respect to the observer used in computing the noise levels is shown in Figure 1-22. The one-third octave band sound pressure level spectra, OASPL, PNL, and PNLT are computed for each source of the aircraft and the summation for the total aircraft at a given observer location along the sideline and at an aircraft location along the flight path. Since the acoustic data base for these aircraft are very limited, the static test data with the theoretical background are used to identify the sources and their characteristics. The effect of aircraft motion is considered separately in formulating the noise-prediction model. In many instances, it has been necessary to apply engineering judgement in estimating the noise levels. A substantial part of the analyses is carried out by Guy Swift.

3.1 RADIATED SOUND FROM THE AIRCRAFT

The noise generated by the various sources of the aircraft are considered to have originated from a single point. Thus, the distance between the various sources (e.g , between the engines) is negligible compared with the distance between the observer and the aircraft. The radiated sound is assumed to vary according to the spherical divergence law ($1/R^2$). Atmospheric attenuation for the sound propagating from the aircraft to observer is computed using the standard procedure given in reference 1-36. The attenuation of each one-third octave band SPL for a distance, R, is given as:

$$\Delta dB_i = \left(\frac{R}{1000}\right) \alpha_i$$

where α_i is the atmospheric absorption coefficient for the ith third-octave band frequency, which is a function of ambient temperature and relative humidity.

In this prediction program, the absorption coefficients for a day with 77°F and 70% relative humidity given in Figure 1-23 are used. These conditions are required by the FAA for aircraft certification as specified in FAR - Part 36[1-36].

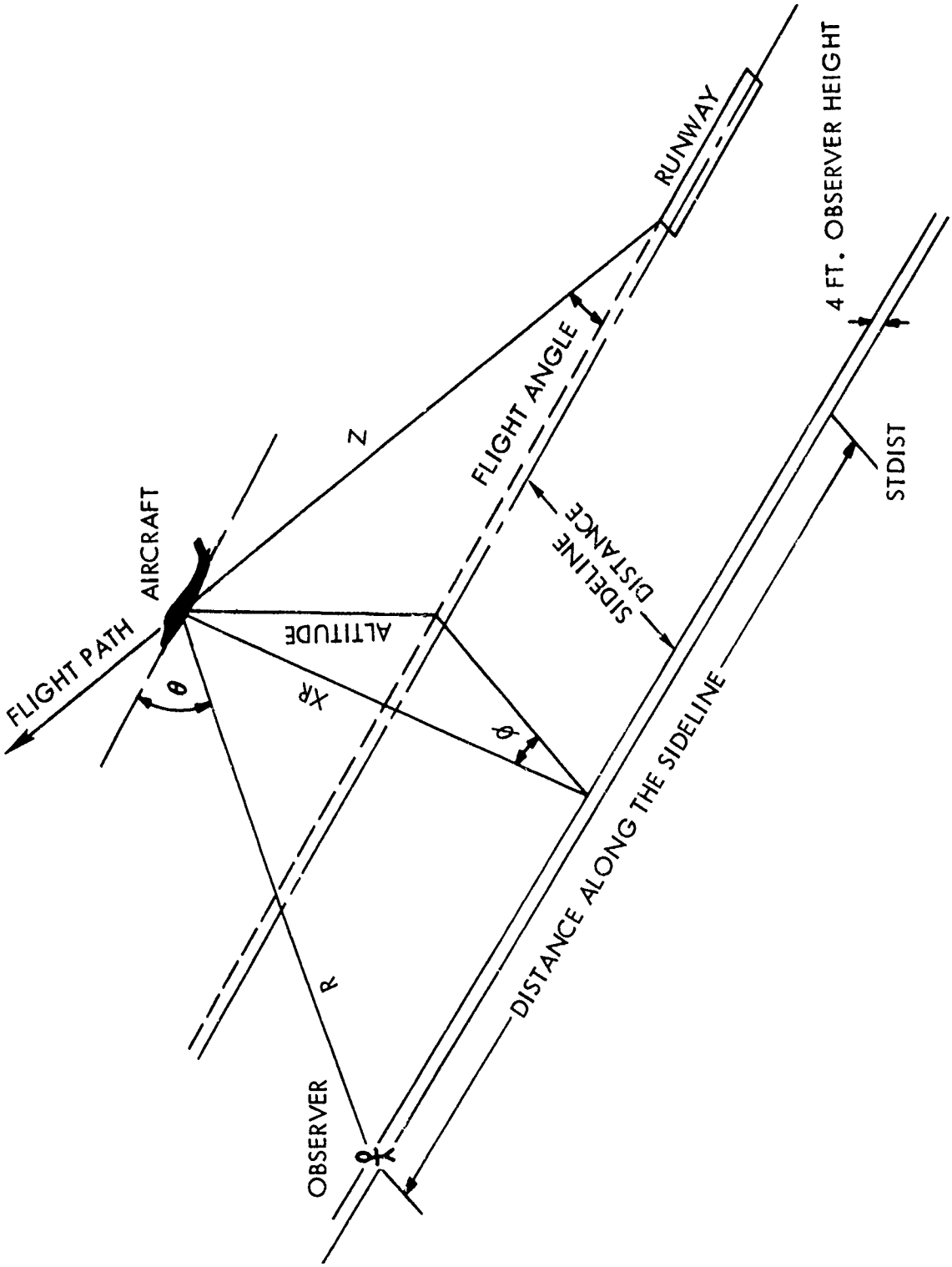

Figure 1-22. Aircraft-Observer Geometry.

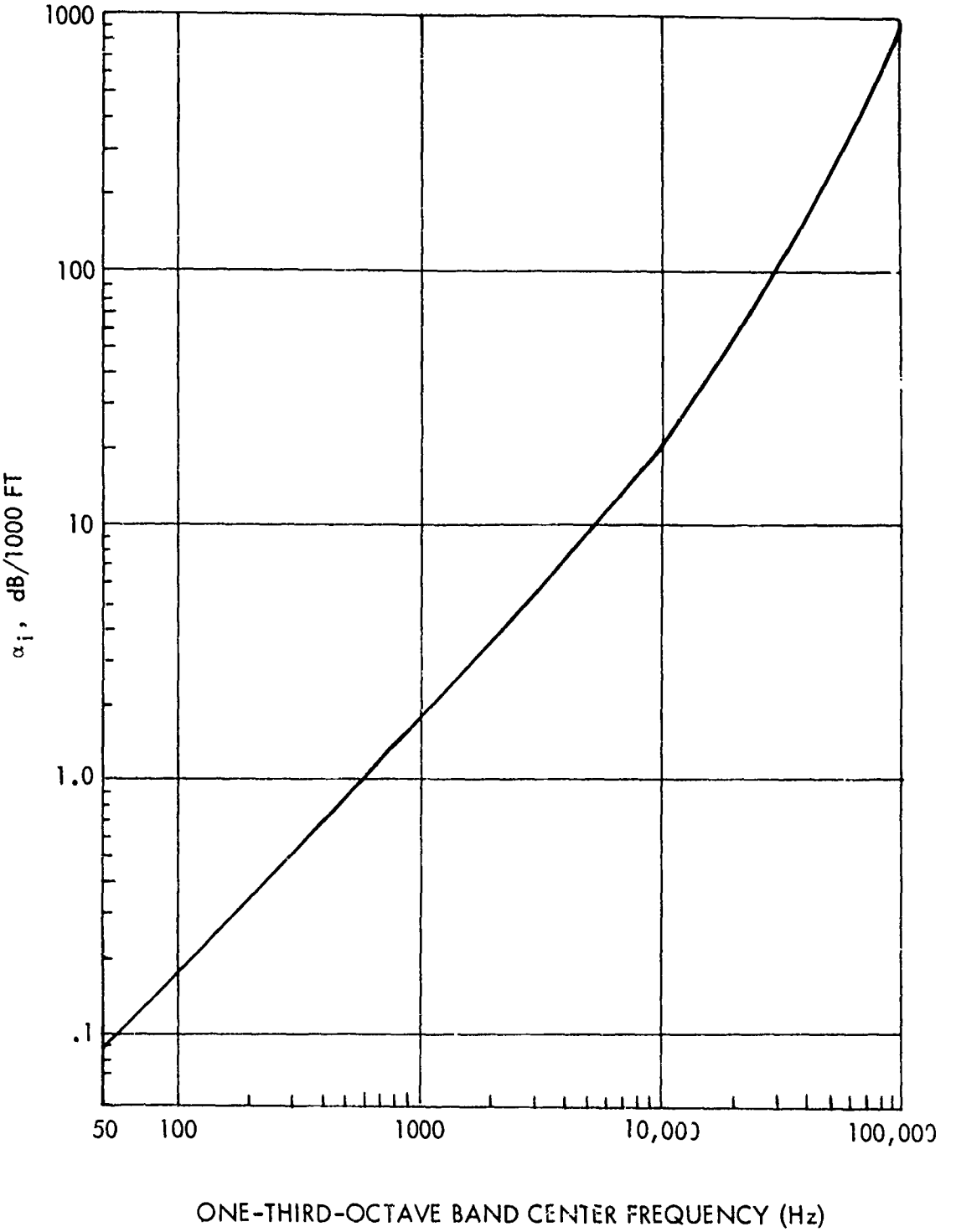

Figure 1-23. Atmospheric Absorption Coefficient

For multiple-engine aircraft, the increase in noise is estimated with the assumption of that each engine produces and radiates noise independently. Therefore, the increase in noise level for N identical engines is given by,

$$\Delta dB = 10 \log_{10} (N).$$

However, depending on the engine locations, configuration of the aircraft, and location of the observer with respect to the aircraft (elevation angle and azimuthal angle), the noise generated by some of the sources will be shielded by the aircraft components and refracted through the other engine flows. Since this type of attenuation is a complicated phenomena and no experimental data are available, these effects are estimated as a function of elevation angle:

$$\Delta dB = - 2 \cos\phi .$$

3.2 EFFECT OF AIRCRAFT MOTION

The characteristics of the noise sources (generation and propagation) are determined based on the static (without forward speed) experiments. The aircraft motion or the freestream flow does influence the noise generation and propagation of the sources. The degree of influence depends on the noise production mechanism and the geometric location of the source. Since V/STOL aircraft noise levels are generally critical during take-off and landing operations, the aircraft speeds considered here are less than 150 knots.

Basically, aerodynamic noise production depends on the fluctuating quantities in the flow such as turbulence, temperature, and density. Sound propagation depends on the inhomogeneities in the path such as flow shear and the presence of the rigid surfaces. The turbulence properties of the flow mixing depends on the relative velocity of the flow with respect to the ambient air. It may be reasonable to assume that the noise-generating mechanism of flow/surface interaction is not influenced by the aircraft motion. However, the flow spreading and thus the velocity gradient is a function of relative jet velocity. Therefore, the propagation characteristics of the aircraft noise sources can also change. In addition, motion of the source with respect to the observer results in Doppler frequency shift and redirectivity. As the data base

for assessing aircraft motion on the aerodynamic noise is limited; it is not possible to assess this effect on the directivity and spectral distribution of each noise component with any degree of confidence. Tests are being conducted at the Lockheed-Georgia Company using a free-jet anechoic room to evaluate the effect of aircraft motion on jet noise. The EBF test data taken in the anechoic wind tunnel for NASA Lewis Research Center during last year (1974) are still being analyzed and are not now available for incorporation in this program. However, the preliminary results of EBF tests published in reference 1-38 and other test results are used in formulating the analytical model to predict the noise.

3.2.1 Effect of Source Motion (Doppler Frequency Shift)

When a sound source is in motion with respect to an observer, the observed frequency is different from the frequency emitted by the source. This shift in frequency, known as Doppler shift, is a function of the source Mach number and the angle between the source direction and an observer (elevation angle). Mangiarotty and Turner[1-39] have derived the following expression for the Doppler frequency shift of the aircraft noise.

$$D(f) = \frac{f_o}{f_s} = \frac{1}{1 - M_A \cos\theta_A} \tag{23}$$

where f_o = observed frequency

f_s = source frequency

M_A = Mach number of the source (aircraft)

θ_A = angle between the flight path and observer

The Doppler shift, D(f), is shown in Figure 1-24 as a function of θ_A and source Mach number.

For angles θ_A close to 90°, and/or for small aircraft Mach numbers, the Doppler frequency shift is negligible as indicated in this figure. Since the maximum noise of V/STOL aircraft occurs for $\theta_A = 90 \pm 45°$, the change in

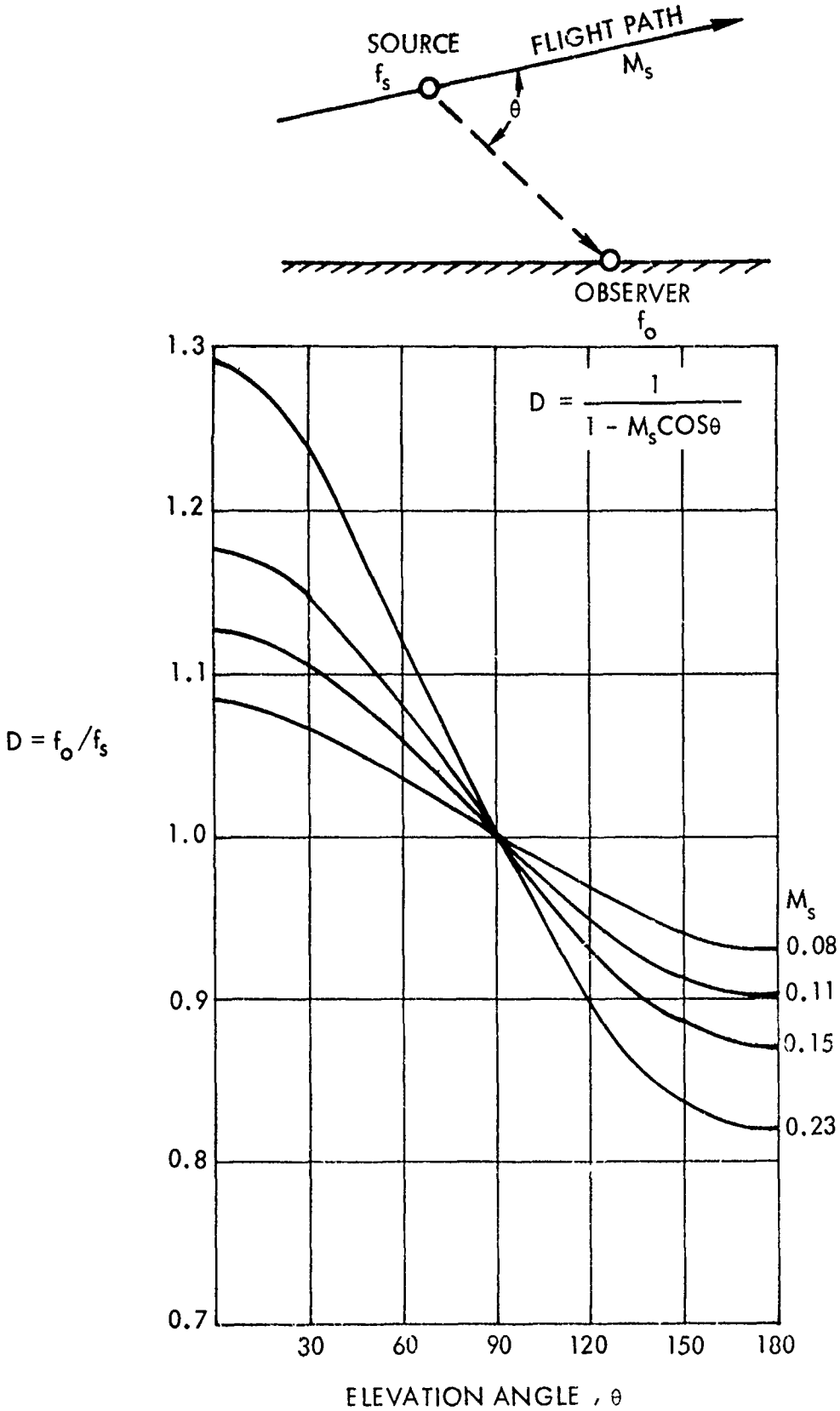

Figure 1-24. Doppler Frequency Shift

frequency due to Doppler shift is negligible. However, this expression is computerized to account for any change in the observed frequency.

3.2.2 Effect of Aircraft Motion on Acoustic Energy

Internally Generated Engine Noise - The experimental results reported by von Glahn and Goodykoontz[1-40] indicate that the internally generated noise is not affected by the aircraft motion. Since the freestream does not influence the fluctuating properties of the flow inside the engine, it is reasonable to assume that the generation mechanism of internally generated engine noise is independent of the aircraft velocity. The change in propagation properties due to change in velocity gradient of the jet flow is assumed to be negligible.

Jet Noise - Jet noise is generated from the turbulent flow developed by the mixing of jet exhaust with the ambient air. Using the similarity relation, it is known that the sound intensity varies as the 8th power of the jet exhaust velocity. It has been customarily assumed that the turbulence intensity depends on the relative velocity of the jet with respect to freestream $(V_J - V_o)$, and thus the sound intensity may be estimated by using the relative velocity in place of jet velocity. Thus, the radiated sound intensity from the jet mixing may be expressed as:

$$I \sim \frac{\rho_a A}{c_a^5} [V_J - V_{A/C}]^8 \tag{24}$$

However, the test results indicate that the reduction in jet noise due to the forward speed is less than this equation indicates. Therefore, an attempt is made to deduce the effect of aircraft motion on jet noise using a global relation between the radiated sound power and the mechanical power of subsonic jets. Lighthill[1-41] has given the acoustic efficiency (relation between the acoustic power and mechanical power) of the jet, in the static cases as:

$$\eta = \frac{\text{Acoustic Power}}{\text{Mechanical Power}} = K \left(\frac{V_J}{c_a}\right)^5 .$$

Since the mechanical power of the jet is independent of forward speed, it is assumed that the acoustic efficiency of the jet varies as $[(V_J - V_a)/c_a]^5$,

and therefore, the radiated sound power of the jet may be written as:

$$\text{Sound Power} \sim \rho_J A_N V_J^3 \cdot \frac{(V_J - V_a)^5}{C_a^5} . \tag{25}$$

The test results of subsonic jet with conical nozzles[1-38, 1-42, 1-43] indicate that the radiated sound intensity in the direction 90° from the inlet axis varies as relative velocity $(V_J - V_{A/C})$ raised to a power between 5 and 6. Therefore, in the prediction program, neglecting the effect of forward speed on directivity and spectral distribution, the incremental SPL to be added to the static results is given as:

$$\Delta dB = 50 \log_{10} \left(1 - \frac{V_a}{V_J}\right) . \tag{26}$$

Even though these results are derived from the subsonic jets with simple conical nozzles, the same equation is also used for nozzles of the other shapes. These results are illustrated in Figure 1-25.

Lift-Augmentation Noise - The noise-generation mechanism of a propulsive lift system is complex and consists of the combination of fluctuating stresses (quadrupole), fluctuating forces (dipole), and fluctuating masses (monopole). It is not possible to evaluate accurately the effect of the freestream velocity (aircraft motion) on the radiated sound from each source of the high-lift system. Therefore, the empirical relation will be derived for each configuration using the limited experimental data and knowledge of the physical phenomena of noise generation and propagation.

Several investigators[1-38, 1-44, 1-45, 1-46] attempted to study experimentally the effect of forward speed on the radiated noise generated by the high-lift systems. The following generalized empirical relation is derived from the data of these references for EBF, USB, and AW:

$$\Delta dB = 10 \log_{10} \left[1 - \frac{V_a}{V_J}\right]^K , \tag{27}$$

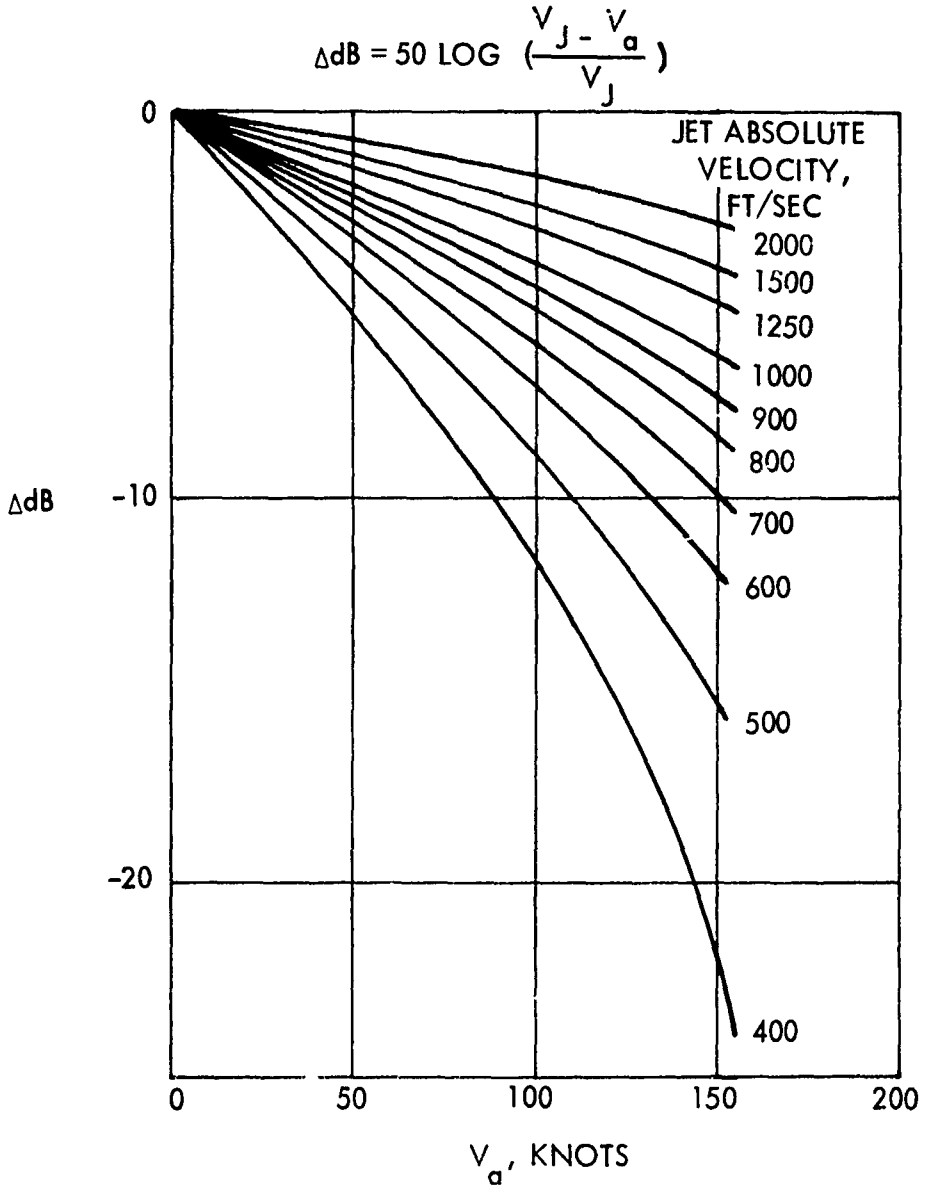

Figure 1-25. Effect of Aircraft Motion on Jet Noise

where K is a function of direction, and high-lift concept. Variation of K with azimuthal angle, ϕ for flyover location is shown in Figure 1-26.

In case of IBF/JF and VT, the equation is modified to account for the deflected angle of the flow. Thus, the relation is given as:

$$\Delta dB = 10 \log_{10} \left[\left(1 - \frac{V_{A/C} \cos\delta_f}{V_J}\right) \right]^K \tag{28}$$

where δ_f = flap angle in the case of IBF and nozzle deflected angle in the case of VT.

The values of K for various V/STOL configurations is given in Table I. The effect of aircraft motion for the vectored thrust concept is shown in Figure 1-27.

3.3 GROUND REFLECTION PROCEDURE

Acoustic measurements taken in the vicinity of the ground (reflecting surface) are distorted as compared with free-field measurements. These effects, discussed by Thomas[1-47] and Miles[1-48], consist of a series of acoustic cancellations and reinforcements in the measured spectra, whether they are the model tests or full-scale flight tests. A generalized method of correcting measured spectra for ground effects is currently being formulated by SAE[1-49]. These are functions of the acoustic impedance of the ground (reflecting surface), the location of the observer with respect to ground and source, source size, and the frequency band width.

The reflection index, N, for a point noise source over a perfectly reflecting plane analyzed in one-third octave bands is taken from reference 1-49 as shown in Figure 1-28. These values are computed from the equation:

$$N_i = 10 \log_{10} \left(1 + \frac{1}{Z^2} + \frac{2}{Z} \frac{\sin\left(\frac{\alpha_i r}{\lambda i}\right)}{\left(\frac{\alpha_i \Delta r}{\lambda i}\right)} \cos\left(\beta \frac{\Delta r}{\lambda i}\right)\right. \tag{29}$$

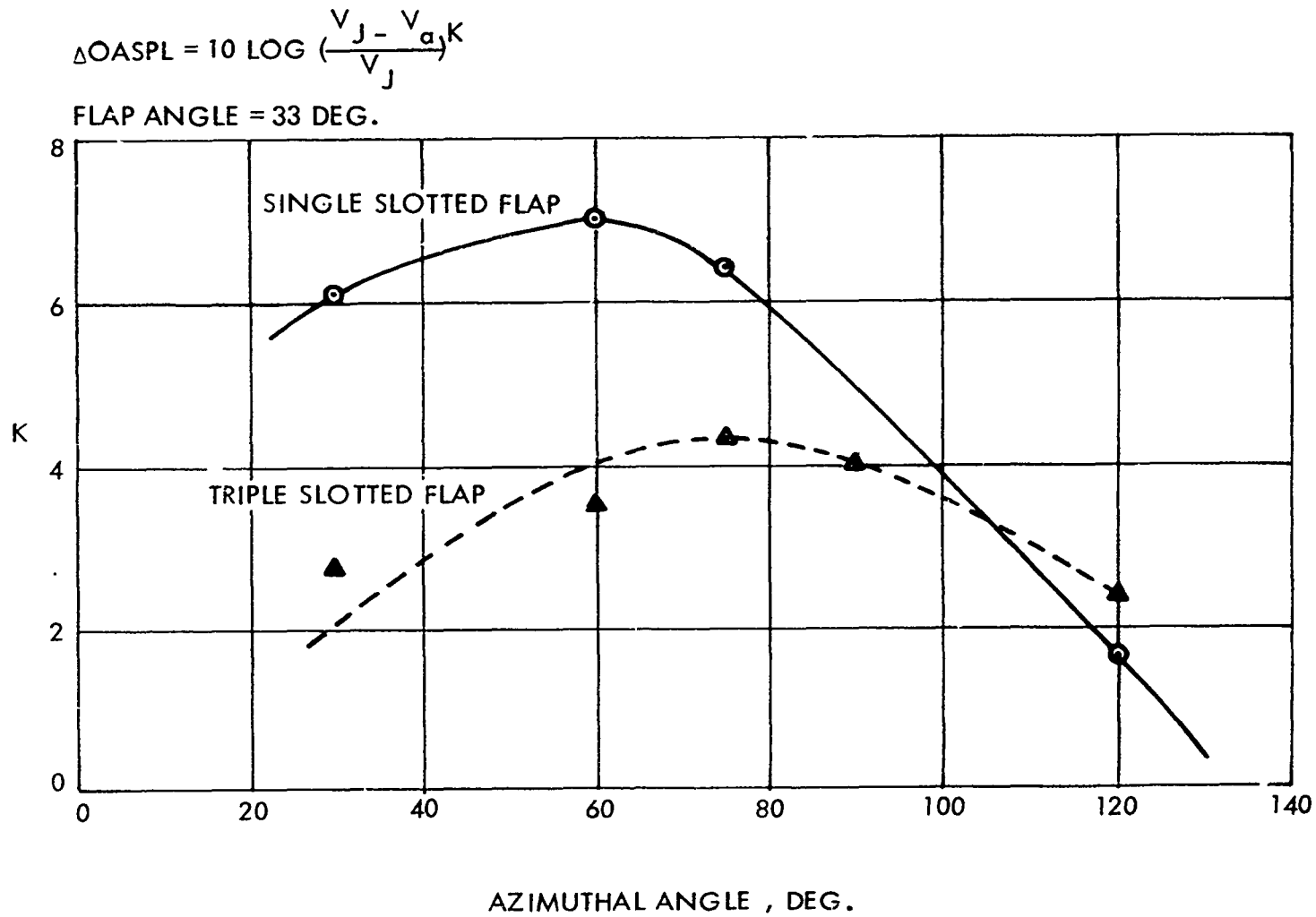

Figure 1-26. Effect of Aircraft Motion on EBF System Noise

TABLE I

RELATIVE AIRSPEED EXPONENTS, k

(θ = 90°)

Configuration	Flyover Plane (ϕ = 90°)	30° Sideline Plane (ϕ = 30°)	0° Sideline Plane (ϕ = 0°)
EBF, Take-off Flaps			
Triple-Slotted Flap	4.0	1.8	-0.8
Double-Slotted Flap	5.05	3.0	0.25
Single-Slotted Flap	6.1	4.2	1.3
USB	1.8	0.8	0
AW (Hardwall with Slot Nozzle)			
Take-off Flaps	1.8	(1.0)	(0)
Landing Flaps	-1.8	(-1.0)	(0)
IBF	5.0	5.0	5.0
VT	5.0	5.0	5.0

$$\Delta dB = 50 \text{ LOG } \frac{V_J - V_a \cos \delta_f}{V_J}$$

CONICAL NOZZLE

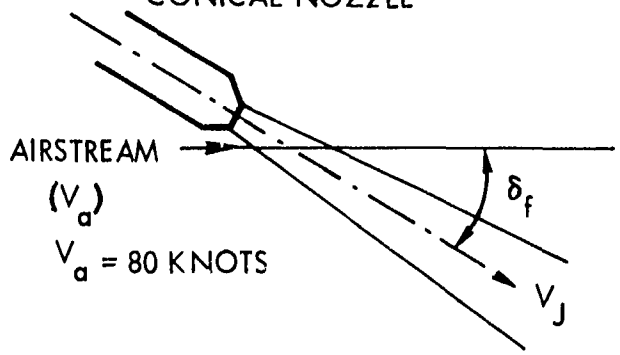

δ_f = JET VECTOR ANGLE WITH REFERENCE TO AIRSTREAM

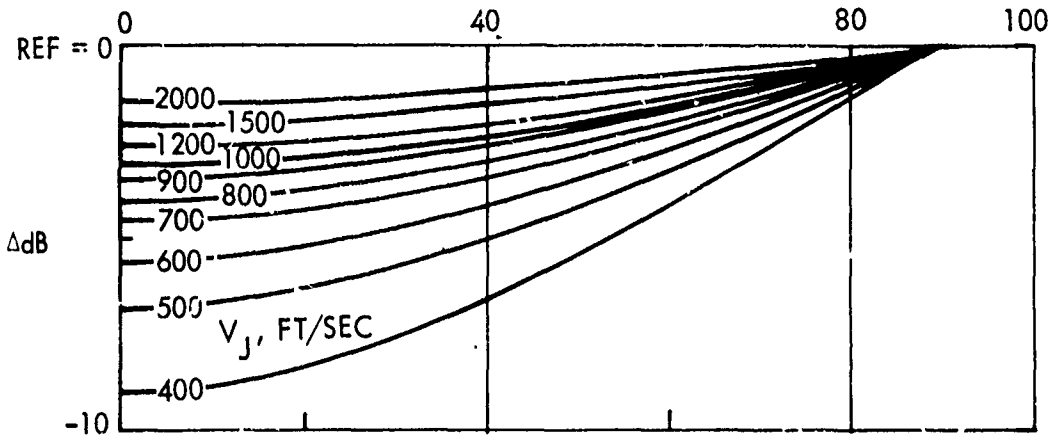

Figure 1-27. Effect of Aircraft Motion on Vectored Thrust Noise

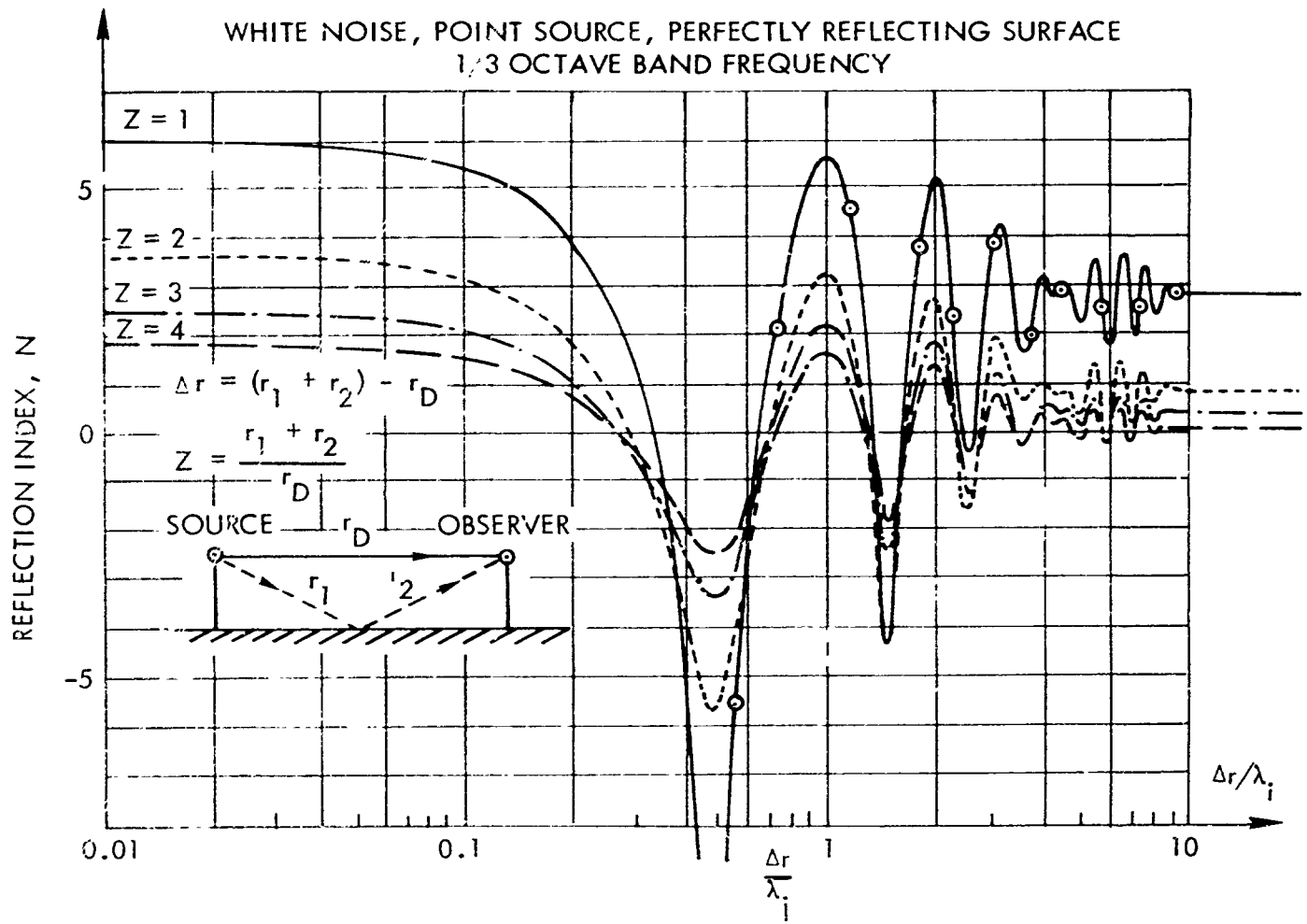

Figure 1-28. Ground Reflections

where

N_i = reflection index for i^{th} one-third-octave band source pressure level, dB

$Z = r_R/r_D$

r_D = length of direct sound ray, ft.

r_R = length of reflected sound ray $(r_{R1} + r_{R2})$, ft.

$r = (r_R - r_D)$, ft.

$\lambda_i = c_a/f_i$ = wave length of the ith one-third-octave band center frequency

c_a = speed of sound

f_i = center frequency of the ith band

$\alpha_i = (\Delta f/2f_i)$

$\beta = 2\pi \sqrt{1 + (\Delta f/2f_i)^2}$

Δf = frequency band width

$\Delta f/f_i$ = 0.231 for one-third-octave band analysis

Figure 1-29 indicates the first few cancellations and reinforcement frequencies as a function of the difference in distance between the direct and reflected wave paths.

For a distributed source in a finite volume, a similar analysis may be conducted by assuming a number of discrete sources, each having the same white-noise characteristics.

Comparisons of theory with experiment, reported in references[1-47, 1-48] indicate that Equation (29) yields very reasonable correction factors for jet and EBF noise. Therefore, in this program, the ground reflections are computed using equation (29) with the assumptions of a perfectly reflected surface and white-noise point source. For the other reflecting surfaces (with different acoustic impedance) the formulation has to be modified.

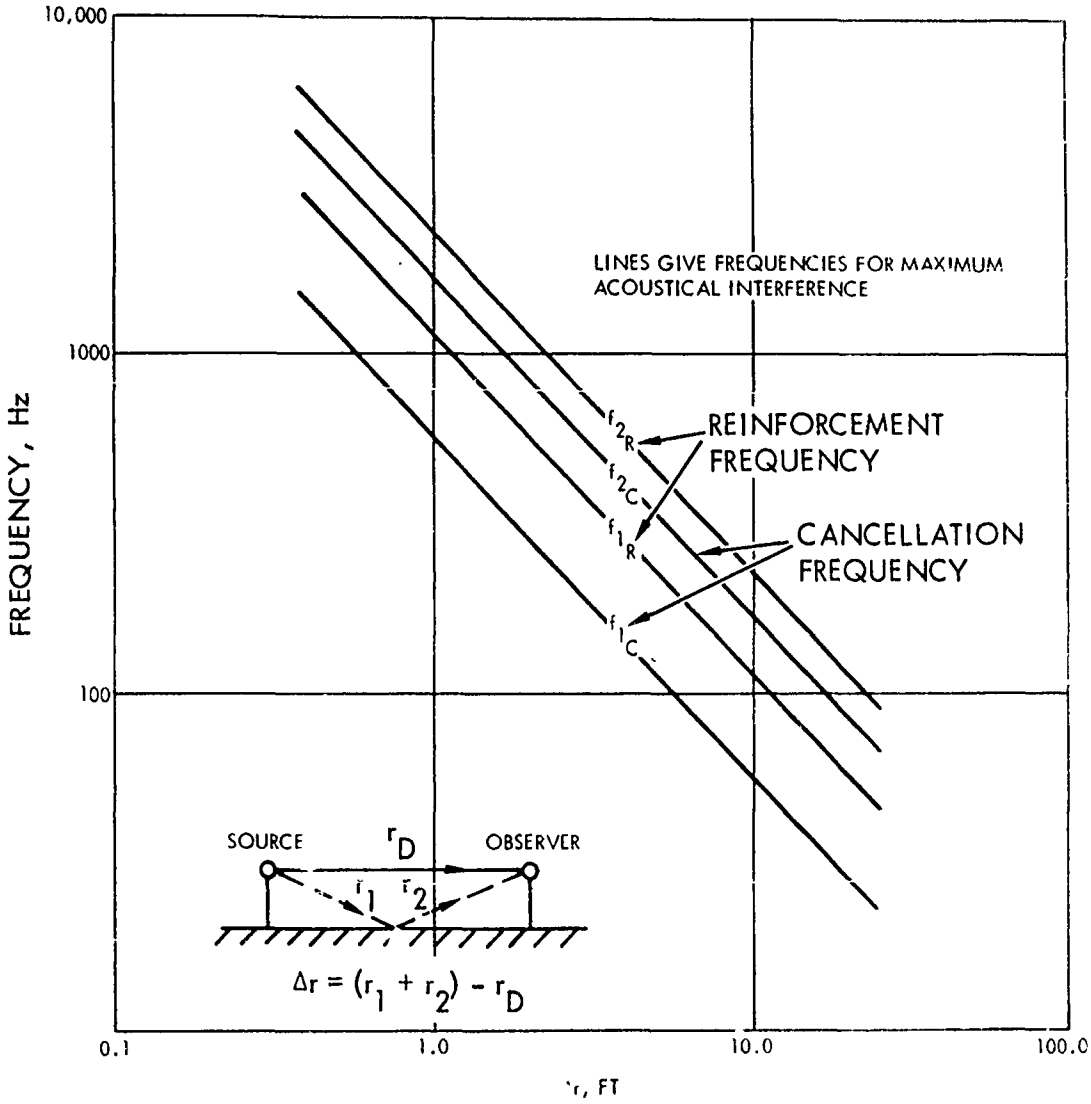

Figure 1-29. Interference Frequencies (Ground Reflection)

3.4 EXTRA GROUND ATTENUATION (EGA)

The presence of open ground terrain influences the characteristics of sound close to the ground propagating in the direction parallel to the ground surface. These effects are known as Extra Ground Attenuation (EGA), and are largely due to the refraction and scatter effect of the inhomogeneities near the ground and the residual ground attenuation. The inhomogeneities are the presence of wind, temperature gradients, and atmospheric turbulence on the boundary of the ground. Reference 1-50 describes a widely accepted industry standard for predicting EGA with the assumption of wind velocity of 10 miles per hour and a thermal gradient of an average day. The EGA contributes mainly for sideline noise with elevation angles of less than about 40 . The attenuation is assumed to be independent of wind direction, and azimuthal angle, equal to that for downwind propagating with a speed of 10 mph. EGA is computed in the computer program using the results presented in Figure 1-30 taken from reference 1-50 for downwind propagating with a speed of 10 mph. Effects of EGA is considered for the aircraft-to-observer distance less than 100 ft.

The ground absorption effect sometimes referred as "ground dip" has been observed in the frequency range of 300 to 600 Hz. The magnitude of this effect depends upon the acoustical impedance of the ground, which could be about 5 dB for distances above 1,000 feet for soft grounds. This effect is negligible if the ground is a perfectly reflecting and, therefore, not included in EGA computation.

3.5 SHIELDING OF SOUND BY AIRCRAFT COMPONENTS

Rigid surfaces can be effective sound barriers for sound sources close to the surface. Since the aerodynamic noise sources of an aircraft are located close to the aircraft, the aircraft components can provide effective shielding in certain directions, although the actual effectiveness of such shielding depends on the location of the sources relative to the structural components. The noise sources of a high-lift system that are most effectively influenced by the shielding phenomena of the aircraft structural components are: (1) aft-radiated engine, (2) jet mixing, (3) impingement, and (4) wall-jet mixing noise. In general, the forward-radiated engine noise is not shielded. For

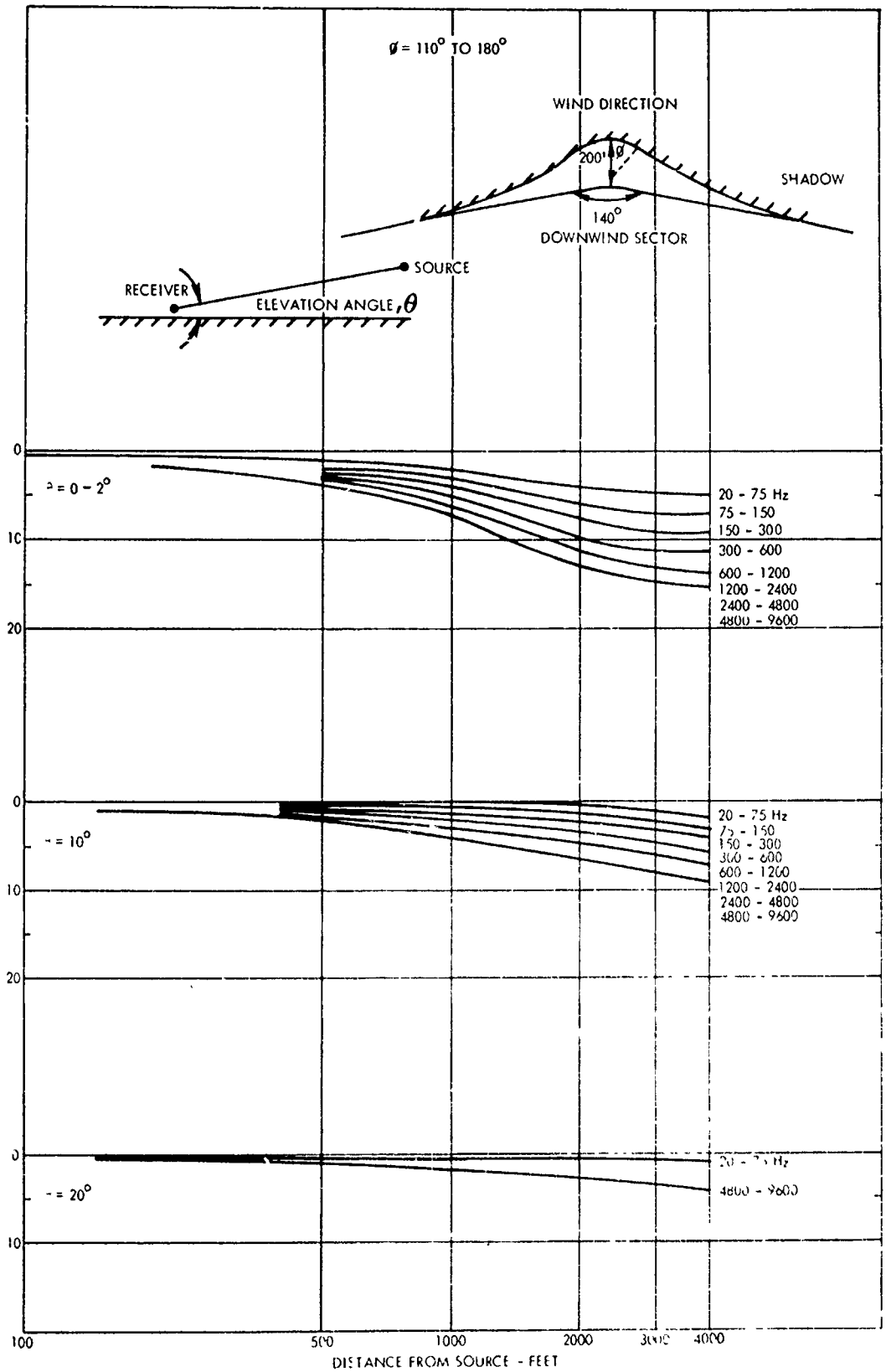

(a) AS A FUNCTION OF FREQUENCY AND ELEVATION ANGLE

Figure 1-30. Extra Ground Attenuation

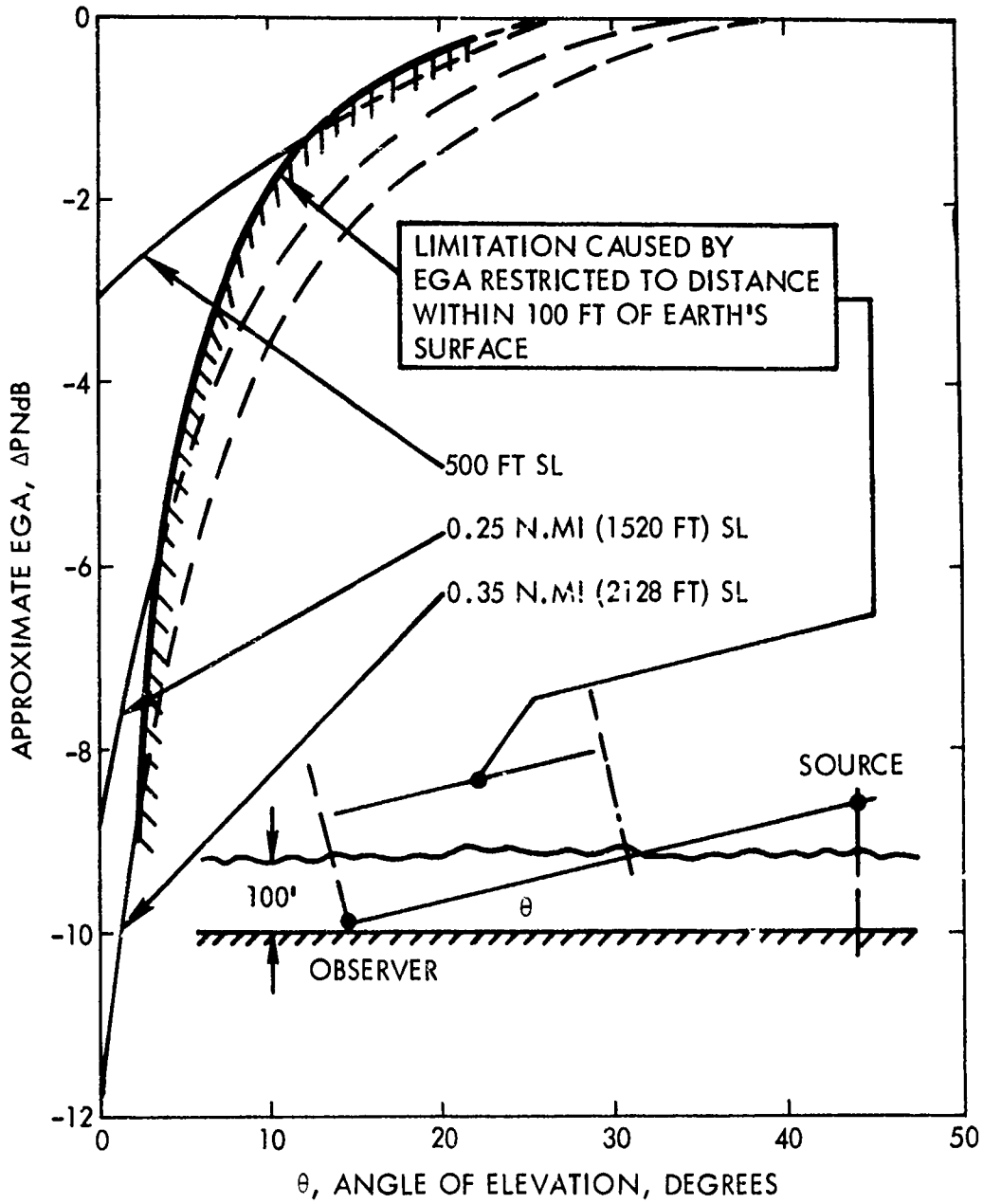

(b) REDUCTION IN PNL AS A FUNCTION OF DISTANCE

Figure 1-30. (Concluded)

the case of multi-engine aircraft, some noise could be shielded by the fuselage and the nacelles.

Feher[1-51] and Wiener[1-52] have adapted optical-diffraction theory to estimate the shielding effect of structural components on sound radiation. Based on these methods, Swift and Tibbetts[1-53] formulated the shielding of aft-radiated engine and jet mixing noise by the wing/flap in the fly-over plane.

In the case of the USB concept, the aft-radiated engine and jet mixing noise sources are located on the wing/flap surface. The reduction in noise levels due to shielding for these sources in the fly-over plane is given by:

$$\Delta dB = 10 \log_{10} (N_F) + 10$$

where $N_F = 2\,[(a+b) - S]/\lambda$, Fresnel number; a, b, and s are defined in Figure 1-31

λ = sound wave length.

The description of directivity and spectral distribution for the flow-surface interaction noise (for example, impingement and wall jet noise) of propulsive-lift systems include the presence of rigid surfaces. Therefore, the shielding is not included separately for these sources.

3.6 NOISE REDUCTION FEATURES

To evaluate the noise reduction possibilities, it is necessary to identify the relative importance of the noise sources and their generation and propagation mechanisms. In the case of V/STOL aircraft, it is very well established that the high-lift noise dominates over the other sources. Several exploratory studies are being conducted at Lockheed and several other organizations to understand the noise characteristics and to develop any feasible noise-suppression techniques. The present state of the art is not advanced enough to develop a method to incorporate a generalized noise reduction method of V/STOL aircraft. However, the possible noise control features for each of the sources and the inclusion of these techniques in the noise-prediction program of each configuration are discussed.

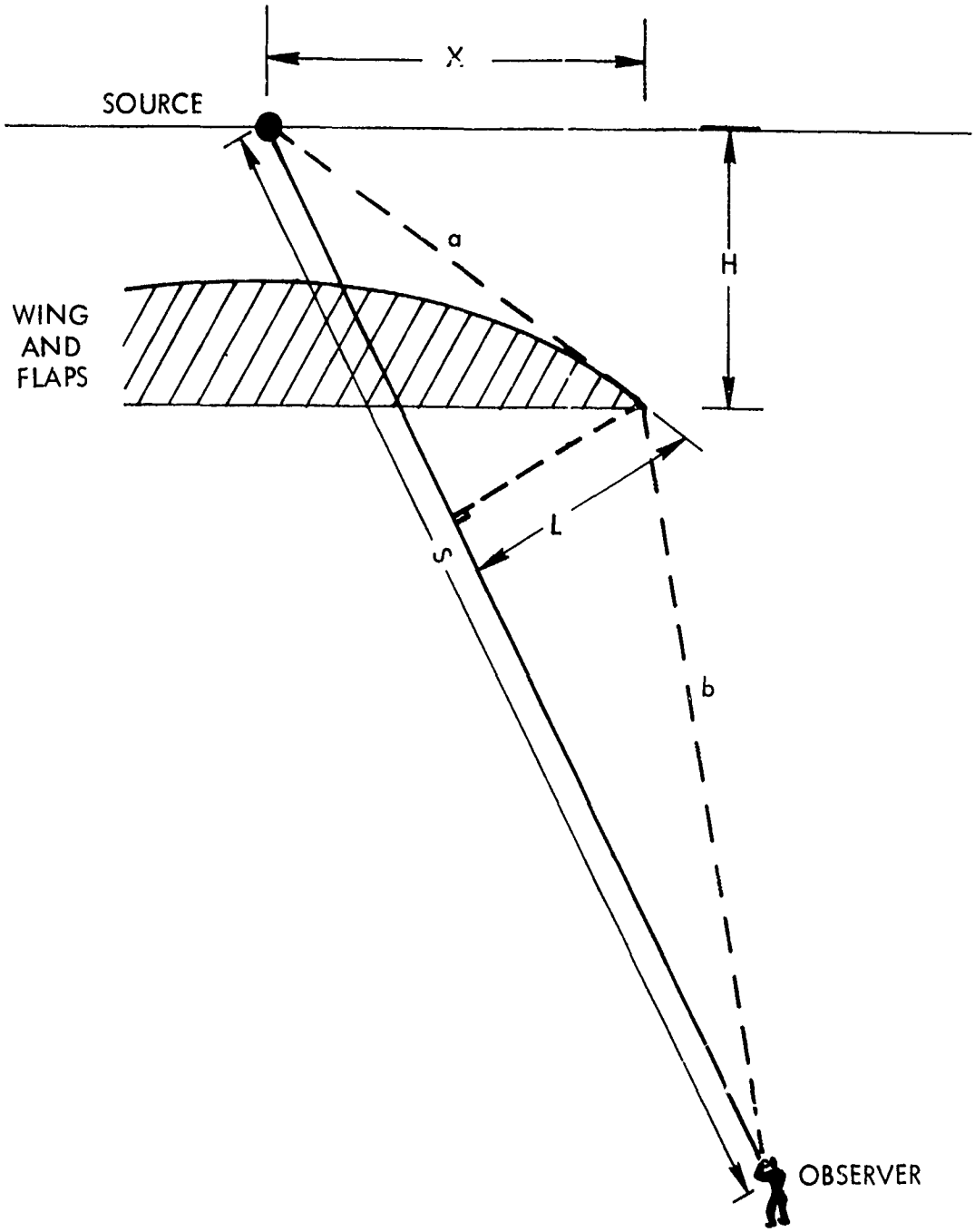

Figure 1-31. Geometry for Wing/Flap Shielding

The best method of reducing jet noise and the high-lift system noise is to reduce the jet velocity. However, the reduction of jet velocity requires that the nozzle exit area be increased to have the same mass flow and thrust, thus calling for larger and heavier powerplants. For cost effectiveness, therefore, noise-control techniques must be adopted to the lift-augmentation system with a minimum performance loss.

3.6.1 Internally Generated Engine Noise

Other than the design of the basic fan, compressor, and turbine, one of the common methods of suppressing this type of noise is by treating the inlet and exhaust system with sound-absorbing materials. Some of the novel liner treatment designs for this purpose are described by Wirt[1-54]. The detailed study of suppression of the engine internal noise is beyond the scope of this program. Therefore, the effect of suppression is added as a reduction in SPL (ΔdB) for the unsuppressed noise sources (fan/compressor, turbine, and core engine).

3.6.2 Jet Mixing Noise

At present, jet noise reduction is achieved by reducing the jet velocity (with an increase in exhaust area) and the use of bypass engines and the multi-lobed or multi-tubed nozzle. In the case of bypass engines, the noise could be minimized by having the velocities of the two streams as close as possible. The use of multi-elements for the nozzle exhaust (tubes or lobes) is effective in reducing the noise at high jet velocities. However, at the low subsonic velocities which are typical in V/STOL takeoff and landing operations, the test results indicate that jet noise actually increases. Although the reasons are still not well known, the tentative explanation is that the noise generated by the interference of turbulence with the nozzle lip and the so-called "tail-pipe noise" increases at low velocities. The use of different nozzle shapes is directly incorporated in the jet-noise prediction program.

3.6.3 Lift-Augmentation Noise

Five methods are currently used for suppressing lift-augmentation or flow-surface interaction noise. (1) Use of a porous or compliant material at the

trailing edge (trailing edge treatment), (2) having a secondary flow at the trailing edge (trailing edge blowing, (3) use of different numbers of slots in the flap, (4) use of different nozzle shapes, and (5) ejector treatment in the case of the augmentor wing.

Externally Blown Flap and Upper Surface Blown Flap - *Trailing-Edge Treatment and Trailing-Edge Blowing* - Hyden *et al*[1-55] have found from their preliminary experimental investigations that the use of porous material in the place of a trailing-edge section and modification of flow field by introducing a secondary flow at the trailing edge offer potential for reducing the radiated EBF and USB noise. However, they have neither evaluated the performance characteristics nor optimized the modifications of the trailing edge. Pennock *et al*[1-38] conducted static tests using a large-scale model of EBF and found that a moderate amount of noise reduction could be achieved either by replacing part of the last flap with a perforated plate or a compliant material, or by using secondary blowing at the trailing edge. Using these results, empirical relationships are established for optimum noise reduction in terms of PNL:

$$PNL = -1\ (0.5 + \sin\phi) \qquad \text{for EBF}$$

$$PNL = -2\ (0.5 + \sin\phi) \qquad \text{for USB}$$

and it is assumed to be independent of azimuthal angle, θ.

Noise reduction obtained with the secondary blowing at the trailing edge is a function of the height of the slot and the velocity of the secondary flow, as illustrated in Figure 1-32. However, at very high secondary flow velocity (>400 fps) the noise generated by the secondary flow itself becomes dominant. Empirical relationships for the maximum (optimum) noise reduction are derived using the experimental data from references 1-35 and 1-56.

$$PNL = -2h \sin\phi \qquad \text{for EBF}$$

$$PNL = -4h \sin\phi \qquad \text{for USB}$$

where h is slot thickness in inches.

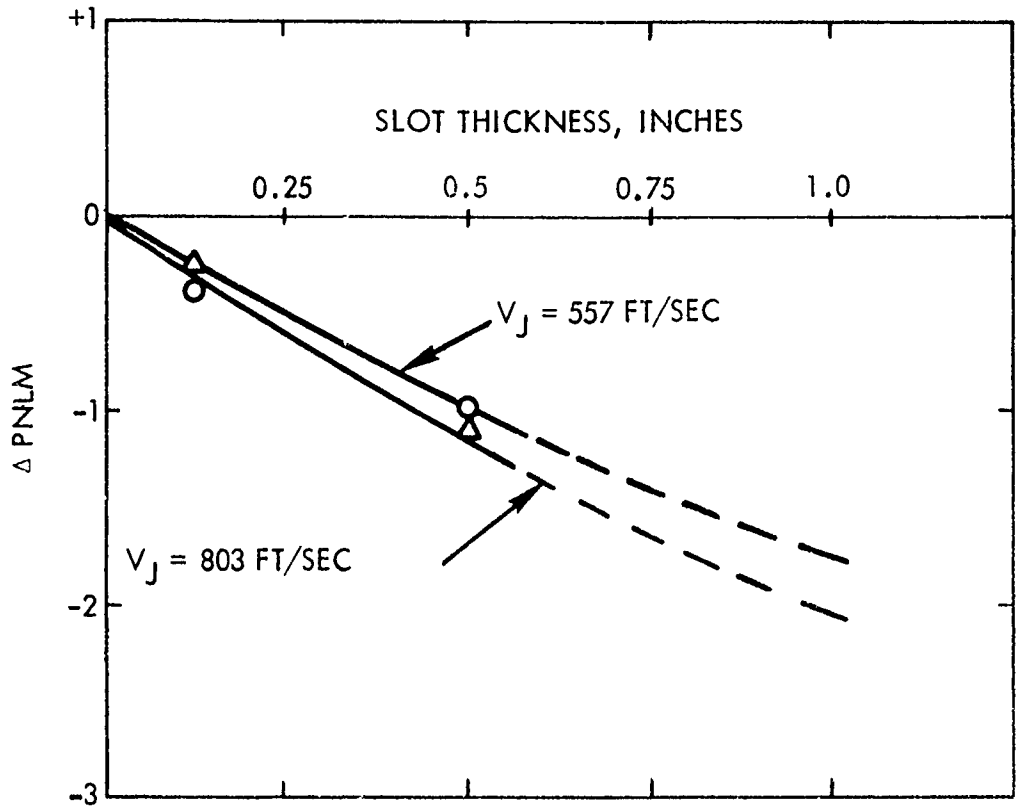

Figure 1-32. Noise Reduction Due to Trailing Edge Blowing for EBF

Effect of Number of Flap Segments - In the case of the EBF, it is found that an increase in flap segments increases the radiated noise levels. From the experimental results of reference 1-38, the following expression is derived for the change in noise levels as a function of jet velocity and the number of flap segments:

$$PNL = -\frac{804}{V_J}(3 - S) \cdot \sin\phi$$

where V_J = jet velocity in ft/sec.

S = number of slots.

Use of Multi-element Nozzle - Replacing a single element (circular or rectangular) nozzle with a multi-element nozzle reduces the impingement velocity in the case of EBF, and thus the flow-surface interaction noise may be reduced. However, at low velocities, it is experimentally found that the EBF noise cannot be reduced by this technique. Replacement of a circular nozzle by a multi-element nozzle and an acoustically treated ejector is found to be an effective way to reduce the noise without any performance penalty, as indicated in references 1-57, 1-58, and 1-59. Using these data, a maximum noise reduction of about 6 PNdB in the flyover plane and 3 PNdB in the sideline plane may be obtained.

Augmentor Wing - A basic design of Augmentor Wing with a slot nozzle and hard-wall ejector is excessively noisy. Extensive experimental noise control studies of AW have been reported in references 1-10 and 1-11, and the important features of noise reductions are summarized in Figure 1-33. High noise reductions are obtained by: (1) replacing the slot nozzle by multi-element nozzles and (2) acoustically lining the internal walls of the ejector. Since the actual noise reductions are sensitive to detail design, it is not possible to generalize concerning the actual results which may be expected.

Internally Blown Flap and Vectored Thrust Configurations - No general trends or novel methods are used to reduce the noise generated by these configuration and flow parameters which are included in the basic noise prediction model.

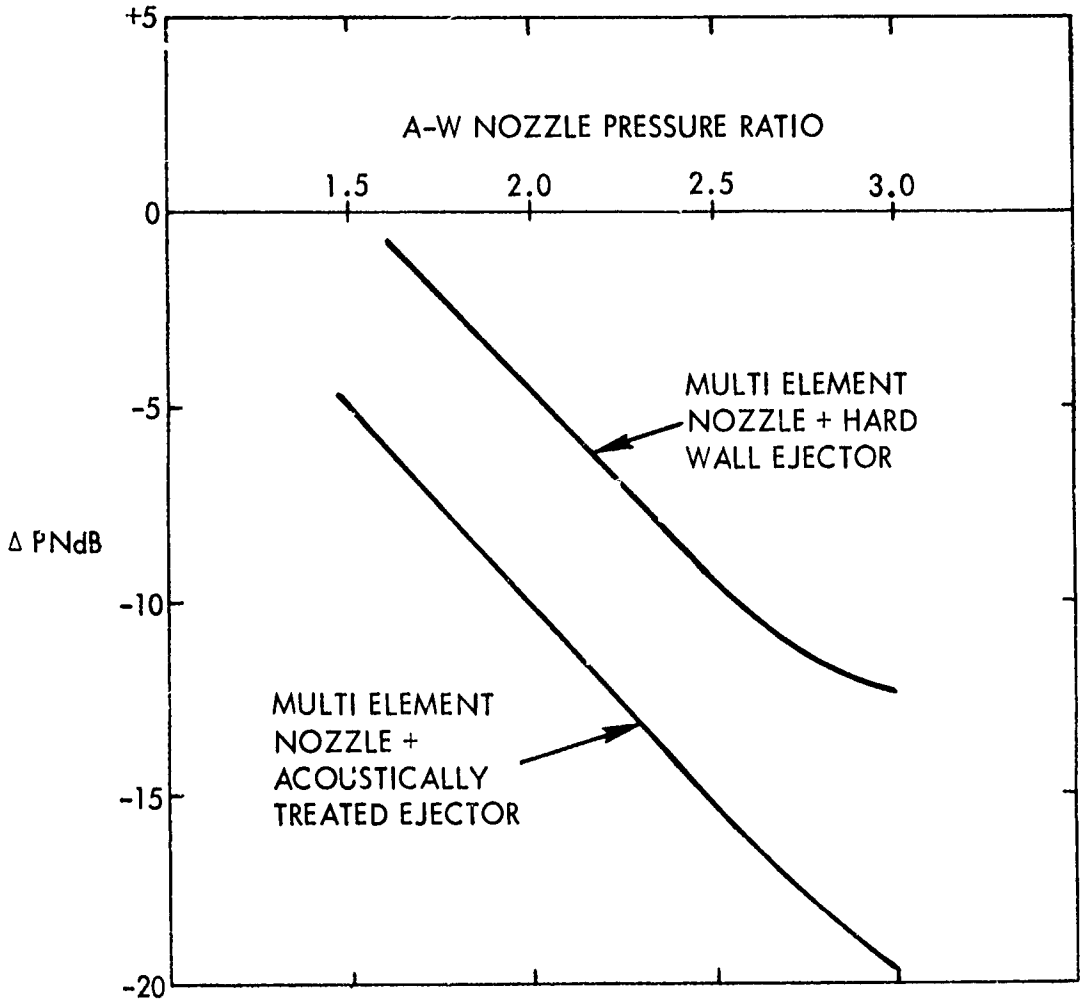

Figure 1-33. Noise Reduction for Augmentor Wing

REFERENCES

1-1. O'Keefe, J. V.; and Kelley, G. S.: "Design Integration and Noise Studies for Jet STOL Aircraft" Final Report, Volume I - Program Summary, NASA CR-114283, May 1972.

1-2. Lockheed-Georgia Co., "Quiet Short-Haul Research Aircraft Design Study" Final Report, NASA CR-137554, Sept. 1974.

1-3. Searle, N., "Acoustic Investigation of a Hybrid Propulsion Lift System" ASME Paper No. 74-WA/Aero-3, Dec. 1974.

1-4. Burdsall, E. A.; Urban, R. H: "Far-Compressor Noise: Prediction, Research and Reduction Studies," FAA Report, FA-RD-71-73, Feb. 1971.

1-5. General Electric, "Advance Transport Technology: Mid-Term Report," October 6, 1971.

1-6. Kazin, S. B. and Matta, R. K.: "Turbine Noise Generation, Reduction and Prediction," AIAA Paper No. 75-449, March 1975.

1-7. Bushell, K. W.: "Survey of Low Velocity and Coaxial Jet Noise with Application to Prediction," *Journal of Sound and Vibration* (1971) 18(2), 271-282.

1-8. Crighton, D. G.: "The Excess Noise Field of Subsonic Jets," *Journal of Fluid Mechanics* (1972), Vol. 56, Part 4, p. 683-694.

1-9. Lockheed-Georgia Co., "The Generation and Radiation of Supersonic Jet Noise," Lockheed-Georgia Engineering Report No. LG74ER0010, Feb. 1974.

1-10. Tester, B. J. and Morfey, C. L.: "Developments in Jet Noise Modeling - Theoretical Predictions and Comparisons with Measured Data," AIAA Paper No. 75-477, March 1975.

1-11. Stone, J. R.: "Interim Prediction Method for Jet Noise," NASA TMX-71618, 1975.

1-12. Olsen, W. O.; Miles, J. H.; and Dorsch, R. G.: "Noise Generated by Impingement of a Jet Upon a Large Flat Board," NASA TN-D-7075, Dec. 1972.

1-13. Reddy, N. N. and Yu, J. C.: "Experimental Investigation of Radiated Acoustic Power of an Externally Blown Flap," Paper presented at the 85th Acoustical Society of America Meeting, April 10-13, 1973, Boston, Mass.

1-14. von Glahn, V. H.; Groesbeck, D. E.; and Huff, R. G.: "Peak Axial-Velocity Decay with Single and Multi-Element Nozzles," AIAA Paper No. 72-48, Jan. 1972 (NASA TMX-67979).

1-15. Bradbury, L. J. S.: "Simple Expressions for the Spread of Turbulent Jets," *The Aeronautical Quarterly*, May 1967, p. 133-142.

1-16. Reddy, N. N. and Brown, W. H.: "Acoustic Characteristics of an Upper-Surface Blowing Concept of Power-Lift System," AIAA Paper No. 75-204, Jan. 1975.

1-17. Reddy, N. N.: "Propulsive-Lift Noise of an Upper Surface Blown Flap Configuration," AIAA Paper No. 75-470, March 1975.

1-18. Hayden, R. E.: "Noise from Interaction of Flow with Rigid Surfaces: A Review of Current Status of Prediction Techniques," NASA CR-2126, 1972.

1-19. Grosche, F. R.: "On the Generation of Sound Resulting from the Passage of Turbulent Air Jet Over a Flat Plate of Finite Dimensions," RAE Library Translation 1460, translated by D. G. Randall, Oct. 1970.

1-20. Ffowcs Williams, J. E. and Hall, L. H.: "Aerodynamic Sound Generated by Turbulent Flow in the Vicinity of Scattering Half Plane," *Journal of Fluid Mechanics*, Vol. 40, Part 4, 1970, p. 657-670.

1-21. Powell, A.: "Aerodynamic Noise and Plane Boundary," *Journal of Acoustical Society of America*, Vol. 32, No. 8, 1960.

1-22. Yu, J. C.; Reddy, N. N.; and Whitesides, J. L. Jr.: "Noise and Flow Characteristics of an Externally Blown Flap," Second Interagency Symposium on University Research in Transportation Noise, North Carolina State University, June 5-7, 1974.

1-23. Schrecker, G. O. and Maus, J. R.: "Noise Characteristics of Jet Flap Exhaust Flows," NASA CR- , 1972.

1-24. Dorsch. R. G. *et al*: "Blown Flap Noise Research," AIAA Paper No. 71-745, June 1971 (NASA TMX-67850).

1-25. Gibson, F. W.: "Noise Measurement Studies of Several Model Jet-Augmented Lift Systems," NASA TND-6710, 1972.

1-26. Healy, G. J., "Measurement and Analysis of Aircraft Far-Field Aerodynamic Noise," NASA CR-2377, Dec. 1974.

1-27. Healy, G. J.: "Aircraft Far-Field Aerodynamic Noise — Its Measurement and Prediction," AIAA Paper No. 75-486, March 1975.

1-28. Gibson, J. S.: "Non-Engine Aerodynamic Noise Investigation of a Large Aircraft," NASA CR-2378, Oct. 1974.

1-29. Gibson, J. S.: "Recent Developments at the Ultimate Noise Barrier," ICAS Paper No. 74-59, Aug. 1974.

1-30. Smith, D. L.; Paxon, R. P.; Talmadge, R. D.; and Holtz, E. R.: Measurements of the Radiated Noise from Sailplanes," AFFDL TM-70-3-FDDA, July 1970.

1-31. Hardin, J. C.; Fratello, D. J.; Hayden, R. E.; and Kadman, Y.: "Prediction of Airframe Noise," NASA TND-7821, 1975.

1-32. Revell, J. D.: "The Calculation of Aerodynamic Noise Generated by Large Aircraft at Landing Approach," Paper JJ9, 87th Acoustical Society of America Meeting, April 1974.

1-33. Revell, J. D.: "Induced Drag Effects on Airframe Noise," AIAA Paper No. 75-487, March 1975.

1-34. Marrow, D. L. and Passage, R. W.: "Acoustic Survey of AiResearch Model GTCP36-4," AiResearch Report No. GT-7618-R, Dec. 1965.

1-35. AiResearch and Lockheed-Georgia Co., "Sound Pressure Level, AiResearch Model GTCP165-1 APU." Report No. GT-8041-R8, Feb. 1968.

1-36. Standard Values of Atmospheric Absorption as a Function of Temperature and Humidity for Use in Evaluating Aircraft Flyover Noise, Aerospace Recommended Practice No. 866, Society of Automatic Engineers, Aug. 31, 1964.

1-37. FAR Part 3b, "Noise Standards: Aircraft Type and Airworthiness Certification," Federal Aviation Regulation, Vol. III, Nov. 1969.

1-38. Pennock, A. P.; Swift, G.; and Marbert, J. A.: "Static and Wind Tunnel Model Tests for the Development of Externally Blown Flap Noise Reduction Technique; NASA CR-134675 (Lockheed-Georgia LG74ER0170), Feb. 1975.

1-39. Mangiarotty, R. A. and Turner, B. A.: "Wave Radiation Doppler Effect Correction of a Source, Observer and Surrounding Medium," *Journal of Sound and Vibration*, Vol. 6, p. 110-116, 1967.

1-40. von Glahn, U. and Goodykoontz, J., "Forward Velocity Effects on Jet Noise with Dominant Internal Noise Sources," NASA TMX-71438.

1-41. Lighthill, M. J.: "Jet Noise," *AIAA Journal*, Vol. 1, No. 7, July 1963.

1-42. von Glahn, U.; Groesbeck, D.; and Goodykoontz, J.: "Velocity Decay and Acoustic Characteristics of Various Nozzle Geometrics in Forward Flight," AIAA Paper No. 73-629.

1-43. Cocking, B. J. and Bryce, W. D.: "An Investigation of the Noise of Cold Air Jets Under Simulated Flight Conditions," National Gas Turbine Establishment Report No. R.334, 1974.

1-44. Goodykoontz, J.: "EBF Noise Tests — Forward Velocity Effects," Short-Haul Aircraft Propulsion Technology, NASA-Lewis Research Center, April 1973.

1-45. Dorsch, R. G.; Clark, B. J.; and Reshotko, M.: "Interim Prediction for EBF Noise," NASA TMX- (To be published in 1974).

1-46. Falaraski, M. D. *et al*, "Comparison of the Acoustic Characteristics of Large-Scale Models of Several Propulsive Lift Concepts," AIAA Paper No. 74-1094.

1-47. Thomas, P.: "Acoustic Interference by Reflection Application to the Sound Pressure Spectrum of Jets," NASA TTF-14, 185, March 1972.

1-48. Miles, J. H.: "Rational Function Representation of Flap Noise Spectra Including Correction for Reflection Effects," NASA TMX-71502, Jan. 1974.

1-49. SAE "Acoustic Effects Produced by a Reflecting Plane," Draft.

1-50. SAE AIR 923, "Method for Calculating the Attenuation of Aircraft Ground-to-Ground Noise Propagation During Takeoff and Landing," Society of Automotive Engineers, August 1966.

1-51. R. O. Feher, Proc. Ann. Nat. Noise Abatement Symposium, 1951, p. 98.

1-52. Wiener, F. M., "Sound Propagation Outdoors," Chapt. IX, p. 193, *Noise Reduction*, L. L. Beranek, Editor, 1960.

1-53. Swift, G. and Tibbets, J. G.: "Wing Shielding," Lockheed-Georgia Co., Interdepartmental Communication E-47-064-73, July 1973 (Proprietary).

1-54. Wirt, L. S.: "Sound-Absorptive Materials to Meet Special Requirements," *Journal of Acoustical Society of America*, 57(1), January 1975.

1-55. Hayden, R. E. *et al*, "A Preliminary Evaluation of Noise Prediction Potential for the Upper Surface Blown Flap," NASA CR- , 1972 (BBN Report No. 2478).

1-56. Cole, T. W. and Rathbun, E. A.: "Small Scale Model Static Acoustic Investigation of Hybrid High Lift Systems Combining Upper Surface Blowing with the Internally Blown Flap," NASA CR114757, July 1974.

1-57. Samanich, W. E., *et al*: "Effect of Exhaust Nozzle Configuration on Aerodynamic and Acoustic Performance of an Externally Blown Flap System with A Quiet 6:1 Bypass Ratio Engine," NASA TMX-71466, Nov. 1973.

1-58. Goodykoontz, J., *et al*: "Mixer Nozzle-Externally Blown Flap Noise Tests," NASA TMX-68021, Feb. 1972.

1-59. Putnam, T. W.; Lasagna, P. L.: "Externally Blown Flap Impingement Noise," AIAA Paper No. 72-664, June 1972.

1-60. O'Keefe, J. V.; Kelley, G. S.: "Design Integration and Noise Studies for Jet STOL Aircraft," NASA CR-114283, May 1972.

1-61. Campbell, J. M., *et al*: "Noise Suppression of Improved Augmentors for Jet STOL Aircraft," NASA CR-114534, January 1973.

PART II

DESCRIPTION AND USE OF COMPUTER PROGRAM

by

D. F. Blakney

J. G. Tibbetts

N. N. Reddy

This is a two-part report. The first part consists of Sections 1 - 3 describing the analyses and analytical model for prediction of V/STOL noise. The second part consists of Sections 4 - 6 describing the development and use of the V/STOL noise prediction program.

PRECEDING PAGE BLANK NOT FILMED

TABLE OF CONTENTS

	Page
LIST OF FIGURES	2-iii
4. NOISE PREDICTION PROGRAM DESCRIPTION	2-1
4.1 General Description	2-1
4.1.1 Program Options	2-2
4.1.2 Input Parameters	2-4
4.1.3 Recommended Subroutine Combinations	2-16
4.2 STOLPROG - Main Program	2-18
4.3 Source Prediction Programs	2-27
4.3.1 AERO - Airframe Aerodynamic Noise	2-28
4.3.2 FAN - Fan Noise	2-31
4.3.3 TURBNE - Turbine Noise	2-37
4.3.4 JET - Jet Exhaust Noise	2-42
4.3.5 EXCESS - Excess Engine Noise	2-53
4.3.6 AUGWNG - Augmentor Wing Noise	2-58
4.3.7 WNGJET - Wing Jet Noise	2-63
4.3.8 IMPING - Impingement Noise	2-69
4.3.9 WALJET - Wall Jet Noise	2-79
4.3.10 WAKE - Trailing Edge Wake Noise	2-88
4.3.11 TRAIL - Trailing Edge Noise	2-96
4.3.12 APU - Auxiliary Power Unit Noise	2-104
4.4 Additional Subroutines	2-106
4.4.1 EGA - Extra Ground Attenuation	2-107
4.4.2 GRE - Ground Reflection Effect	2-111
4.4.3 SHIELD - Shielding from Aircraft Components	2-114
4.4.4 FWDSPD - Forward Speed Effects on Level	2-116
4.4.5 DOPLER - Frequency Shift Due to Forward Speed	2-119
4.4.6 REDUCE - Noise Reduction Features	2-122
4.4.7 PNLREV - Calculation of Perceived Noise Level	2-126
4.4.8 TONE - Calculation of Tone Corrected PNL	2-127
4.4.9 GIRC - One Independent Variable Table Interpolation	2-128
4.4.10 DTAB2 - Two Independent Variable Table Interpolations	2-129

TABLE OF CONTENTS (Continued)

Page

5. MACHINE REQUIREMENTS 2-130
   5.1 Operating System 2-130
   5.2 Resource Estimates 2-130

6. DIAGNOSTICS 2-131

LIST OF FIGURES

Figure No.	Title	Page
2-1	Logic Diagram for V/STOL Noise Prediction	2-3
2-2	High-Lift System Configurations	2-6
2-3	Flight Path Geometry	2-10
2-4	Nozzle Configurations	2-12
2-5	Recommended Subroutine Combinations	2-17
2-6	STOLPROG Flow Chart	2-20
2-7	AERO Flow Chart	2-29
2-8	Shielding Geometry	2-32
2-9	FAN Flow Chart	2-34
2-10	TURBNE Flow Chart	2-39
2-11	JET Flow Chart	2-45
2-12	EXCESS Flow Chart	2-55
2-13	AUGWNG Flow Chart	2-60
2-14	WNGJET Flow Chart	2-65
2-15	High-Lift System Geometry Schematic	2-70
2-16	IMPING Flow Chart	2-72
2-17	Flow Geometry Schematic	2-80
2-18	WALJET Flow Chart	2-82
2-19	WAKE Flow Chart	2-90
2-20	TRAIL Flow Chart	2-97
2-21	APU Flow Chart	2-105
2-22	EGA Geometry	2-108
2-23	EGA Flow Chart	2-109
2-24	GRE Flow Chart	2-112
2-25	SHIELD Flow Chart	2-115

LIST OF FIGURES (Continued)

Figure No.	Title	Page
2-26	FWDSPD Flow Chart	2-117
2-27	DOPLER Flow Chart	2-120
2-28	REDUCE Flow Chart	2-124

4. NOISE PREDICTION PROGRAM DESCRIPTION

The following subsections will describe the computer program developed to predict the noise generated by V/STOL aircraft. They present detailed flow charts of each program, along with the descriptions which include the required input and the applicable limitations.

4.1 GENERAL DESCRIPTION

This program predicts the noise generated on takeoff or approach by six powered-lift systems:

(1) Vectored Thrust (VT)
(2) Externally Blown Flap (EBF)
(3) Upper Surface Blowing (USB)
(4) Internally Blown Flap (IBF/BLC and IBF/JF)
(5) Augmentor Wing (AW)
(6) Hybrid System (Hybrid)

The program consists of a main control program and 22 subroutines. The noise from each source defined for V/STOL aircraft is predicted by a separate subroutine. The following subroutines have been developed to predict the radiated noise from 12 different sources:

(1) AERO - predicts airframe aerodynamic noise
(2) FAN - predicts single stage fan noise
(3) TURBNE - predicts engine turbine noise
(4) JET - predicts jet mixing noise
(5) EXCESS - predicts the excess engine noise (core)
(6) AUGWNG - predicts noise of complete augmentor wing high lift system
(7) WNGJET - predicts jet mixing noise from wing slot nozzle
(8) IMPING - predicts noise from impingement of jet flow on wing flap surface
(9) WALJET - predicts noise from jet flow over surface of wing/flaps
(10) WAKE - predicts noise from trailing-edge wake
(11) TRAIL - predicts trailing-edge noise
(12) APU - predicts noise from Auxiliary Power Unit (PNL only)

In addition, 10 other subroutines calculate the propagation effects or noise reduction, or they perform functions necessary to the prediction procedures:

(1) EGA - calculates spectral effect of extra ground attenuation
(2) GRE - calculates spectral effect of ground reflection
(3) SHIELD - calculates spectral effect of wing shielding
(4) FWDSPD - calculates total effect (ΔPNdB) on noise level of aircraft forward motion
(5) DOPLER - shifts spectrum to account for Doppler frequency shift due to motion of the source
(6) REDUCE - determines total effect (ΔPNdB) of noise reduction features discussed in following sections
(7) PNLREV - calculates perceived noise level (PNL) from a 1/3 octave band spectrum
(8) TONE - calculates tone corrections to PNL from a 1/3 octave band spectrum
(9) GIRC - table interpolation routine for single independent variable tables
(10) DTAB2 - table interpolation routine for tables with two independent variables.

The main program (STOLPROG) and the 22 subroutines listed above form a unique prediction tool for use on V/STOL aircraft. The module concept used, with each source and effect accounted for in a separate subroutine, allows for the future updating of technology for individual elements without a major rewrite of the entire prediction program.

The logic diagram shown in Figure 2-1 gives a macroscopic view of the program operation.

4.1.1 Program Options

As shown in Figure 2-1, the program has three main options:

(1) Predict noise for a fixed aircraft position and a fixed observer position.

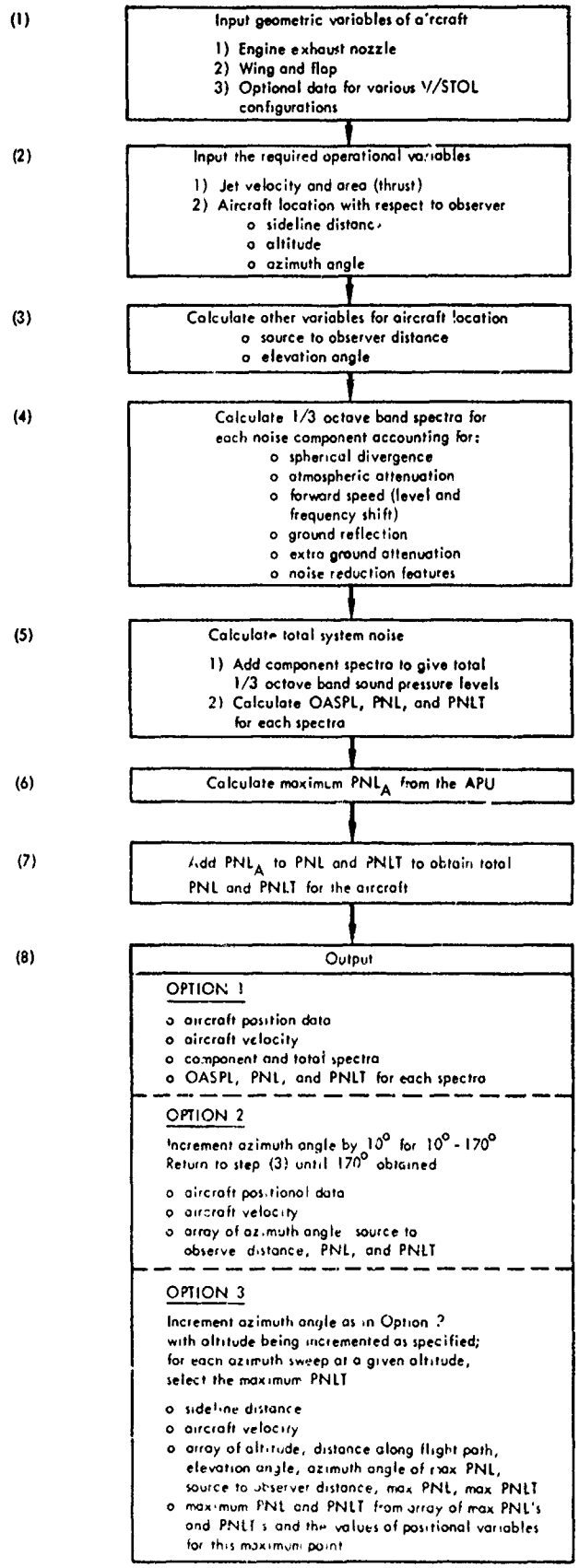

Figure 2-1. Logic Diagram for V/STOL Noise Prediction

(2) Predict noise for a fixed aircraft position and 17 observer locations along the sideline with an azimuth angle range from 10° to 170°.

(3) Predict maximum noise during flight profile segment.

The output for each option is also described in Figure 2-1 and exemplified in the sample cases presented in Appendix A.

The aircraft operational parameters (such as nozzle velocity and flap angle) must remain constant during the flight profile described for option 3. For segmented takeoffs or approaches, each segment must be a separate program execution.

4.1.2 Input Parameters

The required input parameters for the program are presented below. Each line of variables represents one card image. Some parameters are read only when certain program options are used. These optional inputs are also shown with the options which require them.

|TITLE|

|NOPTS|NOPTG|NENG|

|SLDIST|ALT|AZMANG|VAC|FLTANG|

If NOPTG = 3 |NALT|ALTINC|STDIST|

|NK(1)|NK(2)|NK(3)|NK(4)|NK(5)|NK(6)|NK(7)|NK(8)|NK(9)|NK(10)|NK(11)|NK(12)|

|ALPHA1|X1|Y1|

|FLAP1|FLAP2|FLAP3|FLPAG1|FLPAG2|FLPAG3|

If NK(4) = 1

|NOPTJ|

If NOPTJ = 1 or 3 |DPLUG|DPRIM|VJPRIM|TTPRIM|ANGNOZ|

If NOPTJ = 3 |DANIN|DANOUT|VJSEC|TTSEC|

If NOPTJ = 2 |HNOZ|WNOZ|VJPRIM|TTPRIM|ANGNOZ|

If NK(6) = 1 |HWNOZ|WWNOZ|VJWNOZ|EJL|EJANG|

If NK(7) = 1 |HWNOZ|WWNOZ|VJWNOZ|ANGWNZ|TTWNOZ|

If NK(1) = 1 |SA|AR|THICK|

If NK(2) = 1 |WFF|PRF|DF|TF|TREATF|TREATA|

If NK(3) = 1 |PRT|VTIPT|DTURB|BLADES|TRPM|PCTP|TREATT|

If NK(12) = 1 |NOPTA|XX|

|NRED|

If NRED = 1

|NR1|NR2|NR3|

If NR3 = 1 |HSLOT|

The variable TITLE is an alphanumeric list that is input with a 10A6 format. NOPTS, NOPTG, NENG, NALT, NK(I) NOPTJ, NOPTA, NRED, NR1, NR2, and NR3 are all integers and are input with I5 formats. The remaining variables are single-precision real numbers and are input with F10.1 formats.

The input variables, their units, and definitions are as described below.

TITLE — Alphanumeric heading of not more than 60 characters; generally used to identify the V/STOL configuration for which the predictions are made.

NOPTS — Option that denotes which aircraft configuration is to be analyzed as follows (Figure 2-2).

1 = VT
2 = EBF
3 = USB
4 - IBF, either Boundary Layer Control (BLC) or Jet Flap (JF)
5 = AW
6 = Hybrid, combination of USB and IBF/BLC.

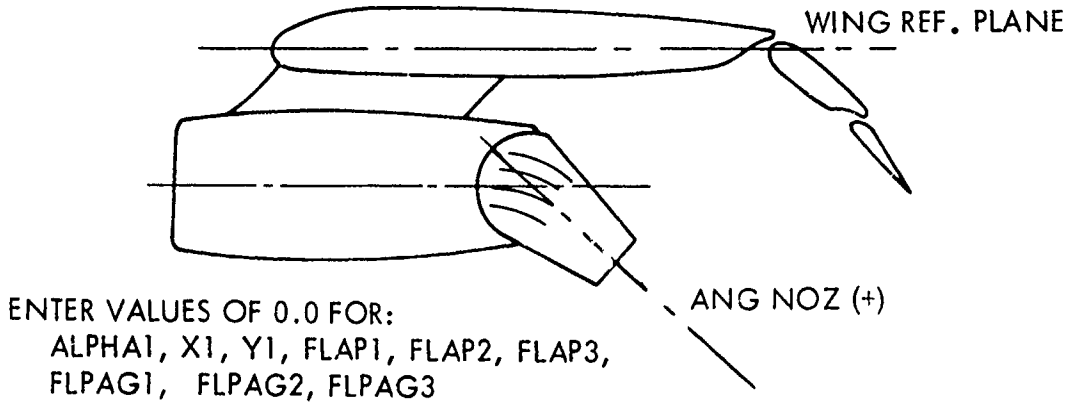

(a) VECTORED THRUST (NOPTS = 1)

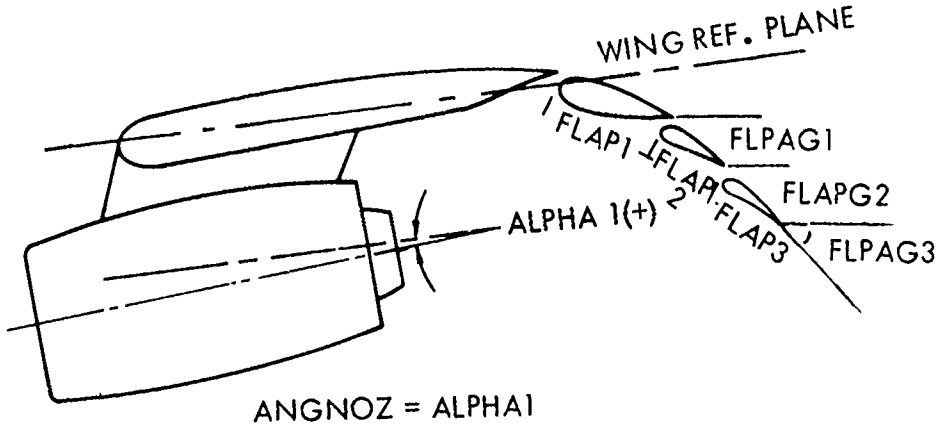

(b) EXTERNALLY BLOWN FLAP (NOPTS = 2)

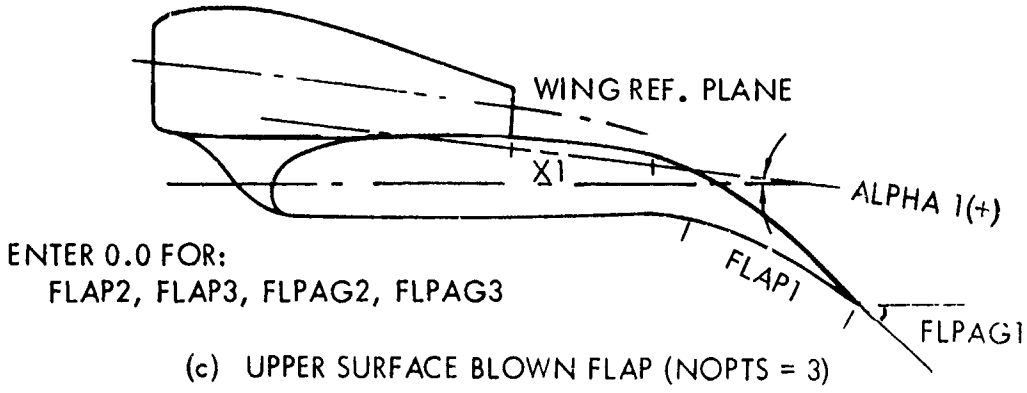

(c) UPPER SURFACE BLOWN FLAP (NOPTS = 3)

Figure 2-2. High Lift System Configurations

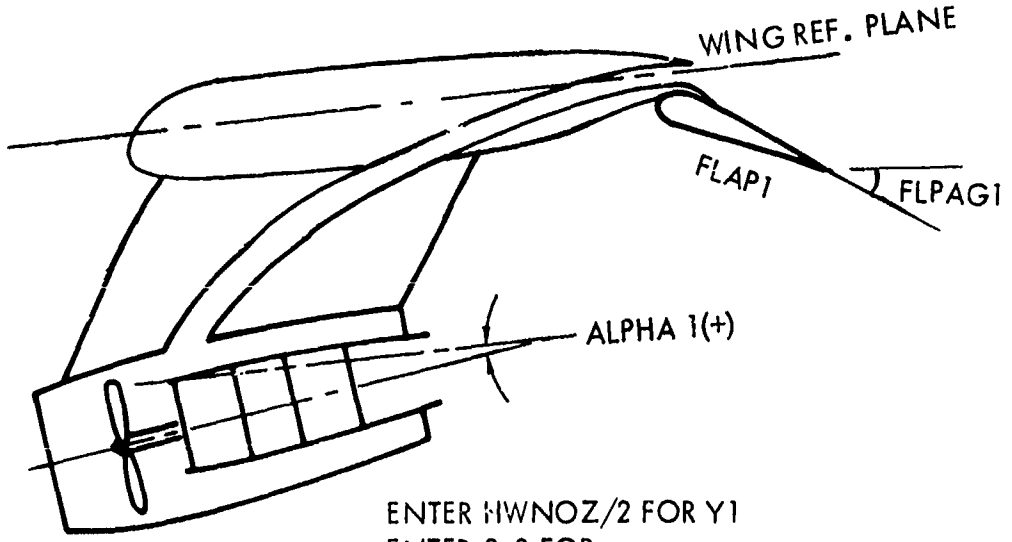

ENTER HWNOZ/2 FOR Y1
ENTER 0.0 FOR:
X1, FLAP2, FLAP3, FLPAG2, FLPAG3

ANGNOZ = ALPHA1

(d) INTERNALLY BLOWN FLAP/BOUNDARY LAYER CONTROL (NOPTS = 4)

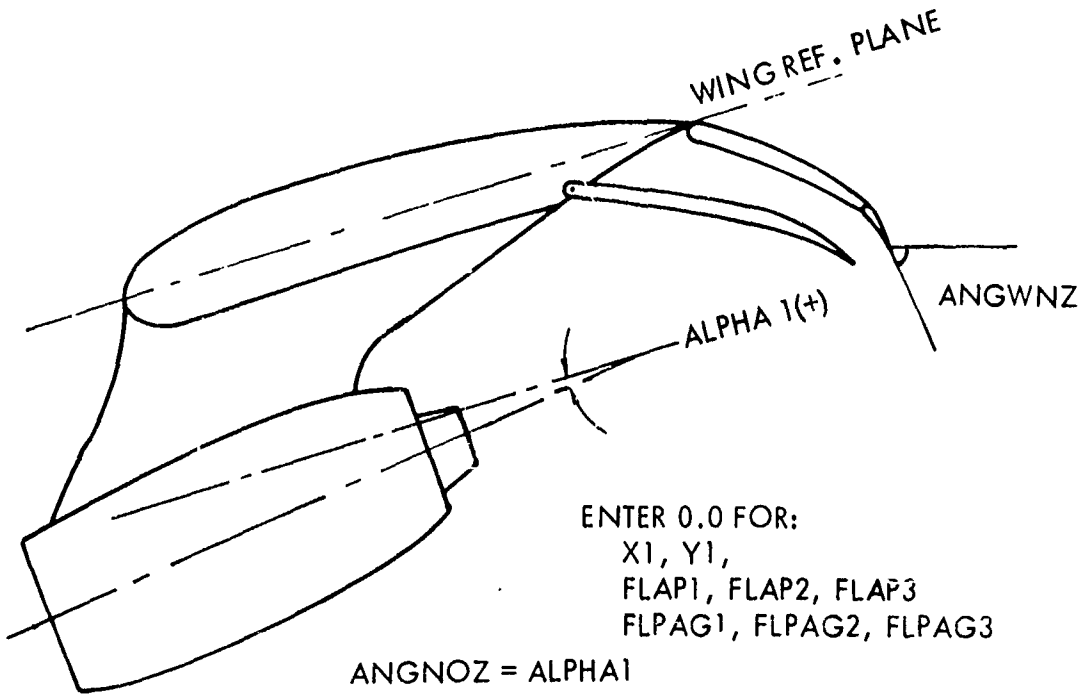

ENTER 0.0 FOR:
X1, Y1,
FLAP1, FLAP2, FLAP3
FLPAG1, FLPAG2, FLPAG3

ANGNOZ = ALPHA1

(e) INTERNALLY BLOWN FLAP/JET FLAP (NOPTS = 4)

Figure 2-2. (Continued)

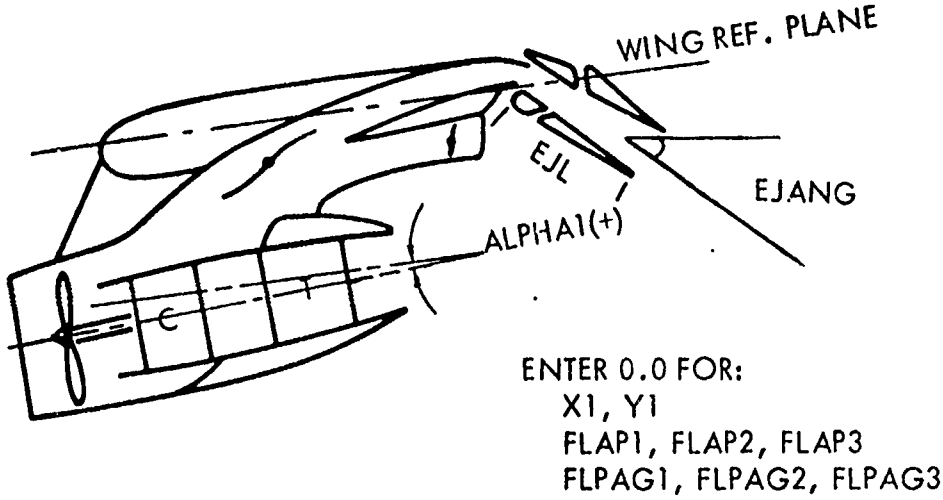

ANGNOZ = -ALPHA1

(f) AUGMENTOR WING (NOPTS = 5)

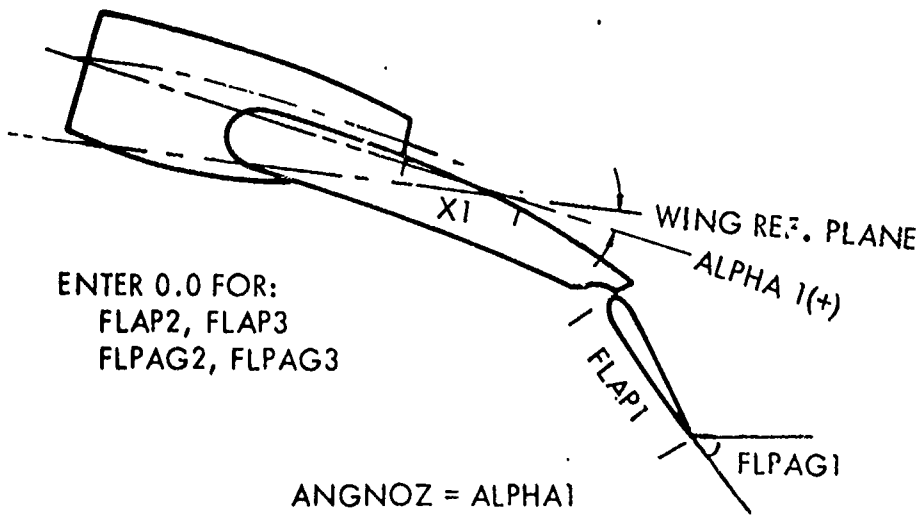

ANGNOZ = ALPHA1

(g) HYBRID (NOPTS = 6)

Figure 2-2. (Concluded)

NOPTG — Key to select the desired program option discussed in Section 4.1.1.

1 = calculate noise for single aircraft location and single observer location

2 = calculate noise for single aircraft location and 17 observer locations along sideline with azimuth angle varying from 10° to 170°.

3 = calculate values in option 2 for several aircraft locations, and select the maximum noise during flight profile.

NENG — Number of engines desired on the aircraft.

SLDIST* — Perpendicular distance from projection of aircraft centerline on horizontal plane to the desired observer sideline as shown in Figure 2-3 (feet).

ALT* — Aircraft altitude for single locations; the starting altitude when NOPTG = 3, (feet), not less than 4 feet.

AZMANG* — Azimuthal angle from forward aircraft centerline to the line from the aircraft to the observer; value is initialized internally to 10 if NOPTG = 1 (degrees).

VAC — Velocity of aircraft along flight path (knots).

FLTANG — Angle between aircraft flight path and horizontal plane, see Figure 2-3, (degrees).

NALT — Number of points on profile to be used with NOPTG = 3.

ALTINC — Increment to be applied to altitude between points on Flight profile for NOPTG = 3, positive (+) for takeoff, negative (-) - for approach, (feet).

**The value of STOD computed from SLDIST, ALT, and AZMANG must be greater than 10 ft.*

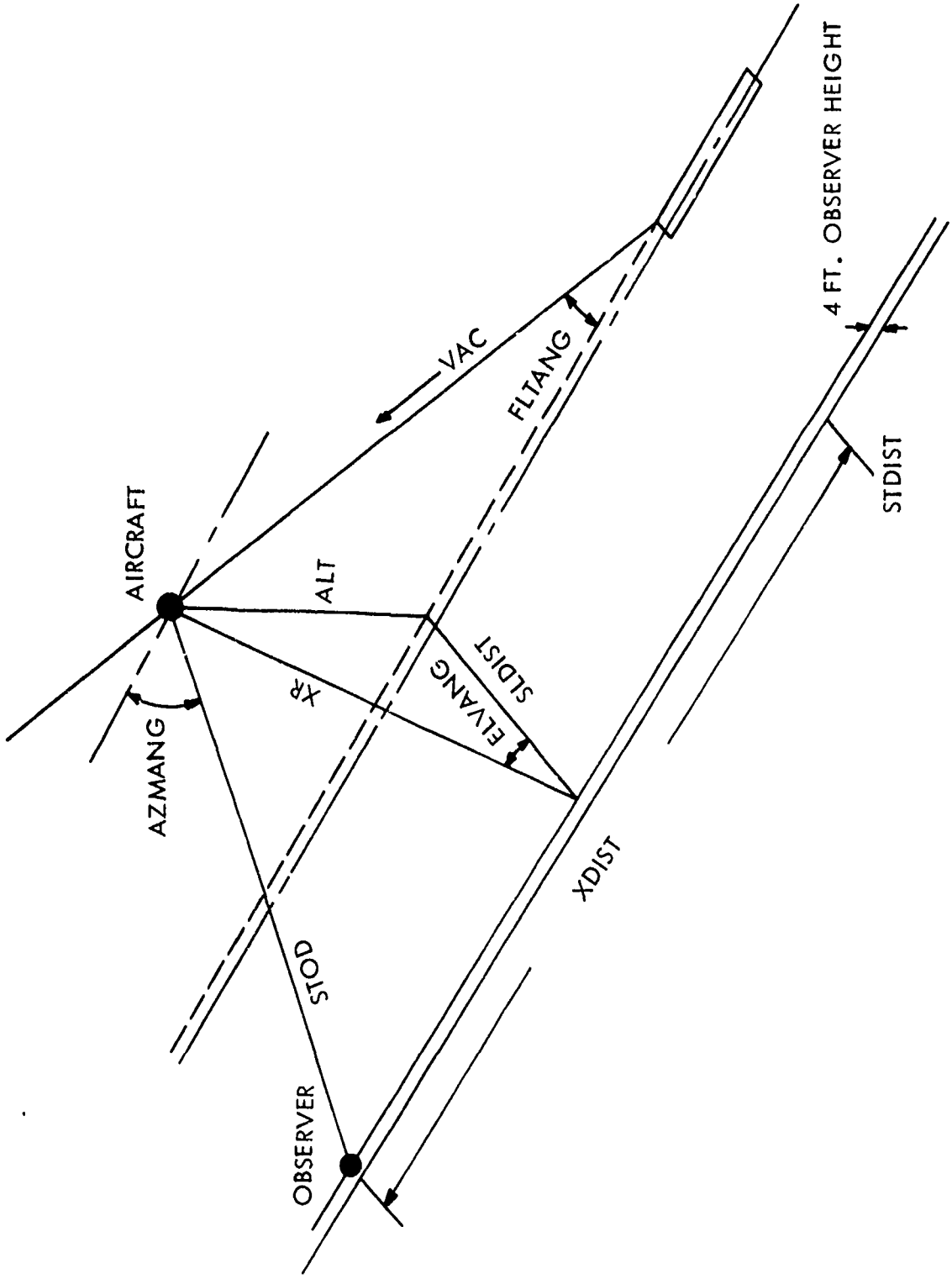

Figure 2-3. Flight Path Geometry

STDIST — Distance to desired reference point from start of flight profile segment for NOPTG = 3, see Figure 2-3 (feet).

NK(1) — Keys to select the noise source subroutines to be called; the value of index I corresponds to the subroutine number listed in Section 4.1 (e.g. NK(1) is for AERO, NK(2) is for FAN, etc.).

0 = subroutine not called.
1 = subroutine called.

ALPHA1 — Angle between the jet exhaust centerline and the wing centerline positive in the direction of the wing, see Figure 2-2 (degrees).

X1 — Distance from projection of the center of the nozzle exit on the wing to the wing trailing edge, see Figure 2-2 (feet).

Y1 — Vertical distance from wing surface to the center of the nozzle exit (feet).

FLAP1 — Length of first flap (feet).

FLAP2 — Length of second flap, 0.0 if only 1 flap (feet).

FLAP3 — Length of third flap, 0.0 if only 1 or 2 flaps (feet).

FLPAG1 — Angle between the centerline of first flap and the wing reference plane (degrees).

FLPAG2 — Angle between the centerline of second flap and the wing reference plane; enter 0.0 if only 1 flap is present (degrees).

FLPAG3 — Angle between the centerline of third flap and the wing reference plane; 0.0 if only 1 or 2 flaps are present (degrees).

NOPTJ — Key to denote type of engine nozzles used, see Figure 2-4.

1 = circular nozzle, with or without plug
2 = slot nozzle
3 = coaxial nozzle, with or without primary plug.

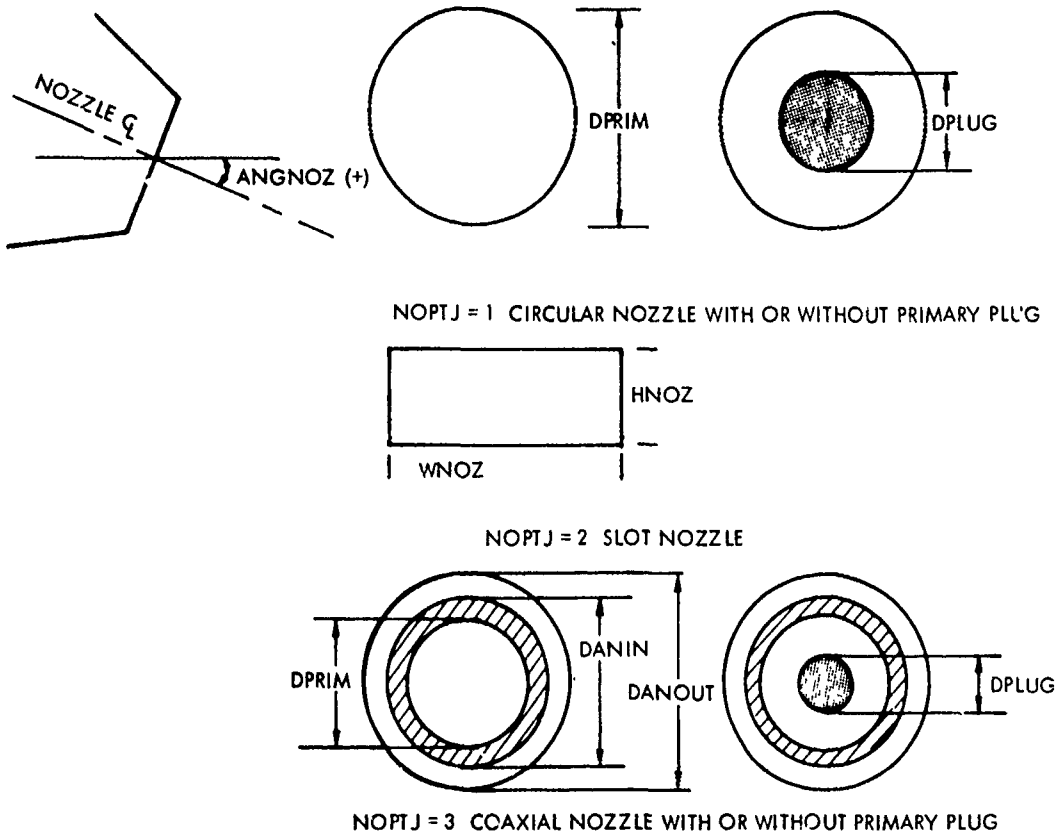

Figure 2-4. Nozzle Configurations

DPLUG	Diameter of nozzle plug; enter 0.0 if no plug is present (feet).
DPRIM	Outer diameter of primary nozzle; diameter of mixed flow nozzle if NOPTG = 1 (feet).
VJPRIM	Velocity of exhaust from primary nozzle; velocity from mixed flow nozzle if NOPTG = 1 (ft/sec.).
TTPRIM	Total temperature of primary flow; total temperature of mixed flow if NOPTJ = 1 (°R).
ANGNOZ	Angle of nozzle centerline relative to wing reference plane [horizontal line through center of nozzle exit; positive (+) in downward direction, see Figure 2-4 (degrees).]
DANIN	Inner diameter of secondary annulus (feet).
DANOUT	Outer diameter of secondary annulus (feet).
VJSEC	Velocity of secondary flow (ft/sec.).
TTSEC	Total temperature of secondary flow (°R).
HNOZ	Height of engine slot nozzle (feet).
WNOZ	Width of engine slot nozzle (feet).
HWNOZ	Height of wing slot nozzle (feet).
WWNOZ	Width of wing slot nozzle (feet).
VJWNOZ	Velocity of flow from wing slot nozzle (ft/sec.).
EJL	Length of ejector AW configuration (feet).
EJANG	Angle of ejector relative to wing reference plane (degrees).

ANGWNG	Angle of centerline of wing slot nozzle relative to wing reference plane [horizontal line center of wing slot nozzle (degrees)]
TTWNOZ	Total temperature of wing slot nozzle flow (°R).
SA	Surface area of wings (Ft^2).
AR	Aspect ratio of wing.
THICK	Maximum thickness of wing (feet).
WFF	Weight flow through fan (lb/sec).
PREF	Pressure ratio of fan.
DF	Diameter of fan (feet).
TF	Temperature of fan exhaust flow (°R)
TREATF	Attenuation of fan noise due to treatment in the fan inlet, input as positive (ΔPNdB).
TREATA	Attenuation of fan noise due to treatment in the exhaust duct, input as positive; set value very high when using AW-2S configuration (ΔPNdB).
PRT	Overall pressure ratio of the turbine.
VTIPT	Maximum tip speed (ft/sec).
DTURB	Maximum diameter of the turbine (feet).
BLADES	Maximum number of blades.
TRPM	Turbine shaft RPM (revolutions/minute)

PCTP Percent thrust.

TREATT Attenuation of turbine noise due to turbine treatment (ΔPNdB).

NOPTA Key to denote the parameter to be used in calculation of APU noise.

1 = use bleed capacity (BC).
2 = use output shaft horsepower (SHP).

XX Value of BC in lb/sec for NOPTA = 1.
Value of SHP in horsepower for NOPTA = 2.

NRED Key to denote the use of noise reduction features on the V/STOL configurations.

0 = not used.
1 = used.

NR1 Key to denote use of first noise reduction feature.

0 = not used.
1 = used.

- o less than 3 flaps on EBF.
- o multi-lobe nozzle with hard wall ejector on AW.

NR2 Key to denote use of second noise reduction feature.

0 = not used.
1 = used.

- o treatment on last flap trailing edge of EBF or USB.
- o multi-lobe nozzle with lined ejector on AW.

NR3 Key to denote use of third noise reduction feature.

0 = not used.

1 = used.

- o blowing at last flap trailing edge on EBF or USB.

HSLOT Height of slot used for trailing-edge blowing (feet).

4.1.3 Suggested Subroutine Combinations

The program is designed to use particular noise sources for each type of V/STOL configuration. However, to allow for possible future program changes or developments, the selection of subroutines to be called is left as an optional input parameter. Figure 2-5 shows the subroutines that should be used with each configuration. Other combinations, which are not described in this report, might be "tailor-made" to fit future high-lift systems which may be evolved.

The AW-2S is a two-stream configuration where all the fan air is used to power the wing slot. The AW-3S has some fan air exiting through the fan nozzle.

(NOPTS=1) VT	(NOPTS=2) EBF	(NOPTS=3) USB	(NOPTS=4) IBF/BLC	(NOPTS=4) IBF/JF	(NOPTS=5) AW-2S	(NOPTS=5) AW-3S	(NOPTS=6) HYBRID
AERO	AERO	AERO	AERO	AERO	AERO	AERO	AERO
FAN	FAN	FAN	FAN	FAN	FAN	FAN	FAN
TURBNE	TURBNE	TURBNE	TURBNE	TURBNE	JET	TURBNE	TURBNE
JET	JET	JET	JET	JET	EXCESS	JET	JET
EXCESS	EXCESS	EXCESS	EXCESS	EXCESS	AUGWNG	EXCESS	EXCESS
APU	IMPING	IMPING	WNGJET	WNGJET	APU	AUGWNG	WNGJET
	WALJET	WALJET	WALJET	APU		APU	IMPING
	WAKE	WAKE	WAKE				WALJET
	TRAIL	TRAIL	TRAIL				WAKE
	APU	APU	APU				TRAIL
							APU

Figure 2-5. Recommended Subroutine Combinations

4.2 STOLPROG - MAIN PROGRAM

STOLPROG is the main control program for the prediction method outlined previously. This program handles all the necessary input and output functions to predict the noise levels for a selected configuration. It also issues all call commands to the desired noise-source prediction subroutines.

The program receives partially corrected 1/3 octave-band spectra (SPL) from the source prediction subroutines, as described in Section 4.3. Through calculations and subroutine calls, STOLPROG determines values to account for the following effects:

- o number of engines on the aircraft
- o ground reflection
- o fuselage shielding
- o extra ground attenuation
- o level change due to forward speed
- o noise reduction features.

The effect of number of engines is computed as $10 \cdot \mathrm{Log}_{10}(N)$, where N is the number of engines. This single value is applied throughout the entire spectrum. The value of fuselage shielding for the multiple engines is determined by $2 \cdot \cos$ (ELVANG), where ELVANG is the aircraft elevation angle. The other effects are calculated in the individual subroutines discussed in the following sections.

The values of the above corrections are applied to the individual source spectra as,

- o number of engines and fuselage shielding — all spectra except AERO
- o level correction for forward speed — JET, AUGWNG, WNGJET, IMPING, WALJET, WAKE, and TRAIL
- o noise reduction features -- AUGWNG, WNGJET, IMPING, WALJET, WAKE, and TRAIL.

The spectra from FAN and TURBINE are combined to form the spectra output under the heading Fan and Turbine when NOPTG = 1 (see Appendix A, Sample Output). The spectra from AUGWNG, WNGJET, IMPING, WALJET, WAKE, and TRAIL are combined to form the spectrum output under the heading High Lift System when NOPTG = 1.

STOLPROG also calculates a total spectrum for all the noise source spectra and determines the overall sound pressure level (OASPL), perceived noise noise level (PNL), and tone-corrected PNL (PNLT) for each spectrum.

Data are stored, parameters are incremented, and the above process is repeated as required to obtain the necessary data for the output option selected (NOPTG).

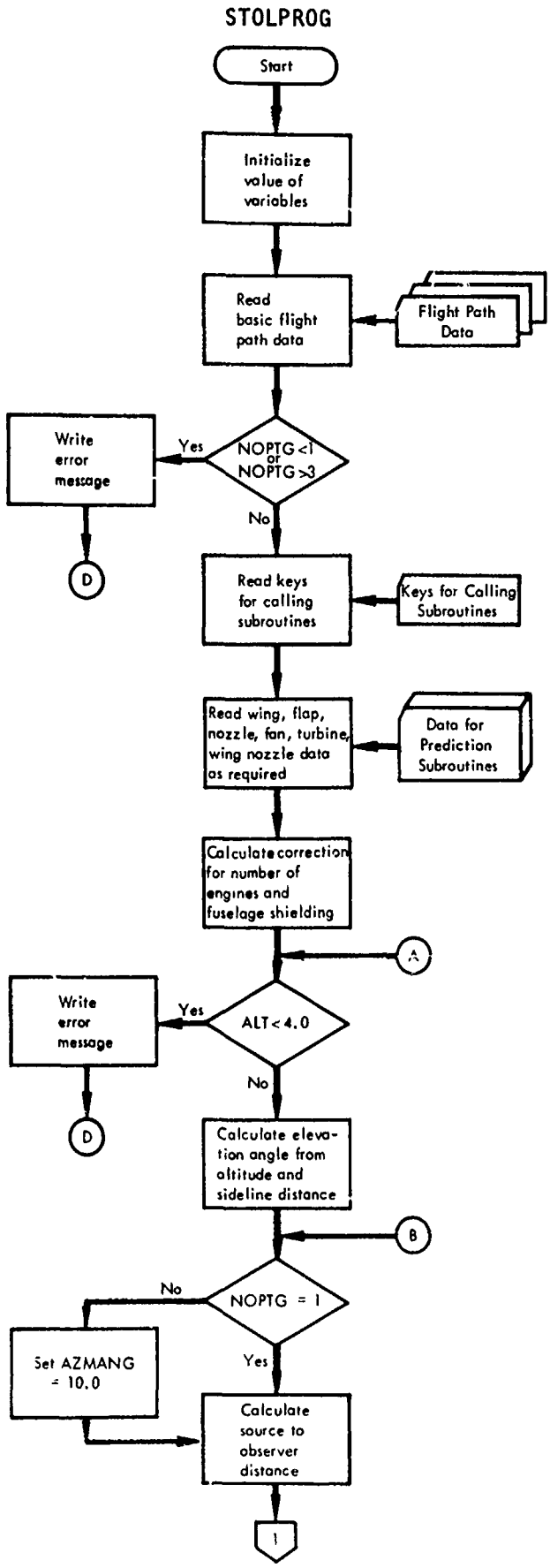

Figure 2-6. STOLPROG Flow Chart.

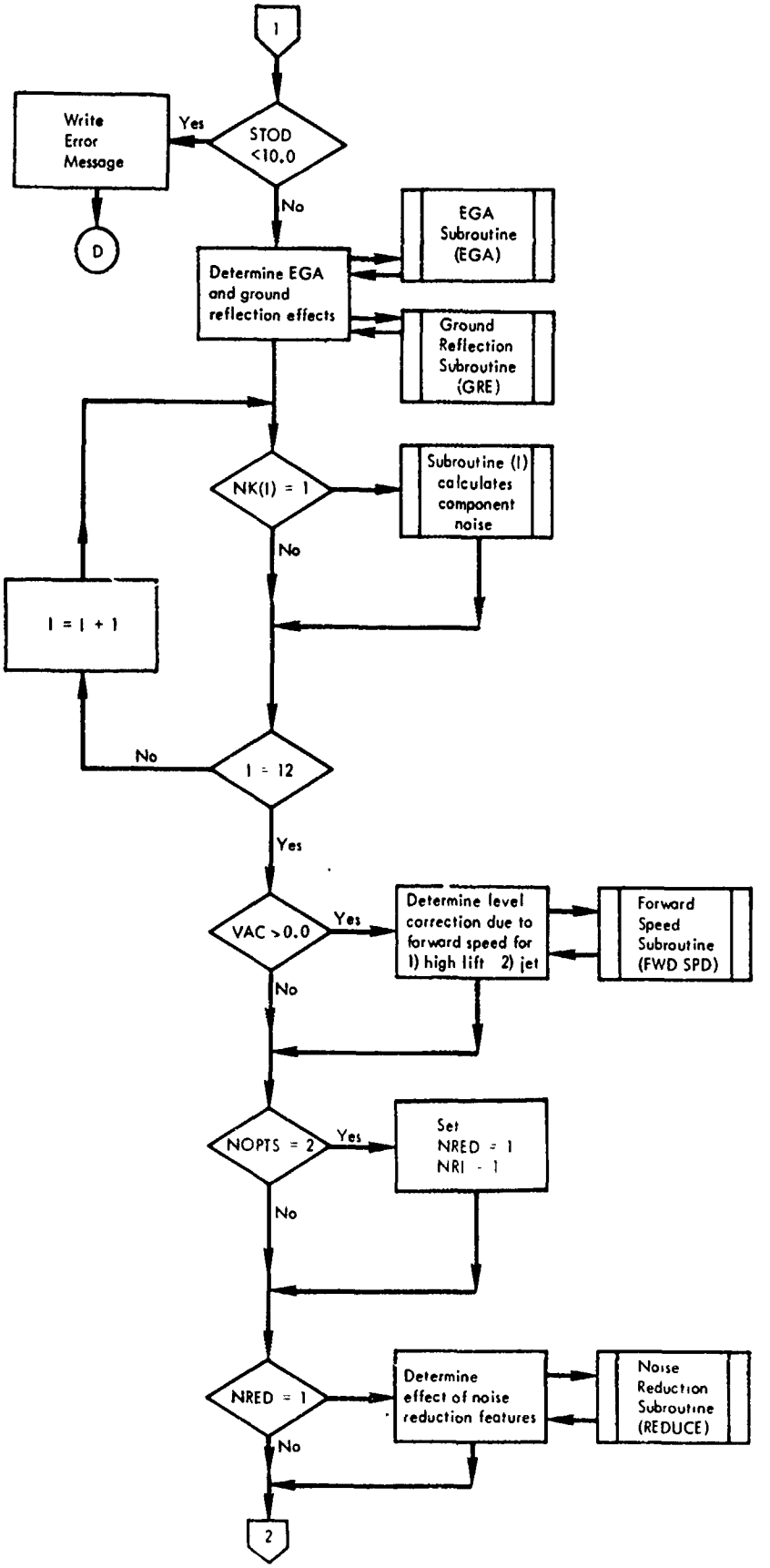

Figure 2-6. Continued.

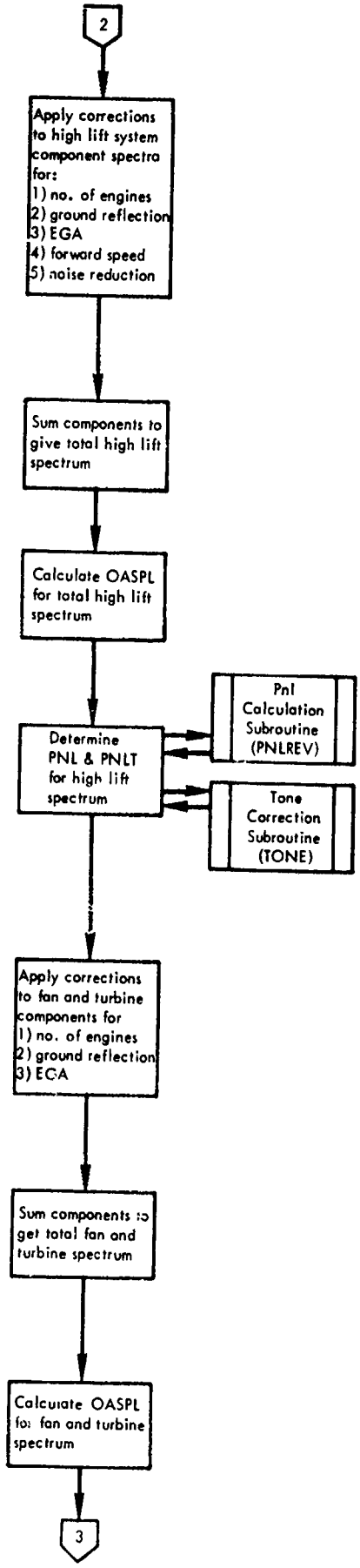

Figure 2-6. Continued.

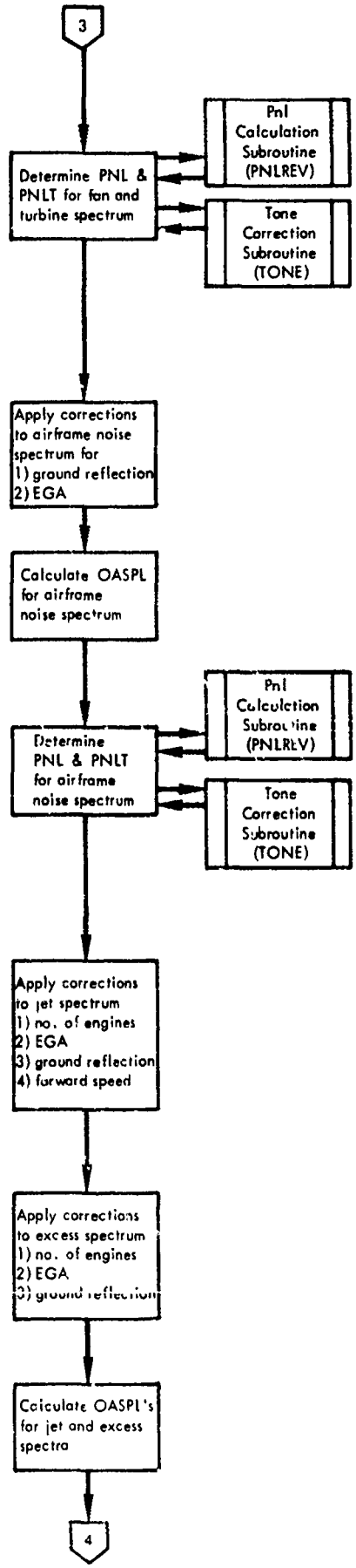

Figure 2-6. Continued.

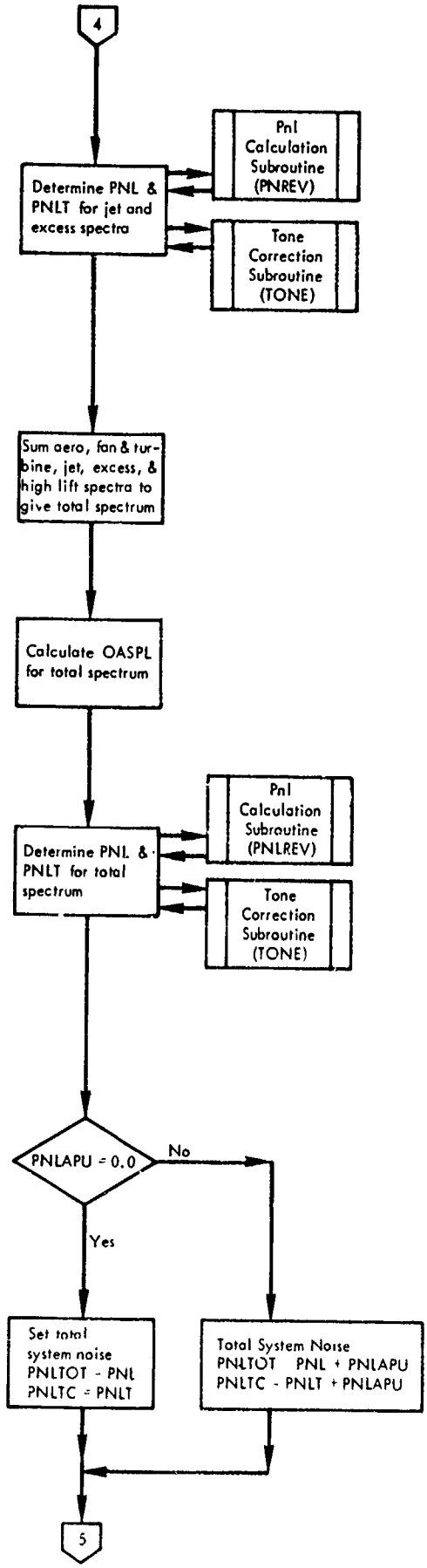

Figure 2-6. Continued.

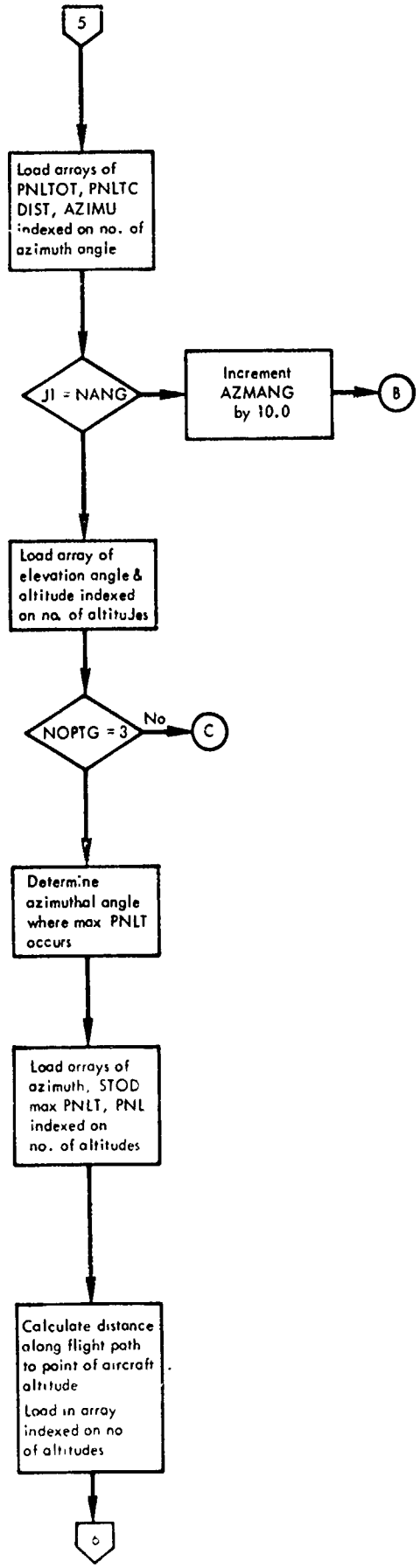

Figure 2-6. Continued.

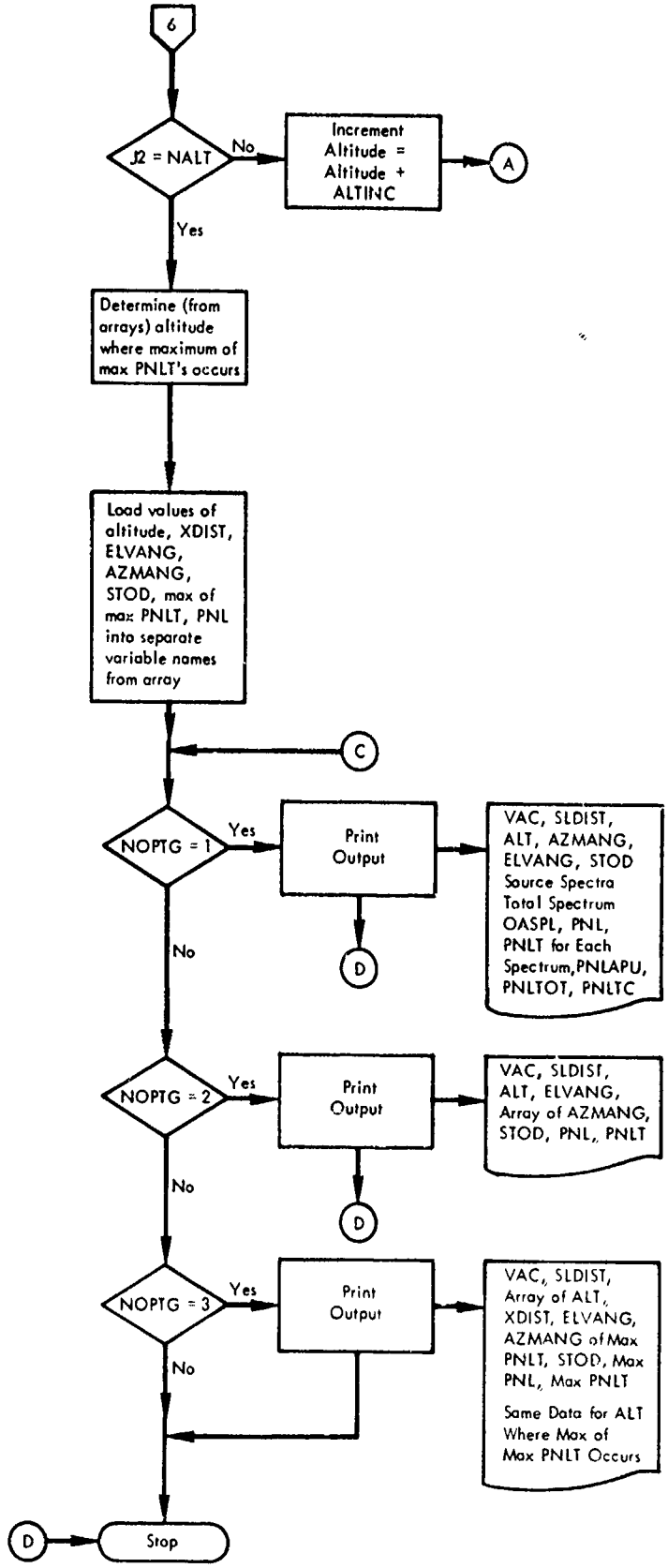

Figure 2-6. Continued.

4.3 SOURCE PREDICTION PROGRAMS

The individual noise source prediction subroutines, with the exception of APU, compute an index value of OASPL at one foot from the source in a reference direction (elevation and azimuth). Although this index OASPL is calculated at one foot from the source, it is equivalent to far-field radiated noise. From this index value, the 1/3 octave-band spectrum of sound pressure level (SPL) at a given distance, azimuth, and elevation angle from the source is calculated considering the following effects:

(1) directivity (azimuthal and elevation)
(2) spectral distribution (conversion to 1/3 o.b. SPL's)
(3) spherical divergence
(4) atmospheric attenuation (using values for a FAA day, 77°F, 70% R.H.)
(5) Doppler frequency shift.

These 1/3 octave-band spectra are then returned to the main program where they are modified to account for other effects, as described in Section 4.2, to give the actual spectrum received by the observer.

The subroutine APU calculates only PNL corrected for spherical divergence.

The following subsections describe and present detailed flow charts for the noise source prediction subroutines.

4.3.1 AERO - Airframe Aerodynamic Noise

This subroutine calculates the 1/3 octave-band spectrum resulting from the motion of the airframe through the atmosphere. The calculation procedure is based on the methodology discussed in Section 2.4.1.

The required variables are:

(1) source to observer distance (STOD)
(2) azimuthal angle (AZMANG)
(3) atmospheric absorption coefficients (ALPHA)
(4) 1/3 o.b. center frequencies (F)
(5) aircraft velocity (VAC)
(6) wing surface area (SA)
(7) aspect ratio (AR)
(8) maximum wing thickness (THICK)

The reference OASPL at a distance of one foot is given by

$$OASPL = 10 \log_{10} \frac{VAC^5 \cdot SA}{AR^2 \quad (1 - XMN)^4} + 7.0$$

where XMN is the aircraft Mach number.

The output is the 1/3 octave-band spectrum.

The subroutine logic path is shown in the following flow chart (Figure 2-7).

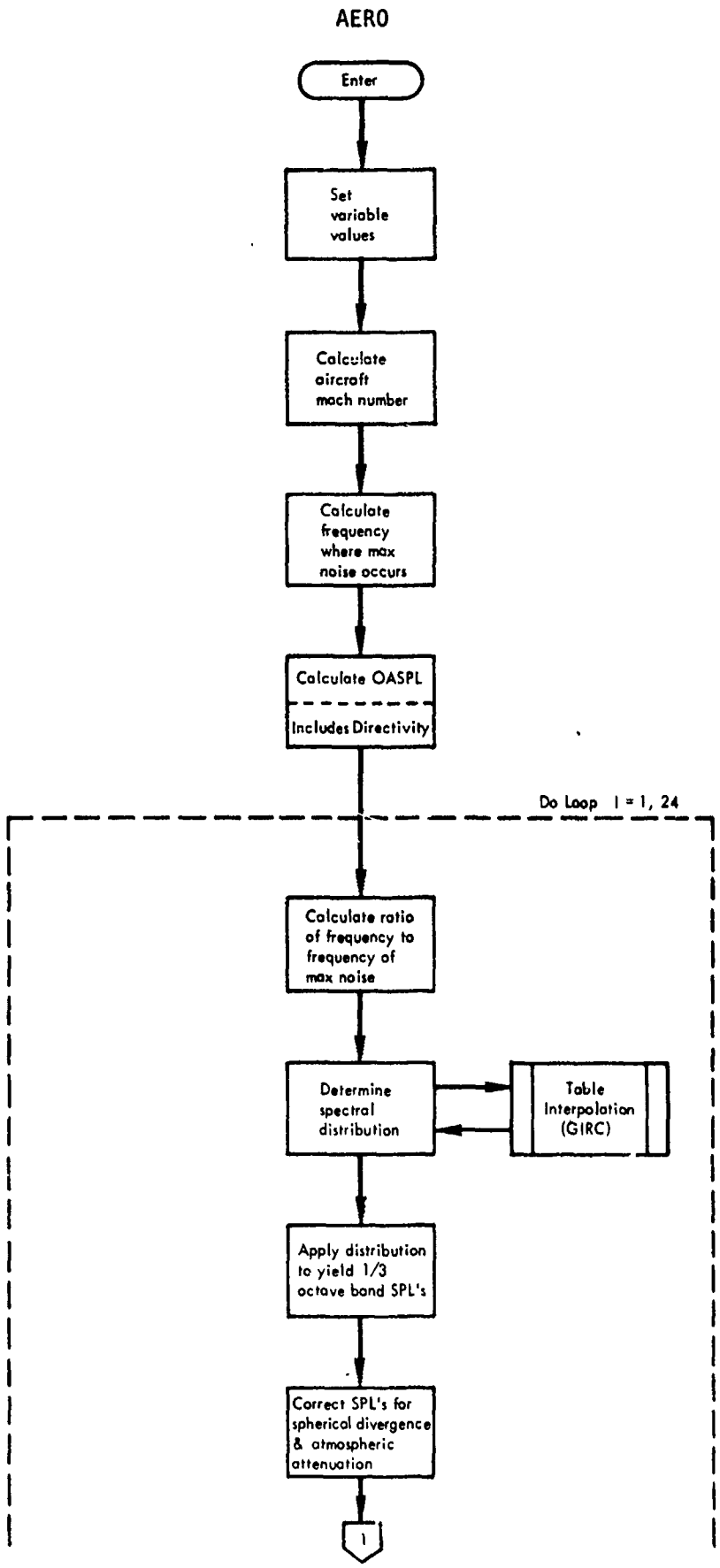

Figure 2-7. AERO Flow Chart.

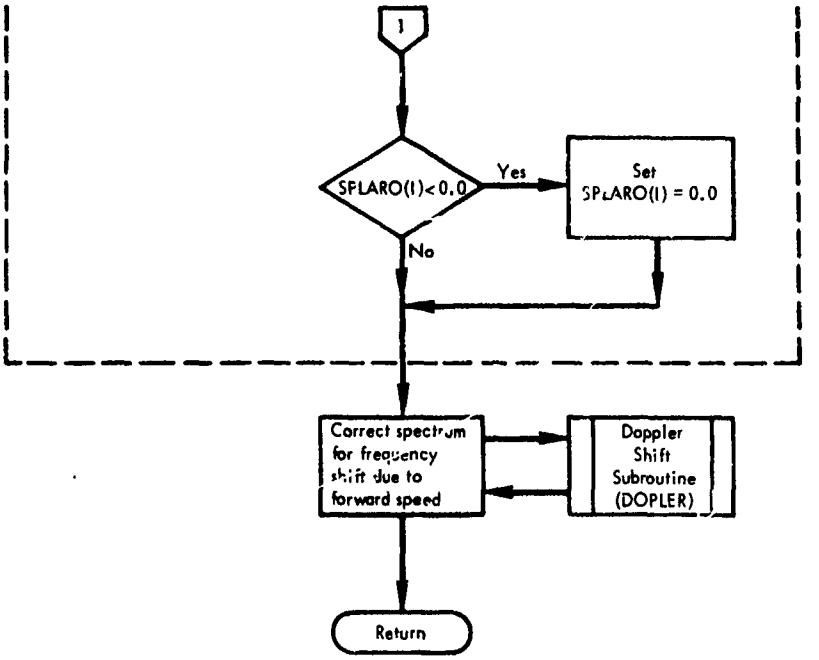

Figure 2-7. Continued.

4.3.2 FAN - Fan Noise

This subroutine calculates the total 1/3 octave-band spectrum for the forward and aft components of fan noise produced by a single-stage turbofan engine. The methodology for the calculation procedure is described in Sections 2.1.1.

Provisions are made to account for inlet and/or exhaust duct treatment effects. The subroutine also calculates the geometrical relations (shown in Figure 2-8) needed to calculate the shielding effect on the aft fan component when the USB (NOPTS = 3) or Hybrid (NOPTS = 6) option is exercised. The source is located at the center of the nozzle exit for these calculations.

The required variables are:

(1) source-to-observer distance (STOD)
(2) azimuthal angle (AZMANG)
(3) atmospheric absorption coefficients (ALPHA)
(4) 1/3 o.b. center frequencies (F)
(5) weight flow through fan (WFF)
(6) pressure ratio of fan (PRF)
(7) diameter of fan (DF)
(8) temperature of fan flow (TF)
(9) insertion loss (ΔPNdB) due to inlet treatment (TREATF)
(10) insertion loss (ΔPNdB) due to exhaust duct treatment (TREATA)
(11) key to determine type of high-lift system (NOPTS)

If NOPTS = 3 or NOPTS = 6, the following are also required:

(1) distance along wing from projection of nozzle exit to wing trailing edge (X1)

(2) vertical distance from wing surface to center of nozzle exit (Y1)

(3) length of flaps (FLAP1, FLAP2, and FLAP3)

(4) flap angles (FLPAG1, FLPAG2, and FLPAG3).

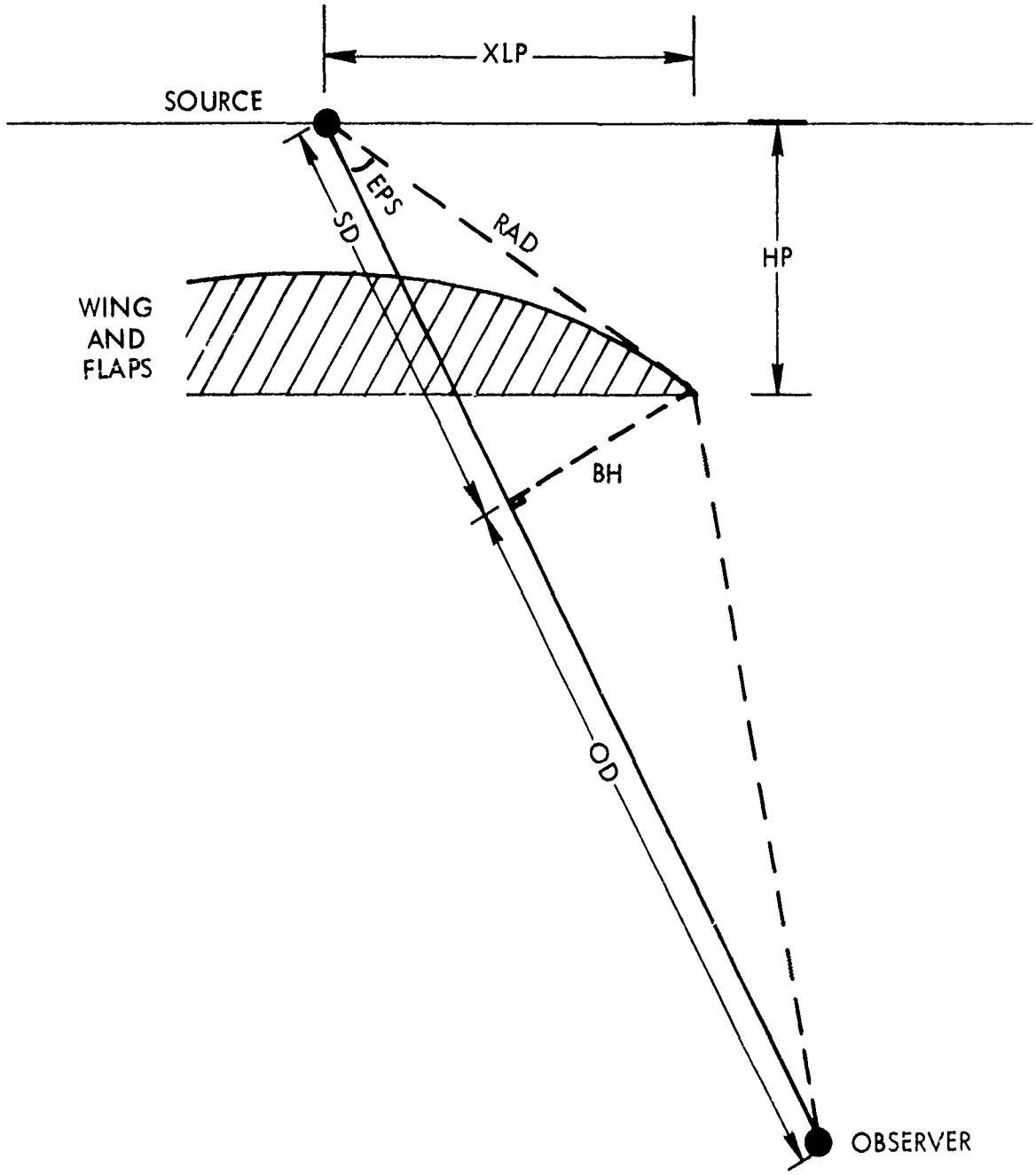

Figure 2-8. Shielding Geometry

The reference OASPL is given by

$$OASPL = 10 \cdot \log_{10} (WFF) + 20 \cdot \log_{10} (PRF^{0.286} - 1) + 127.0$$

The output is the total 1/3 octave-band spectrum composed of the forward and aft component spectra.

The subroutine logic path is shown in the following flow chart (Figure 2-9).

FAN

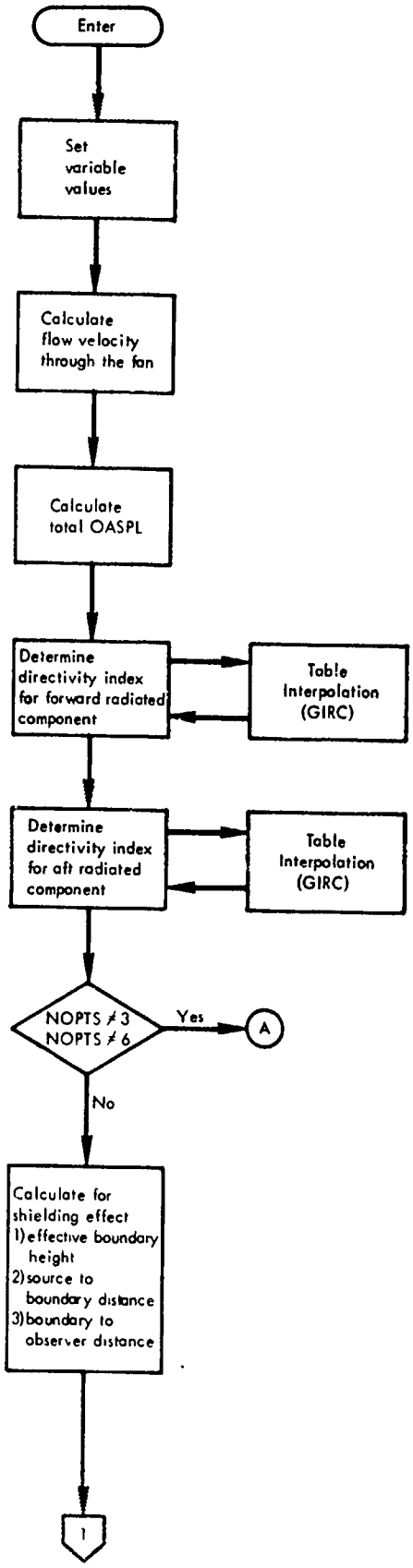

Figure 2-9. FAN Flow Chart.

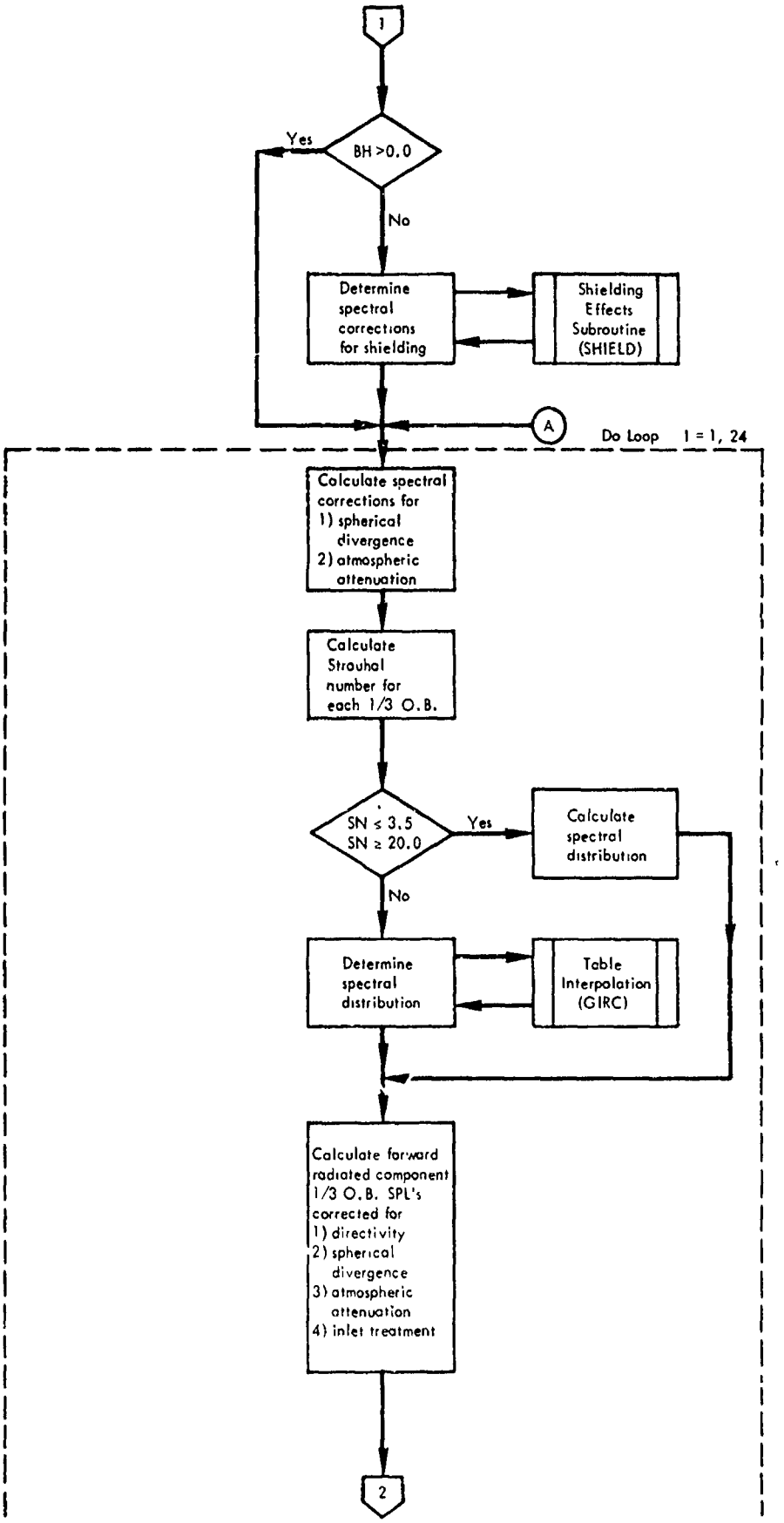

Figure 2-9. Continued.

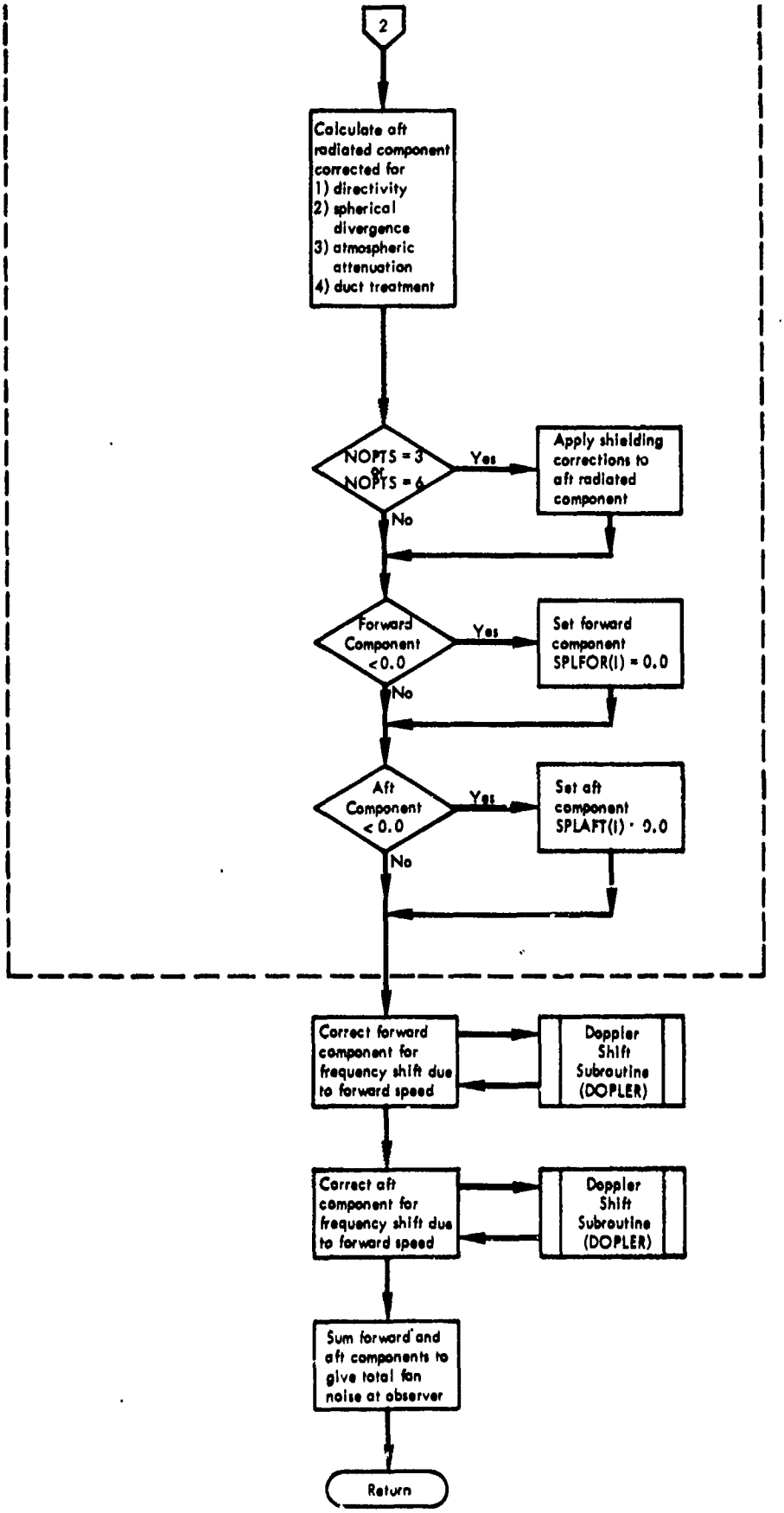

Figure 2-9. Continued.

4.3.3 TURBNE - Turbine Noise

This subroutine calculates the 1/3 octave-band spectrum from the engine turbine. The methodology used to develop this prediction procedure is discussed in Section 2.1.2. The shielding effects are determined as discussed for fan noise (Section 4.3.2) for the source located at the nozzle exit. The required variables are:

(1) source-to-observer distance (STOD)
(2) azimuthal angle (AZMANG)
(3) atmospheric absorption coefficients (ALPHA)
(4) 1/3 o.b. center frequencies (F)
(5) pressure ratio of turbine (PRT)
(6) velocity of blade tip (VTIPT)
(7) diameter of turbine main stage (DTURB)
(8) number of turbine blades in main stage (BLADES)
(9) turbine RPM (TRPM)
(10) percent power of operation (PCTP)
(11) insertion loss (ΔPNdB) due to turbine treatment (TREATT)
(12) key to determine the type of high-lift system (NOPTS)

If NOPTS = 3 or NOPTS = 6, the following are also required:

(1) distance along the wing from projection of nozzle exit to wing trailing edge (X1)

(2) vertical distance from wing surface to the center of the nozzle exit (Y1)

(3) length of flaps (FLAP1, FLAP2, and FLAP3)

(4) flap angles (FLPAG1, FLPAG2, and FLPAG3).

The reference OASPL is given by

$$\text{OASPL} = 8.75 \cdot \log_{10} \left(1 - \left(\frac{1}{\text{PRT}}\right)^{0.286}\right) + 20 \cdot \log_{10} \left(\frac{\text{VTIPT}}{1116.0}\right)$$

$$+ 10 \cdot \log_{10}(\text{AREA}) + 138.9$$

where AREA = turbine area $\left(\frac{DTURB^2 \cdot \pi}{4}\right)$. The output is the 1/3 octave-band spectrum.

The subroutine logic path is shown in Figure 2-10.

TURBNE

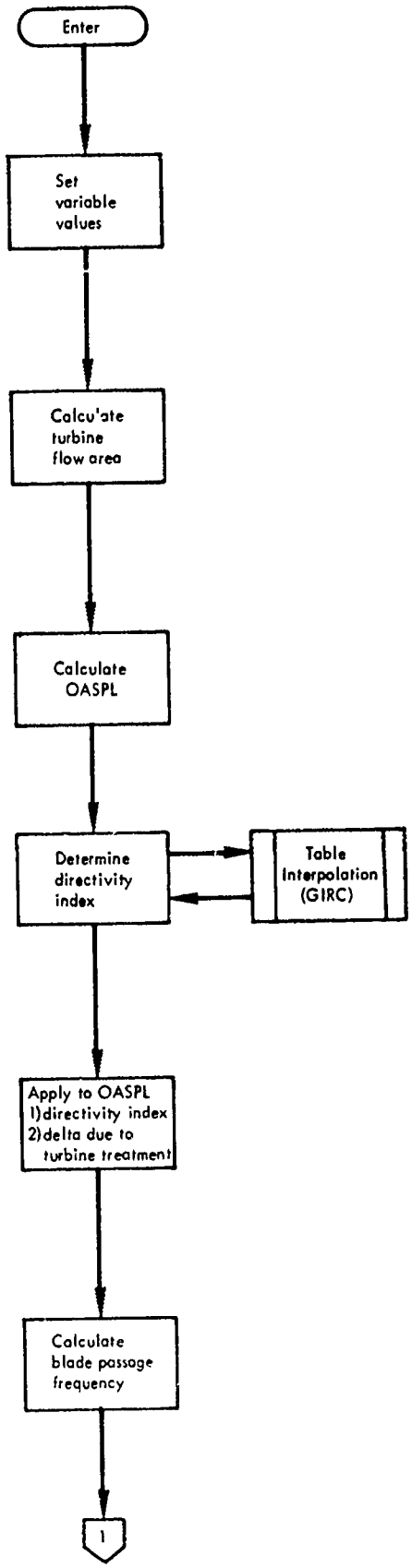

Figure 2-10. TURBNE Flow Chart.

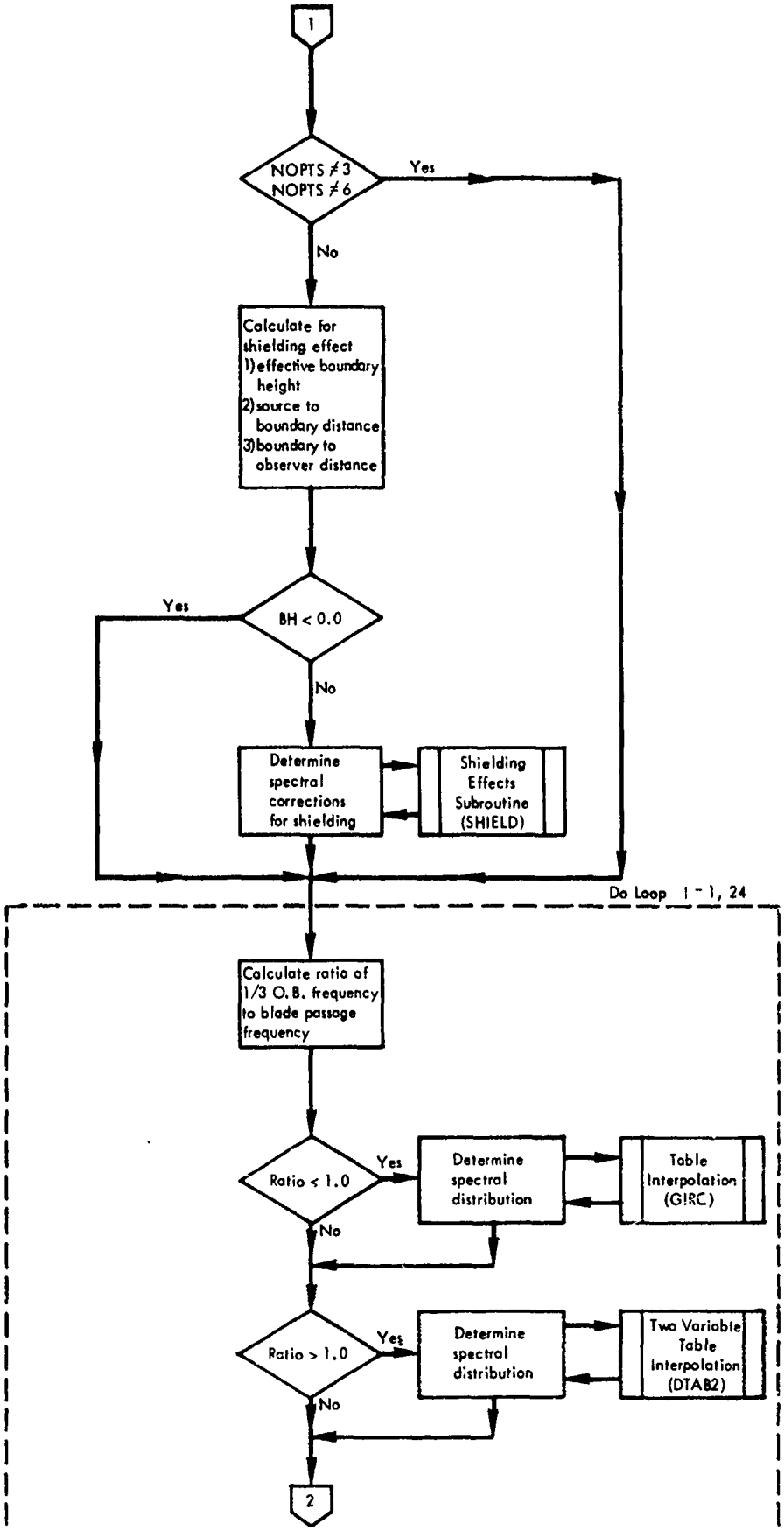

Figure 2-10. Continued.

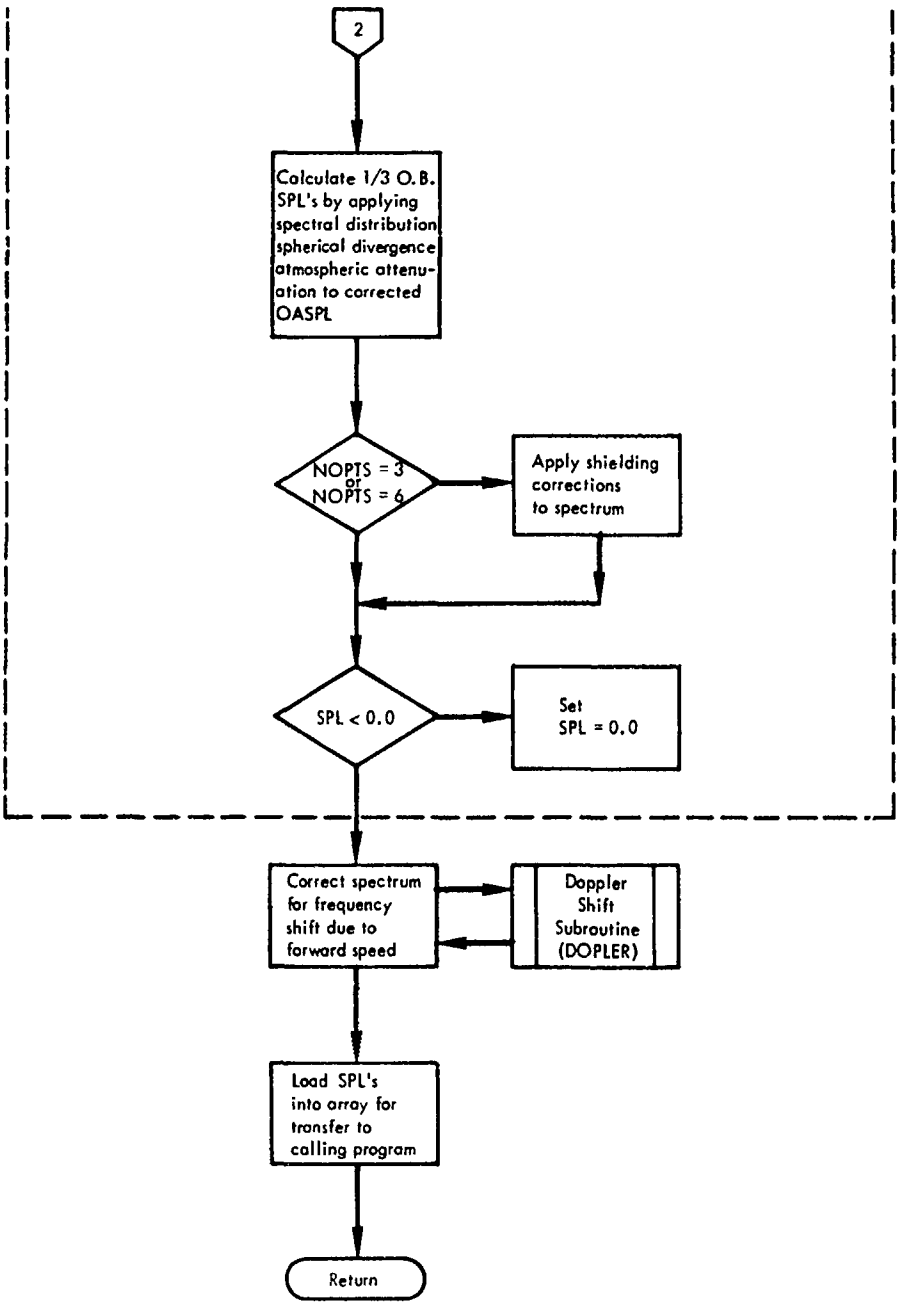

Figure 2-10. Continued.

4.3.4 JET - Jet Exhaust Noise

This subroutine calculates the 1/3 octave-band spectrum (SPL) from the engine core and/or fan exhaust. The methodology used to develop this prediction procedure is discussed in Section 2.2.

This subroutine will calculate the noise for three nozzle configurations as shown in Figure 2-4 and listed below:

(1) circular, with or without plug
(2) slot
(3) coaxial, with or without plug in primary nozzle.

For each configuration, the diameter (DEQUIV) of an equivalent area unplugged circular nozzle, an equivalent velocity (VEQUIV), a hydraulic diameter, and an equivalent temperature (TTEQ) are calculated. These four values are a'so used in EXCESS and the "high-lift source" subroutines for values of NOPTS equal to 2, 3, and 6. Therefore, JET must be called before these subroutines.

The subroutine accounts for the effect of the presence of turning vanes in the flow of the vectored thrust configuration. It also calculates the geometrical relations (shown in Figure 2-8) needed to calculate the shielding effect when the USB (NOPTS = 3) or Hybrid (NOPTS = 6) option is e ercised. The source is assumed to be located 2·DEQUIV downstream of the nozzle exit for these calculations. The shielding values are applied to the jet noise spectrum.

The required variables are:

(1) source-to-observer distance (STOD)
(2) azimuthal angle (AZMANG)
(3) atmospheric absorption coefficients (ALPHA)
(4) 1/3 o.b. center frequencies (F)
(5) key to determine nozzle configurations (NOPTJ)

For NOPT3 = 1 or 3,

(6) diameter of primary plug (DPLUG)

(7) outer diameter of primary nozzle (DPRIM)

(8) velocity of exhaust from primary nozzle (VJPRIM)

(9) total temperature of exhaust from primary nozzle (TTPRIM)

(10) angle of nozzle ℄ relative to the horizontal (ANGNOZ)

For NOPTJ = 3,

(11) inner diameter of secondary nozzle (DANIN)

(12) outer diameter of secondary nozzle (DANOUT)

(13) velocity of exhaust of secondary nozzle (VJSEC)

(14) total temperature of exhaust of secondary nozzle (TTSEC)

For NOPTJ = 2,

(15) height of nozzle (HNOZ)

(16) width of nozzle (WNOZ)

(17) velocity of exhaust (VJPRIM)

(18) total temperature of exhaust (TTPRIM)

(19) angle of nozzle ℄ relative to the horizontal (ANGNOZ)

If NOPTS = 3 OF NOPTS = 6, the following are also required:

(1) distance along the wing from projection of nozzle exit to wing trailing edge (X1)

(2) vertical distance from wing surface to the center of the nozzle exit (Y1)

(3) length of flaps (FLAP1, FLAP2, and FLAP3)

(4) flap angles (FLPA61, FLPA62, and FLPA63)

The reference OASPL is given by

$$OASPL = KA + A + B + C$$

where

$$KA = 134 \text{ when no plug is used}$$

$$= 134 + 3 \cdot \log_{10}\left(0.1 + 2 \left(\frac{H}{B2}\right)\right) \text{ with plug}$$

H = annulus height of primary

B2 = outer diameter of primary (DPRIM),

$$A = 10 \cdot \log_{10}\left(AN \cdot \left(\frac{RHOA}{0.0765}\right)^2 \left(\frac{CA}{11160}\right)^4\right)$$

AN = nozzle area

RHOA = density of ambient air

CA = speed of sound in ambient air,

$$B = 10 \cdot \left(\frac{3.K^{3.5}}{0.6 + K^{3.5}} - 1\right) \cdot \log_{10}\left(\frac{RHOJ}{RHOA}\right)$$

K = ratio of primary jet velocity to speed of sound in ambient air (VPRIM/CA)

RHOJ = density of primary exhaust

$$C = 10 \cdot \log_{10}\left(\frac{K^{7.5}}{1 + 0.01.K^{4.5}}\right)$$

The output is the 1/3 octave-band spectrum.

The subroutine logic path is shown in the following flow chart (Figure 2-11).

JET

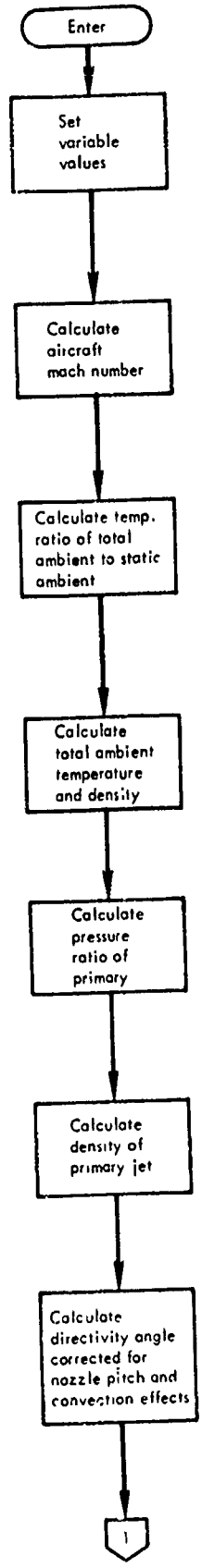

Figure 2-11. JET Flow Chart.

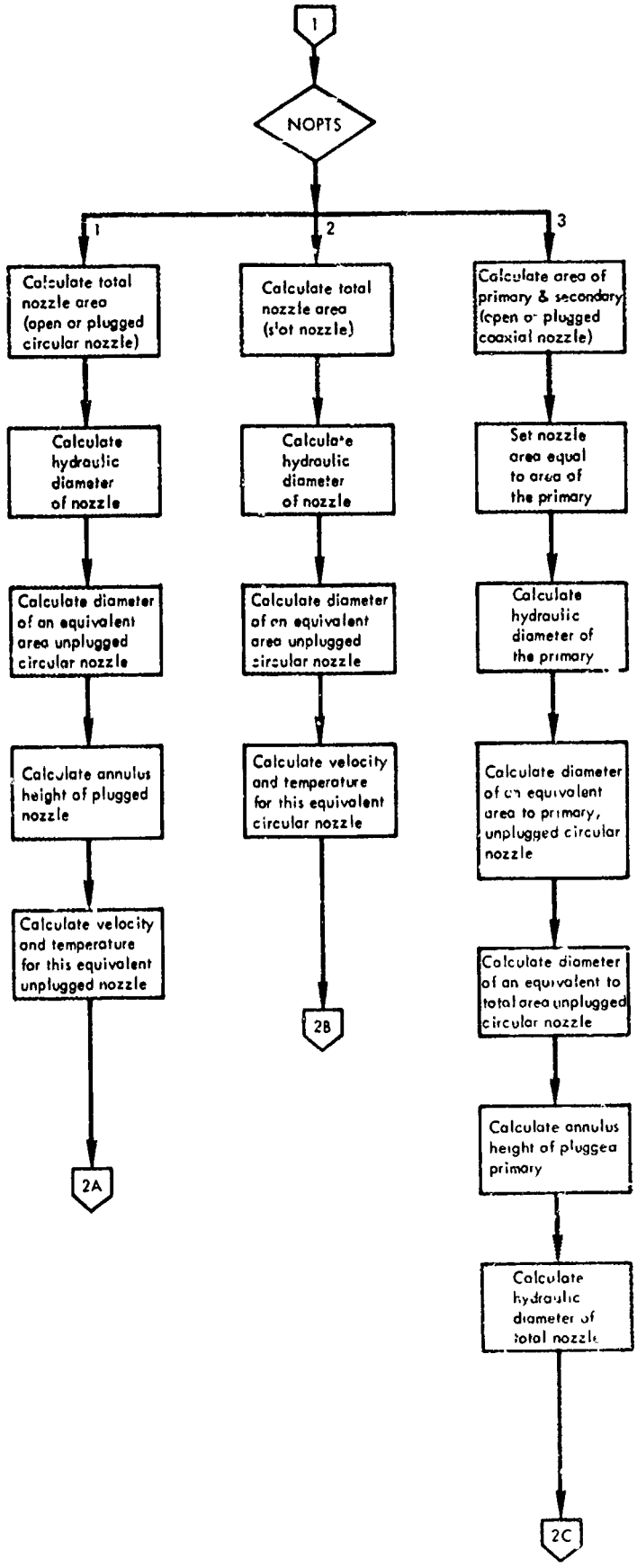

Figure 2-11. Continued.

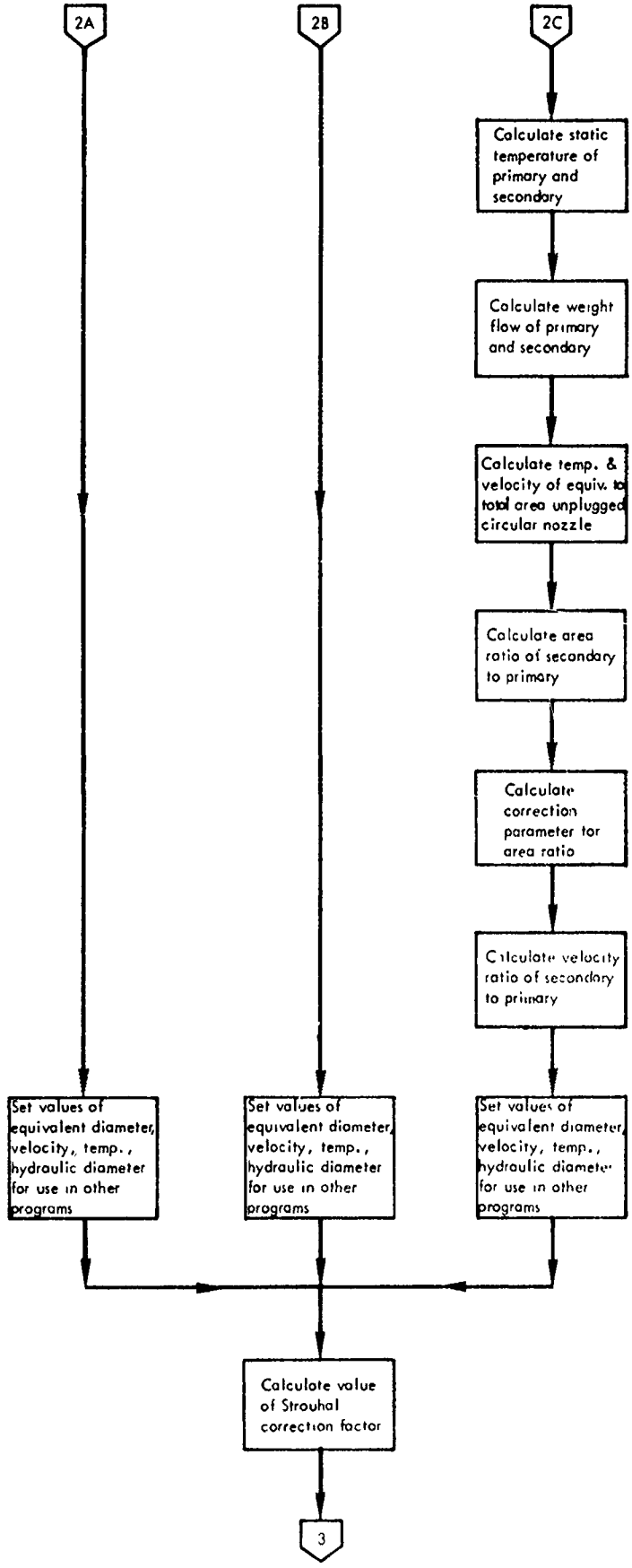

Figure 2-11. Continued.

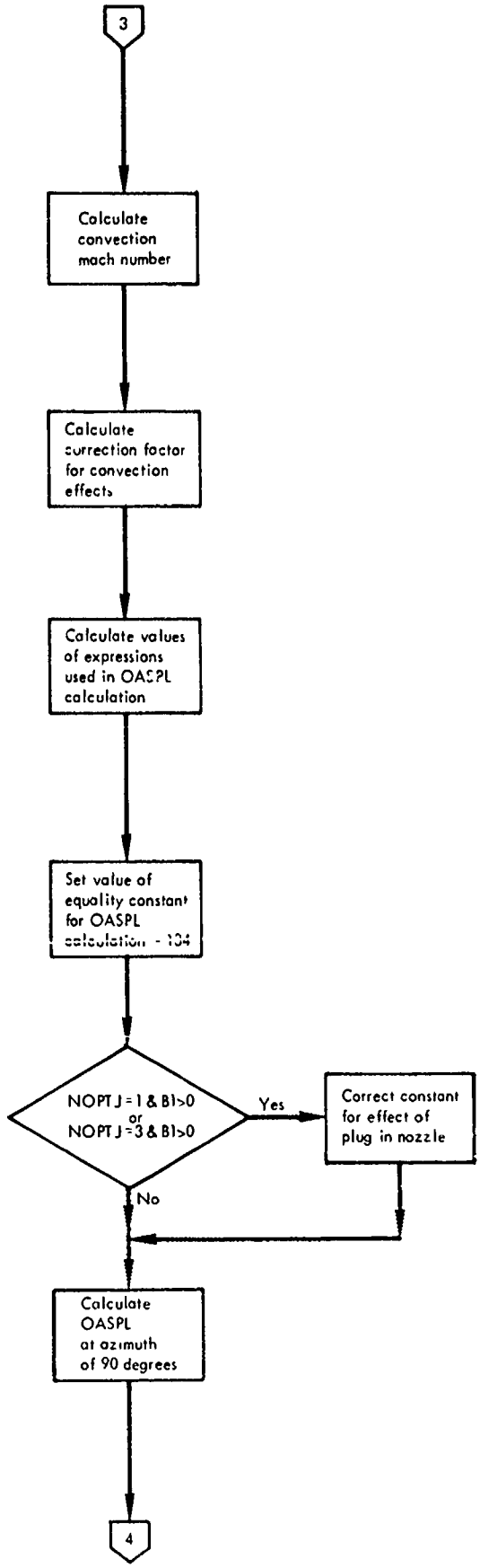

Figure 2-11. Continued.

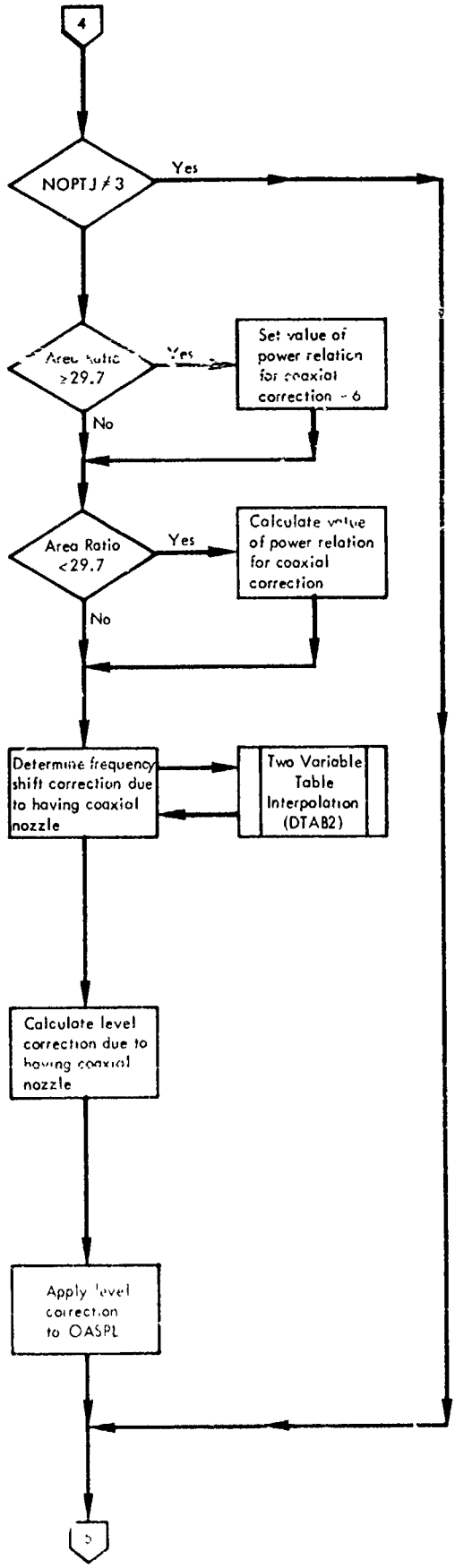

Figure 2-11. Continued.

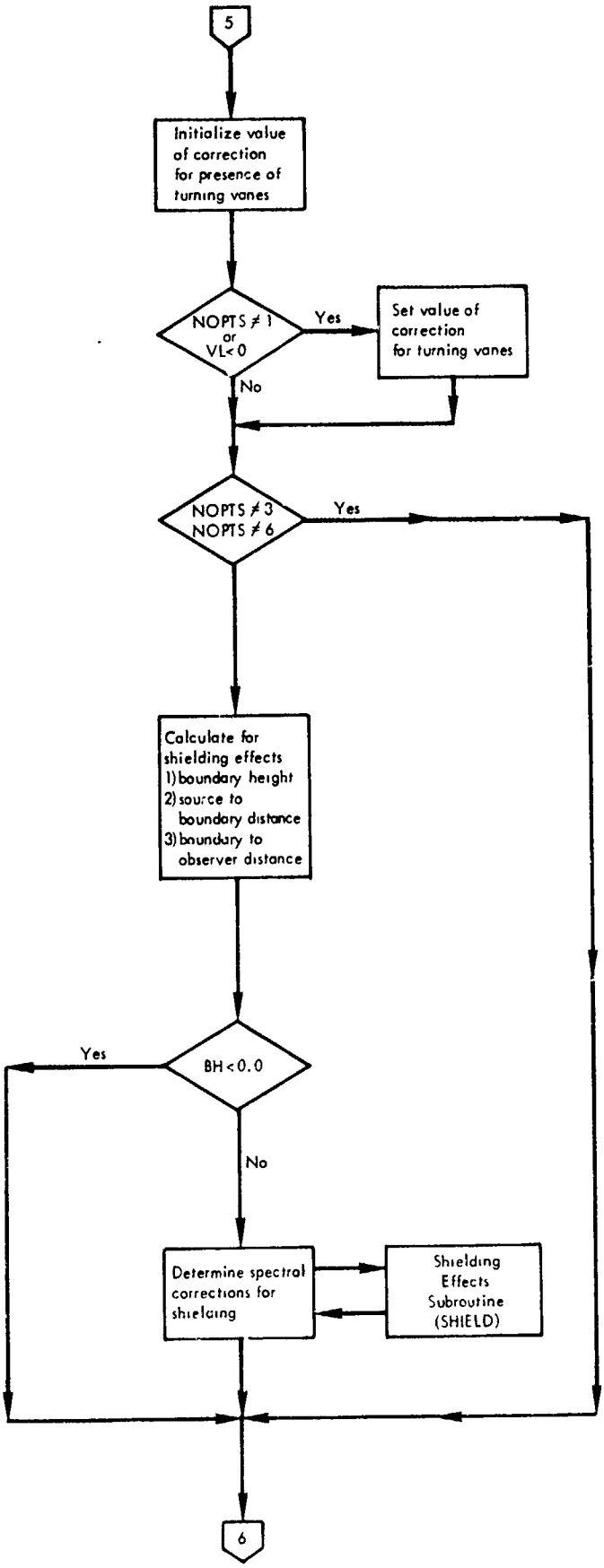

Figure 2-11. Continued.

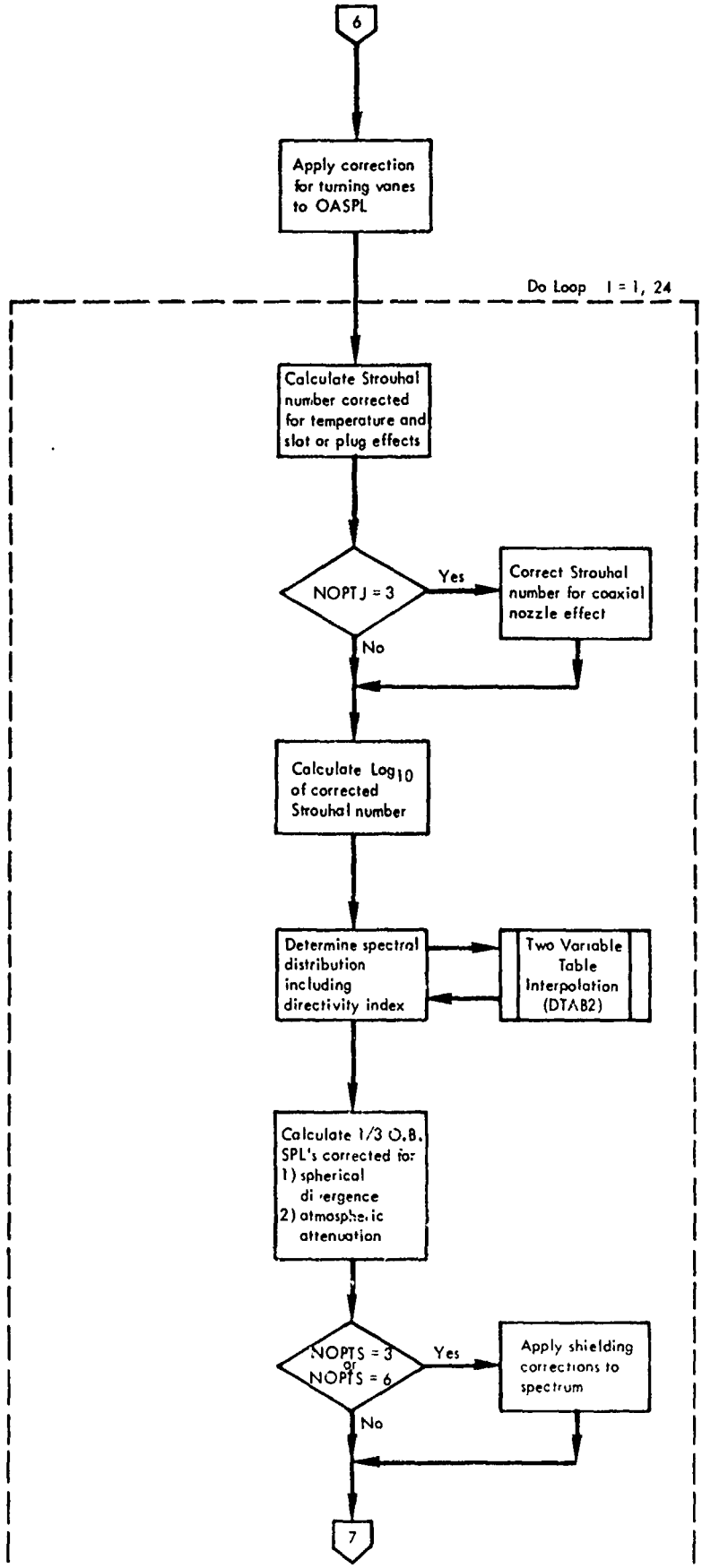

Figure 2-11. Continued.

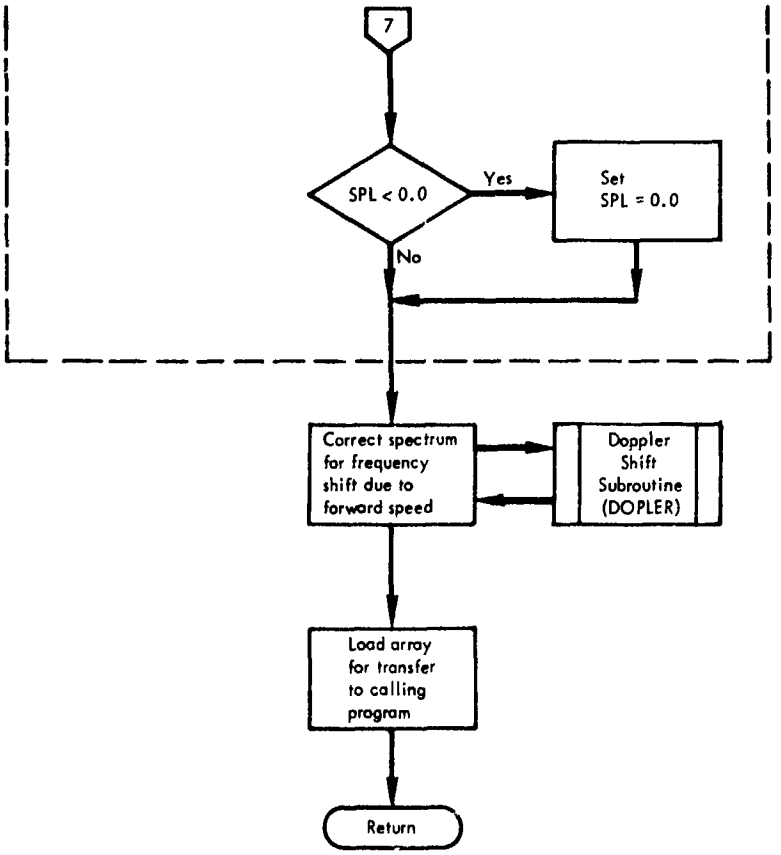

Figure 2-11. Continued.

4.3.5 EXCESS - Excess Engine Noise

This subroutine calculates the 1/3 octave-band spectrum for the excess engine noise source which includes core and tailpipe noise. The definition and discussion of this source and the prediction method is presented in Section 2.1.3.

The subroutine also calculates the geometrical relations (shown in Figure 2-8) needed to calculate the shielding effect when the USB (NOPTS = 3) or Hybrid (NOPTS = 6) option is exercised. The source is assumed to be located at the center of the nozzle exit for these calculations.

The required variables are:

(1) source to observer distance (STOD)
(2) azimuthal angle (AZMANG)
(3) atmospheric absorption coefficients (ALPHA)
(4) 1/3 o.b. center frequencies (F)
(5) engine nozzle angle relative to horizontal (ANGNOZ)
(6) diameter of equivalent unplugged circular nozzle (DEQUIV)
(7) velocity of equivalent unplugged circular nozzle (VEQUIV)
(8) key to determine type of high lift system (NOPTS).

If NOPTS = 3 or NOPTS = 6, the following are also required:

(1) distance along wing from projection of nozzle exit to wing trailing edge (X1)
(2) vertical distance from wing surface to center of nozzle exit (Y1)
(3) length of flaps (FLAP1, FLAP2, and FLAP3)
(4) flap angles (FLPAG1, FLPAG2, and FLPAG3).

The reference OASPL is given by

$$OASPL = 10 \cdot \log_{10}(100 \quad A \quad U^6)$$

where A = equivalent nozzle area $\left(\frac{DEQUIV^2 \cdot \pi}{4}\right)$

U = VEQUIV

The output is the 1/3 octave band spectrum.

Since this subroutine uses two values calculated in JET, it must never be called unless JET has previously been called.

The subroutine logic path is shown in the following chart (Figure 2-12).

EXCESS

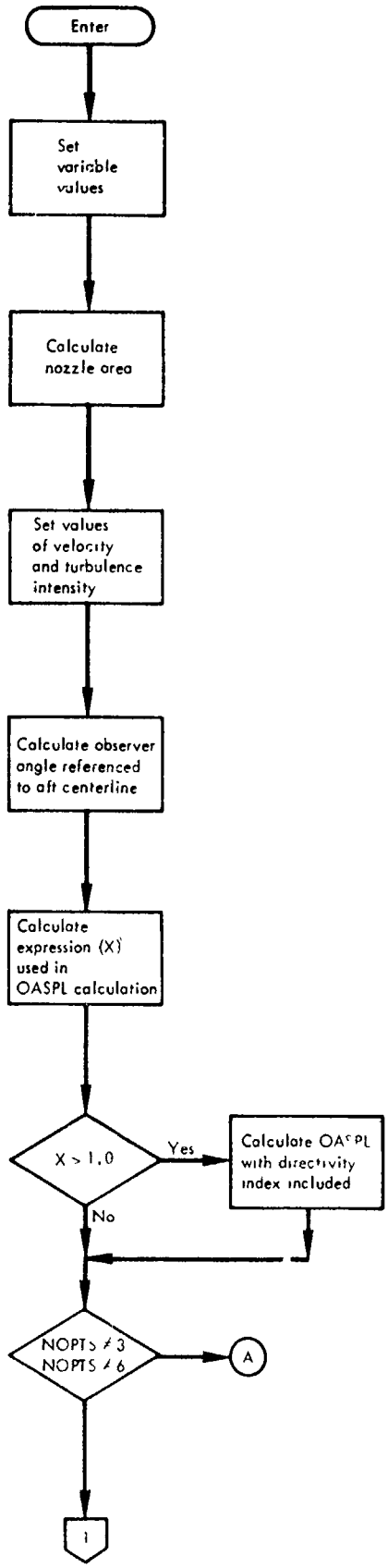

Figure 2-12. EXCESS Flow Chart.

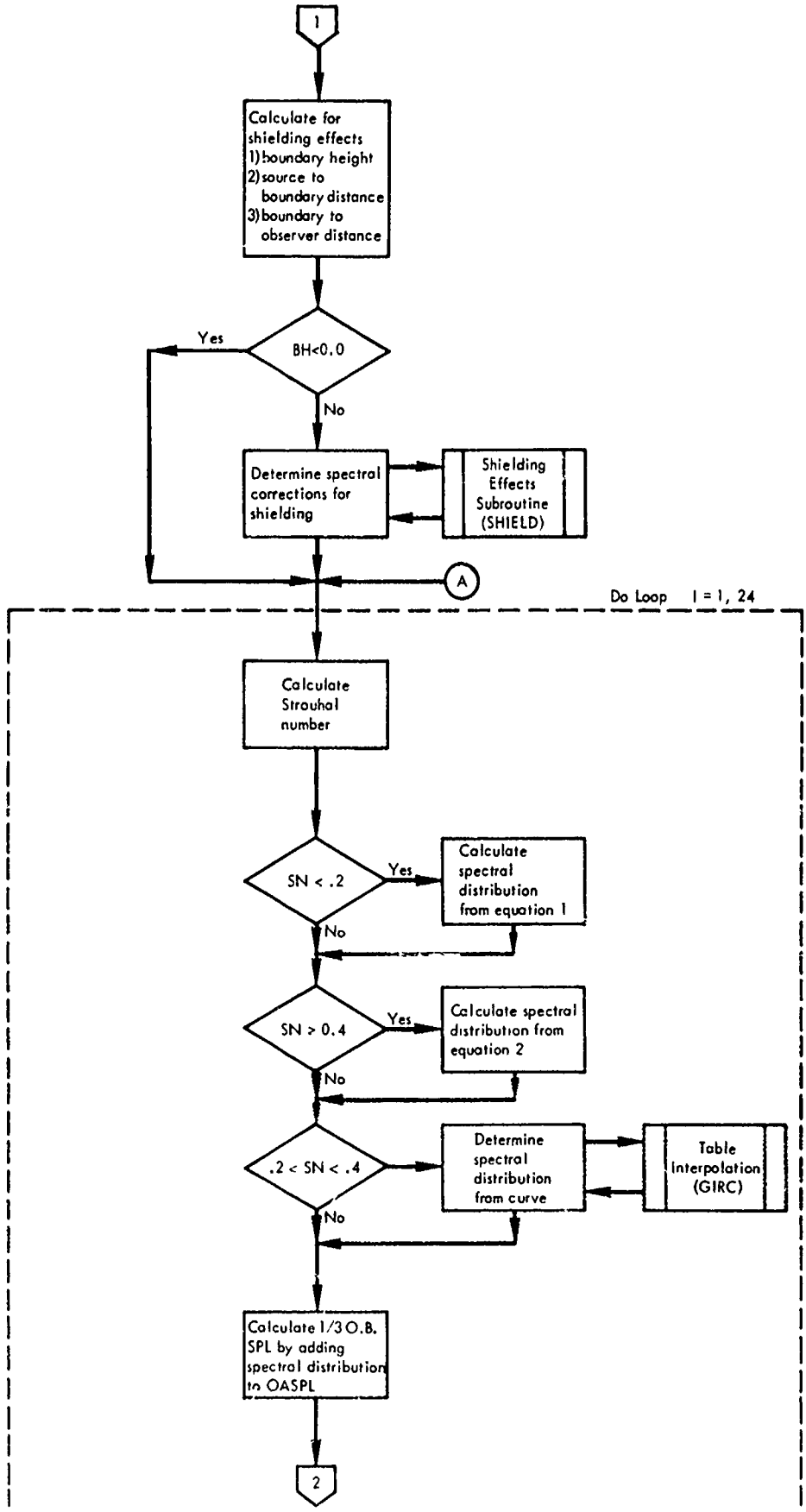

Figure 2-12. Continued.

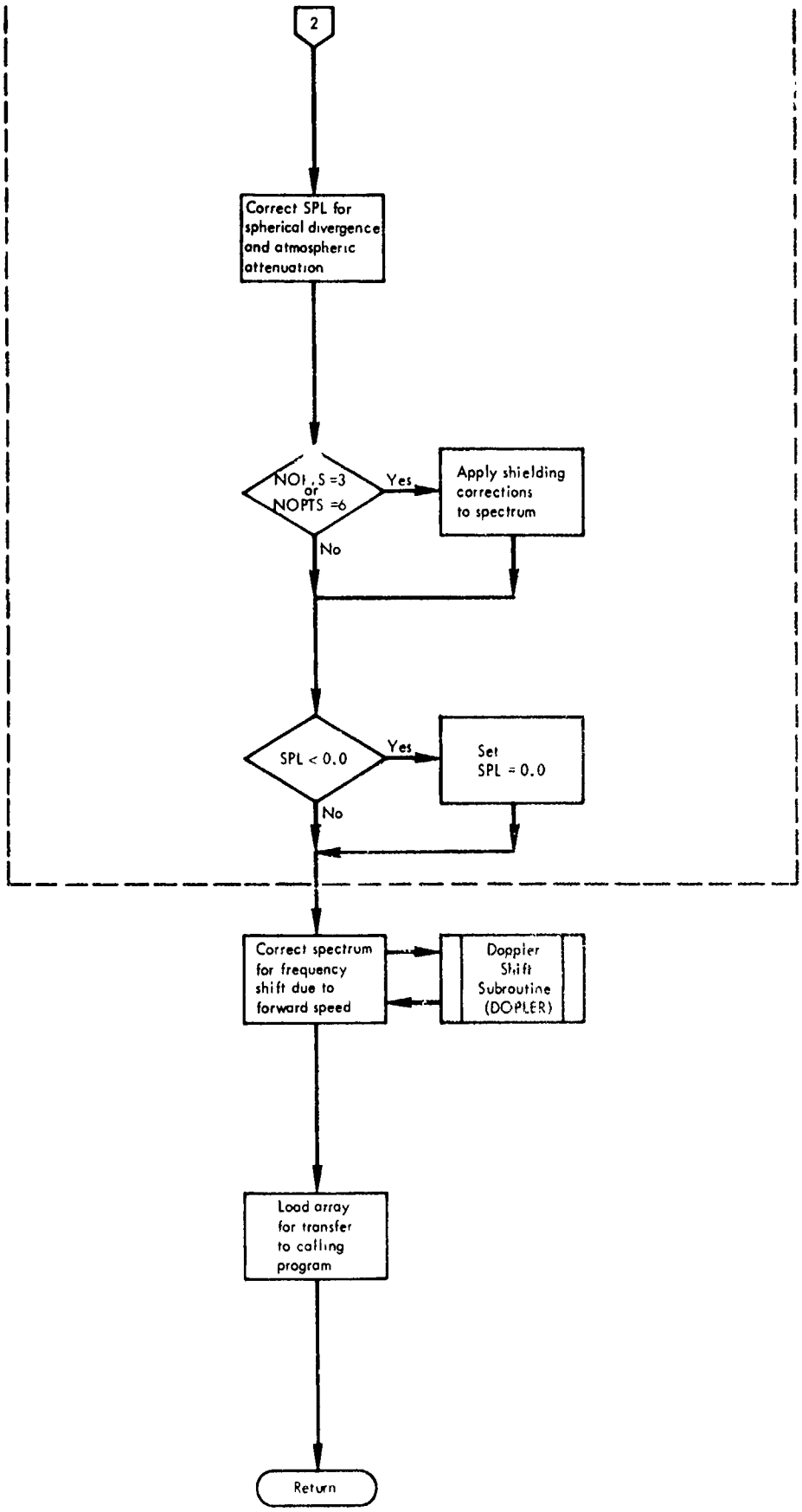

Figure 2-12. Continued.

4.3.6 AUGWNG - Augmentor Wing Noise

This subroutine calculates the 1/3 octave band-spectrum considering the entire augmentor wing high lift system as one source. This subroutine, therefore, should be called only for NOPTS = 5 (AW configuration) and should be the only high-lift noise source subroutine called. The methodology used to develop this prediction procedure is described in Section 2.3.5.

The required variables are:

(1) source-to-observer distance (STOD)
(2) azimuthal angle (AZMANG)
(3) elevation angle (ELVANG)
(4) atmospheric absorption coefficients (ALPHA)
(5) 1/3 o.b. center frequencies (F)
(6) height of wing slot nozzle (HWNOZ)
(7) width of wing slot nozzle (WWNOZ)
(8) velocity of wing slot nozzle exhaust (VJWNOZ)
(9) length of ejector (EJL)
(10) ejector angle (EJANG)

The reference OASPL is calculated using the expression,

$$OASPL = 60 \cdot \log_{10}(VJWNOZ) + 10 \cdot \log_{10}(AREA) - 5 \cdot \log_{10}(EJLHW/10) - 30.6$$

where

AREA = nozzle area (HWNOZ · WWNOZ)

EJLHW = ratio of ejector length to nozzle height (EJL/HWNOZ).

The output is the total 1/3 octave-band spectrum produced by the augmentor wing high-lift system.

In this calculation procedure the AW is considered to be a slot nozzle with hard-wall ejector. The use of multi-lobe nozzle with/or without lined ejector can reduce the noise levels substantially. The effect of these modifications

are determined in the noise reduction option described in Sections 4.1.2 and 4.4.6.

The subroutine logic path is shown in the following flow chart (Figure 2-13).

AUGWNG

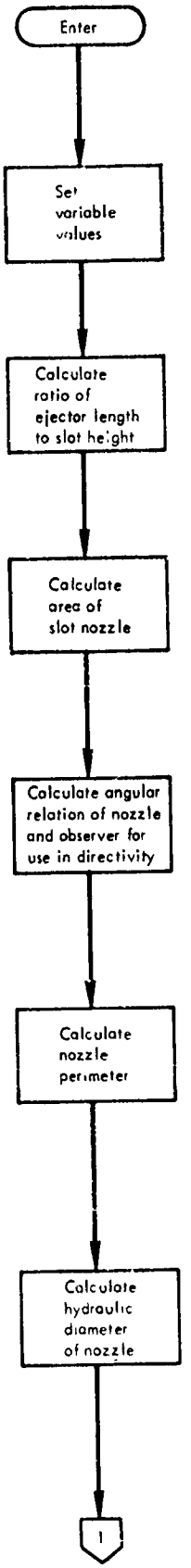

Figure 2-13. AUGWNG Flow Chart.

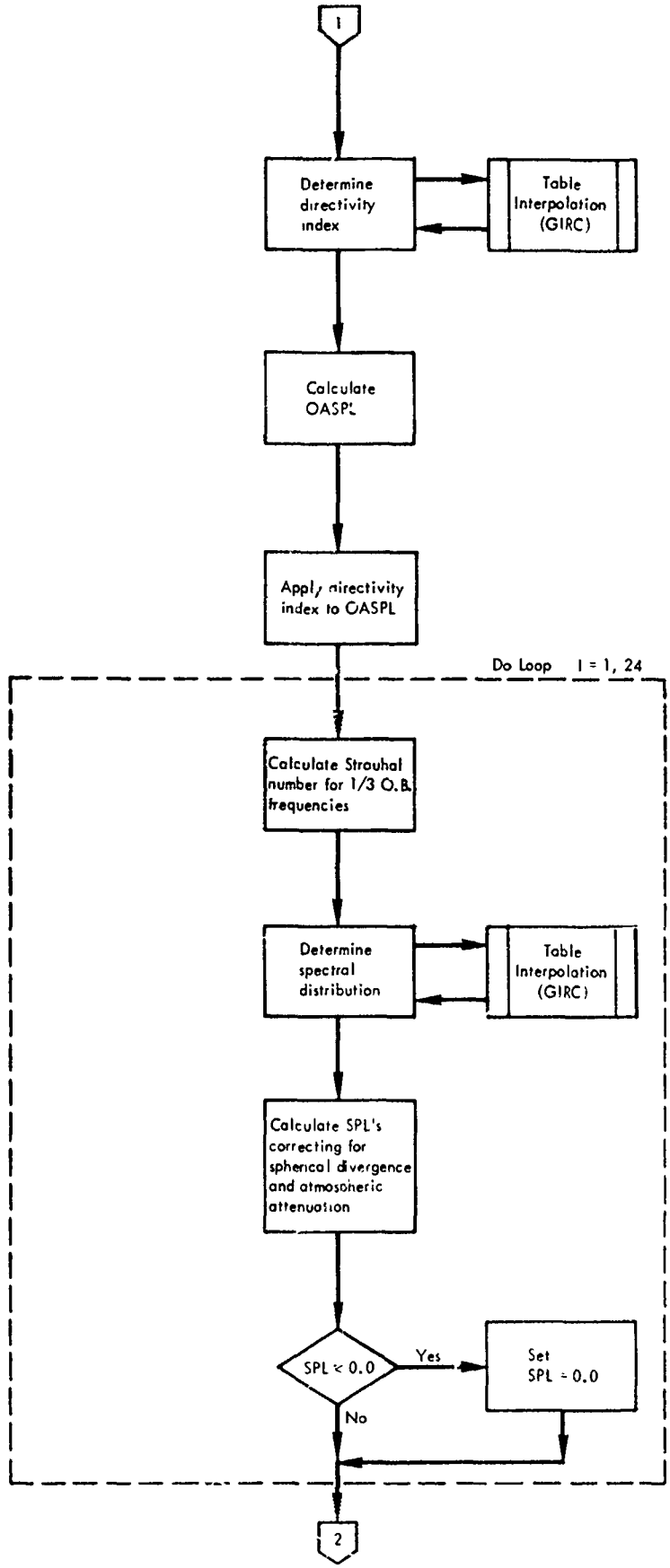

Figure 2-13. Continued.

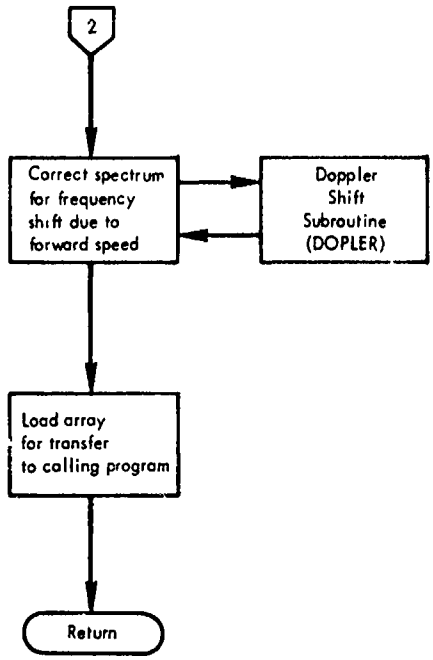

Figure 2-13. Continued.

4.3.7 WNGJET - Wing Jet Noise

This subroutine calculates the 1/3 octave band spectrum of jet noise from a wing slot nozzle. The methodology is the same used in JET. It assumes that the nozzle will be located at the wing trailing edge for the Hybrid (NOPTS = 6) and IBF/BLC (NOPTS = 4) configurations and at the last flap trailing edge for the IBF/JF (NOPTS = 4).

This subroutine calculates the diameter (DE) of the equivalent area circular nozzle; DEQUIV will be set to that value for the IBF (NOPTS = 4). Also, the value of VEQUIV is set to VJWNOZ for the IBF case.

The geometrical relations (Figure 2-8) needed to calculate the shielding effect are also calculated in this subroutine. The source is assumed to be located 2DE downstream from the nozzle exit. The shielding values are applied to the wing jet noise spectrum. The value of the shielding effect is set to 0.0 for the IBF/JF since the wing slot nozzle is at the flap trailing edge.

The required variables are:

(1) source-to-observer distance (STOD)
(2) azimuthal angle (AZMANG)
(3) atmospheric absorption coefficients (ALPHA)
(4) 1/3 o.b. center frequencies (F)
(5) height of wing slot nozzle (HWNOZ)
(6) width of wing slot nozzle (WWNOZ)
(7) velocity of wing slot nozzle (VJWNOZ)
(8) angle of nozzle centerline relative to horizontal plane (ANGWNZ)
(9) total temperature of wing slot nozzle exhaust (TTWNOZ)
(10) flap lengths (FLAP1, FLAP2, and FLAP3)
(11) flap angles (FLPAG1, FLPAG2, and FLPAG3).

The values of items 10 and 11 should be 0.0 for the IBF/JF configuration.

The reference OASPL is calculated using the same equation as shown in JET, Section 4.3.4, with the nozzle dimensions being those of the wing slot nozzle instead of the engine nozzle and the value of KA is always 134.

The output is the 1/3 octave band spectrum.

The subroutine logic path is shown in the following flow chart (Figure 2-14).

WNGJET

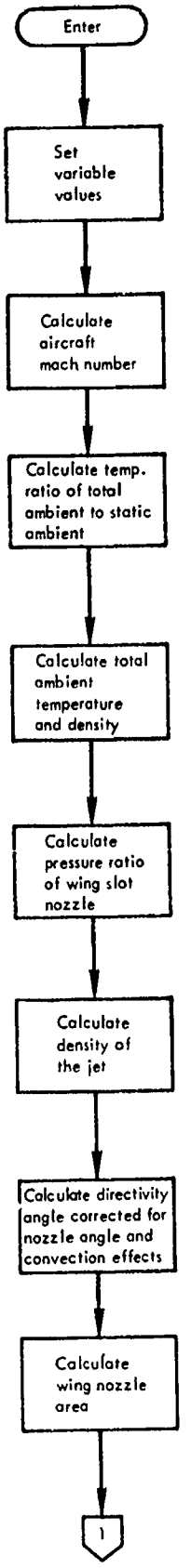

Figure 2-14. WNGJET Flow Chart.

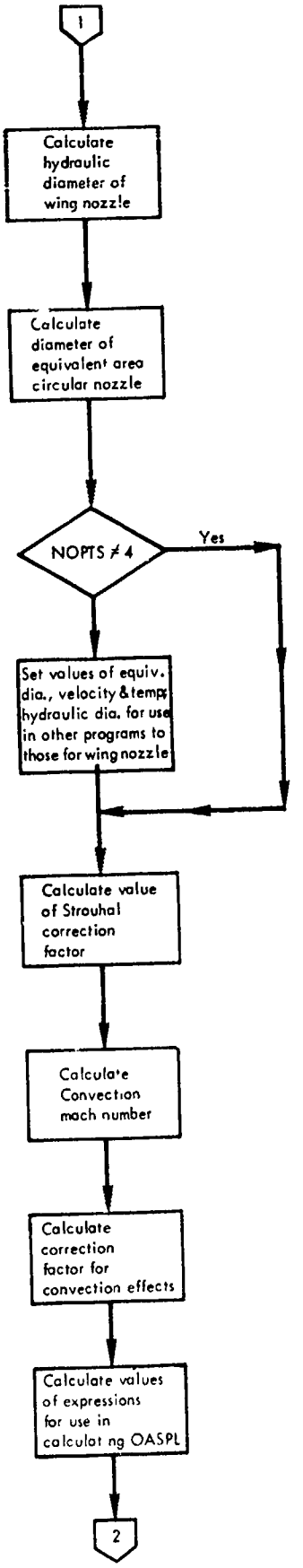

Figure 2-14. Continued.

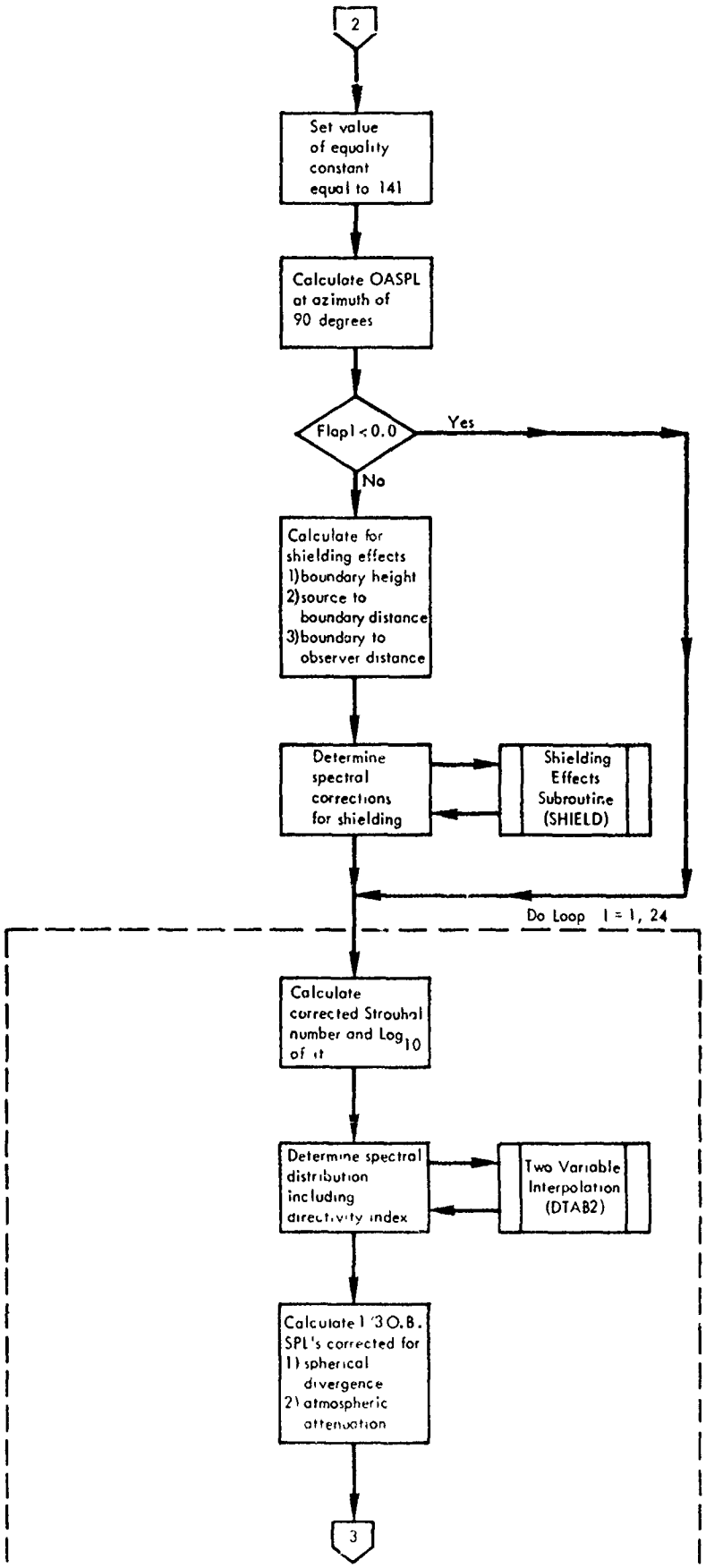

Figure 2-14. Continued.

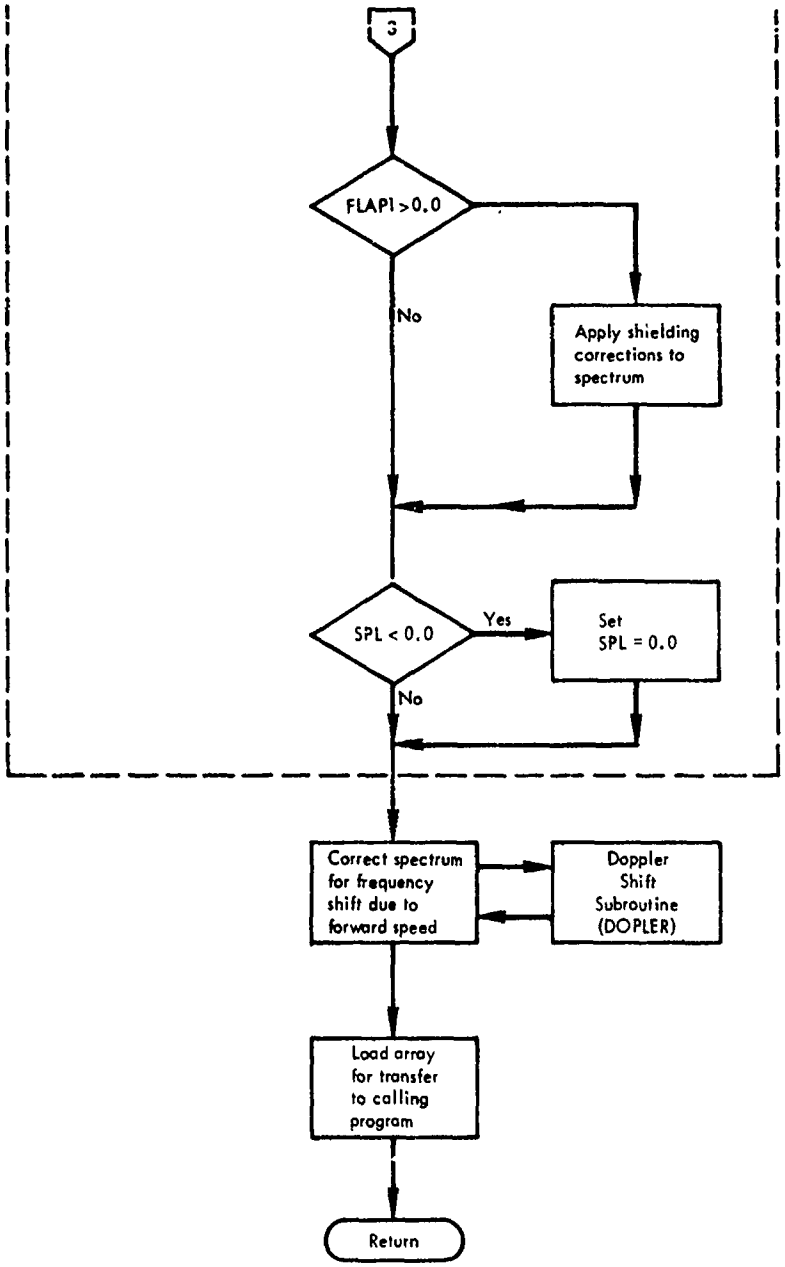

Figure 2-14. Continued.

4.3.8 IMPING - impingement Noise

This subroutine calculates the 1/3 octave-band spectrum for the jet flow impinging on the wing or flaps using the methodology developed in Section 2.3.1.

It is assumed that only the EBF, USB, and Hybrid can have impingement noise; therefore, this subroutine is set up to handle only these three configurations.

Using the geometrical parameters in Figure 2-15, the impingement area (AI) is calculated as a function of impingement velocity (VIP) and angle of impingement (ALPH) for calculating the reference OASPL.

The shielding effects of the wing and flaps for the USB and Hybrid configurations are programmed into the directivity indices which are applied in the calculation of OASPL.

The required variables are:

(1) key to determine type of high-lift system (NOPTS)
(2) source-to-observer distance (STOD)
(3) azimuthal angle (AZMANG)
(4) elevation angle (ELVANG)
(5) atmospheric absorption coefficients (ALPHA)
(6) 1/3 o.b. center frequencies (F)
(7) equivalent nozzle diameter from JET (DEQUIV)
(8) equivalent exhaust velocity from JET (VEQUIV)
(9) equivalent exhaust total temperature from JET (TTEQ)
(10) hydraulic diameter from JET (HD)
(11) angle between nozzle centerline and wing centerline (ALPHA1)
(12) distance along wing from projection of nozzle exit on the wing to wing t.e. (X1)
(13) vertical distance from the wing surface to the center of the nozzle exit (Y1)
(14) length of flaps (FLAP1, FLAP2, and FLAP3)
(15) flap angles (FLPAG1, FLPAG2, and FLPAG3)
(16) key to determine nozzle configuration (NOPTJ)

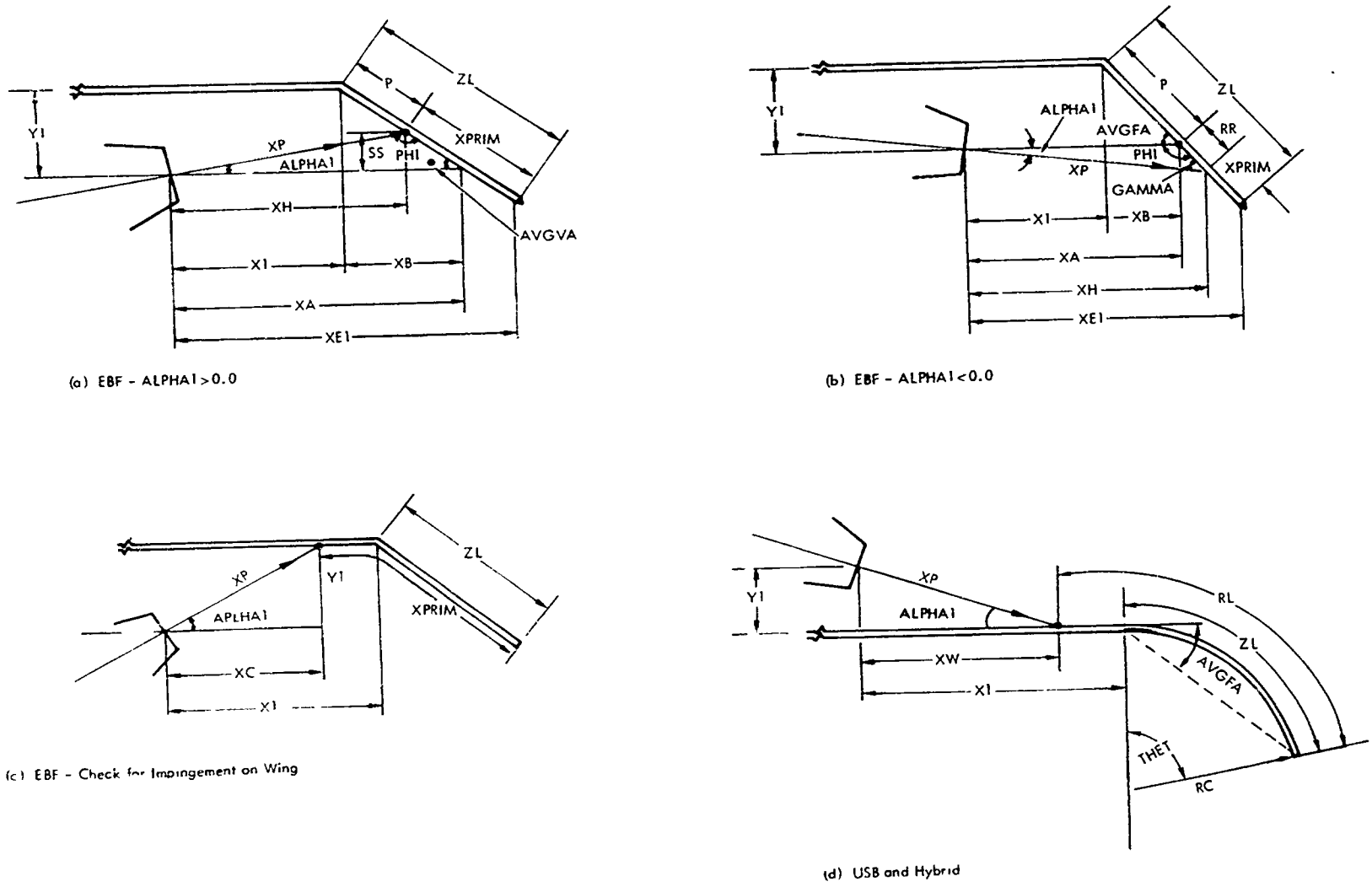

Figure 2-15. High Lift System Geometry Schematic

NOPTJ = 2

(17) height of engine slot nozzle (HNOZ)

(18) width of engine slot nozzle (WNOZ).

The reference OASPL is calculated using the expression,

$$OASPL = 10 \cdot \log_{10} \left(AI \cdot \sin^2 (ALPH)\right) + 80 \cdot \log_{10} (VIP) - 74.$$

The output is the 1/3 octave band spectrum.

The restrictions of this subroutine are:

(1) NOPTS must be 2, 3, or 6; values of 4 or 5 will send control back to STOLPROG with no calculations.

(2) flow for the USB and Hybrid must impinge on wing.

(3) JET must be called prior to IMPING.

The subroutine logic path is shown in the following chart (Figure 2-16).

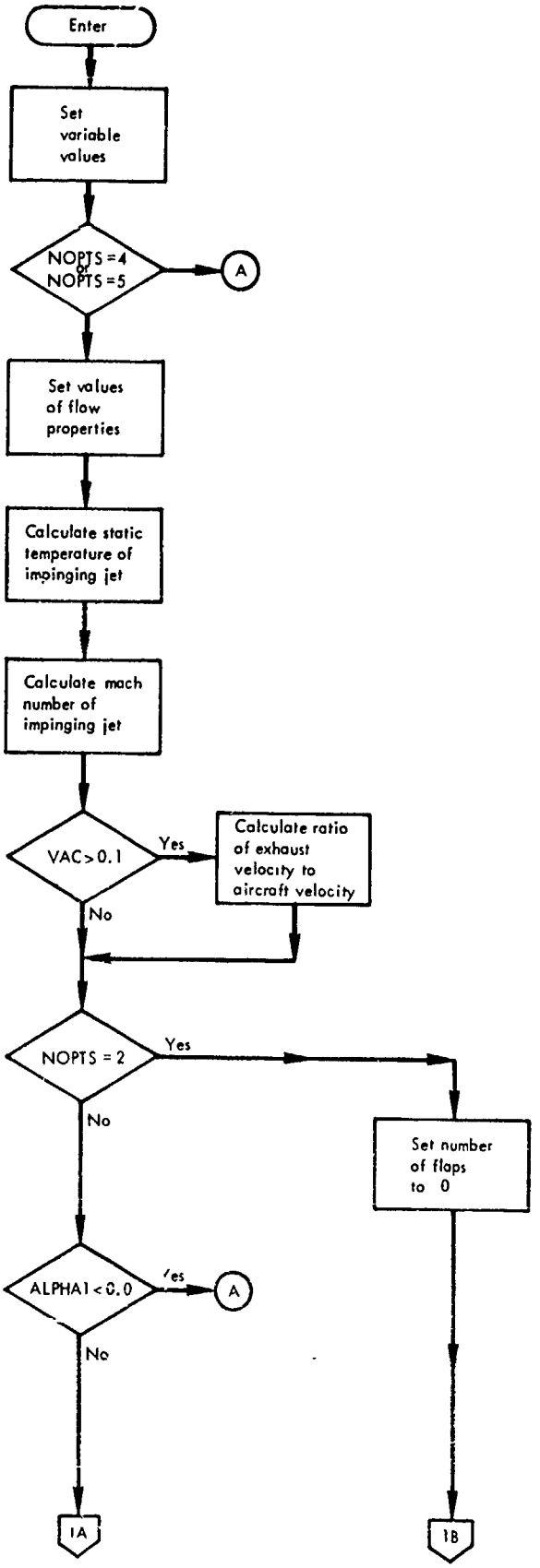

Figure 2-16. IMPING Flow Chart.

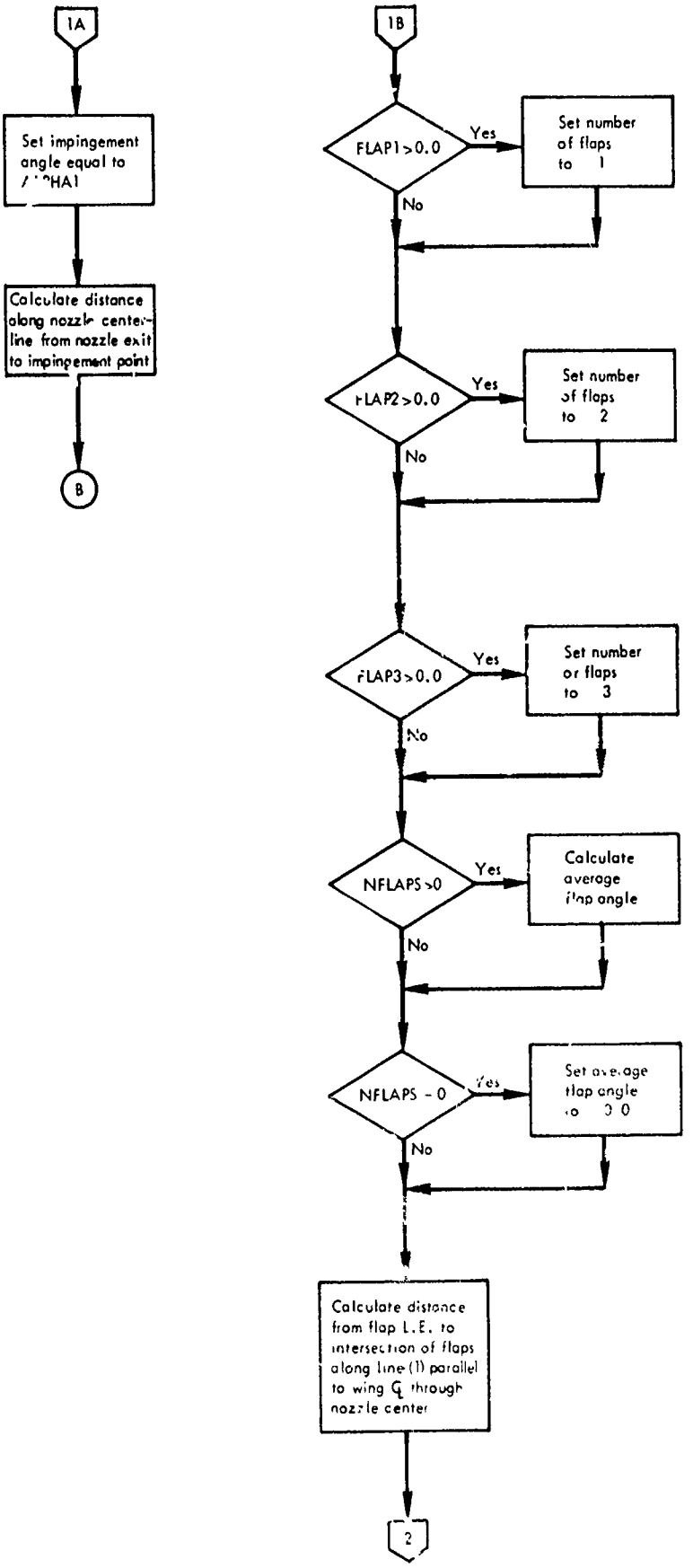

Figure 2-16. Continued.

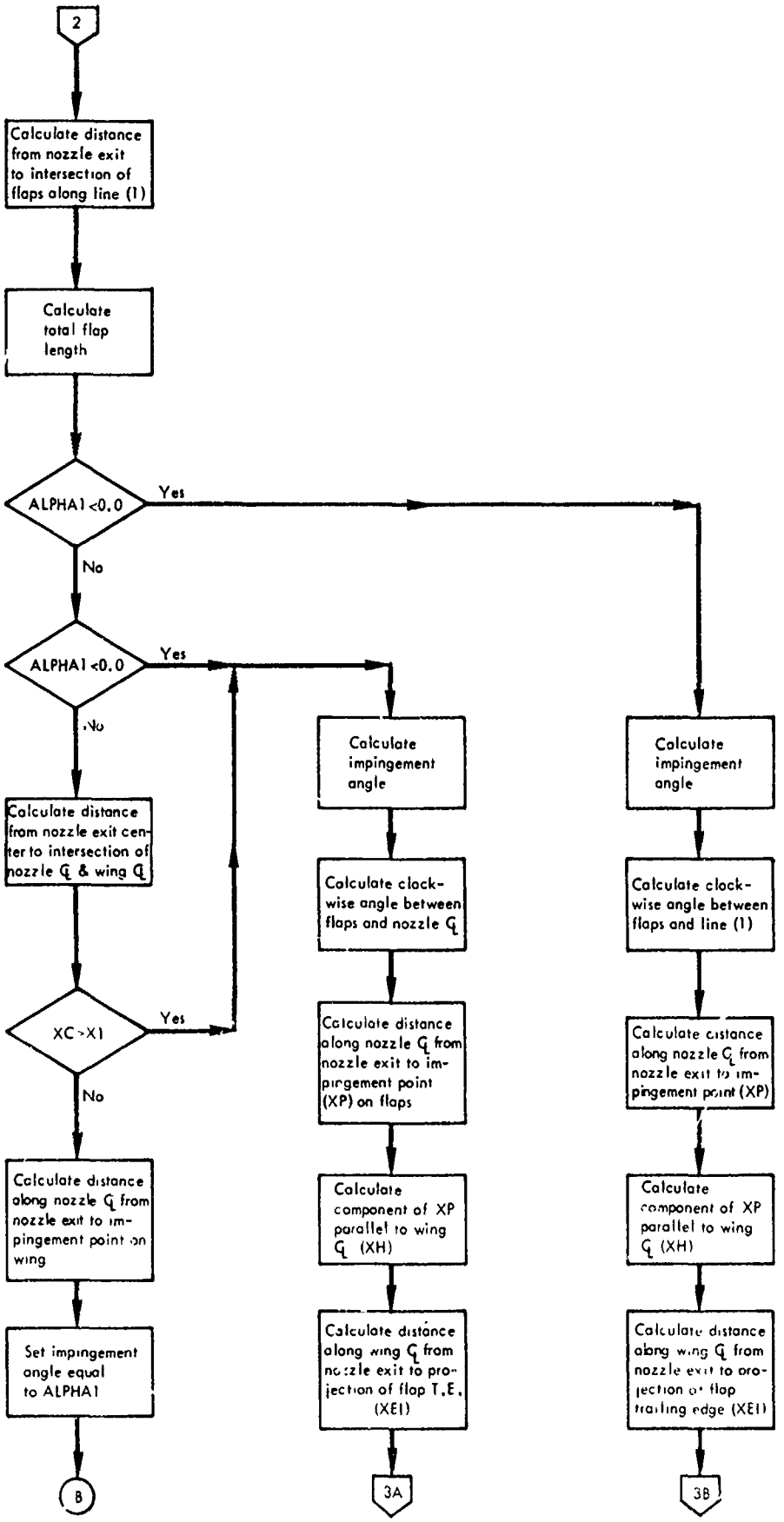

Figure 2-16. Continued.

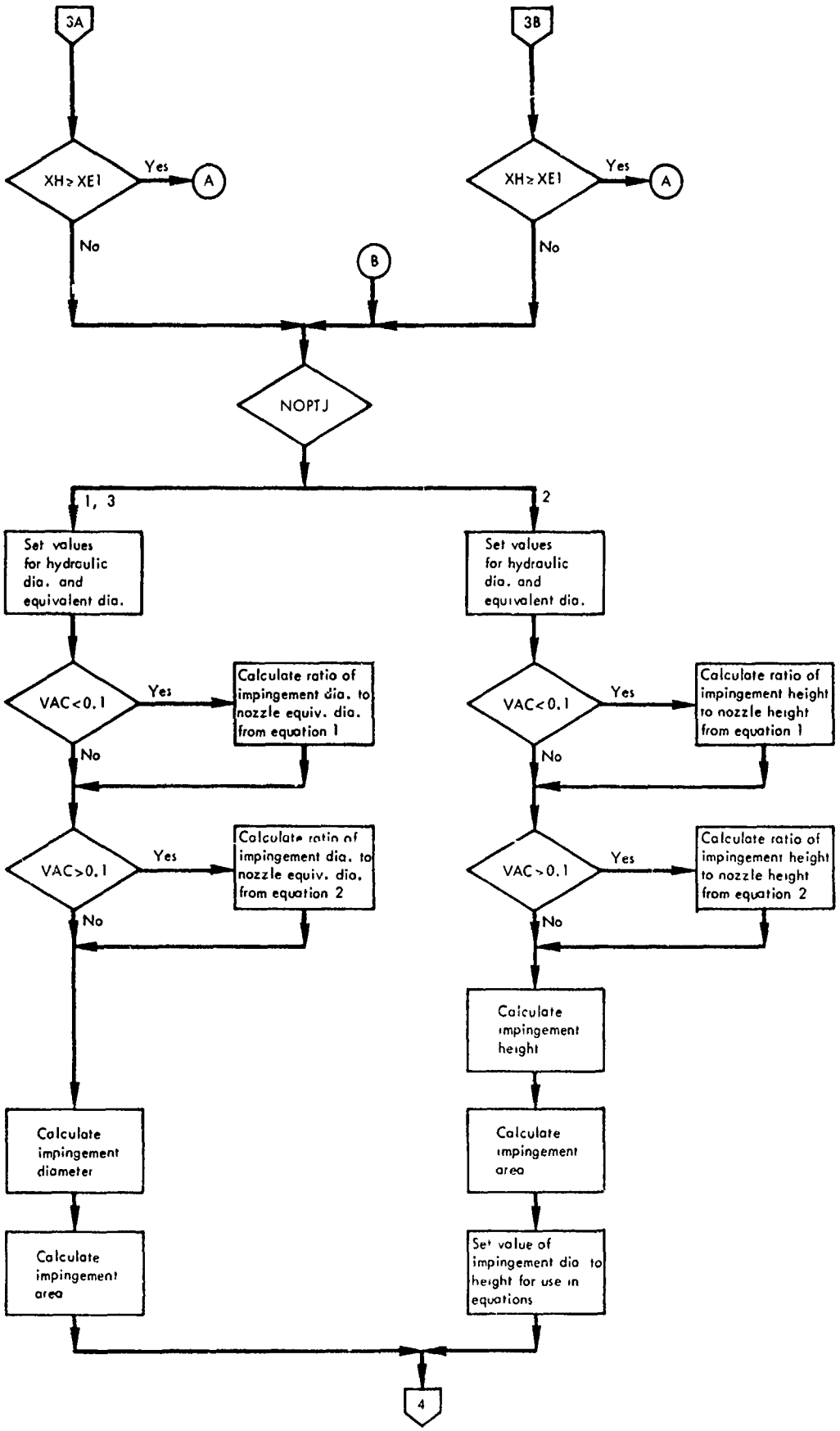

Figure 2-16. Continued.

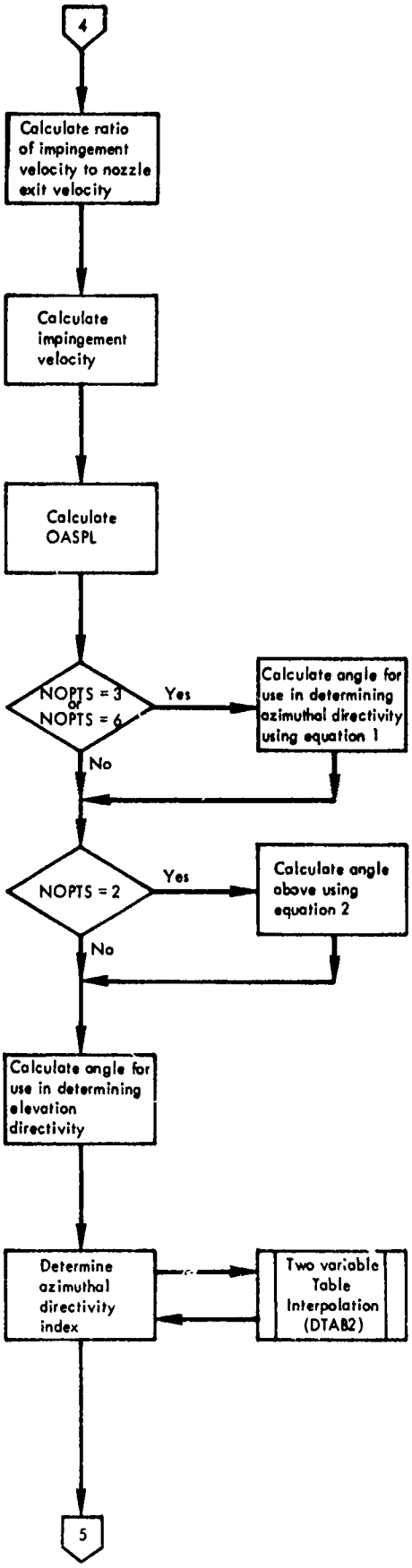

Figure 2-16. Continued.

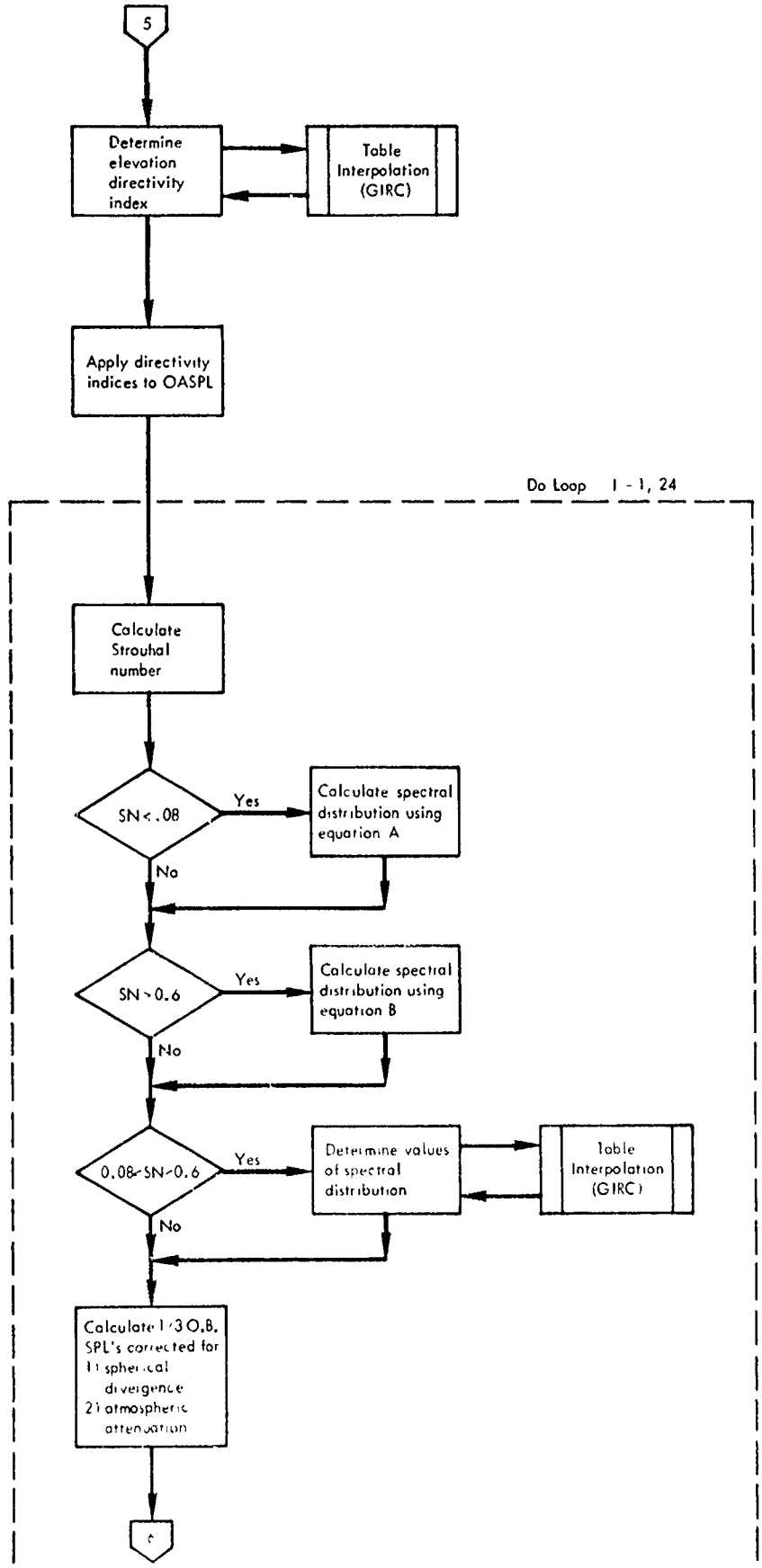

Figure 2-16. Continued.

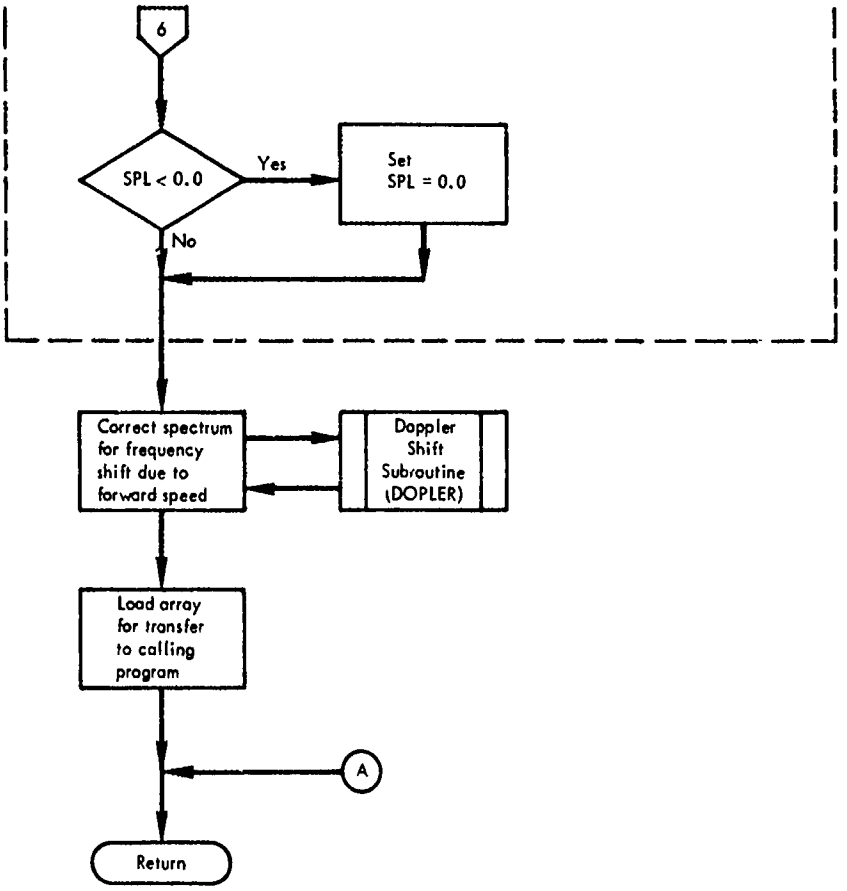

Figure 2-16. Continued.

4.3.9 WALJET - Wall Jet Noise

This subroutine calculates the 1/3 octave-band spectrum from the formation of the wall jet on the wing and/or flap surface, using the methodology developed in Section 2.3.2.

The basic geometrical relations used in this subroutine are the same as those shown in Figure 2-15 for IMPING. However, this subroutine must also calculate values of the flow parameters from the IBF/BLC wing slot nozzle over the surface. The relations used for IBF/BLC are the same as those shown for the USB and Hybrid with ALPHA1 and X1 being assumed to be 0.0.

The parameters associated with the flow over the surface are also calculated as shown in Figure 2-17. The EBF may have either a slot or circular/coaxial nozzle but the USB and Hybrid are assumed to have only a slot nozzle. The IBF/BLC is assumed to have a wing slot nozzle. The other three (VT, IBF/JF and AW) configurations do not have any wall jet flow and therefore, no provision is made to account for them.

The shielding effects of the wing and flaps for the USB, Hybrid and IBF/BLC configurations are programmed into the directivity indices which are applied to the reference OASPL.

The required variables are:

(1) key to determine type of high lift system (NOPTS)
(2) source-to-observer distance (STOD)
(3) azimuthal angle (AZMANG)
(4) elevation angle (ELVANG)
(5) atmospheric absorption coefficients (ALPHA)
(6) 1/3 o.b. center frequencies (F)
(7) flap lengths (FLAP1, FLAP2, and FLAP3)
(8) flap angle (FLPAG1, FLPAG2, and FLPAG3).

NOPTS = 2, 3, or 6

(1) equivalent nozzle diameter form JET (DEQUIV)
(2) equivalent exhaust velocity from JET (VEQUIV)

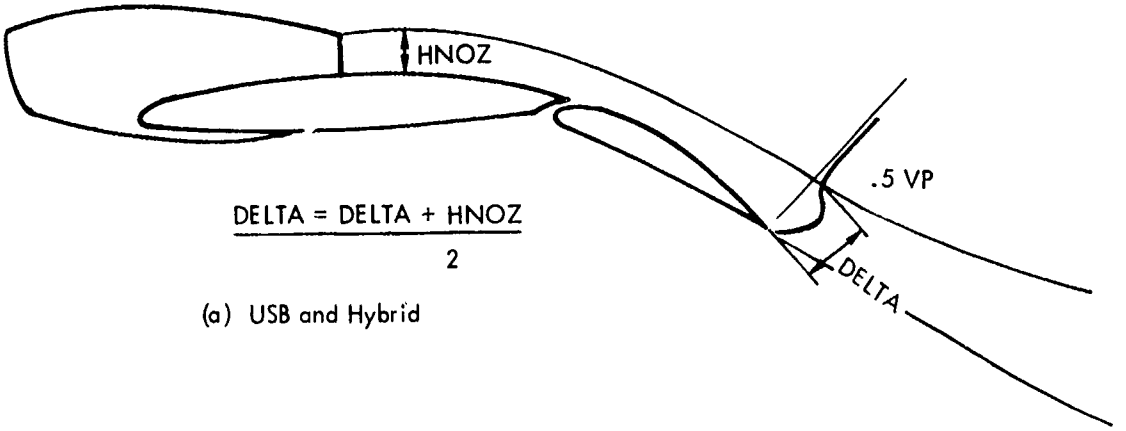

(a) USB and Hybrid

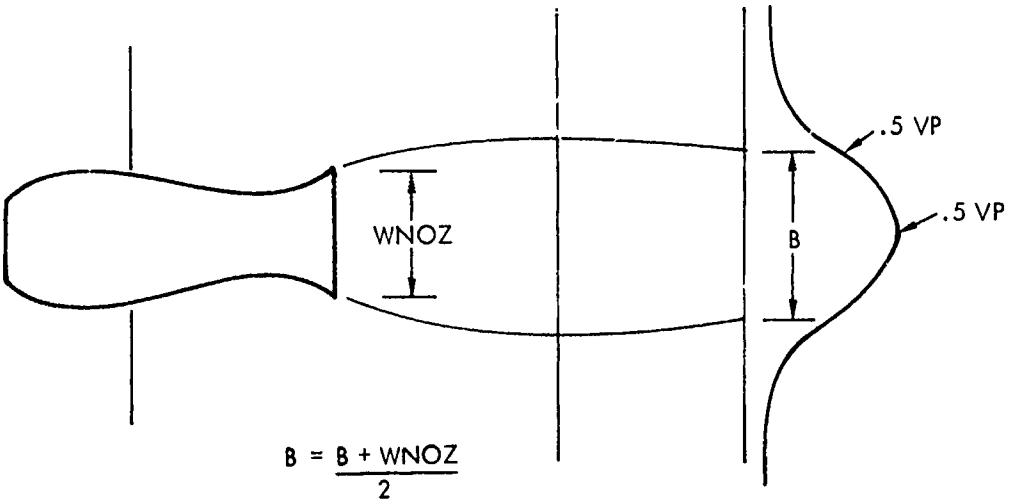

(b) USB and Hybrid

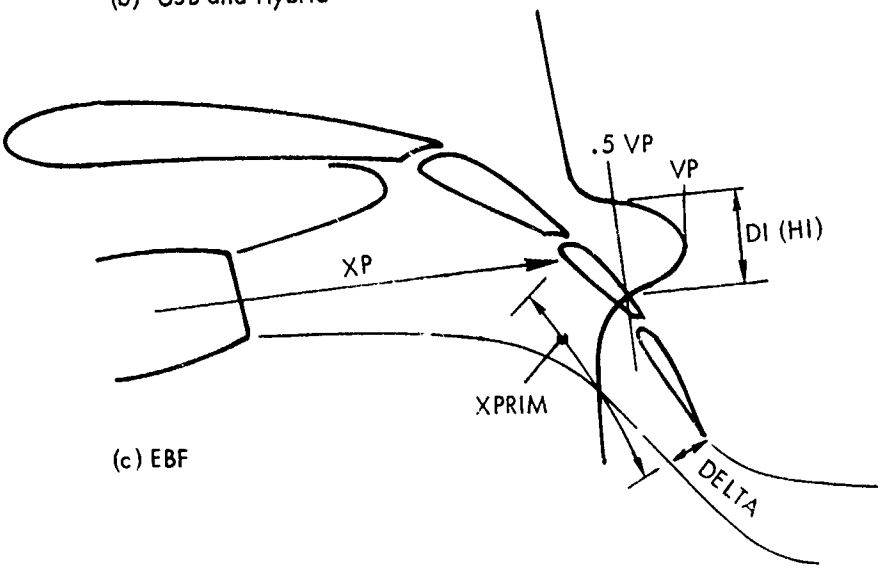

(c) EBF

Figure 2-17. Flow Geometry Schematic

(3) equivalent exhaust total temperature from JET (TTEQ)

(4) angle between engine nozzle ℄ and wing ℄ (ALPHA1)

(5) distance along the wing from projection of engine nozzle center to wing t.e. (X1)

(6) vertical height from the wing surface to nozzle center (Y1)

(7) key to determine engine nozzle configuration (NOPTJ)

NOPTJ = 2

(8) height of engine slot nozzle (HNOZ)

(9) width of engine slot nozzle (WNOZ)

NOPTS = 4

(1) equivalent nozzle diameter from WNGJET (DEQUIV)

(2) equivalent exhaust velocity from WNGJET (VEQUIV)

(3) equivalent exhaust total temperature from WNGJET (TTEQ)

(4) height of wing slot nozzle (HWNOZ)

(5) width of wing slot nozzle (WWNOZ)

The reference OASPL is calculated using one of the following expressions,

NOPTS = 2

$$OASPL = 10 \cdot \log_{10} (XPRIM \cdot B) + 80 \log_{10}(U) - 105$$

where U = VEQUIV,

NOPTS = 3, 4, or 6

$$OASPL = 10 \cdot \log_{10} (RL \cdot B) + 80 \log_{10}(U) - 105$$

where U = VEQUIV.

The output is the 1/3 octave-band spectrum.

The restrictions of this subroutine are:

(1) USB, Hybrid and IBF/BLC must use slot nozzles.

(2) JET or WNGJET must be called prior to WALJET.

The subroutine logic path is shown in the following flow chart (Figure 2-18).

WALJET

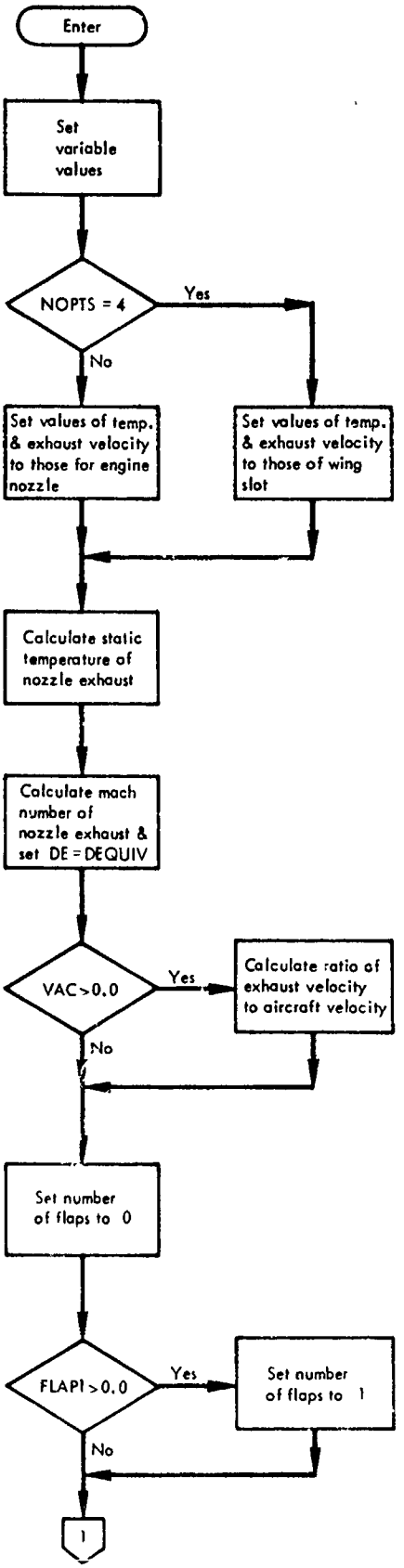

Figure 2-18. WALJET Flow Chart.

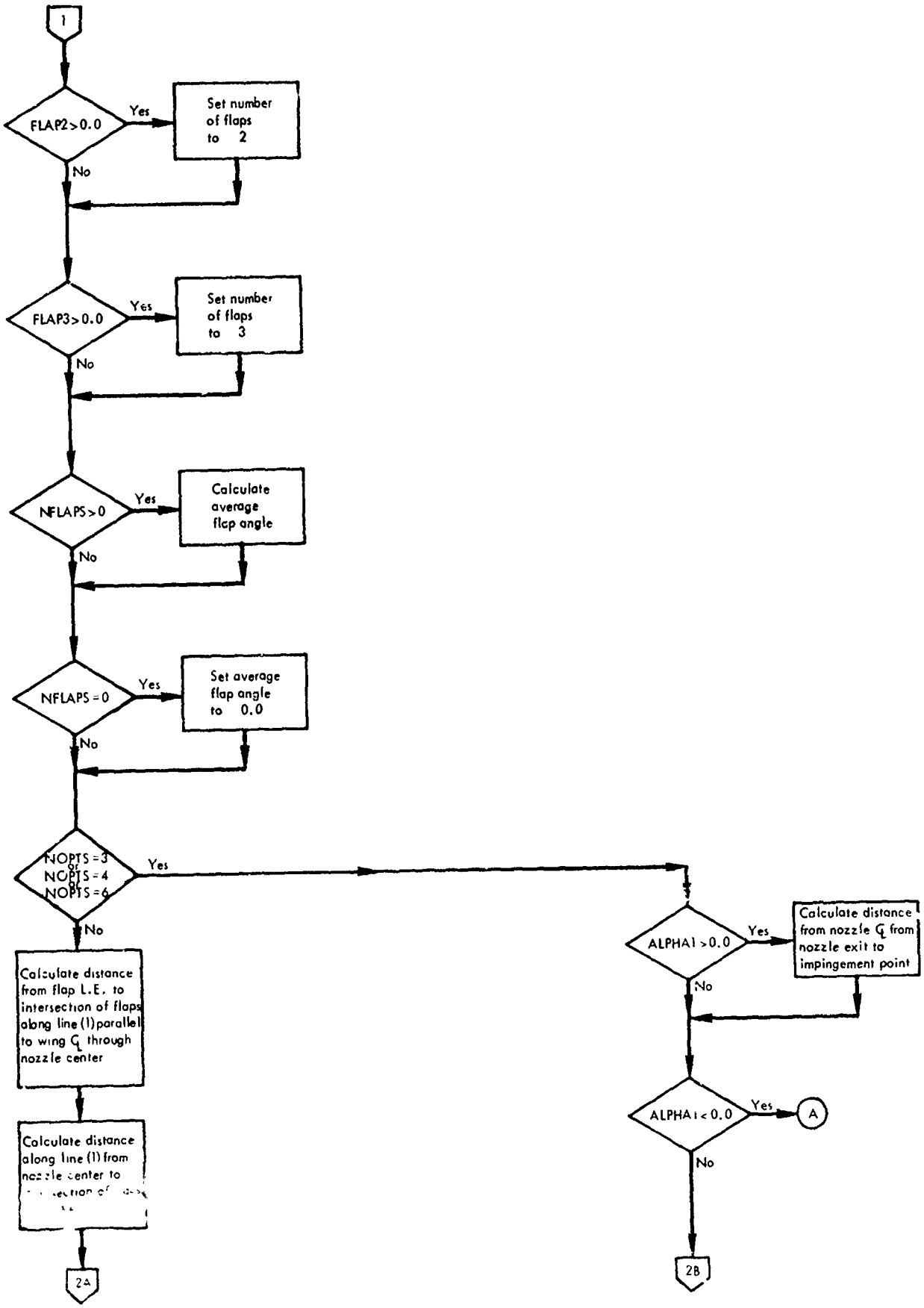

Figure 2-18. Continued.

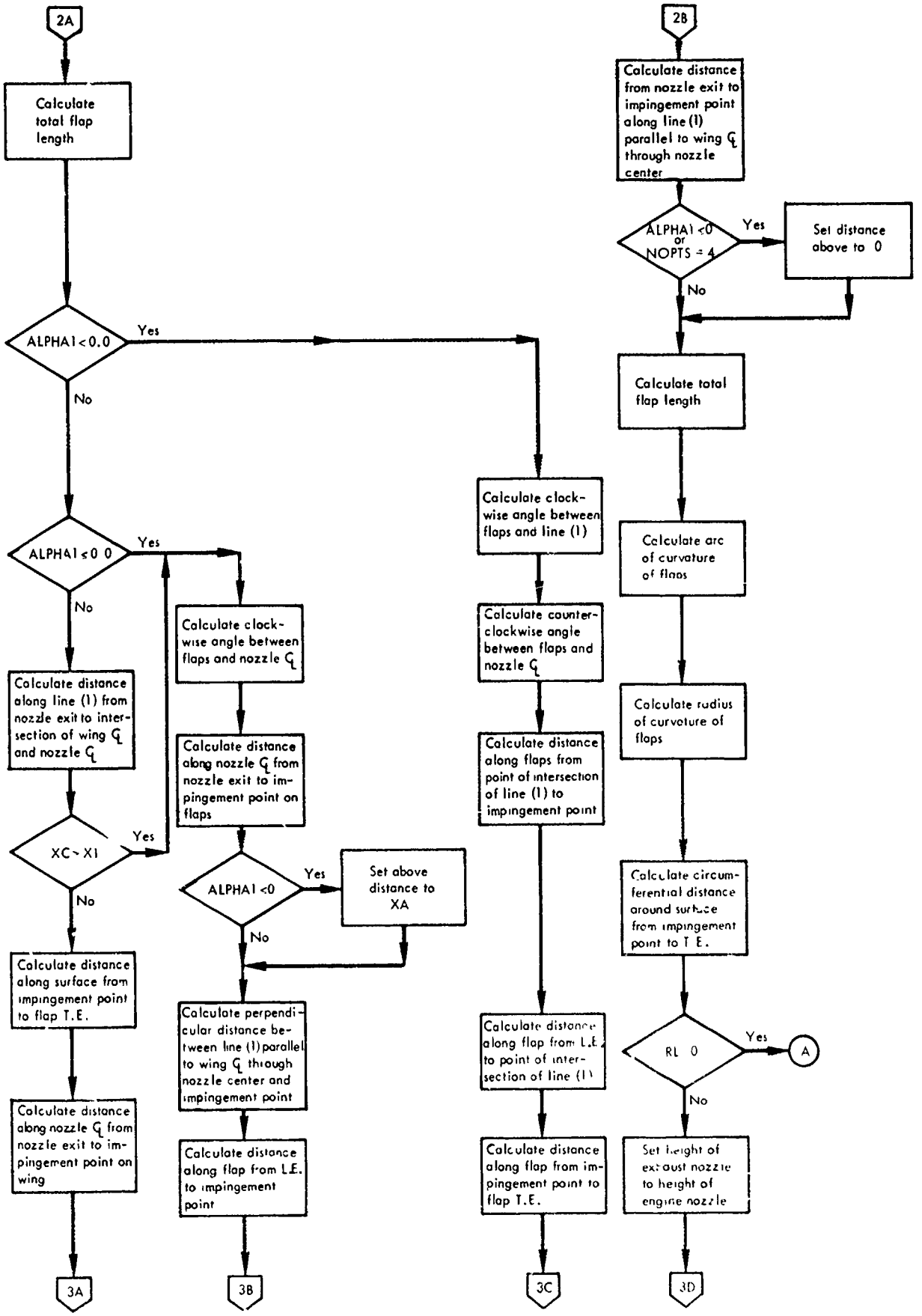

Figure 2-18. Continued.

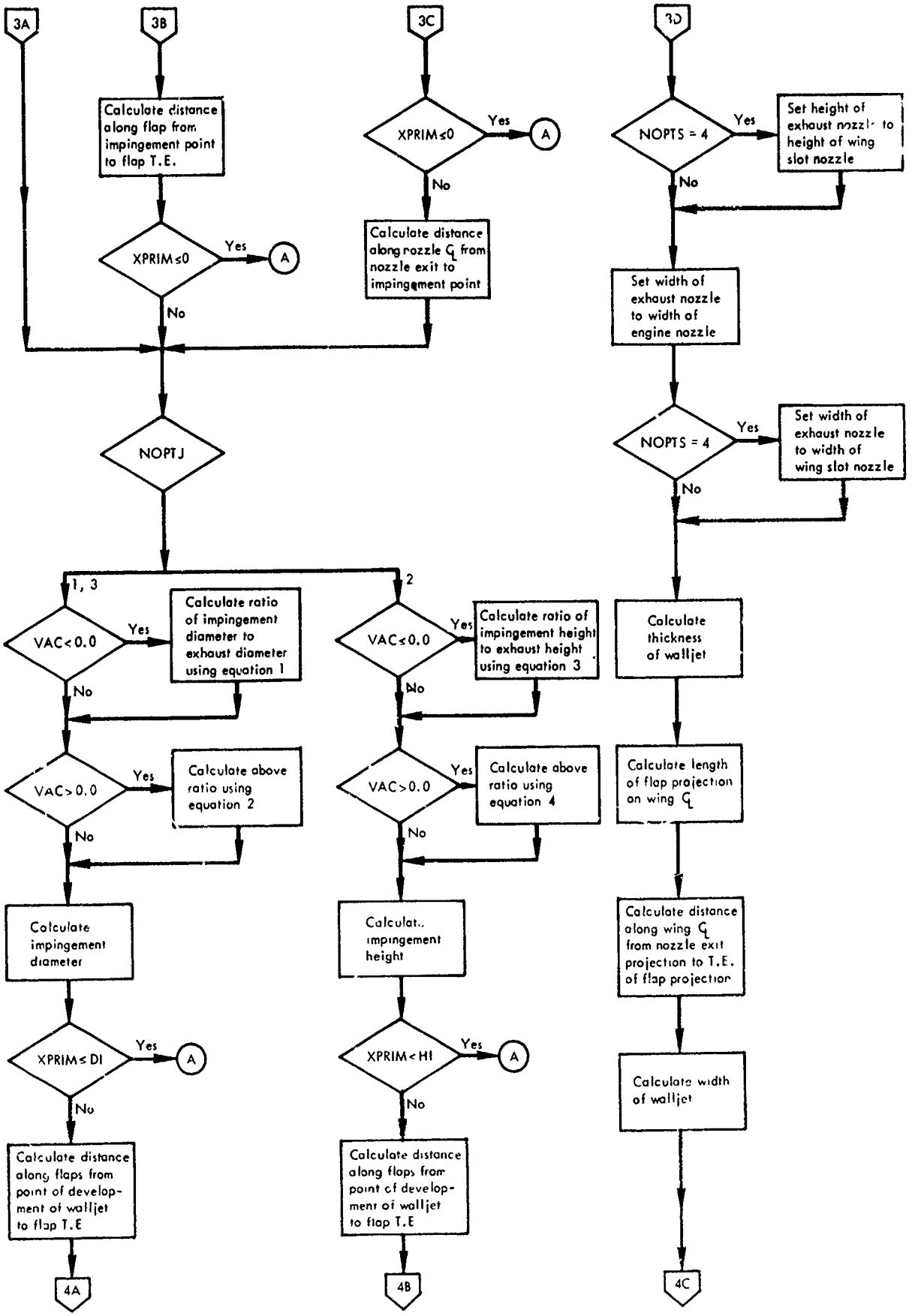

Figure 2-18. Continued.

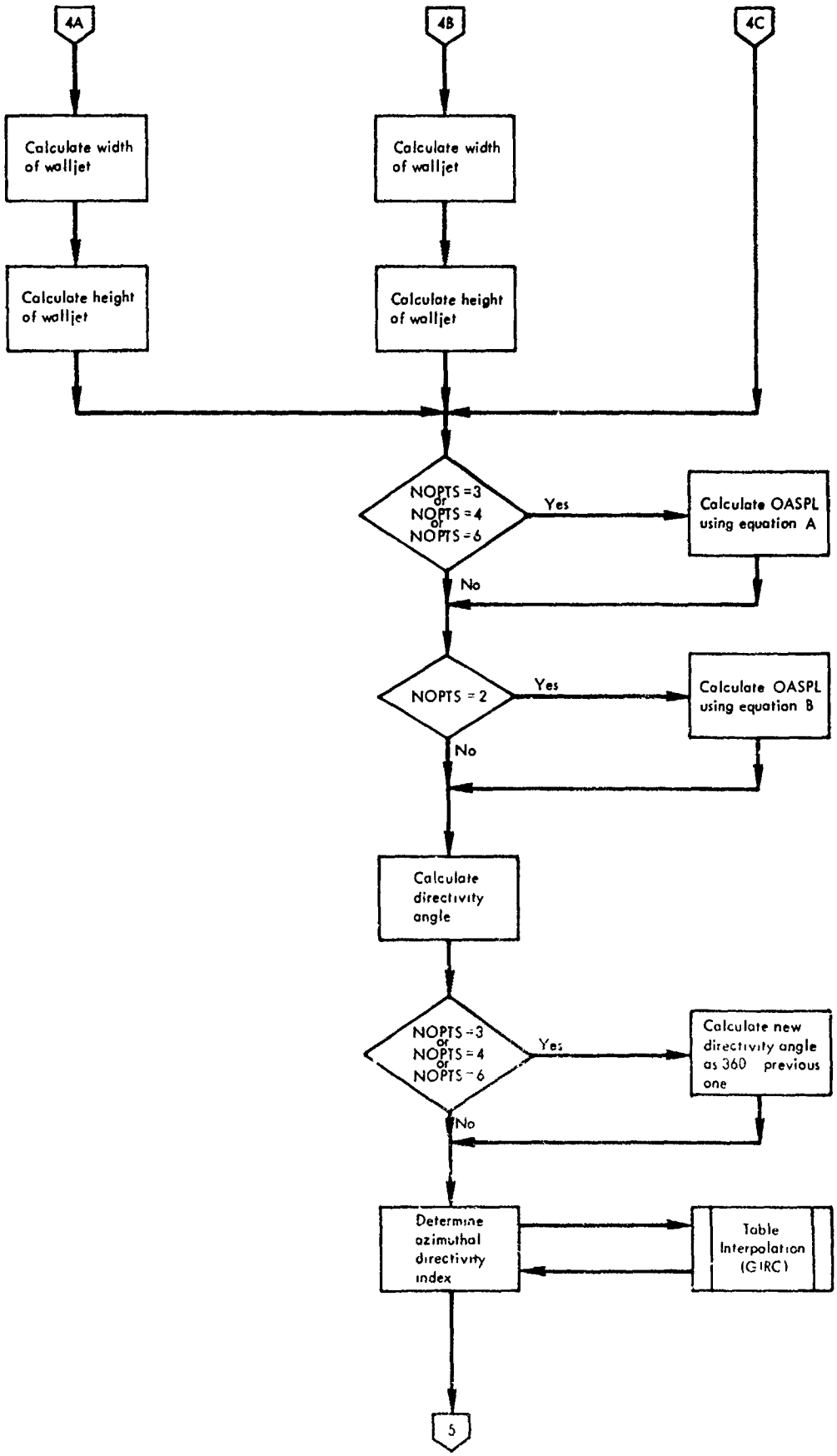

Figure 2-18. Continued.

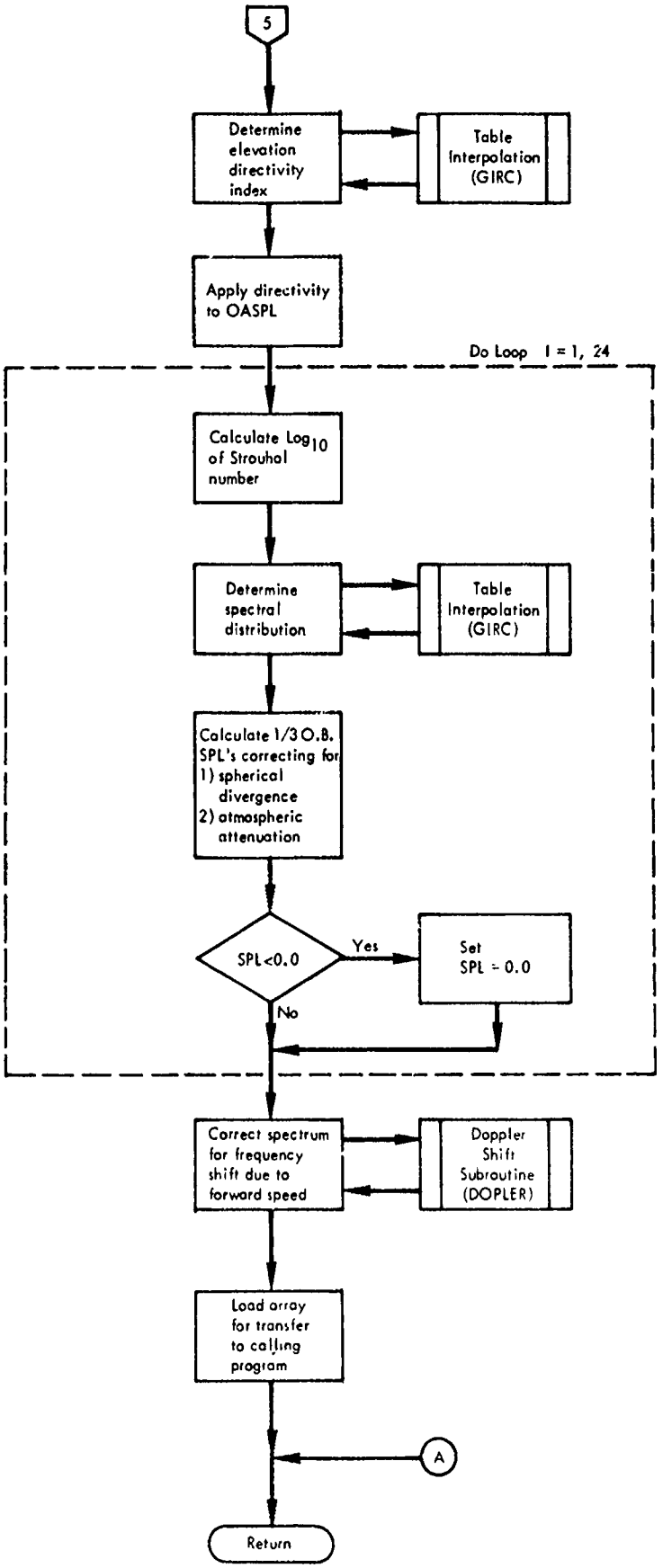

Figure 2-18. Continued.

4.3.10 WAKE - Trailing Edge Wake Noise

This subroutine calculates the total 1/3 octave-band spectrum of the noise levels generated in the wake of the propulsive high-lift airflow downstream of the flap trailing edge. The methodology for the calculation procedure is discussed in Section 2.3.4.

This subroutine should normally be called for NOPTS = 2 (EBF), 3 (USB), 4 (IBF/BLC), and 6 (HYBRID). For NOPTS = 4 (IBF/JF), this subroutine should not be called. For the Hybrid configuration, wake noise is calculated only for the engine exhaust airflow; the wake noise component of the flow from the slot nozzle is assumed to be insignificant.

The geometrical relationships required by WAKE are calculated within the subroutine and are shown in Figure 2-15. The geometry for IBF/BLC is similar to Figure 2-15(d), except ALPHA1 is assumed equal to zero. Shielding is not applied to wake noise.

The key input variables are:

(1) key to determine type of high-lift system (NOPTS)
(2) 1/3 o.b. center frequencies (F)
(3) atmospheric absorption coefficients (ALPHA)
(4) source-to-observer distance (STOD)
(5) azimuthal angle (AZMANG)
(6) flap lengths (FLAP1, FLAP2, and FLAP3)
(7) flap angles (FLPAG1, FLPAG2, and FLPAG2).

If NOPTS = 2, 3, or 6, the following are required for the engine exhaust nozzle:

(1) distance from nozzle exit to wing trailing edge measured parallel to wing centerline (X1)
(2) distance from nozzle exit to wing surface measured perpendicular to wing centerline (Y1)
(3) angle between nozzle centerline and wing centerline (ALPHA1)
(4) jet equivalent exhaust velocity (VEQUIV)
(5) jet equivalent exhaust total temperature (TTEQ)

(6) nozzle exit equivalent diameter (DEQUIV)

(7) nozzle exit hydraulic diameter (HD).

For NOPTS = 2, NOPTJ is also required; a key to indicate nozzle exit geometry.

For NOPTS = 2, NOPTJ is also required; a key to indicate nozzle exit geometry. ters required are:

(1) height of the slot nozzle (HNOZ)

(2) width of the slot nozzle (WNOZ).

If NOPTS = 4, the following wing nozzle parameters are needed:

(1) jet total temperature (TTWNOZ)

(2) jet exhaust velocity (VJWNOZ)

(3) height of the wing nozzle (HWNOZ)

(4) width of the wing nozzle (WWNOZ)

(5) distance from nozzle exit to wing trailing edge measured parallel to wing centerline (normally = 0.0) (X1).

The expression used for OASPL in this subroutine is:

$$OASPL = 10 \log_{10} (DELTA \cdot B) + 80 \log_{10} (VTE) - 111.0$$

where VTE is the velocity at the trailing edge and DELTA and B are illustrated in Figure 2-17.

The restrictions are: (1) For NOPTS = 4 (IBF/BLC), this subroutine assumes that ALPHA1 will be input as zero and that Y1 will be input as HWNOZ/2, and (2) for NOPTS = 3 (USB) and 6 (HYBRID), the engine nozzle exit dimensions must be described in terms of an equivalent nozzle height and width if a slot nozzle is not used.

The output is the 1/3 octave-band spectrum for the wake noise component.

The subroutine logic path is shown in the following flow chart (Figure 2-19).

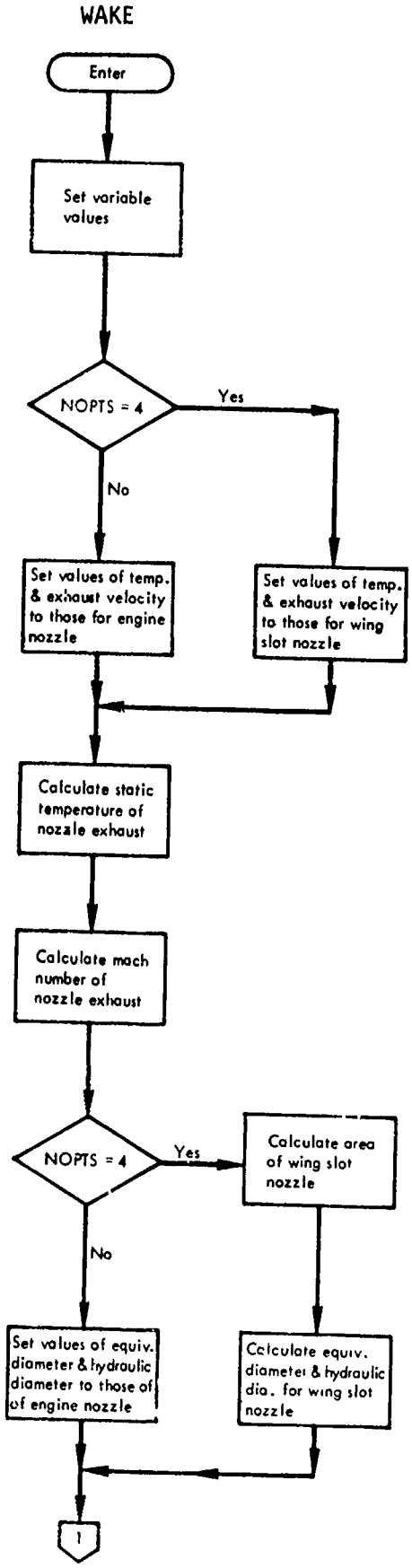

Figure 2-19. WAKE Flow Chart.

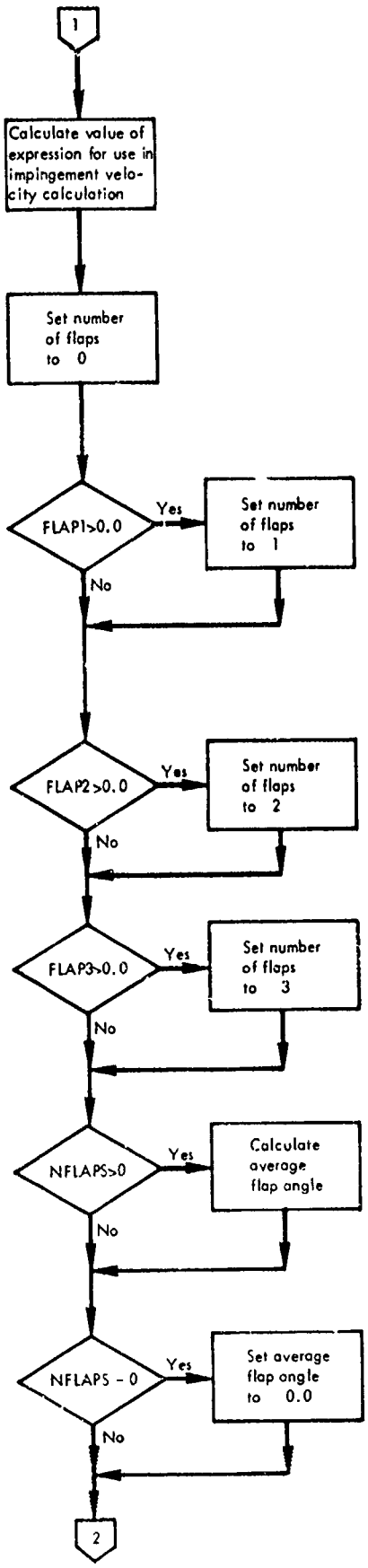

Figure 2-19. Continued.

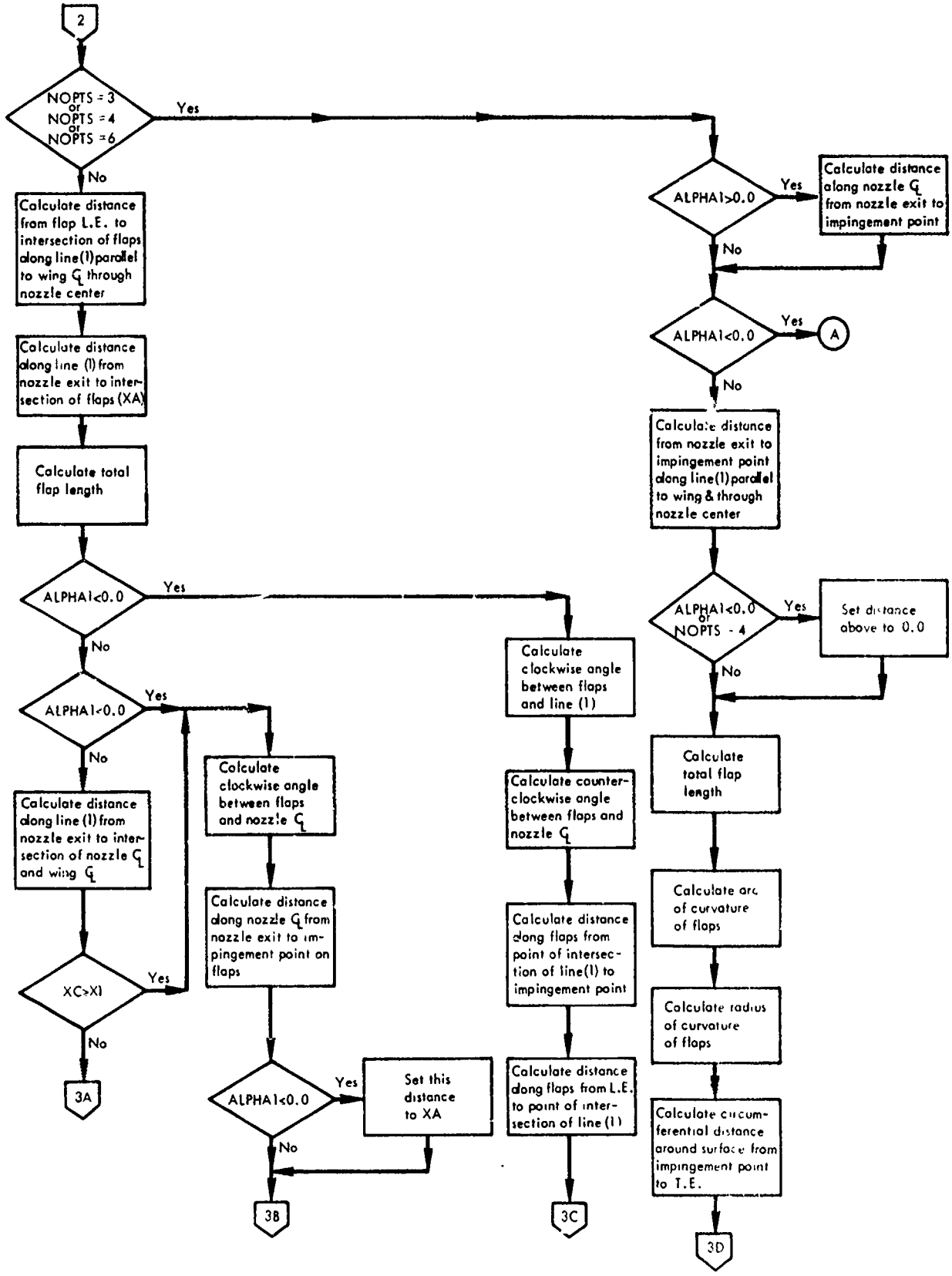

Figure 2-19. Continued.

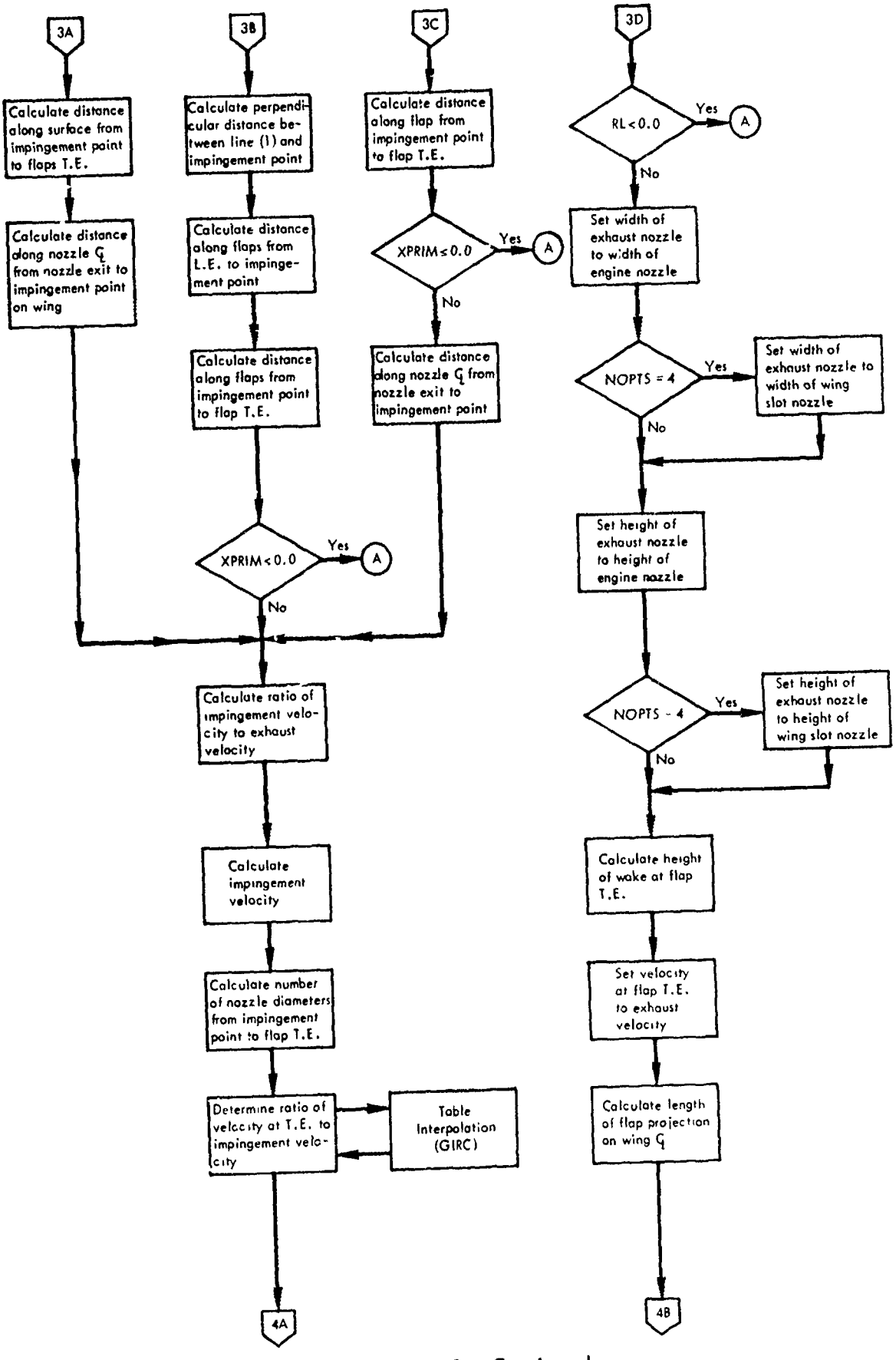

Figure 2-19. Continued.

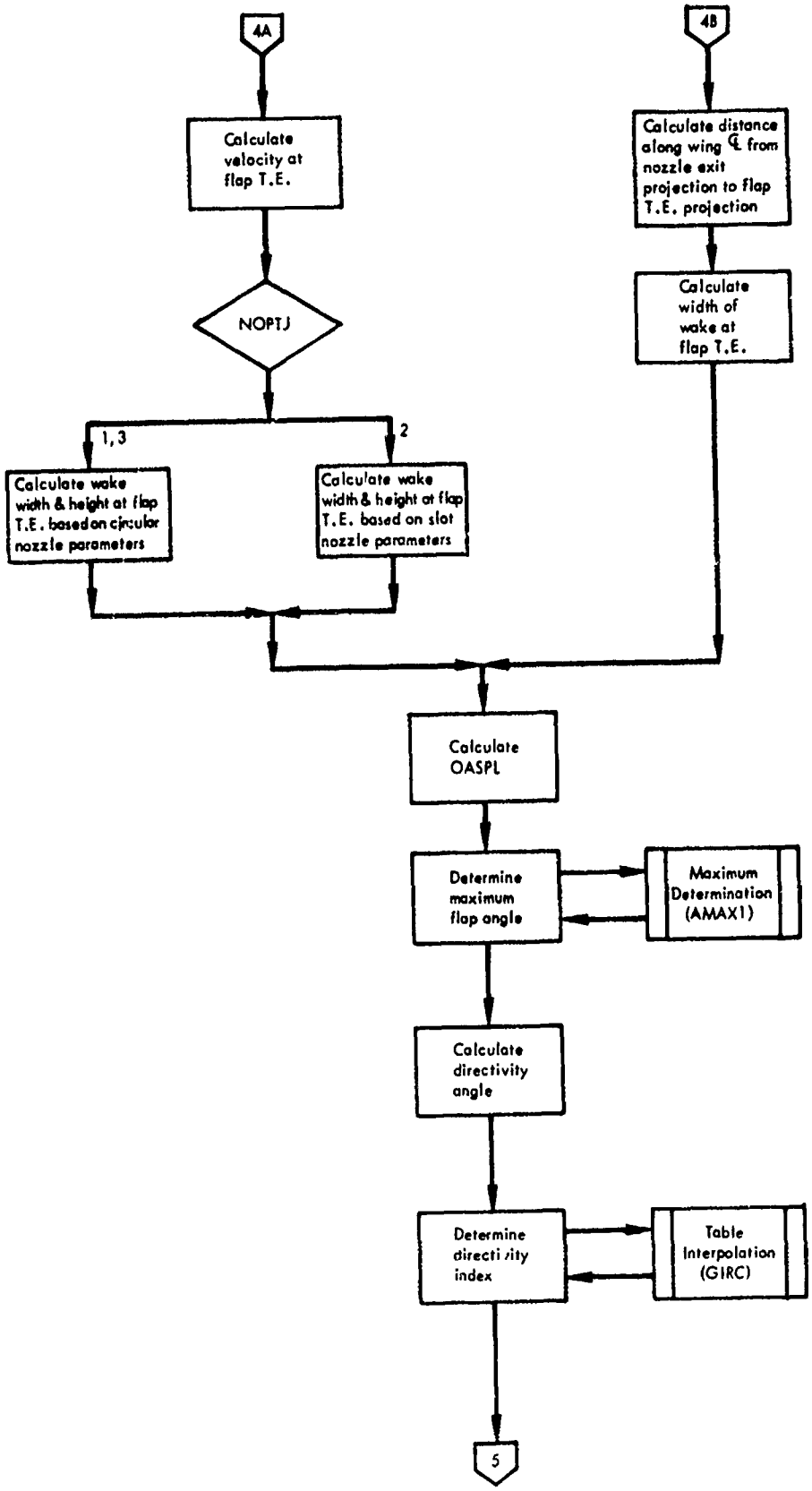

Figure 2-19. Continued.

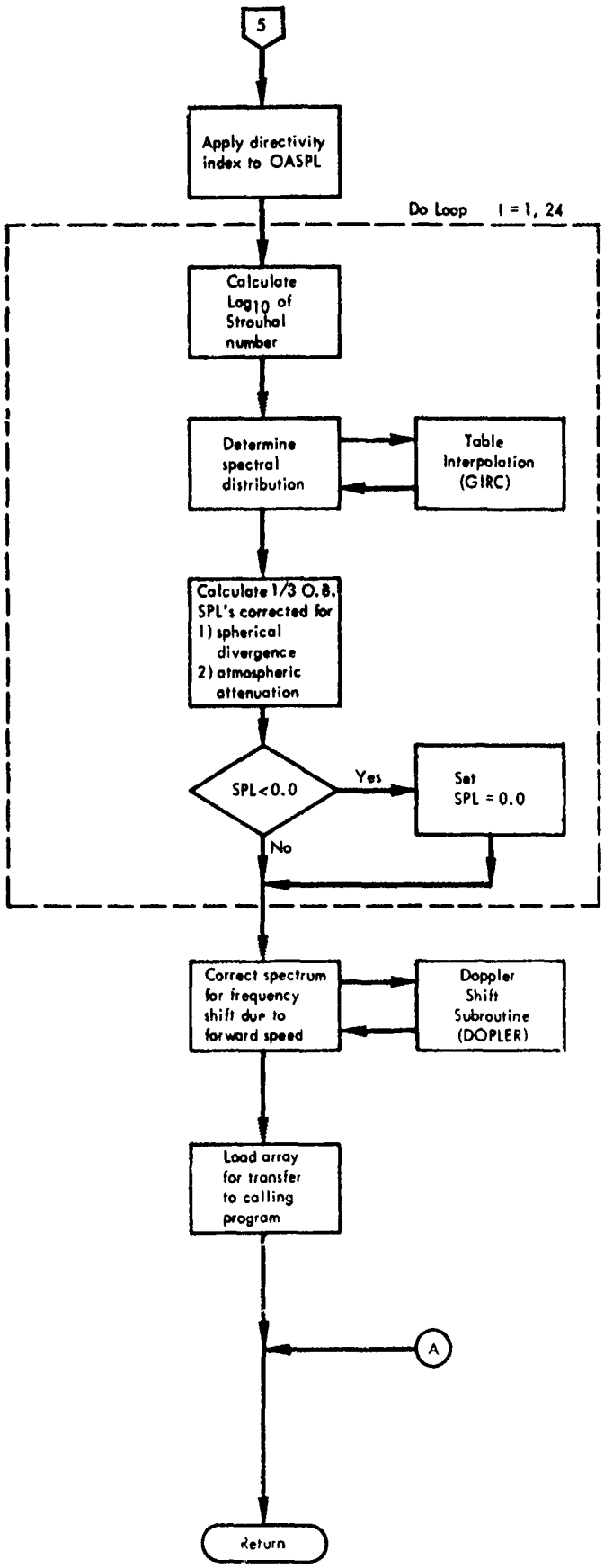

Figure 2-19. Continued.

4.3.11 TRAIL - Trailing Edge Noise

This subroutine calculates the 1/3 octave-band spectrum of the noise generated by engine high-lift airflow leaving the flap trailing edge. The methodology for the calculation procedure is discussed in Section 2.3.3.

This subroutine should normally be called for NOPTS = 2 (EBF), 3 (USB), 4 (IBF/BLC), and 6 (HYBRID), but should not be called for NOPTS = 4 (IBF/JET FLAP). For the Hybrid configuration, this is based on engine nozzle geometry and airflow parameters. As with all the high-lift noise sources (impingement, wall-jet, wake, and trailing edge), for the Hybrid configuration, it is assumed that the dominant component of these sources is derived from the engine nozzle airflow and that the wing nozzle contribution may be neglected.

The geometrical relationships used in TRAIL are calculated within the subroutine and are illustrated in Figure 2-15. The geometry for IBF/BLC configurations is similar to the USB and Hybrid as shown in Figure 2-15(d), except ALPHA1 is assumed to be zero. Wing shielding is not calculated separately but is included in the directivity of the noise.

The required input variables for TRAIL are the same as those described for WAKE in the preceding section, except that WAKE also requires the aircraft elevation angle relative to the observer (ELVANG).

The reference OASPL is calculated from the following expression:

$$OASPL = 10 \log_{10} (DELTA \cdot B) + 50 \log_{10} (VTE) - 6.0 + TURB$$

where VTE is the velocity at the trailing edge and DELTA and B are shown in Figure 2-17. TURB is a factor added to account for the location of the turbulence center.

The restrictions which apply to WAKE (Section 4.3.10) also apply to TRAIL.

The output is the 1/3 octave-band spectrum of sound pressure levels.

The subroutine logic path is shown in the following flow chart (Figure 2-20).

TRAIL

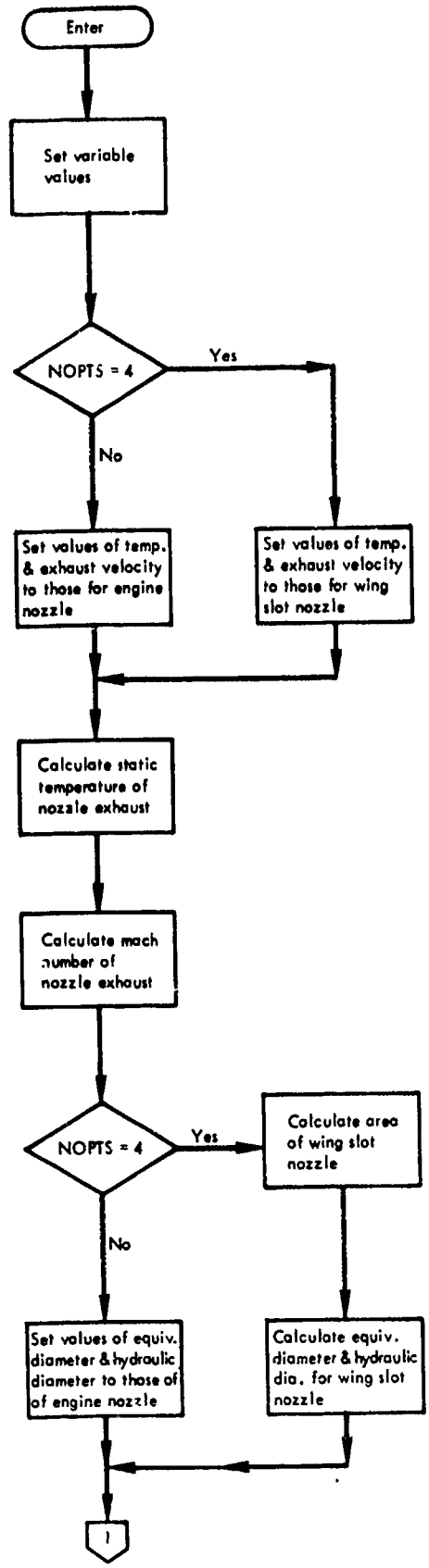

Figure 2-20. TRAIL Flow Chart.

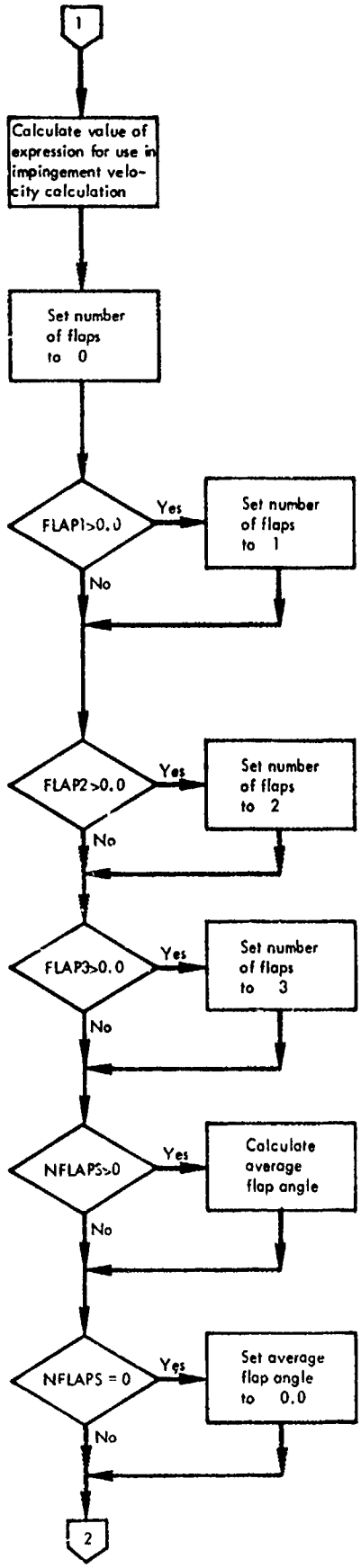

Figure 2-20. Continued.

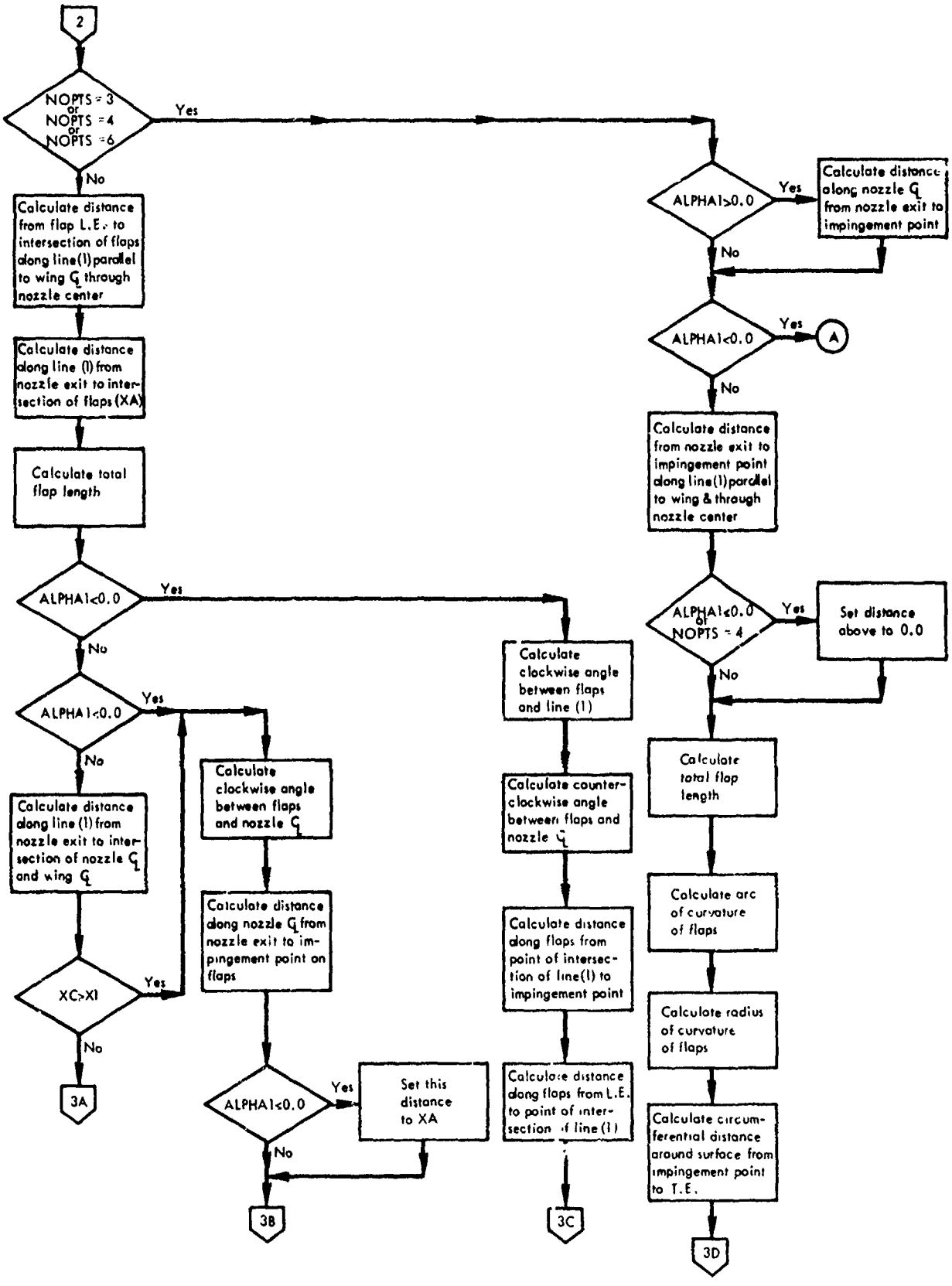

Figure 2-20. Continued.

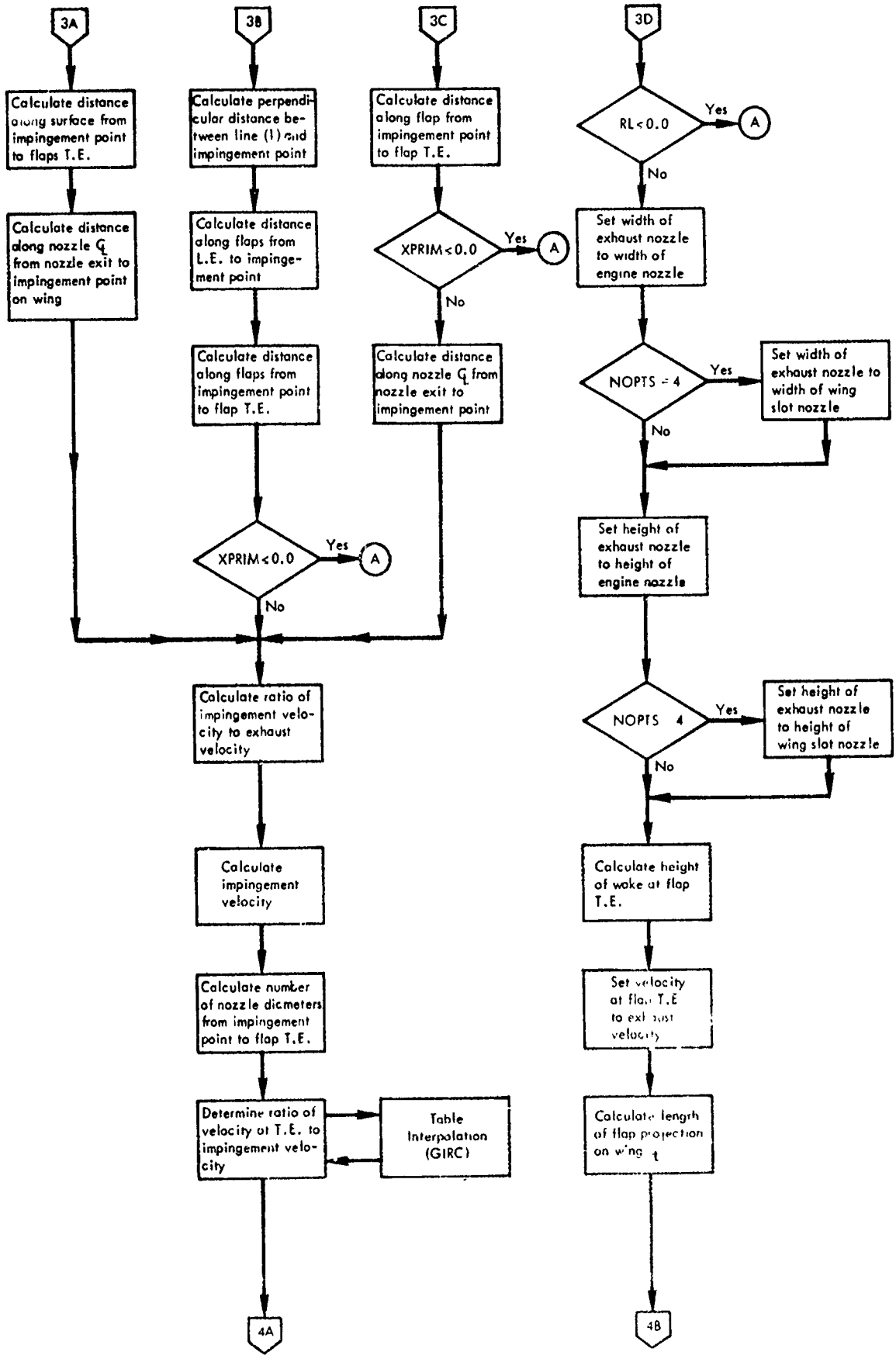

Figure 2-20. Continued.

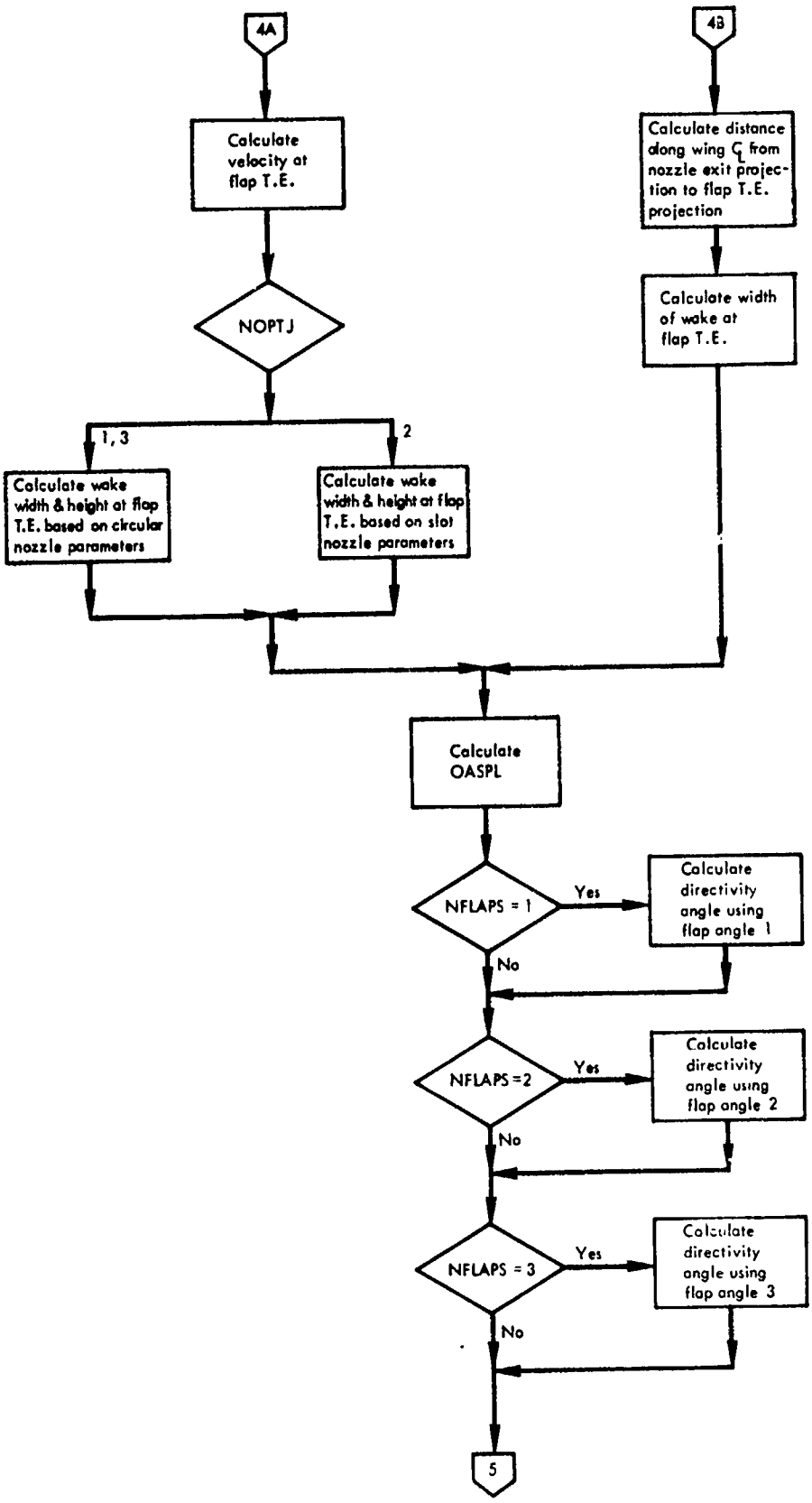

Figure 2-20. Continued.

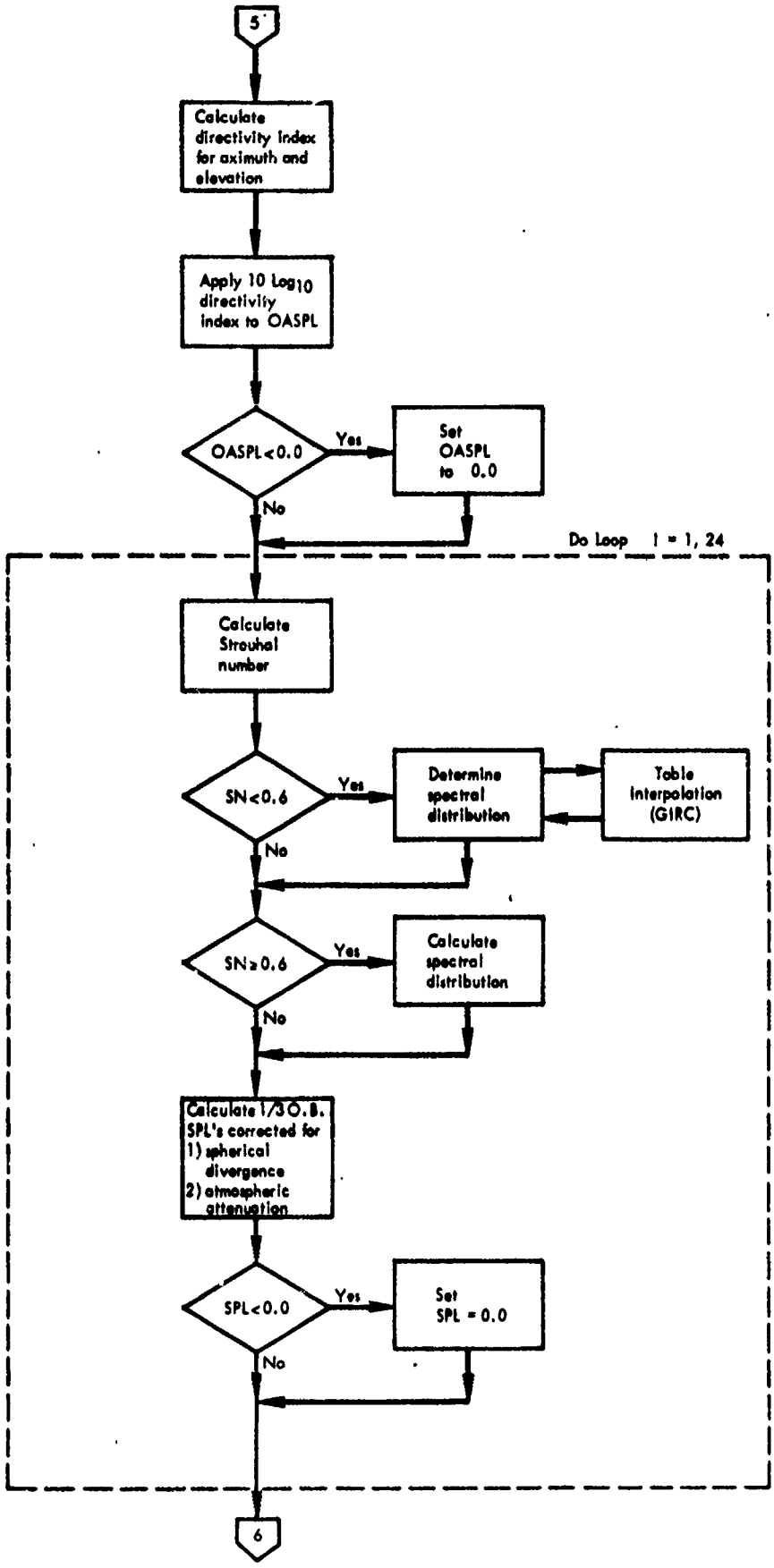

Figure 2-20. Continued.

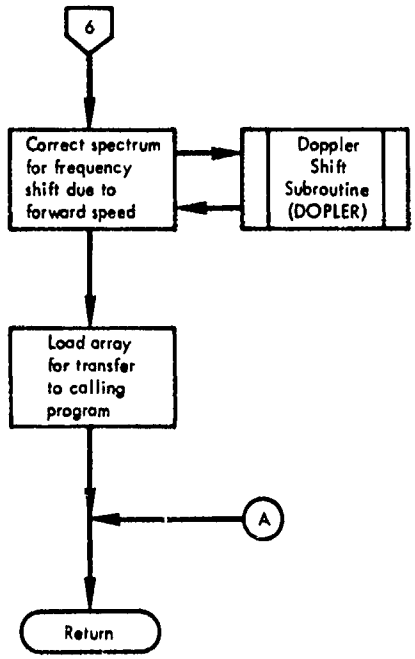

Figure 2-20. Continued.

4.3.12 APU - Auxiliary Power Unit

This subroutine calculates the noise level produced by the auxiliary power unit and radiated to an observer located some finite distance from the source. Due to the limited amount of data available for this noise source this prediction method, discussed in Section 2.4.2, yields only the perceived noise level corrected for spherical divergence to the source-to-observer distance. It does not account for any directional effects.

There are two options for this prediction: one is based on the bleed capacity, and the other is based on the shaft horsepower output of the APU.

The required variables are:

(1) key to denote which option of calculation is used (NOPTA)
- = 1 uses bleed capacity (BC)
- = 2 uses shaft horsepower (SHP)

(2) source-to-observer distance (STOD).

Method one (NOPTA = 1) uses the expression,

$$PNLAPU = 103.0 + 0.11 \cdot BC$$

to determine the perceived noise level (PNLAPU) at distance of 1 foot. Method two (NOPTA = 2) uses the expression,

$$PNLAPU = 106.0 + 0.106 \cdot SHP .$$

The output is the perceived noise level radiated to the observer.

The subroutine logic path is shown in the following flow chart (Figure 2-21).

APU

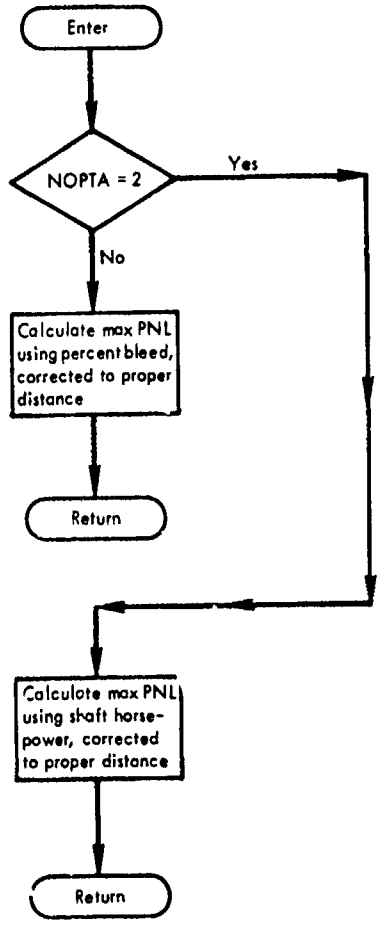

Figure 2-21. APU Flow Chart.

4.4 ADDITIONAL SUBROUTINES

In addition to the twelve major noise source prediction subroutines, discussed in Section 4.3, the overall program includes ten subroutines which perform auxiliary functions. These functions, due to their length and frequent use by the main program and/or the twelve major subroutines, were programmed as separate subroutines. The following are the descriptions, with detailed flow charts (for the six subroutines programmed for this prediction procedure), and explanatory figures for these ten subroutines.

4.4.1 EGA - Extra Ground Attenuation

This subroutine calculates the changes in SPL spectra resulting from all or a portion of the acoustic ray path being within the turbulent boundary layer of the earth, estimated to be 100 feet. The curves presented in SAE AIR 923 for the 10 knots downwind condition form the basis for this calculation as described in Section 3.4. The conditions could be varied to accommodate other wind conditions by replacing the stored data in the subroutine with that for the desired conditions.

The required variables are:

(1) source-to-observer distance (STOD)

(2) aircraft altitude (ALT)

(3) 1/3 o.b. center frequencies (F).

Using these values and the known observer height (4 ft), the length of the acoustic ray within the 100 ft. boundary layer of the earth can be determined based on the geometrical relations shown in Figure 2-22.

The output is an array of spectral corrections to be subtracted from the predicted SPL spectra.

These values are maximum when ANGLE (see Figure 2-22) is 0.0 degrees and are 0 when ANGLE is greater than or equal to 30.0 degrees.

The subroutine logic path is shown in the following flow chart (Figure 2-23).

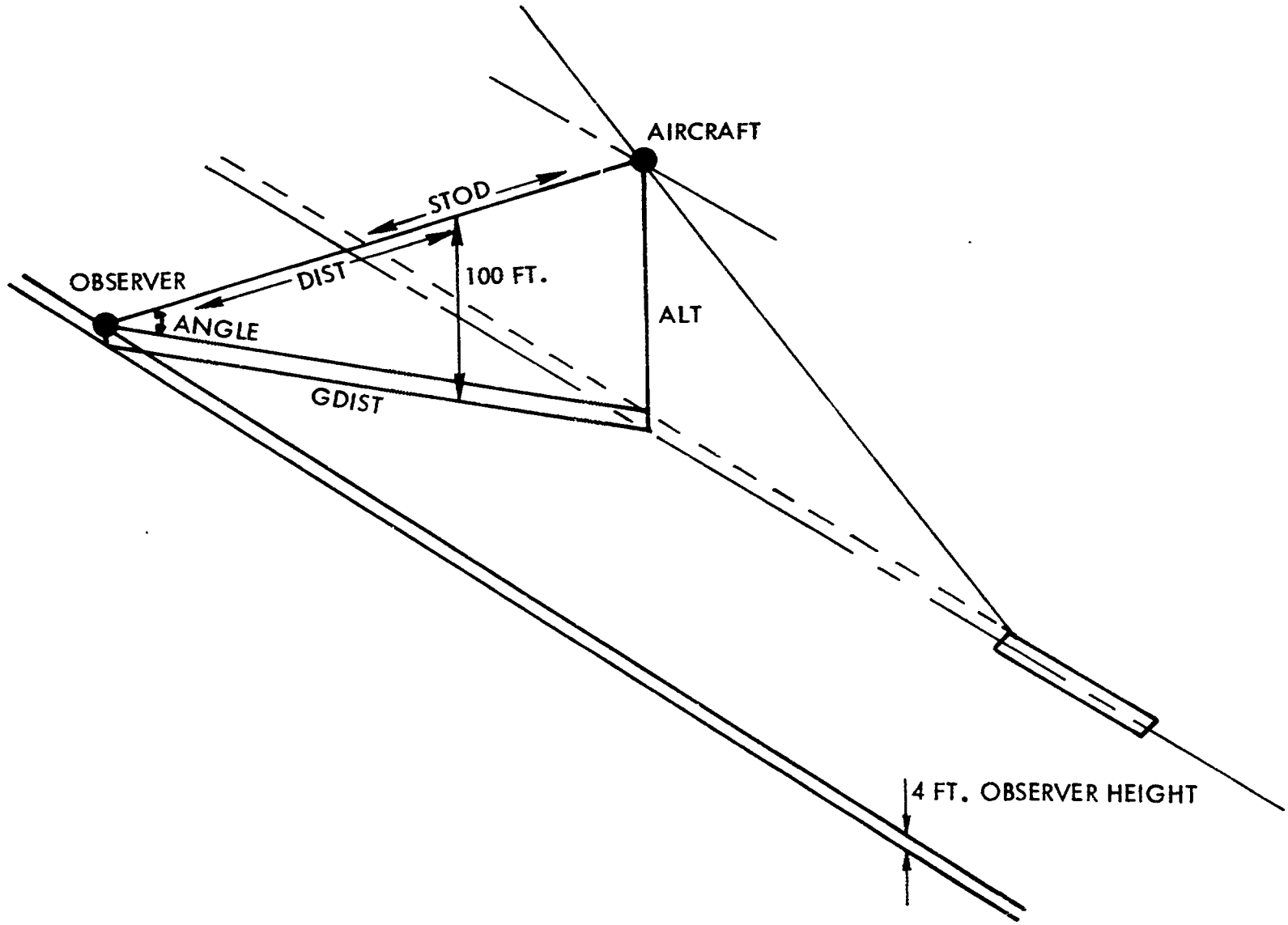

Figure 2-22. EGA Geometry

EGA

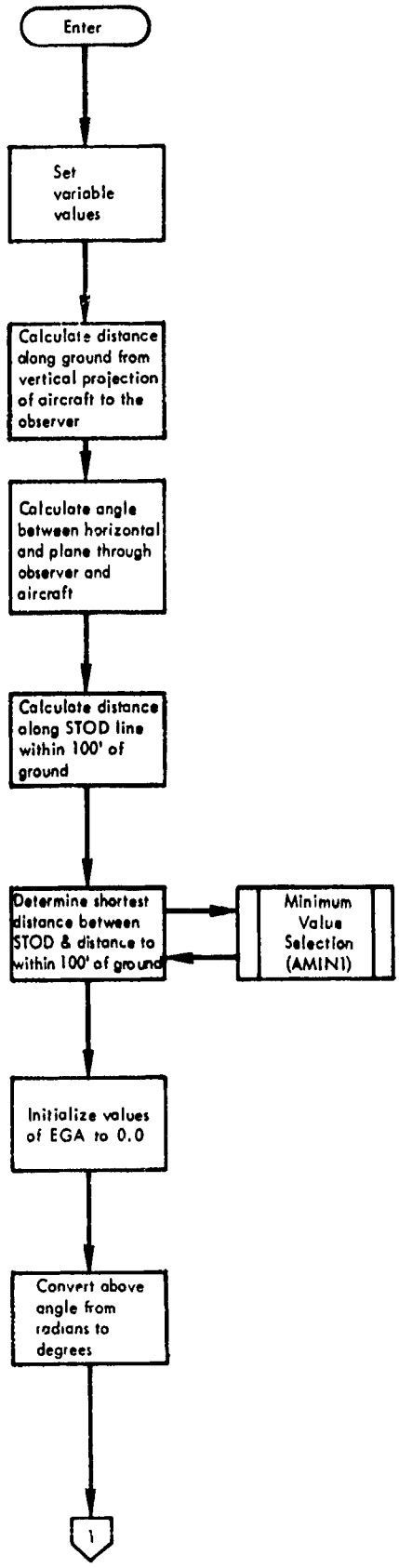

Figure 2-23. EGA Flow Chart.

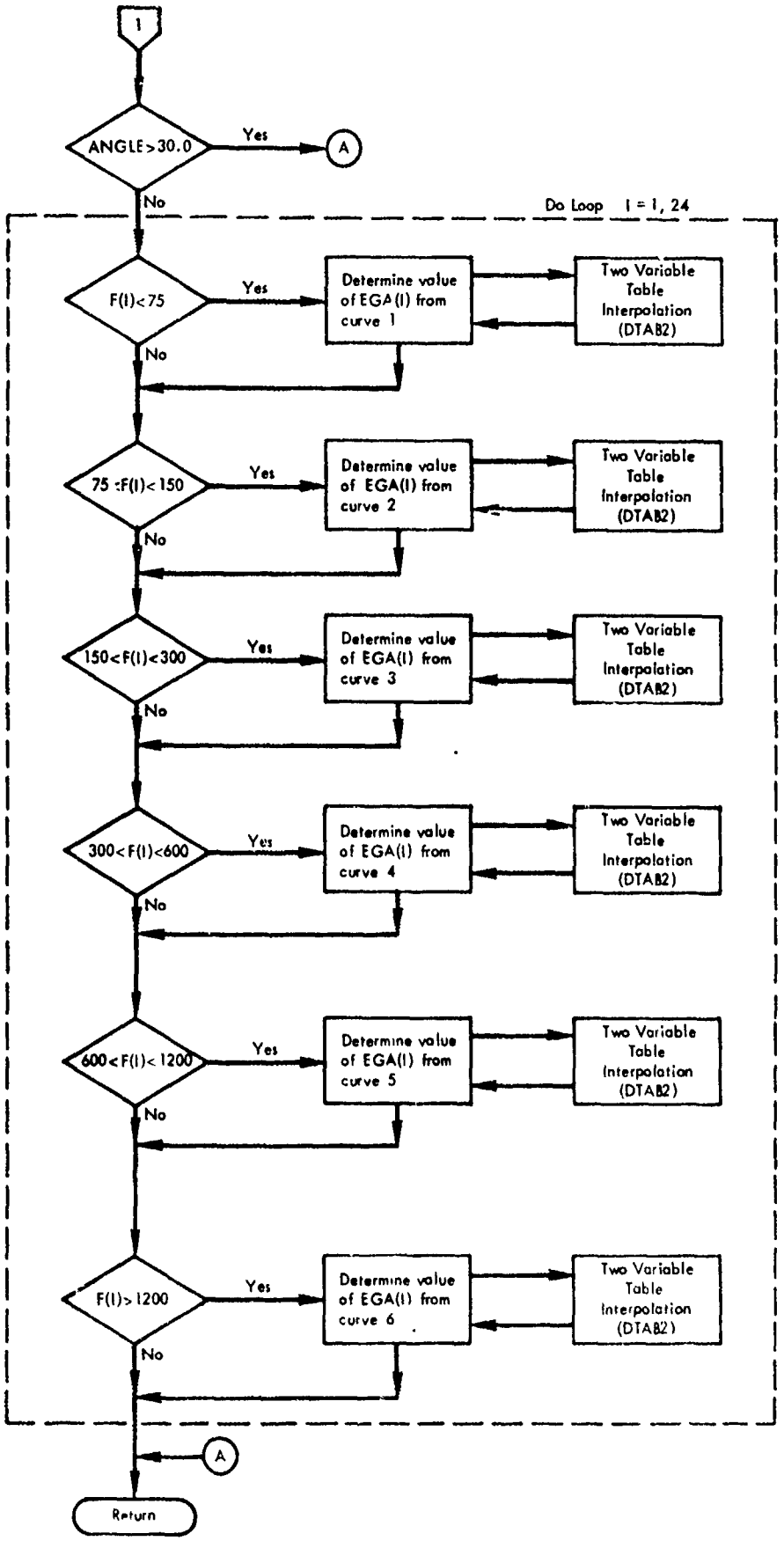

Figure 2-23. Continued.

4.4.2 GRE - Ground Reflection Effect

This subroutine calculates the spectral changes resulting from the acoustic cancellations and reinforcements caused by the reflection of the acoustic rays from a surface. These effects are calculated considering a perfect reflecting surface; however, the equations can be modified to include other surfaces as described in Section 3.3.

The required variables are:

(1) source-to-observer distance (STOD)
(2) aircraft elevation angle (ELVANG)
(3) aircraft altitude (ALT)
(4) 1/3 o.b. center frequencies (F).

From these and the known observer height (4 ft.) the length of the direct ray and the reflected ray can be determined, for use in the above methodology.

The output is an array of spectral corrections to be added to the predicted free-field spectrum.

The restrictions for this subroutine are:

(1) the elevation angle must be between 0° - 90°
(2) the value of acoustic cancellations are limited to -30 dB.

The subroutine logic path is shown in the following flow chart (Figure 2-24).

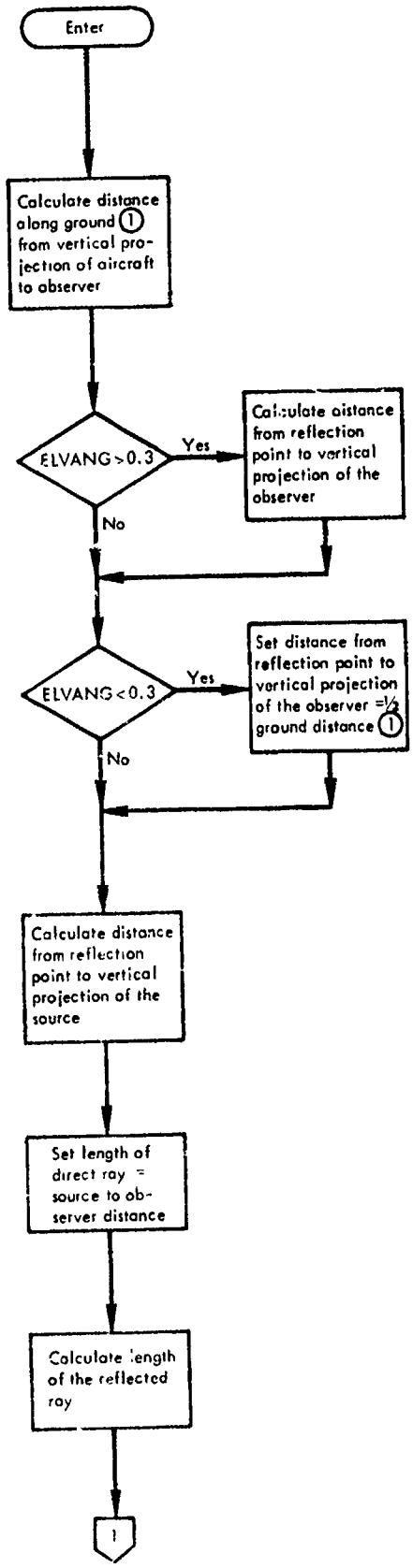

Figure 2-24. GRE Flow Chart.

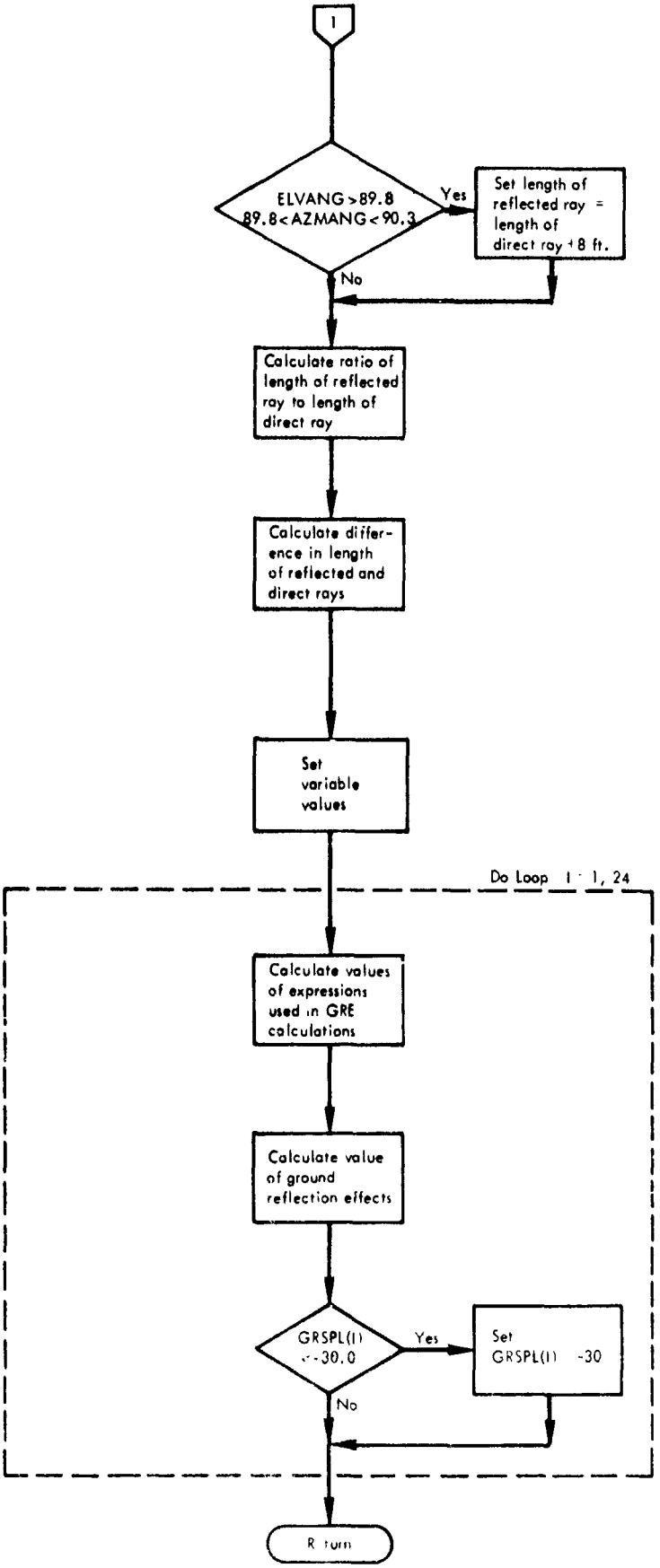

Figure 2-24. Continued.

4.4.3 SHIELD - Shielding from Aircraft Components

This subroutine calculates the spectral change produced by shielding of the noise source by the wing/flaps. The wing shielding effect is computed spectrally using the optical diffraction method described in Section 3.5

The required variables are:

(1) aircraft elevation angle (ELVANG)
(2) source-to-barrier distance (SD)
(3) equivalent barrier height (BH)
(4) boundary-to-observer distance (OD)
(5) 1/3 o.b. center frequencies (F).

SD, BH, and OD are calculated by the calling subroutines based on the individual source locations. The geometrical variables used for these calculations are shown in Figure 2-8.

The output is the change in SPL resulting from the shielding. The values of wing/flap shielding are limited to a minimum of 0 and a maximum of 20 in any 1/3 octave band. The value of fuselage shielding is discussed in Section 4.2 .

The subroutine logic path is shown in the following flow chart (Figure 2-25).

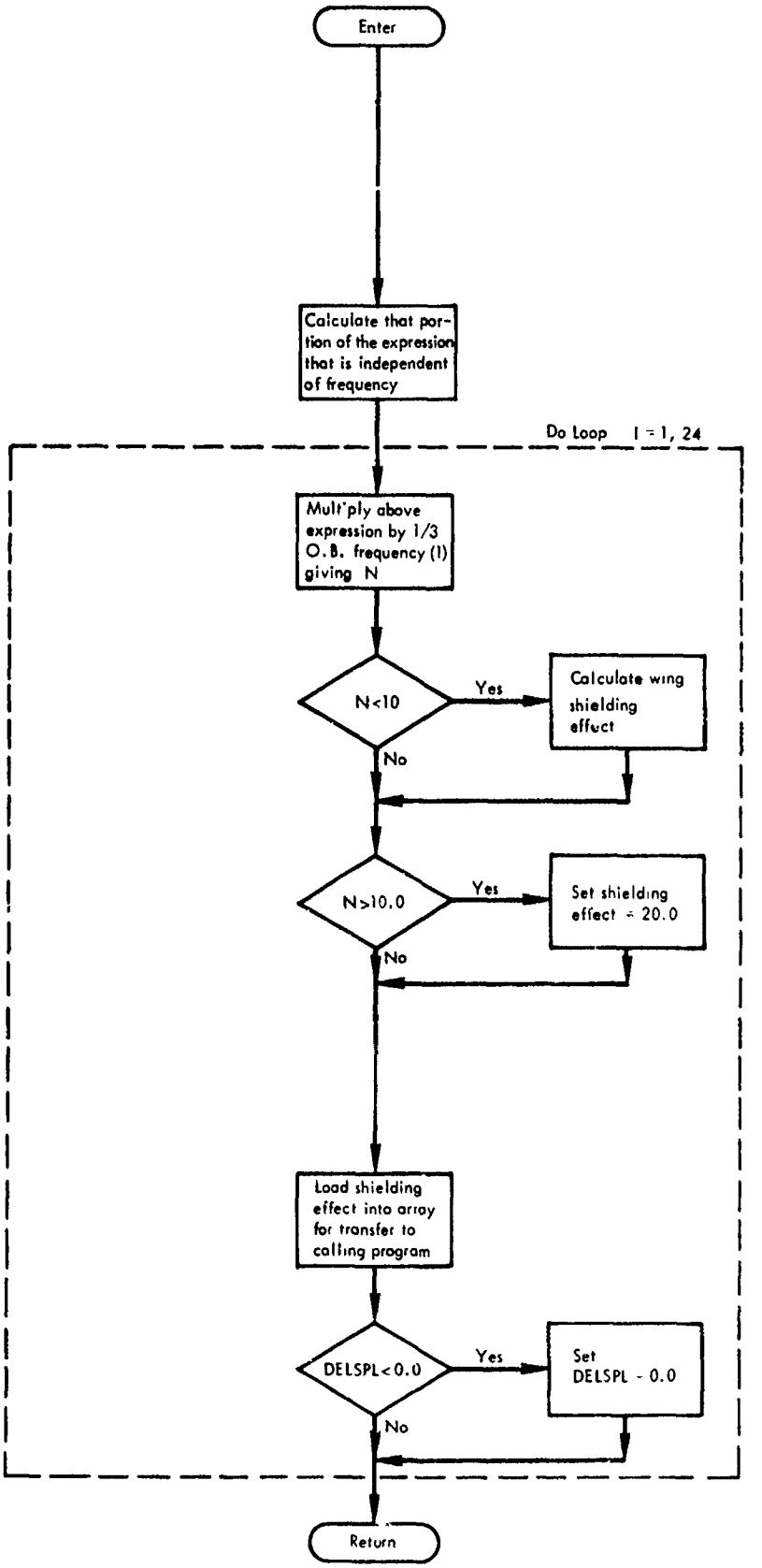

Figure 2-25. SHIELD Flow Chart.

4.4.4 FWDSPD - Forward Speed Effects on Level

This subroutine calculates the change in PNL (ΔPNdB) resulting from the forward speed of the aircraft, as described in Section 3.2. Values are calculated using the equation

$$\Delta PNdB = 10 \cdot k \cdot \log_{10} (1 - VAC \ \cos(ANG)/VEL)$$

where:

k = power factor which varies with high lift system and configuration as described in Section 3.2.2.

VAC = aircraft velocity along flight path.

ANG = nozzle angle (ANGNOZ for NOPTS = 1, 2, 3, 6;
ANGWNZ for NOPTS = 4)

VEL = nozzle velocity (VEQUIV for NOPTS = 1, 2, 3, 6;
VJWNOZ for NOPTS = 4, 5)

The required variables are:

(1) key to determine type of high-lift system (NOPTS)
(2) NOPTS = 1, 4 none
(3) NOPTS = 2, flap length (FLAP1, FLAP2, FLAP3)
(4) NOPTS = 3, 6 , elevation angle (ELVANG)
(5) NOPTS = 5, elevation angle (ELVANG)
ejector angle (EJANG)
(6) all values of NOPTS require values of ANG and VEL described above
(7) aircraft velocity (VAC).

The output is the change in PNL level (ΔPNdB) of the system specified by the incoming value of NOPTS.

The restriction for this subroutine is that the aircraft velocity (VAC) must be less than the nozzle velocity (VEL).

The subroutine logic path is shown in the following flow chart (Figure 2-26).

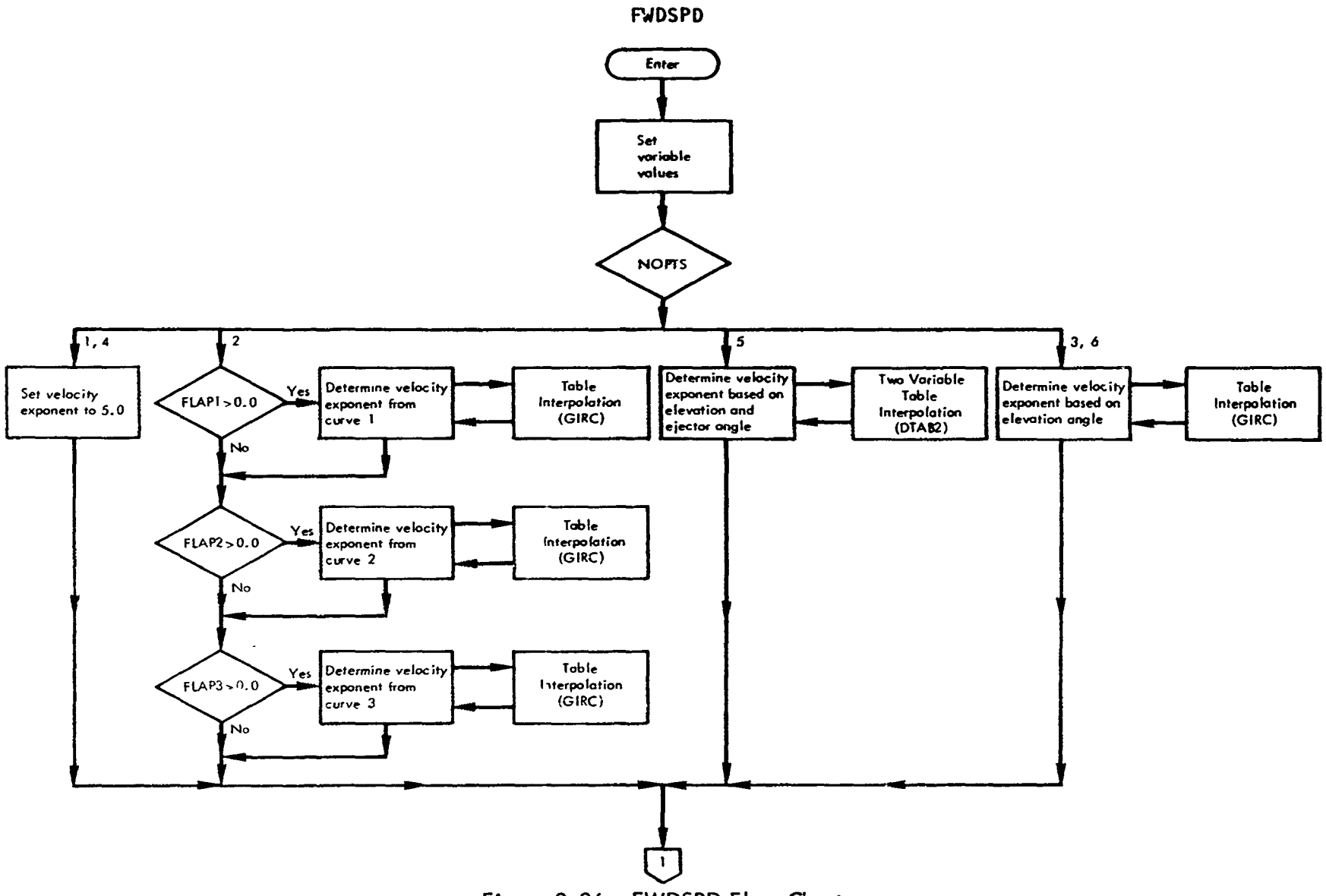

Figure 2-26. FWDSPD Flow Chart.

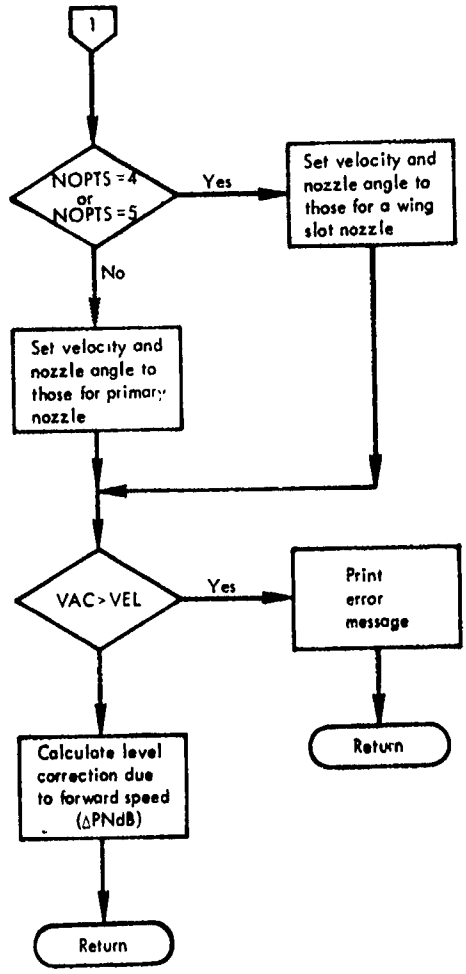

Figure 2-26. Continued.

4.4.5 DOPLER - Frequency Shift Due to Forward Speed

This subroutine shifts 1/3 octave-band spectra up or down in frequency as required to account for the change in frequency resulting from the aircraft moving toward or away from the observer. The Doppler frequency shift methodology is briefly described below. The detailed discussion is presented in Section 3.2.1.

The value of the Doppler ratio (D) is calculated and determines the amount of frequency shift as follows:

$D \leq 0.445449$	no shift; print diagnostic
$0.445449 < D \leq 0.56123$	3 1/3 o.b. downward
$0.561231 < D \leq 0.707107$	2 1/3 o.b. downward
$0.707107 < D \leq 0.890899$	1 1/3 o.b. downward
$0.890899 < D < 1.122462$	no shift
$1.122462 \leq D < 1.414213$	1 1/3 o.b. upward
$1.414213 \leq D < 1.781797$	2 1/3 o.b. upward
$1.781797 \leq D < 2.244924$	3 1/3 o.b. upward
$D \geq 2.244924$	no shift; print diagnostic

where D is the ratio of source frequency to observed frequency (f/f_o).

The required variables are:

(1) aircraft velocity along the flight path (VAC)
(2) azimuthal angle from aircraft centerline to the observer (AZMANG)
(3) 24 - 1/3 o.b. sound pressure levels.

The output is the shifted 1/3 o.b. spectrum.

The restrictions for this subroutine are:

(1) there must be 24 - 1/3 o.b. SPL's in a single subscripted array input
(2) the value of D must be $0.445449 < D < 2.244924$.

The subroutine logic path is shown in the following flow chart (Figure 2-27).

DOPLER

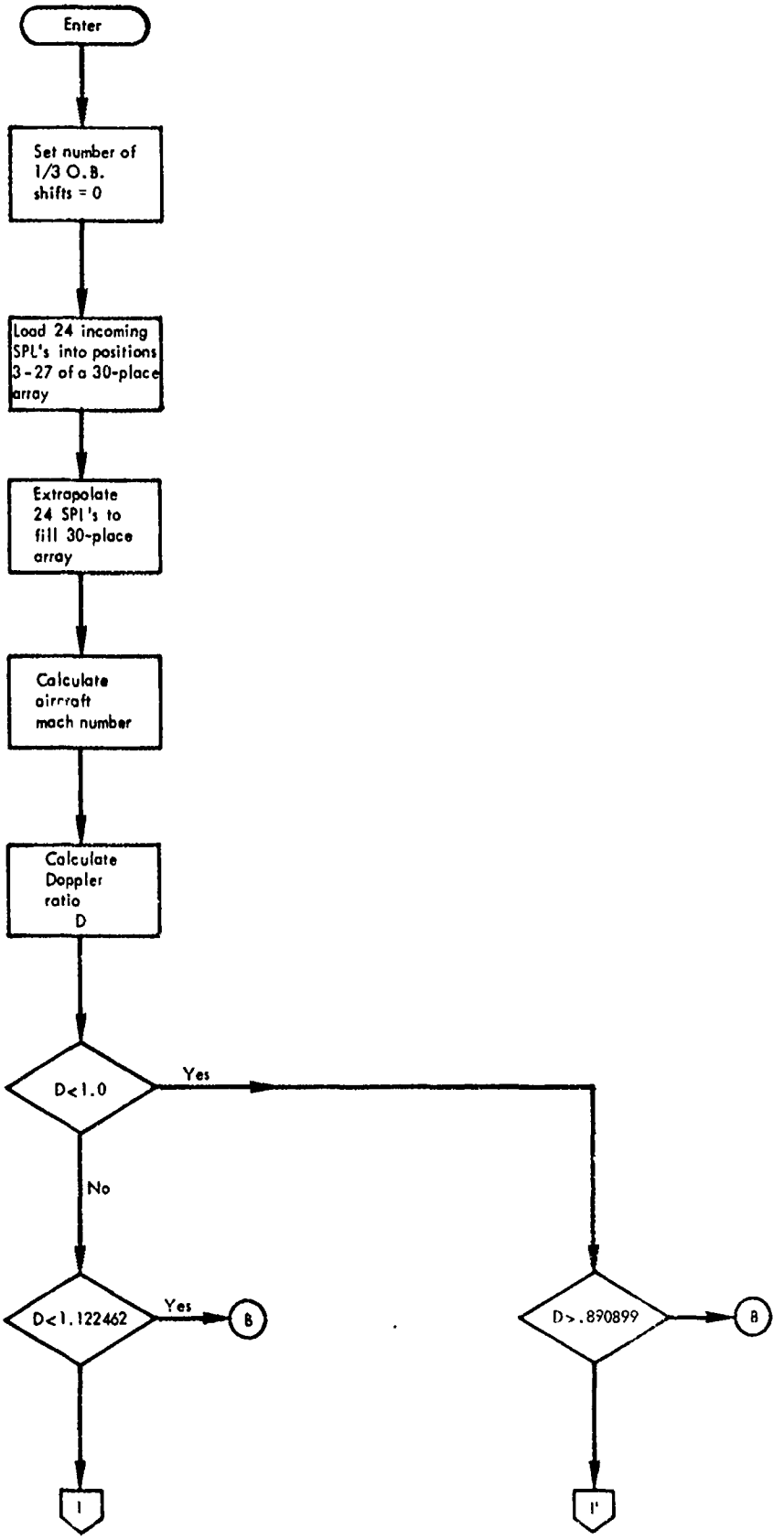

Figure 2-27. DOPLER Flow Chart.

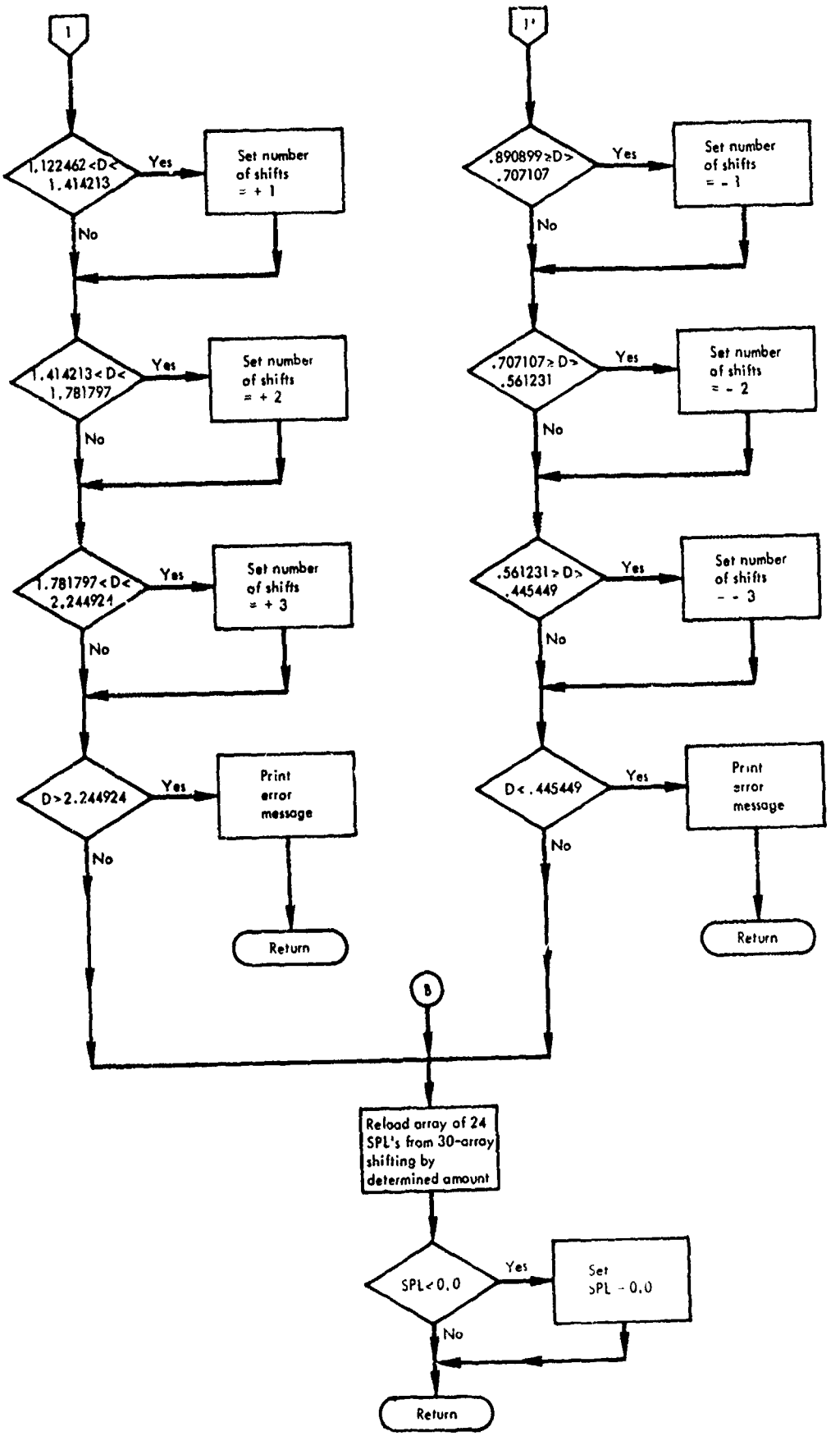

Figure 2-27. Continued.

4.4.6 REDUCE - Noise Reduction Features

This subroutine calculates the reduction in PNL (ΔPNdB) achieved through the use of certain noise reduction features, described in Section 3.6. These are defined for three types of high lift systems, only, as follows:

EBF (NOPTS = 2)

NR1 = 1 Number of flaps (1-3)

NR2 = 1 Treatment on the last flap trailing edge

NR3 = 1 Slot blowing at last trailing edge

USB (NOPTS = 3)

NR1 = 1 No reduction applied

NR2 = 1 Treatment on the last flap trailing edge

NR3 = 1 Slot blowing at last trailing edge

AW (NOPTS = 5)

NR1 = 1 Multi-element nozzle with hard-wall ejector

NR2 = 2 Multi-element nozzle with lined ejector

NR3 = 1 No reduction applied.

A value of 1 input for NRED implies that one of the noise reduction features has been applied and the values for NR1, NR2, and NR3 should be checked.

The required variables are:

(1) key to determine the type of high-lift system (NOPTS)
(2) which noise reduction features applied (NR1, NR2, NR3)
(3) length of flaps (FLAP1, FLAP2, FLAP3)
(4) elevation angle (ELVANG)
(5) equivalent nozzle velocity if system is EBF or USB (VEQUIV)
(6) slot height if trailing edge blowing is used (HSLOT)
(7) wing nozzle temperature if system is AW (TTWNOZ)
(8) wing nozzle velocity if system is AW (VJWNOZ).

The output is the ΔPNdB produced by one or more of the noise reduction features.

The restrictions for this subroutine are:

(1) system type must be EBF, USB, or AW

(2) only one noise reduction feature may be used with AW.

The subroutine logic path is shown in the following flow chart (Figure 2-28).

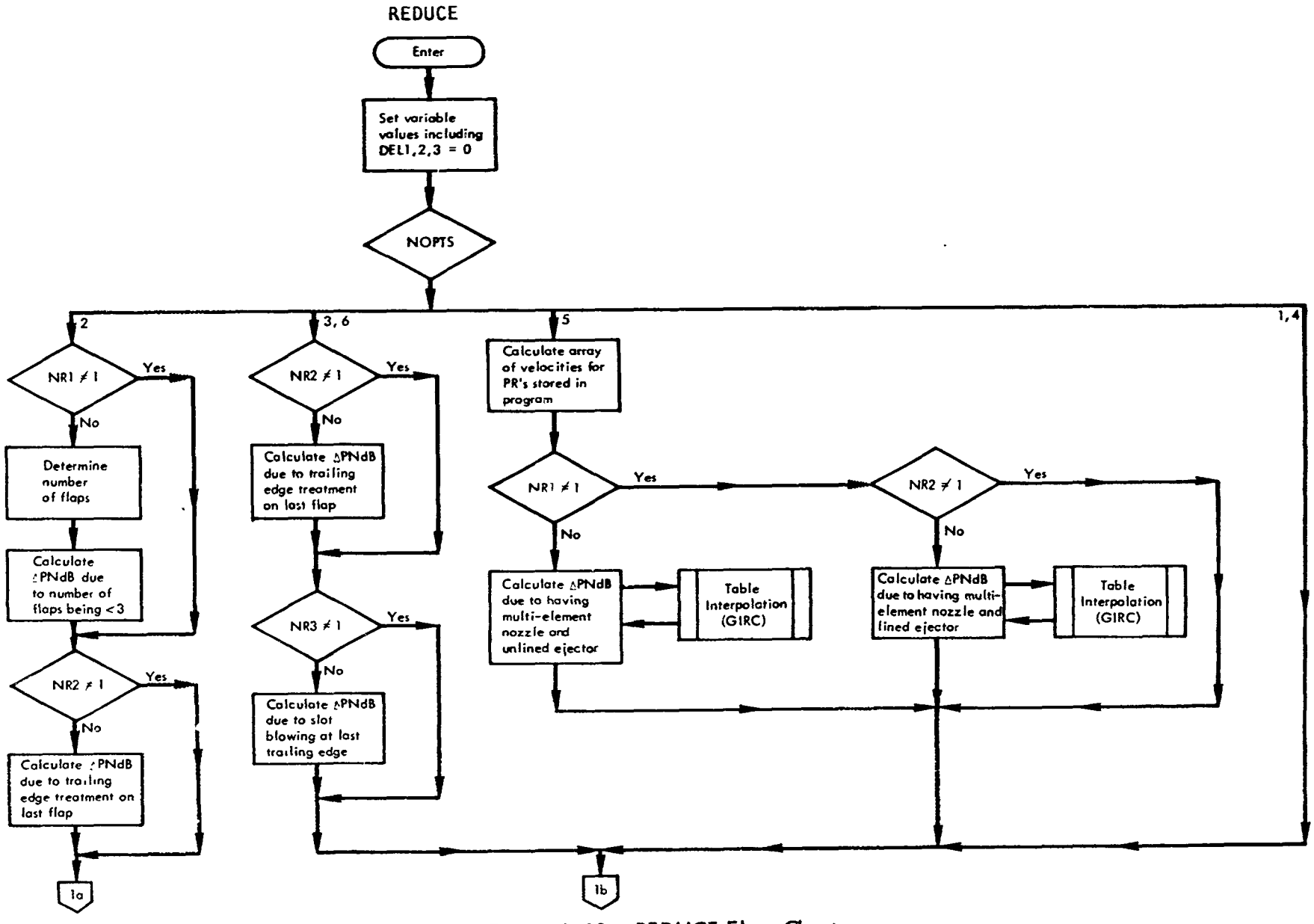

Figure 2-28. REDUCE Flow Chart.

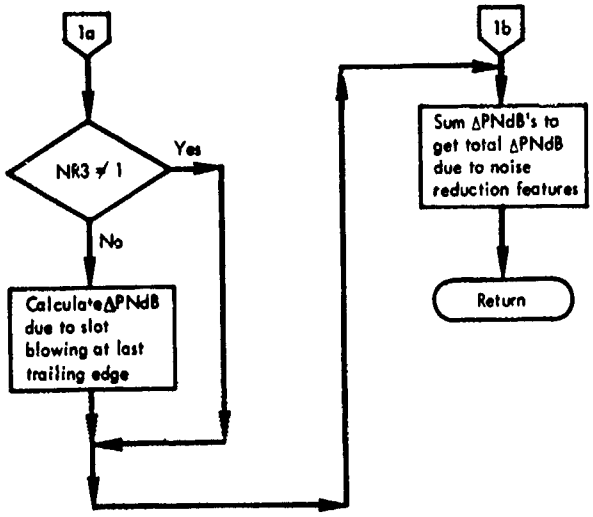

Figure 2-28. Continued.

4.4.7 PNLREV - Calculation of Perceived Noise Level

This subroutine calculates the perceived noise level (PNL) from octave or 1/3 octave-band spectrum. It utilizes the methods defined in SAE ARP-865A. The mathematical formulation of the Noy Table, defined in that document, is used in order to save both space and time during program execution.

The required variables are:

(1) spectrum

(2) code to distinguish between octave band and 1/3 octave band spectra (NOCT)

1 = octave band

2 = 1/3 octave band.

The output is the perceived noise level of the input spectrum.

The restrictions for the subroutine are:

(1) The frequency range of the spectrum must be

(a) 24 - 1/3 octave bands centered from 50 Hz to 10,000 Hz or

(b) 8 octave bands centered from 63 Hz to 8,000 Hz.

(2) The sound pressure level in any band must not exceed 150 dB.

The procedures for this calculation are well defined and have been in use for several years. Therefore, no flow chart is presented for this subroutine.

4.4.8 TONE - Calculation of Tone Corrected PNL

This subroutine calculates the correction to be applied to the perceived noise level, due to irregularities in the spectrum. The program uses the methods and equations defined in Appendix B of FAR Part 36.

The required inputs are:

(1) 1/3 octave-band spectrum

(2) perceived noise leve the spectrum.

The output is the value of the tone corrected perceived noise level.

This program requires that the input spectrum consists of 24 values of sound pressure level.

The methods for this calculation are well defined and have been in use for several years. Therefore, no flow chart is presented for this subroutine.

4.4.9 GIRC - One Independent Variable Table Interpolation

This function routine interpolates a value of a dependent variable for the desired value of the independent variable. It requires an array of independent variables and the corresponding array of dependent variables.

Entrance into this function is of the form

ANS = GIRC (ARG, X, Y, NX, IORDER)

where

ARG = interpolant
X = array of independent variable
Y = array of dependent variable
NX = length of arrays X and Y
IORDER = 1 indicates first order interpolation
= 2 indicates second order interpolation.

Upon return from this function ANS will contain the interpolated value.

This is provided as a system routine to users of the Lockheed-Georgia Company UNIVAC 1106 computer. It has been operational for several years and is generally accepted as accurate for interpolations. Therefore, the internal workings of this routine were not investigated and no flow chart is provided.

4.4.10 DTAB2 - Two Independent Variable Table Interpolation

This function routine interpolates a value of a dependent variable for the desired values of the two independent variables. This is done from arrays of the independent variables and the corresponding double-subscripted array of the dependent variables.

Entrance into this function is of the form

```
ANS = DTAB2 (XX, ZI, X, Z, NX, NZ, KX, KZ, Y, M, IERR)
```

where

```
   ANS = interpolated value from Y
    XX = interpolant in X direction
    ZI = interpolant in Z direction
     X = array of X value (single subscript)
     Z = array of Z value (single subscript)
    NX = number of values in X
    NZ = number of values in Z
    KX = 1 for linear interpolation in X
       = 2 for curvilinear interpolation in X
    KZ = 1 for linear interpolation in Z
       = 2 for curvilinear interpolation in Z
     Y = array of Y [double subscripted:  Y (NZ, NX)]
     M = row dimension of Y
  IERR = 1 for successful interpolation
       = 2 for unsuccessful interpolation
```

The value of IERR is returned from the function routine.

The interpolation is first performed in the Z direction for enough values so that the interpolation can then be performed in the X direction using these interpolated values.

This routine is provided for UNIVAC 1106 users at the Lockheed-Georgia Company. It has been operational for several years and is generally accepted as accurate. Therefore, the internal workings of this routine were not investigated and no flow chart is provided.

5. MACHINE REQUIREMENTS

This program is designed to operate on the UNIVAC 1106. Approximately 20K decimal words of 36 bits each are required for execution. Data input is through cards or 80 character card images. Output may be obtained on a line printer only.

5.1 OPERATING SYSTEM

The program has been developed on a UNIVAC 1106 under EXEC-8 level 27. However, it is also checked out on the NASA Langley CDC 6600 under KRONOS with a FTN compiler.

5.2 RESOURCE ESTIMATES

The central processor time required to process a job depends on three major factors:

(1) number of noise source subroutines used to describe aircraft system
(2) output option (NOPTG) selected
(3) number of points on flight profile for NOPTG = 3.

The most computational time is required when NOPTG = 3 is selected since it requires data for 17 observer locations for each point on the flight profile.

The noise levels for the baseline aircraft, of each type of high-lift system, were computed using NOPTG = 3 with 16 points on each flight profile. The subroutines called for each system were those suggested in Section 4.1.3. The following table shows the time required for each execution and output cycle of the computations:

Aircraft Type	CPU Time-minutes
Vectored Thrust	3.58
Externally Blown Flap	3.57
Upper Surface Blowing	3.43
Internally Blown Flap	4.23
Augmentor Wing	4.55
Hybrid	5.05

6. DIAGNOSTICS

The following are a list of the error messages which may be printed, and the program which prints them:

(1) ALTITUDE CANNOT BE LESS THAN 4.0 FEET
YOUR VALUE IS NOW XXXXX.XX STOLPROG)
occurs when ALT is less than 4.0.

(2) NOPTG CANNOT BE SET EQUAL XXXXX (STOLPROG)
occurs when NOPTG is other than 1, 2, or 3.

(3) STOD CANNOT BE LESS THAN 10.0 FEET
YOUR VALUE IS NOW XX.XXX (STOLPROG)
INCREASE YOUR VALUE OF ALT OR SLDIST.
occurs when STOD is <10.0 ft.

(4) RELATIVE VELOCITY NOT ACCEPTABLE TO SUBROUTINE FWDSPD (FWDSPD)
occurs when VAC $\geq$ VEL.

(5) THIS VALUE OF D X.XXXXXXXXXX $\pm$ XX IS NOT ACCEPTABLE FOR SUBROUTINE DOPLER THEREFORE NO SHIFT WAS USED (DOPLER)
occurs when D is ≥ 2.244924 or D ≤ 0.44599.

(6) SPL EXCEEDS 150 dB (PNLREV)
occurs when 1 of the 1/3 o.b. SPL's is greater than 150 dB; the returned value of PNL will be 0.0.

PRECEDING PAGE BLANK NOT FILMED

APPENDICES

PRECEDING PAGE BLANK NOT FILMED

A. SAMPLE CASES

The following pages contain sample input and output for the three program options (NOPTG) available with this prediction program.

DATA FOR NOPTG=1 OPTION

```
 1    BASELINE HYBRID AIRCRAFT
 2      6     1     4
 3 500.       4.0        90.        80.        8.0
 4      1     1     1     1     1     0     1     1     1     1     1     1
 5 12.        8.6162     0.6710
 6 5.5815     0.0        0.0        30.        0.0        0.0
 7      2
 8 1.3206     8.54       600.       565.       12.
 9 0.0456     17.3086    640.       0.0        565.
10 2304.      6.72       1.367
11 214.       1.255      6.0999     519.       17.5       18.0
12 1.105      1400.      2.8974     60.        17400.     59.        0.0
13      2 200.
14      0
```

BASELINE HYBRID AIRCRAFT

AIRCRAFT VELOCITY = 80.0 KNOTS
SIDELINE DISTANCE = 500.0 FEET
AIRCRAFT ALTITUDE = 4.0 FEET
AZIMUTHAL ANGLE = 90.0 DEG.
ELEVATION ANGLE = .0 DEG.
SOURCE TO OBSERVER DISTANCE = 500.0 FEET

FREQUENCY (HZ)	AIRFRAME AERODYNAMIC (DB)	FAN AND TURBINE (DB)	JET EXHAUST (DB)	EXCESS ENGINE (DB)	HIGH LIFT SYSTEM (DB)	TOTAL (DB)
50.	49.2	54.8	60.8	75.2	73.7	77.6
63.	58.2	55.1	61.8	73.4	75.1	77.5
80.	61.5	54.5	61.6	69.4	75.6	76.8
100.	66.2	54.9	62.2	66.5	77.1	77.9
125.	72.0	55.4	62.7	63.8	78.5	79.6
160.	70.6	55.7	62.6	60.4	78.9	79.7
200.	68.5	56.4	62.7	57.6	78.6	79.2
250.	65.9	57.0	62.5	54.8	77.6	78.1
315.	62.5	57.1	61.5	51.2	75.7	76.2
400.	59.1	57.6	61.0	48.2	74.7	75.1
500.	55.1	58.2	60.4	45.3	73.4	73.8
630.	52.0	59.9	59.3	42.1	71.8	72.3
800.	48.5	61.2	58.4	39.0	70.3	71.0
1000.	44.3	59.8	57.2	36.0	68.7	69.5
1250.	40.6	59.0	55.1	32.1	65.2	67.3
1600.	36.7	58.6	53.5	28.6	64.3	65.6
2000.	32.1	58.2	51.8	25.2	62.4	64.0
2500.	28.7	58.5	49.9	21.6	60.2	62.7
3150.	24.3	59.2	47.5	17.6	57.5	61.7
4000.	18.2	59.1	44.4	12.7	54.3	60.5
5000.	13.4	58.3	41.2	7.8	50.8	59.1
6300.	5.6	55.1	35.3	.3	44.8	55.6
8000.	.0	45.7	23.3	.0	32.5	45.9
10000.	.0	48.6	24.3	.0	33.4	48.7
OASPL	76.8	71.3	73.0	78.6	87.5	88.5
PNL	76.1	83.3	77.8	70.1	91.6	93.3
PNLT	76.7	85.4	80.0	70.1	93.8	95.4

MAXIMUM APU NOISE = 73.2 PNDB

```
*****************************************
* TOTAL SYSTEM PNL  =  93.3 PNDB *
*                                *
* TOTAL SYSTEM PNLT =  95.4 PNDB *
*****************************************
```

DATA FOR NOPTG=2 OPTION

```
 1    BASELINE HYBRID AIRCRAFT
 2      6     2     4
 3 500.       4.0        90.        80.        8.0
 4      1     1     1     1     1     0     1     1     1     1     1     1
 5 12.        8.6162     0.6710
 6 5.5815     0.0        0.0        30.        0.0        0.0
 7      2
 8 1.3206     8.54       600.       565.       12.
 9 0.0456     17.3086    640.       0.0        565.
10 2304.      6.72       1.367
11 214.       1.255      6.0999     519.       17.5       18.0
12 1.105      1400.      2.8974     60.        17400.     59.        0.0
13      2 200.
14      0
```

BASELINE HYBRID AIRCRAFT

AIRCRAFT VELOCITY = 80.0 KNOTS
SIDELINE DISTANCE = 500.0 FEET
AIRCRAFT ALTITUDE = 4.0 FEET
ELEVATION ANGLE = .0 DEG.

AZIMUTHAL ANGLE (DEG)	SOURCE TO OBSERVER DISTANCE (FT)	TOTAL PNL (PNDB)	TOTAL PNLT (PNDB)
10.0	2879.4	67.6	67.6
20.0	1461.9	78.8	78.8
30.0	1000.0	86.2	86.2
40.0	777.9	89.4	89.4
50.0	652.7	91.2	91.2
60.0	577.4	92.3	92.3
70.0	532.1	92.8	92.8
80.0	507.7	93.2	94.8
90.0	500.0	93.3	95.4
100.0	507.7	93.6	95.3
110.0	532.1	93.7	93.7
120.0	577.4	92.7	92.7
130.0	652.7	90.4	90.4
140.0	777.9	87.2	87.2
150.0	1000.0	82.8	82.8
160.0	1461.9	75.5	75.5
170.0	2879.4	64.2	65.1

DOVRS 000021 FPOF 000000 FPUF 000000 ERMD 000000
TASK: UNITS=2 CPU=11 REF=41 WDS=45778 CORE=21

DATA FOR NOPTG=3 OPTION

```
 1    BASELINE HYBRID AIRCRAFT
 2     6    3    4
 3 500.       4.0        90.        80.        8.0
 4    10 50.0      2000.0
 5     1    1    1    1    1    0    1    1    1    1    1    1
 6 12.        8.6162     0.6710
 7 5.5815     0.0        0.0        30.        0.0        0.0
 8     2
 9 1.3206     8.54       600.       565.       12.
10 0.0456     17.3086    640.       0.0        565.
11 2304.      6.72       1.367
12 214.       1.255      6.0999     519.       17.5       18.0
13 1.105      1400.      2.8974     60.        17400.     59.        0.0
14     2 200.
15     0
```

BASELINE HYBRID AIRCRAFT

AIRCRAFT VELOCITY = 80.0 KNOTS
SIDELINE DISTANCE = 500.0 FEET

ALTITUDE (FT)	DISTANCE ALONG FLIGHT PATH (FT)	ELEVATION ANGLE (DEG)	AZIMUTHAL ANGLE (DEG)	SOURCE TO OBSERVER DISTANCE (FT)	MAXIMUM PNL (PNDB)	MAXIMUM PNLT (PNDB)
4.0	2000.0	.0	90.0	500.0	93.3	95.4
54.0	2355.8	5.7	100.0	510.2	92.5	94.7
104.0	2711.5	11.3	90.0	509.9	91.5	93.4
154.0	3067.3	16.7	110.0	555.5	92.2	94.3
204.0	3423.1	21.8	110.0	573.1	92.1	93.9
254.0	3778.8	26.6	110.0	594.9	91.6	94.0
304.0	4134.6	31.0	90.0	583.1	91.2	93.4
354.0	4490.4	35.0	110.0	649.5	90.9	93.1
404.0	4846.1	38.7	60.0	739.4	89.7	92.0
454.0	5201.9	42.0	90.0	672.7	90.1	91.3

***** MAXIMUM NOISE *****

ALTITUDE (FT)	DISTANCE ALONG FLIGHT PATH (FT)	ELEVATION ANGLE (DEG)	AZIMUTHAL ANGLE (DEG)	SOURCE TO OBSERVER DISTANCE (FT)	MAXIMUM PNL (PNDB)	MAXIMUM PNLT (PNDB)
4.0	2000.0	.0	90.0	500.0	93.3	95.4

B. COMPUTER PROGRAM LISTINGS

The following pages contain the program listings for all the programs developed and/or used in this prediction procedure for V/STOL aircraft noise.

```
      DIMENSION SPLL(6,24),SPLF(2,24),SPLARO(24),SPLLFT(24),SPLFAN(24)
     2 SPLT(24),PNLTOT(17),PNLTC(17),PNLMAX(50),PNLTMX(50),ALTUDE(50),
     3 AZMAX(50),DISTMX(50),XDIST(50),ELV(50),AZIMU(17),DIST(17)
     4 ,TITLE(10),NK(12),SPLJET(24),SPLEXS(24),GRSPL(24),EGSPL(24)
C*
C***** COMMON BLOCK  ********
C*
      COMMON NOPTS,NOPTJ,STOD,ALT,AZMANG,ELVANG,
     2 VAC,DPLUG,DEQUIV,VEQUIV,FLAP1,FLAP2,FLAP3,FLPAG1,FLPAG2,
     3 FLPAG3,TTEQ,HNOZ,WNOZ,VJWNOZ,HWNOZ,WWNOZ,ANGNOZ,ANGWNZ,NRED,
     4 NR1,NR2.NR3,HSLOT,EJL,EJANG,WFF,PRF,DF,TF,TREATF,TREATA,PRT,
     5 DTURB,BLADES,TRPM,PCTP,SA,AR,THICK,NOPTA,BC,SHP,DPRIM,DANIN,
     6 DANOUT,X1,Y1,VTIPT,VJPRIM,VJSEC,TTPRIM,TTSEC,XCN,TTWNOZ,HD
     7 ,ALPHA1,TREATT
      COMMON /ATMO/F(24),ALPHA(24)
C*
C***** DATA STATEMENTS AND VALUE INITIALIZATION *****
C*
      DATA F/50.,63.,80.,100.,125.,160.,200.,250.,315.,400.,500.,
     2 630.,800.,1000.,1250.,1600.,2000.,2500.,3150.,4000.,5000.,
     3 6300.,8000.,10000./
C***** ATMOSPHERIC ABSORPTION IS FOR 77 DEG.F. AND 70 % R.H. *****
      DATA ALPHA/0.09,0.11,0.14,0.17,0.22,0.28,0.35,0.44,0.55,0.70,
     2 0.88,1.11,1.41,1.77,2.23,2.88,3.63,4.59,5.87,7.61,8.56,11.08,
     3 15.08,20.34/
      NALT=1
      NANG=1
      XCN=1.0
      DELDBL=0.0
      DELDBJ=0.0
      DELL=0.0
      DO 20 I=1,24
      DO 10 J=1,6
   10 SPLL(J,I)=0.0
   20 CONTINUE
      DO 40 I=1,24
      DO 30 J=1,2
   30 SPLF(J,I)=0.0
      SPLJET(I)=0.0
      SPLEXS(I)=0.0
      SPLARO(I)=0.0
      SPLFAN(I)=0.0
      SPLLFT(I)=0.0
   40 CONTINUE
      PNLAPU=0.0
C*
C***** READ BASIC FLIGHT PATH DATA *****
C*
      READ(5,505) TITLE
      READ(5,501) NOPTS,NOPTG,NENG
      IF(NOPTG.LT.1.OR.NOPTG.GT.3) GO TO 280
      READ(5,502) SLDIST,ALT,AZMANG,VAC,FLTANG
      IF(NOPTG.EQ.3) READ(5,503) NALT,ALTINC,STDIST
      VAC=VAC*1.69*COS(FLTANG/57.2957795)
```

```
C*
C***** READ KEYS FOR SUBROUTINE CALLS *****
C*
      READ(5,501) (NK(I),I=1,12)
C*
C***** READ INPUT DATA FOR PREDICTION SUBROUTINES *****
C*
C***** READ FLAP GEOMETRY AND NOZZLE LOCATION *****
      READ(5,502) ALPHA1,X1,Y1
      READ(5,502) FLAP1,FLAP2,FLAP3,FLPAG1,FLPAG2,FLPAG3
C***** READ ENGINE NOZZLE DATA *****
      IF(NK(4).NE.1) GO TO 44
      READ(5,501) NOPTJ
      IF(NOPTJ.EQ.2) GO TO 42
      READ(5,502) DPLUG,DPRIM,VJPRIM,TTPRIM,ANGNOZ
      IF(NOPTJ.EQ.3) READ(5,502) DANIN,DANOUT,VJSEC,TTSEC
      GO TO 44
   42 READ(5,502) HNOZ,WNOZ,VJPRIM,TTPRIM,ANGNOZ
   44 CONTINUE
C***** READ WING NOZZLE DATA *****
      IF(NK(6).EQ.1) READ(5,502) HWNOZ,WWNOZ,VJWNOZ,EJL,EJANG
      IF(NK(7).EQ.1) READ(5,502) HWNOZ,WWNOZ,VJWNOZ,ANGWNZ,TTWNOZ
C***** READ DATA FOR OPTIONAL SOURCES *****
      IF(NK(1).EQ.1) READ(5,502) SA,AR,THICK
      IF(NK(2).EQ.1) READ(5,502) WFF,PRF,DF,TF,TREATF,TREATA
      IF(NK(3).EQ.1) READ(5,502) PRT,VTIPT,DTURB,BLADES,TRPM,PCTP,TREATT
      IF(NK(12).NE.1) GO TO 46
      READ(5,503) NOPTA,XX
      IF(NOPTA.EQ.1) BC=XX
      IF(NOPTA.EQ.2) SHP=XX
   46 CONTINUE
C****** READ INPUT FOR NOISE REDUCTION OPTIONS *****
      READ(5,501) NRED
      IF(NRED.NE.1) GO TO 48
      READ(5,501) NR1,NR2,NR3
      IF(NR3.EQ.1) READ(5,502) HSLOT
   48 CONTINUE
C*
C***** CALCULATE GEOMETRIC VALUES PLUS EXTRA GROUND ATTENUATION,
C*****   GROUND REFLECTION EFFECTS,AND FORWARD SPEED EFFECT *****
C*
      ENG=FLOAT(NENG)
      ENJC=10.0*ALOG10(ENG)
      IF(NOPTG.NE.1) NANG=17
      DO 210 J2=1,NALT
      IF(ALT.LT.4.0) GO TO 270
      IF(NOPTG.NE.1) AZMANG=10.0
      XR=SQRT(SLDIST**2+(ALT-4.0)**2)
      IF(XR.LT.0.01) GO TO 50
      ELVANG=ASIN((ALT-4.0)/XR)*57.2957795
      GO TO 60
   50 ELVANG=90.0
   60 CONTINUE
      ENJCOR=ENJC-2.0*COS(ELVANG/57.2957795)
```

```
      DO 160 J1=1,NANG
      STOD=XR/SIN(AZMANG/57.2957795)
      IF(STOD.LT.10.0) GO TO 285
      CALL EGA(EGSPL)
      CALL GRE(GRSPL)
C*
C***** CALL STATEMENTS FOR SUBROUTINES  *****
C*
      IF(NK(1).EQ.1) CALL AERO(SPLARO)
      IF(NK(2).EQ.1) CALL FAN(SPLF)
      IF(NK(3).EQ.1) CALL TURBNE(SPLF)
      IF(NK(4).EQ.1) CALL JET(SPLJET)
      IF(NK(5).EQ.1) CALL EXCESS(SPLEXS)
      IF(NK(6).EQ.1) CALL AUGWNG(SPLL)
      IF(NK(7).EQ.1) CALL WNGJET(SPLL)
      IF(NK(8).EQ.1) CALL IMPING(SPLL)
      IF(NK(9).EQ.1) CALL WALJET(SPLL)
      IF(NK(10).EQ.1) CALL WAKE(SPLL)
      IF(NK(11).EQ.1) CALL TRAIL(SPLL)
      IF(NK(12).EQ.1) CALL APU(PNLAPU)
      IF(VAC.LE.0.0) GO TO 70
      CALL FWDSPD(DELDBL)
      NOPTF=NOPTS
      NOPTS=1
      CALL FWDSPD(DELDBJ)
      NOPTS=NOPTF
   70 CONTINUE
      IF(NOPTS.NE.2) GO TO 75
      NRED=1
      NR1=1
   75 IF(NRED.NE.1) GO TO 80
      CALL REDUCE(DELL)
   80 CONTINUE
C*
C***** CALCULATE TOTAL OF HIGH LIFT NOISE *****
C*
      SUM2=0.0
      DO 110 I=1,24
      SUM1=0.0
      DO 100 J=1,6
      IF(NK(J+5).NE.1) GO TO 95
      IF(SPLL(J,I).LE.0.1) GO TO 95
      SPLL(J,I)=SPLL(J,I)+ENJCOR+GRSPL(I)-EGSPL(I)+DELDBL+DELL
   95 IF(SPLL(J,I).LT.0.0) SPLL(J,I)=0.0
      IF(SPLL(J,I).GT.0.0) SUM1=SUM1+10.0**(SPLL(J,I)/10.0)
  100 CONTINUE
      IF(SUM1.GT.0.0) SPLLFT(I)=10.0*ALOG10(SUM1)
      IF(SUM1.GT.0.0) SUM2=SUM2+SUM1
  110 CONTINUE
      IF(SUM2.GT.0.0) OASPLL=10.0*ALOG10(SUM2)
      CALL PNLREV(SPLLFT,PN,2)
      PNLLFT=PN
      CALL TONE(SPLLFT,PN,PNLC)
      PNLFTT=PNLC
```

```
C*
C***** CALCULATE TOTAL OF FAN AND TURBINE NOISE *****
C*
      SUM2=0.0
      DO 130 I=1,24
      SUM1=0.0
      DO 120 J=1,2
      IF(NK(J+1).NE.1) GO TO 115
      SPLF(J,I)=SPLF(J,I)+ENJCOR-EGSPL(I)+GRSPL(I)
  115 IF(SPLF(J,I).LT.0.0) SPLF(J,I)=0.0
      IF(SPLF(J,I).GT.0.0) SUM1=SUM1+10.0**(SPLF(J,I)/10.0)
  120 CONTINUE
      IF(SUM1.GT.0.0) SPLFAN(I)=10.0*ALOG10(SUM1)
      IF(SUM1.GT.0.0) SUM2=SUM2+SUM1
  130 CONTINUE
      IF(SUM2.GT.0.0) OASPLF=10.0*ALOG10(SUM2)
      CALL PNLREV(SPLFAN,PN,2)
      PNLFAN=PN
      CALL TONE(SPLFAN,PN,PNLC)
      PNLFNT=PNLC
C*
C***** CALCULATE OASPL AND PNL FOR AIRFRAME NOISE *****
C*
      IF(NK(1).NE.1) GO TO 141
      SUM1=0.0
      DO 140 I=1,24
      SPLARO(I)=SPLARO(I)-EGSPL(I)+GRSPL(I)
      IF(SPLARO(I).LT.0.0) SPLARO(I)=0.0
      IF(SPLARO(I).GT.0.0) SUM1=SUM1+10.0**(SPLARO(I)/10.0)
  140 CONTINUE
      IF(SUM1.GT.0.0) OASPLA=10.0*ALOG10(SUM1)
      CALL PNLREV(SPLARO,PN,2)
      PNLARO=PN
      CALL TONE(SPLARO,PN,PNLC)
      PNLART=PNLC
  141 CONTINUE
C*
C ***** CALCULATE OASPL AND PNL FOR JET AND EXCESS NOISE *****
C*
      SUM1=0.0
      SUM2=0.0
      DO 145 I=1,24
      IF(NK(4).NE.1) GO TO 142
      SPLJET(I)=SPLJET(I)+ENJCOR-EGSPL(I)+GRSPL(I)+DELDBJ
  142 IF(NK(5).NE.1) GO TO 144
      SPLEXS(I)=SPLEXS(I)+ENJCOR-EGSPL(I)+GRSPL(I)
  144 IF(SPLJET(I).LT.0.0) SPLJET(I)=0.0
      IF(SPLEXS(I).LT.0.0) SPLEXS(I)=0.0
      IF(SPLJET(I).GT.0.0) SUM1=SUM1+10.0**(SPLJET(I)/10.0)
      IF(SPLEXS(I).GT.0.0) SUM2=SUM2+10.0**(SPLEXS(I)/10.0)
  145 CONTINUE
      IF(SUM1.GT.0.0) OASPLJ=10.0*ALOG10(SUM1)
      IF(SUM2.GT.0.0) OASPLE=10.0*ALOG10(SUM2)
      CALL PNLREV(SPLJET,PN,2)
```

```
      PNLJET=PN
      CALL TONE(SPLJET,PN,PNLC)
      PNLTJT=PNLC
      CALL PNLREV(SPLEXS,PN,2)
      PNLEXS=PN
      CALL TONE(SPLEXS,PN,PNLC)
      PNLTEX=PNLC
C*
C***** CALCULATE TOTAL NOISE FROM COMPONENTS *****
C*
      SUM2=0.0
      DO 150 I=1,24
      SUM1=0.0
      IF(SPLARO(I).GT.0.0) SUM1=SUM1+10.0**(SPLARO(I)/10.0)
      IF(SPLFAN(I).GT.0.0) SUM1=SUM1+10.0**(SPLFAN(I)/10.0)
      IF(SPLJET(I).GT.0.0) SUM1=SUM1+10.0**(SPLJET(I)/10.0)
      IF(SPLEXS(I).GT.0.0) SUM1=SUM1+10.0**(SPLEXS(I)/10.0)
      IF(SPLLFT(I).GT.0.0) SUM1=SUM1+10.0**(SPLLFT(I)/10.0)
      SUM2=SUM2+SUM1
      IF(SUM1.GT.0.0) SPLT(I)=10.0*ALOG10(SUM1)
  150 CONTINUE
      IF(SUM2.GT.0.0) OASPLT=10.0*ALOG10(SUM2)
      CALL PNLREV(SPLT,PN,2)
      PNL=PN
      CALL TONE(SPLT,PN,PNLC)
      PNLT=PNLC
      IF(PNLAPU.LE.0.0) GO TO 152
      SUM1=10.0**(PNL/10.0)+10.0**(PNLAPU/10.0)
      SUM2=10.0**(PNLT/10.0)+10.0**(PNLAPU/10.0)
      PNLTOT(J1)=10.0*ALOG10(SUM1)
      PNLTC(J1)=10.0*ALOG10(SUM2)
      GO TO 154
  152 PNLTOT(J1)=PNL
      PNLTC(J1)=PNLT
  154 CONTINUE
      DIST(J1)=STOD
      AZIMU(J1)=AZMANG
      AZMANG=AZMANG+10.0
  160 CONTINUE
      ELV(J2)=ELVANG
      ALTUDE(J2)=ALT
      IF(NOPTG.NE.3) GO TO 230
C*
C***** DETERMINE MAXIMUM NOISE FOR SIDELINE POSITIONS *****
C*
      PNLM=0.0
      DO 170 J1=1,NANG
      IF(PNLTC(J1).LT.PNLM) GO TO 170
      PNLM=PNLTC(J1)
      NMAX=J1
  170 CONTINUE
      PNLMAX(J2)=PNLTOT(NMAX)
      PNLTMX(J2)=PNLTC(NMAX)
      AZMAX(J2)=AZIMU(NMAX)
```

```
      DISTMX(J2)=DIST(NMAX)
C*
C***** CALCULATE DISTANCE ALONG THE FLIGHT PATH *****
C*
      IF(J2.GT.1) GO TO 180
      XDIST(1)=STDIST
      GO TO 200
  180 IF(ALTINC.LT.0.0) GO TO 190
      XDIST(J2)=STDIST+((ALTUDE(J2)-ALTUDE(1))/TAN(FLTANG/57.2957795))
      GO TO 200
  190 XDIST(J2)=STDIST-(((ALTUDE(1)-4.0)/TAN(FLTANG/57.2957795))-((
     2 ALTUDE(J2)-4.0)/TAN(FLTANG/57.2957795)))
  200 CONTINUE
      ALT=ALT+ALTINC
  210 CONTINUE
C*
C***** DETERMINE THE MAXIMUM NOISE DURING FLIGHT PROFILE *****
C*
      PNLM=0.0
      DO 220 J2=1,NALT
      IF(PNLTMX(J2).LT.PNLM) GO TO 220
      PNLM=PNLTMX(J2)
      NMAX=J2
  220 CONTINUE
      PMAX=PNLMAX(NMAX)
      PTMAX=PNLTMX(NMAX)
      ATMAX=ALTUDE(NMAX)
      ELMAX=ELV(NMAX)
      AZMX=AZMAX(NMAX)
      DMAX=DISTMX(NMAX)
      XMAX=XDIST(NMAX)
  230 CONTINUE
      VAC=VAC/(1.69*COS(FLTANG/57.2957795))
      GO TO (235,240,250),NOPTG
C*
C***** WRITE STATEMENTS FOR NOPTG = 1 *****
C*
  235 WRITE(6,601) TITLE,VAC,SLDIST,ALT,AZIMU(1),ELVANG,STOD
      WRITE(6,602)
      WRITE(6,603) ((F(I),SPLARO(I),SPLFAN(I),SPLJET(I),SPLEXS(I),
     2 SPLLFT(I),SPLT(I)),I=1,24)
      WRITE(6,604) OASPLA,OASPLF,OASPLJ,OASPLE,OASPLL,OASPLT
      WRITE(6,605) PNLARO,PNLFAN,PNLJET,PNLEXS,PNLLFT,PNL
      WRITE(6,606) PNLART,PNLFNT,PNLTJT,PNLTEX,PNLFTT,PNLT
      WRITE(6,607) PNLAPU,PNLTOT(1),PNLTC(1)
      WRITE(6,608)
      GO TO 260
C*
C***** WRITE STATEMENTS FOR NOPTG = 2 *****
C*
  240 WRITE(6,609) TITLE,VAC,SLDIST,ALT,ELVANG
      WRITE(6,610)
      WRITE(6,611) ((AZIMU(J),DIST(J),PNLTOT(J),PNLTC(J)),J=1,NANG)
      WRITE(6,608)
```

```
      GO TO 260
C*
C***** WRITE STATEMENTS FOR NOPTG = 3 *****
C*
  250 WRITE(6,612) TITLE,VAC,SLDIST
      WRITE(6,613)
      WRITE(6,614) ((ALTUDE(J),XDIST(J),ELV(J),AZMAX(J),DISTMX(J),
     2 PNLMAX(J),PNLTMX(J)),J=1,NALT)
      WRITE(6,615)
      WRITE(6,613)
      WRITE(6,614) ATMAX,XMAX,ELMAX,AZMX,DMAX,PMAX,PTMAX
      WRITE(6,608)
  260 CONTINUE
      GO TO 290
C*
C***** ERROR MESSAGES *****
C*
  270 WRITE(6,616) ALT
      GO TO 290
  280 WRITE(6,617) NOPTG
      GO TO 290
  285 WRITE(6,618) STOD
  290 CONTINUE
C*
C***** FORMAT STATEMENTS FOR INPUT *****
C*
  501 FORMAT(12I5)
  502 FORMAT(8F10.1)
  503 FORMAT(1I5,3F10.1)
  505 FORMAT(10A6)
C*
C***** FORMAT STATEMENTS FOR OUTPUT *****
C*
  601 FORMAT(1H1,/,15X,10A6,//,35X,'AIRCRAFT VELOCITY =   ',F5.1,
     1 ' KNOTS',/,
     2 35X,'SIDELINE DISTANCE =  ',F6.1,' FEET',/,35X,'AIRCRAFT ALTIT'
     3 ,'UDE = ',F7.1,' FEET',/,37X,'AZIMUTHAL ANGLE =   ',F5.1,' DEG.'
     4 /,37X,'ELEVATION ANGLE =   ',F5.1,' DEG.',/,25X,
     5 'SOURCE TO OBSERVER DISTANCE = ',F7.1,' FEET')
  602 FORMAT(//,23X,'AIRFRAME',5X,'FAN AND',5X,'JET',5X,'EXCESS',3X,
     2 'HIGH LIFT',/,10X,'FREQUENCY',3X,'AERODYNAMIC',3X,'TURBINE',
     3 3X,'EXHAUST',3X,'ENGINE',4X,'SYSTEM',5X,'TOTAL',/,13X,'(HZ)',
     4 9X,'(DB)',8X,'(DB)',6X,'(DB)',5X,'(DB)',6X,'(DB)',7X,'(DB)',/)
  603 FORMAT(12X,F6.0,7X,F5.1,7X,F5.1,5X,F5.1,4X,F5.1,5X,F5.1,6X,F5.1)
  604 FORMAT(//,12X,'OASPL',8X,F5.1,7X,F5.1,5X,F5.1,4X,F5.1,5X,F5.1,6X,
     2 F5.1)
  605 FORMAT(13X,'PNL',9X,F5.1,7X,F5.1,5X,F5.1,4X,F5.1,5X,F5.1,6X,F5.1)
  606 FORMAT(13X,'PNLT',8X,F5.1,7X,F5.1,5X,F5.1,4X,F5.1,5X,F5.1,6X,
     2 F5.1)
  607 FORMAT(///,34X,'MAXIMUM APU NOISE = ',F5.1,' PNDB',////,32X,
     2 34('*'),/,32X,'* TOTAL SYSTEM PNL  = ',F5.1,' PNDB *',/,32X,
     3 '*',32X,'*',/,32X,'* TOTAL SYSTEM PNLT = ',F5.1,' PNDB *',/,
     4 32X,34('*'))
  608 FORMAT(1H1)
```

```
609 FORMAT(1H1,/,10X,10A6,//,19X,'AIRCRAFT VELOCITY =   ',F5.1,
   1 ' KNOTS',/,19X,
   2 'SIDELINE DISTANCE =  ',F6.1,' FEET',/,19X,'AIRCRAFT ALTITUDE = ',
   3 F7.1,' FEET',/,21X,'ELEVATION ANGLE =   ',F5.1,' DEG.')
610 FORMAT(//,26X,'SOURCE TO',/,10X,'AZIMUTHAL',8X,'OBSERVER',7X,
   2 'TOTAL',7X,'TOTAL',/,12X,'ANGLE',10X,'DISTANCE',8X,'PNL',8X,
   3 'PNLT',/,12X,'(DEG)',12X,'(FT)',8X,'(PNDB)',6X,'(PNDB)',/)
611 FORMAT(12X,F5.1,10X,F7.1,7X,F5.1,7X,F5.1)
612 FORMAT(1H1,/,20X,10A6,//,39X,'AIRCRAFT VELOCITY =  ',F5.1,
   1 ' KNOTS',/,39X,
   2 'SIDELINE DISTANCE = ',F6.1,' FEET')
613 FORMAT(//,23X,'DISTANCE',28X,'SOURCE TO',/,24X,'ALONG',6X,
   2 'ELEVATION',3X,'AZIMUTHAL',4X,'OBSERVER',3X,'MAXIMUM',3X,
   3 'MAXIMUM',/,10X,'ALTITUDE',3X,'FLIGHT PATH',5X,'ANGLE',7X,
   4 'ANGLE',6X,'DISTANCE',5X,'PNL',7X,'PNLT',/,12X,'(FT)',9X,'(FT)',
   5 8X,'(DEG)',7X,'(DEG)',8X,'(FT)',6X,'(PNDB)',4X,'(PNDB)',/)
614 FORMAT(10X,F7.1,5X,F8.1,7X,F5.1,7X,F5.1,6X,F7.1,5X,F5.1,5X,F5.1)
615 FORMAT(/////,37X,'***** MAXIMUM NOISE *****')
616 FORMAT(1H1,/,10X,'ALTITUDE CANNOT BE LESS THAN 4.0 FEET',/,
   2 10X,'YOUR VALUE IS NOW ',F8.2,/,1H1)
617 FORMAT(1H1,/,10X,'NOPTG CANNOT BE SET EQUAL ',1I5,/1H1)
618 FORMAT(1H1,/,10X,'STOD CANNOT BE LESS THAN 10.0',
   2 /,10X,'YOUR VALUE IS NOW ',F6.3,/,10X,
   3 'INCREASE YOUR VALUE OF ALT OR SLDIST')
    STOP
    END
```

```
      SUBROUTINE AERO(SPLARO)
      DIMENSION RATIO(20),DIFF(20),SPLARO(24)
      COMMON NOPTS,NOPTJ,F(24),ALPHA(24),STOD,ALT,AZMANG,ELVANG,
     2 VAC,DPLUG,DEQUIV,VEQUIV,FLAP1,FLAP2,FLAP3,FLPAG1,FLPAG2,
     3 FLPAG3,TTEQ,HNOZ,WNOZ,VJWNOZ,HWNOZ,WWNOZ,ANGNOZ,ANGWNZ,NRED,
     4 NR1,NR2,NR3,HSLOT,EJL,EJANG,WFF,PRF,DF,TF,TREATF,TREATA,PRT,
     5 DTURB,BLADES,TRPM,PCTP,SA,AR,THICK,NOPTA,BC,SHP,DPRIM,DANIN,
     6 DANOUT,X1,Y1,VTIPT,VJPRIM,VJSEC,TTPRIM,TTSEC,XCN,TTWNOZ,HD
     7 ,ALPHA1,TREATT
      DATA RATIO/0.001953125,0.00390625,0.0078125,0.015625,0.03125,
     2 0.0625,0.125,0.25,0.5,1.0,2.0,4.0,8.0,16.0,32.0,64.0,128.0,
     3 256.0,512.0,1024.0/
      DATA DIFF/201.,179.,157.,135.,113.,91.,69.,47.,25.,10.,16.5,26.5,
     2 36.5,46.5,56.5,66.5,76.5,86.5,96.5,106.5/
      XMN=VAC/1116.0
      FMAX=1.3*VAC/(THICK*(1.-XMN*COS(AZMANG/57.2957/95)))
      OASPL=10.*ALOG10(((SIN(AZMANG/57.2957/95))**2*VAC**5*SA)/
     2 (AR**2*(1.-XMN)**4))+7.0
      DO 10 I=1,24
      FRAT=F(I)/FMAX
      SPEC=GIRC(FRAT,RATIO,DIFF,20,1)
      SPLARO(I)=OASPL-SPEC-20.*ALOG10(STOD)-(STOD/1000.)*ALPHA(I)
      IF(SPLARO(I).LT.0.0) SPLARO(I)=0.0
   10 CONTINUE
      CALL DOPLER(SPLARO)
      RETURN
      END
```

```
      SUBROUTINE FAN(SPLF)
      DIMENSION SPLF(2,24),SPLSH(24),SPLFOR(24),SPLAFT(24),
     2 XANGLE(19),XDIRA(19),XDIRF(19),XSN(9),XSPEC(9)
      COMMON NOPTS,NOPTJ,F(24),ALPHA(24),STOD,ALT,AZMANG,ELVANG,
     2 VAC,DPLUG,DEQUIV,VEQUIV,FLAP1,FLAP2,FLAP3,FLPAG1,FLPAG2,
     3 FLPAG3,TTEQ,HNOZ,WNOZ,VJWNOZ,HWNOZ,WWNOZ,ANGNOZ,ANGWNZ,NRED,
     4 NR1,NR2,NR3,HSLOT,EJL,EJANG,WFF,PRF,DF,TF,TREATF,TREATA,PRT,
     5 DTURB,BLADES,TRPM,PCTP,SA,AR,THICK,NOPTA,BC,SHP,DPRIM,DANIN,
     6 DANOUT,X1,Y1,VTIPT,VJPRIM,VJSEC,TTPRIM,TTSEC,XCN,TTWNOZ,HD
     7 ,ALPHA1,TREATT
      DATA XANGLE/0.,10.,20.,30.,40.,50.,60.,70.,80.,90.,100.,110.,
     2 120.,130.,140.,150.,160.,170.,180./
      DATA XDIRA/-16.,-15.,-14.,-13.,-12.,-11.,-10.,-9.,-7.4,-4.6,-2.0,
     2 1.6,2.4,2.0,-1.4,-2.3,-4.0,-5.2,-7.0/
      DATA XDIRF/-2.6,-1.8,1.0,1.4,0.8,1.0,0.2,-0.6,-2.6,-4.6,-6.7,
     2 -9.4,-10.,-11.,-12.,-13.,-14.,-15.,-16./
      DATA XSN/3.5,5.,6.,7.,9.,11.,14.,17.,20./
      DATA XSPEC/-13.7,-12.5,-10.5,-7.5,-9.9,-10.5,-9.5,-11.9,-12.2/
      DO 2 I=1,24
    2 SPLSH(I)=0.0
      VF=109.595*SQRT(TF*(1.0-1.0/(PRF**0.286)))
      OASPL=10.0*ALOG10(WFF)+20.0*ALOG10(PRF**0.286-1.0)+127.0
      DIRF=GIRC(AZMANG,XANGLE,XDIRF,19,1)
      DIRA=GIRC(AZMANG,XANGLE,XDIRA,19,1)
      IF(NOPTS.NE.3.AND.NOPTS.NE.6) GO TO 5
      XLP=X1+FLAP1*COS(FLPAG1/57.2957795)+FLAP2*COS(FLPAG2/57.2957795)
     2 +FLAP3*COS(FLPAG3/57.2957795)
      HP=Y1+FLAP1*SIN(FLPAG1/57.2957795)+FLAP2*SIN(FLPAG2/57.2957795)
     2 +FLAP3*SIN(FLPAG3/57.2957795)
      EPS=180.0-AZMANG-((ATAN(HP/XLP))*57.2957795)
      RAD=SQRT(XLP**2+HP**2)
      BH=RAD*SIN(EPS/57.2957795)
      SD=SQRT(RAD**2-BH**2)
      OD=STOD-SD
      IF(BH.LE.0.0) GO TO 5
      CALL SHIELD(SPLSH,SD,BH,OD,F,ELVANG)
    5 CONTINUE
      DO 10 I=1,24
      DISTOF=20.0*ALOG10(STOD)+(STOD/1000.0)*ALPHA(I)
      SN=F(I)*DF/VF
      IF(SN.LE.3.5) SPEC=11.0*ALOG10(SN)-19.55
      IF(SN.GT.3.5.AND.SN.LT.20.0) SPEC=GIRC(SN,XSN,XSPEC,9,1)
      IF(SN.GE.20.0) SPEC=-7.6*ALOG10(SN)-2.3
      SPLFOR(I)=OASPL-DIRF-DISTOF+SPEC-TREATF
      SPLAFT(I)=OASPL-DIRA-DISTOF+SPEC-TREATA
      IF(NOPTS.EQ.3.OR.NOPTS.EQ.6) SPLAFT(I)=SPLAFT(I)-SPLSH(I)
      IF(SPLFOR(I).LT.0.0) SPLFOR(I)=0.0
      IF(SPLAFT(I).LT.0.0) SPLAFT(I)=0.0
   10 CONTINUE
      CALL DOPLER(SPLFOR)
      CALL DOPLER(SPLAFT)
      SUM=0.0
      DO 20 I=1,24
      FOR=0.0
```

```
      AFT=0.0
      IF(SPLFOR(I).GT.0.0) FOR=10.0**(SPLFOR(I)/10.0)
      IF(SPLAFT(I).GT.0.0) AFT=10.0**(SPLAFT(I)/10.0)
      SUM=FOR+AFT
      IF(SUM.GT.0.0) SPLF(1,I)=10.0*ALOG10(SUM)
   20 CONTINUE
      RETURN
      END
```

```
      SUBROUTINE TURBNE(SPLF)
      DIMENSION SPLF(2,24),XANGLE(19),XDIR(19),XFR1(10),XFR2(10),
     2 XSPEC1(10),SPL(24),SPLSH(24),XSPEC2(6,10),XPCT(6)
      COMMON NOPTS,NOPTJ,F(24),ALPHA(24),STOD,ALT,AZMANG,ELVANG,
     2 VAC,DPLUG,DEQUIV,VEQUIV,FLAP1,FLAP2,FLAP3,FLPAG1,FLPAG2,
     3 FLPAG3,TTEQ,HNOZ,WNOZ,VJWNOZ,HWNOZ,WWNOZ,ANGNOZ,ANGWNZ,NRED,
     4 NR1,NR2,NR3,HSLOT,EJL,EJANG,WFF,PRF,DF,TF,TREATF,TREATA,PRT,
     5 DTURB,BLADES,TRPM,PCTP,SA,AR,THICK,NOPTA,BC,SHP,DPRIM,DANIN,
     6 DANOUT,X1,Y1,VTIPT,VJPRIM,VJSEC,TTPRIM,TTSEC,XCN,TTWNOZ,HD
     7 ,ALPHA1,TREATT
      DATA XANGLE/0.,10.,20.,30.,40.,50.,60.,70.,80.,90.,100.,110.,
     2 120.,130.,140.,150.,160.,170.,180./
      DATA XDIR/14.5,13.5,12.2,11.5,10.2,9.2,8.2,7.2,6.2,5.2,3.5,1.7,
     2 0.0,1.0,3.2,4.5,5.7,6.2,6.8/
      DATA XFR1/0.1,0.2,0.3,0.4,0.5,0.6,0.7,0.8,0.9,1.0/
      DATA XFR2/1.1,1.2,1.3,1.4,1.5,1.6,1.7,1.8,1.9,2.0/
      DATA XSPEC1/25.0,18.0,15.5,13.5,12.5,12.0,11.0,10.5,10.0,10.0/
      DATA XPCT/50.,60.,70.,80.,90.,100./
      DATA ((XSPEC2(NZ,NX),NX=1,10),NZ=1,6)/10.5,11.0,11.5,12.0,12.5,
     2 13.0,13.2,13.7,14.0,14.5,10.7,11.4,12.2,13.2,14.1,15.0,15.36,
     3 15.86,16.2,16.7,10.9,11.8,12.9,14.4,15.7,17.0,17.52,18.02,18.4,
     4 18.9,11.1,12.2,13.6,15.6,17.3,19.0,19.68,20.18,20.6,21.1,11.3,
     5 12.6,14.3,16.8,18.9,21.0,21.84,22.24,22.8,23.4,11.5,13.0,15.0,
     6 18.0,20.5,23.0,24.0,24.5,25.0,25.5/
      DO 2 I=1,24
    2 SPLSH(I)=0.0
      AREA=3.141592654*(DTURB**2)/4.0
      OASPL=8.75*ALOG10(1.0-(1.0/PRT)**0.286)+20.0*ALOG10(VTIPT/
     2 1116.0)+10.0*ALOG10(AREA)+138.9
      DIR=GIRC(AZMANG,XANGLE,XDIR,19,1)
      OASPL=OASPL-DIR-TREATT
      BPF=BLADES*TRPM/60.0
      IF(NOPTS.NE.3.AND.NOPTS.NE.6) GO TO 5
      XLP=X1+FLAP1*COS(FLPAG1/57.2957795)+FLAP2*COS(FLPAG2/57.2957795)
     2 +FLAP3*COS(FLPAG3/57.2957795)
      HP=Y1+FLAP1*SIN(FLPAG1/57.2957795)+FLAP2*SIN(FLPAG2/57.2957795)
     2 +FLAP3*SIN(FLPAG3/57.2957795)
      EPS=180.0-AZMANG-((ATAN(HP/XLP))*57.2957795)
      RAD=SQRT(XLP**2+HP**2)
      BH=RAD*SIN(EPS/57.2957795)
      SD=SQRT(RAD**2-BH**2)
      OD=STOD-SD
      IF(BH.LE.0.0) GO TO 5
      CALL SHIFLD(SPLSH,SD,BH,OD,F,ELVANG)
    5 CONTINUE
      DO 10 I=1,24
      RATIO=F(I)/BPF
      IF(RATIO.LE.1.0) SPEC=GIRC(RATIO,XFR1,XSPEC1,10,1)
      IF(RATIO.GT.1.0) SPEC=DTAB2(RATIO,PCTP,XFR2,XPCT,10,6,1,1,
     2 XSPEC2,6,IERR)
      SPL(I)=OASPL-SPEC-20.0*ALOG10(STOD)-(STOD/1000.)*ALPHA(I)
      IF(NOPTS.EQ.3.OR.NOPTS.EQ.6) SPL(I)=SPL(I)-SPLSH(I)
      IF(SPL(I).LT.0.0) SPL(I)=0.0
   10 CONTINUE
```

```
      CALL DOPLER(SPL)
      DO 20 I=1,24
      SPLF(2,I)=SPL(I)
   20 CONTINUE
      RETURN
      END
```

```
      SUBROUTINE JET(SPLJET)
      DIMENSION SPL(24),SPLSH(24)
     1,SPLJET(24)
     2,THTP(9),OASDIR(9,17),VRAT(5),ARATP(12),FSP(5,12)
      REAL MA,MC,MCF,NPR,K,KA,LOGST(17),LOGS
      COMMON NOPTS,NOPTJ,F(24),ALPHA(24),STOD,ALT,AZMANG,ELVANG,
     2 VAC,DPLUG,DEQUIV,VEQUIV,FLAP1,FLAP2,FLAP3,FLPAG1,FLPAG2,
     3 FLPAG3,TTEQ,HNOZ,WNOZ,VJWNOZ,HWNOZ,WWNOZ,ANGNOZ,ANGWNZ,NRED,
     4 NR1,NR2,NR3,HSLOT,EJL,EJANG,WFF,PRF,DF,TF,TREATF,TREATA,PRT,
     5 DTURB,BLADES,TRPM,PCTP,SA,AR,THICK,NOPTA,BC,SHP,DPRIM,DANIN,
     6 DANOUT,X1,Y1,VTIPT,VJPRIM,VJSEC,TTPRIM,TTSEC,XCN,TTWNOZ,HD
     7 ,ALPHA1,TREATT
      DATA VRAT/0.2,0.4,0.6,0.8,1.0/
      DATA ARATP/0.,.2,.3,.4,.5,.6,.7,.8,1.0,1.2,1.4,1.6/
      DATA ((FSP(I,J),J=1,12),I=1,5)/0.0,.135,.19,.235,.265,.285,.29,
     1 .295,.30,.30,.30,.30,
     2 0.0,.17,.245,.315,.375,.435,.48,.53,.61,.675,.73,.78,
     3 0.0,.23,.325,.41,.475,.535,.585,.63,.71,.765,.82,.86,
     4 0.0,.20,.285,.365,.43,.49,.54,.585,.66,.715,.76,.805,
     5 0.0,.16,.23,.29,.35,.405,.45,.50,.58,.645,.70,.75/
      DATA THTP/0.0,110.,120.,130.,140.,150.,160.,170.,180./
      DATA LOGST/-1.6,-1.4,-1.2,-1.0,-0.8,-0.6,-0.4,-0.2,0.0,
     1 0.2,0.4,0.6,0.8,1.0,1.2,1.4,1.6/
      DATA ((OASDIR(I,J),J=1,17),I=1,9)/34.2,29.6,25.,20.7,17.1,
     1 14.4,12.5,11.3,10.8,11.1,12.,13.4,15.3,17.5,19.8,22.1,24.5,
     2 34.2,29.6,25.,20.7,17.1,14.4,12.5,11.3,10.8,11.1,
     3 12.,13.4,15.3,17.5,19.8,22.1,24.5,
     4 38.1,32.5,26.7,21.5,17.2,14.,11.9,10.8,10.5,11.,12.4,
     5 14.2,16.5,18.8,21.1,23.6,25.9,
     6 35.5,29.6,23.5,17.6,14.1,11.8,10.4,9.9,10.6,12.,14.1,16.5,
     7 19.2,21.6,24.,26.5,28.9,
     8 32.6,26.5,20.1,15.,11.5,9.7,9.4,10.7,
     9 12.8,15.5,18.3,21.1,24.,26.7,29.6,32.4,35.1,
     1 31.5,25.2,18.6,13.6,10.,7.8,9.2,12.1,15.3,
     2 18.6,22.,25.3,28.6,31.9,35.2,38.6,41.9,
     3 30.2,23.8,17.3,12.4,10.6,11.3,14.3,17.9,21.7,
     4 25.6,29.4,33.3,37.2,40.9,44.7,48.5,52.2,
     5 33.5,27.4,21.1,15.6,13.8,15.7,18.3,21.8,26.1,30.4,
     6 34.5,38.8,42.9,47.,51.1,55.2,59.3,
     7 34.7,28.7,22.8,17.7,16.1,18.7,22.1,26.4,31.4,
     8 36.1,40.9,45.6,50.4,55.1,60.,64.8,69.6/
      DO 10 I=1,24
   10 SPLSH(I)=0.0
      R=53.34
      G=32.174
      TSA=519.
      T=TTPRIM
      U=VJPRIM
      B1=DPLUG
      B2=DPRIM
      B3=DANIN
      B4=DANOUT
      GAM=1.4
      CA=1116.
```

```
      MA=VAC/CA
      TRA=1.+((GAM-1.)/2.)*MA**2
      TTA=TSA*TRA
      RHOA=39.7/TSA
      NPR=1./(1.-U**2/(2.*G*(GAM/(GAM-1.))*R*T))**(GAM/(GAM-1.))
      RHOJ=(39.7/T)*NPR**((GAM-1.)/GAM)
      THETA=AZMANG+ANGNOZ
      THETAP=THETA*(U/CA)**0.1
      GO TO (12,13,14), NOPTJ
   12 AN=3.14*(B2*B2-B1*B1)/4.
      DH=B2-B1
      HD=DH
      DEQUIV=SQRT(B2*B2-B1*B1)
      IF(B1.GT.0.0) H=(B2-B1)/2.
      DE=DEQUIV
      VEQUIV=VJPRIM
      TTEQ=TTPRIM
      GO TO 15
   13 AN=WNOZ*HNOZ
      DH=4.*AN/(2.*WNOZ+2.*HNOZ)
      DEQUIV=SQRT(4.*AN/3.14)
      DE=DEQUIV
      HD=DH
      VEQUIV=VJPRIM
      TTEQ=TTPRIM
      GO TO 15
   14 APRI=3.14*(B2*B2-B1*B1)/4.
      ASEC=3.14*(B4*B4-B3*B3)/4.
      AN=APRI
      DH=B2-B1
      DE=SQRT(B2*B2-B1*B1)
      DEQUIV=SQRT(4.*(APRI+ASEC)/3.14)
      IF(B1.GT.0.0) H=(B2-B1)/2.
      HD=4.*(APRI+ASEC)/(3.14*(B1+B2+B3+B4))
      TSPRI=TTPRIM-(((GAM-1.)/2.)*VJPRIM**2)/(GAM*R*G)
      TSSEC=TTSEC-(((GAM-1.)/2.)*VJSEC**2)/(GAM*R*G)
      WPRI=(2116.*APRI*VJPRIM)/(R*TSPRI)
      WSEC=(2116.*ASEC*VJSEC)/(R*TSSEC)
      TTEQ=(TTSEC*WSEC+TTPRIM*WPRI)/(WSEC+WPRI)
      VEQUIV=(VJSEC*WSEC+VJPRIM*WPRI)/(WSEC+WPRI)
      ARAT=ASEC/APRI
      ARP=ALOG10(1.+ASEC/APRI)
      VR=VJSEC/VJPRIM
      U=VJPRIM
   15 CONTINUE
      STF=(T/TTA)**(0.4*(1.+COS(THETAP/57.3)))*(DH/DE)**0.4
      MC=0.62*U/CA
      MCF=30.*ALOG10(1.+MC*((1.+MC**5)**-0.2)*COS(THETA/57.3))
      A=10.*ALOG10(AN*((RHOA/0.0765)**2)*(CA/1116.)**4)
      K=U/CA
      B=10.*(((3.*K**3.5)/(0.6+K**3.5))-1.)*ALOG10(RHOJ/RHOA)
      C=10.*ALOG10((K**7.5)/(1.+0.010*K**4.5))
C
C  CALCULATE OASPL AT 90 DEG FROM EQN #6 OF NASA TMX71618
```

```
C
      KA=134.
      IF(NOPTJ.EQ.1.AND.B1.GT.0.0.OR.NOPTJ.EQ.3.AND.B1.GT.0.0) KA=
     1 134.+3.*ALOG10(0.10+2.*(H/B2))
      OAS90=KA+A+B+C
      IF(NOPTJ.NE.3) GO TO 16
      IF(ARAT.GE.29.7) M=6.0
      IF(ARAT.LT.29.7) M=1.1*SQRT(ARAT)
      FS=DTAB2(ARP,VR,ARATP,VRAT,12,5,1,1,FSP,5,IERP)
      OASDEL=5.*ALOG10(TTPRIM/TTSEC)+10.*ALOG10((1.-
     1 VR)**M+1.2*(1.+((ARAT)*VR*VP))
     2 **4/(1.+ARAT)**3)
      OAS90=OAS90+OASDEL
   16 CONTINUE
      DELV=0.0
      IF(NOPTS.EQ.1) DELV=3.0
      IF(NOPTS.NE.3.AND.NOPTS.NE.6) GO TO 35
      XLP=X1+FLAP1*COS(FLPAG1/57.2957795)+FLAP2*COS(FLPAG2/
     1 57.2957795)+FLAP3*COS(FLPAG3/57.2957795)
      XLP=XLP-2.*DE
      HP=Y1+FLAP1*SIN(FLPAG1/57.2957795)+FLAP2*SIN(FLPAG2/
     2 57.2957795)+FLAP3*SIN(FLPAG3/57.2957795)
      EPS=180.-AZMANG-((ATAN(HP/XLP))*57.2957795)
      RAD=SQRT(XLP*XLP+HP*HP)
      BH=RAD*SIN(EPS/57.2957795)
      SD=SQRT(RAD*RAD-BH*BH)
      OD=STOD-SD
      IF(BH.LE.0.0) GO TO 35
      CALL SHIELD(SPLSH,SD,BH,OD,F,ELVANG)
   35 CONTINUE
      OAS90=OAS90+DELV
C
      IF(NOPTJ.EQ.3) SFCOAX=1./(1.-(TTSEC/TTPRIM)*FS)
      DO 18 J=1,24
      ST=(F(J)*DE/D)*STF
      IF(NOPTJ.EQ.3) ST=ST*SFCOAX
      LOGS=ALOG10(ST)
      DIFF=DTAB2(LOGS,THETAP,LOGST,THTP,17,9,1,1,OASDIR,9,IERP)
      SPL(J)=OAS90-DIFF-MCF-20.*ALOG10(STOD)-ALPHA(J)*(STOD/1000.)
C
C ********     DIFF = OASPL - SPL - MCF
C     REF FIG #5  NASA TMX 71618
C
      IF(NOPTS.EQ.3.OR.NOPTS.EQ.6) SPL(J)=SPL(J)-SPLSH(J)
   18 IF(SPL(J).LT.0.0) SPL(J)=0.0
      CALL DOPLER(SPL)
      DO 82 J=1,24
   82 SPLJET(J)=SPL(J)
      RETURN
      END
```

```
      SUBROUTINE EXCESS(SPLEXS)
      DIMENSION SN1(5),Y10(5),
     1SPL(24),SPLEXS(24),SPLSH(24)
      COMMON NOPTS,NOPTJ,F(24),ALPHA(24),STOD,ALT,AZMANG,ELVANG,
     2 VAC,DPLUG,DEQUIV,VEQUIV,FLAP1,FLAP2,FLAP3,FLPAG1,FLPAG2,
     3 FLPAG3,TTEQ,HNOZ,WNOZ,VJWNOZ,HWNOZ,WWNOZ,ANGNOZ,ANGWNZ,NRE
     4 NR1,NR2,NR3,HSLOT,EJL,EJANG,WFF,PRF,DF,TF,TREATF,TREATA,PR
     5 DTURB,BLADES,TRPM,PCTP,SA,AR,THICK,NOPTA,BC,SHP,DPRIM,DANI
     6 DANOUT,X1,Y1,VTIPT,VJPRIM,VJSEC,TTPRIM,TTSEC,XCN,TTWNOZ,HD
     7 ,ALPHA1,TREATT
      DATA SN1/.2,.25,.3,.35,.4/
      DATA Y10/-11.4,-7.2,-5.8,-6.4,-7.9/
      DO 10 I=1,24
   10 SPLSH(I)=0.0
      A=3.14*DEQUIV*DEQUIV/4.
      U=VEQUIV
      E=10.
      THETA=180.-AZMANG-ANGNOZ
      X=E*E*A*U**6*(1.-COS(THETA/57.3))
      OASPL=0.0
      IF(X.GT.1.0) OASPL=10.*ALOG10(X)-70.0
      IF(NOPTS.NE.3.AND.NOPTS.NE.6) GO TO 35
      XLP=X1+FLAP1*COS(FLPAG1/57.2957795)+FLAP2*COS(FLPAG2/
     1 57.2957795)+FLAP3*COS(FLPAG3/57.2957795)
      HP=Y1+FLAP1*SIN(FLPAG1/57.2957795)+FLAP2*SIN(FLPAG2/
     2 57.2957795)+FLAP3*SIN(FLPAG3/57.2957795)
      EPS=180.-AZMANG-((ATAN(HP/XLP))*57.2957795)
      RAD=SQRT(XLP*XLP+HP*HP)
      BH=RAD*SIN(EPS/57.2957795)
      SD=SQRT(RAD*RAD-BH*BH)
      OD=STOD-SD
      IF(BH.LE.0.0) GO TO 35
      CALL SHIELD(SPLSH,SD,BH,OD,F,ELVANG)
   35 CONTINUE
      DO 26 J=1,24
      SN=F(J)*DEQUIV/U
      IF(SN.LE.0.2) SPEC=52.36*ALOG10(SN)+25.2
      IF(SN.GE.0.4) SPEC=-28.5*ALOG10(SN)-19.25
      IF(SN.GT.0.2.AND.SN.LT.0.4) SPEC=GIRC(SN,SN1,Y10,5,1)
      SPL(J)=OASPL+SPEC-20.*ALOG10(STOD)-ALPHA(J)*(STOD/1000.)
      IF(NOPTS.EQ.3.OR.NOPTS.EQ.6) SPL(J)=SPL(J)-SPLSH(J)
   26 IF(SPL(J).LT.0.0) SPL(J)=0.0
      CALL DOPLER(SPL)
      DO 82 J=1,24
   82 SPLEXS(J)=SPL(J)
      RETURN
      END
```

```
      SUBROUTINE AUGWNG(SPLL)
      DIMENSION SPLL(6,24),SPL(24),XANGLE(16),XDIR(16),XSN(18),XSPEC(18)
     2 ,XELV(10),XEDIR(10)
      COMMON NOPTS,NOPTJ,F(24),ALPHA(24),STOD,ALT,AZMANG,ELVANG,
     2 VAC,DPLUG,DEQUIV,VEQUIV,FLAP1,FLAP2,FLAP3,FLPAG1,FLPAG2,
     3 FLPAG3,TTEQ,HNOZ,WNOZ,VJWNOZ,HWNOZ,WWNOZ,ANGNOZ,ANGWNZ,NRED,
     4 NR1,NR2,NR3,HSLOT,EJL,EJANG,WFF,PRF,DF,TF,TREATF,TREATA,PRT,
     5 DTURB,BLADES,TRPM,PCTP,SA,AR,THICK,NOPTA,BC,SHP,DPRTM,DANIN,
     6 DANOUT,X1,Y1,VTIPT,VJPRIM,VJSEC,TTPRIM,TTSEC,XCN,TTWNOZ,HD
     7 ,ALPHA1,TREATT
      DATA XANGLE/-70.0,-60.,-50.,-40.,-30.,-20.,-10.,0.0,10.,20.,30.,
     2 40.,50.,60.,70.,80./
      DATA XDIR/12.5,10.0,8.0,6.5,5.0,3.0,1.0,0.0,0.5,1.0,2.5,7.5,
     2 11.0,11.0,8.0,7.0/
      DATA XSN/0.01,0.02,0.04,0.06,0.08,0.1,0.2,0.3,0.4,0.5,0.6,0.8,
     2 1.0,1.5,2.0,4.0,6.0,10.0/
      DATA XSPEC/31.0,25.,19.5,16.5,14.7,13.0,9.5,9.0,9.5,10.5,11.5,
     2 13.,14.5,18.5,22.5,33.0,39.0,47.0/
      DATA XELV/0.,10.,20.,30.,40.,50.,60.,70.,80.,90./
      DATA XEDIR/3.,2.1,1.5,1.,0.7,0.4,0.2,0.1,0.05,0.0/
      EJLHW=EJL/HWNOZ
      AREA=HWNOZ*WWNOZ
      ANGPRM=AZMANG-(180.0-(EJANG+45.0))
      PERM=2.0*HWNOZ+2.0*WWNOZ
      HDIA=4.0*AREA/PERM
      DIR=GIRC(ANGPRM,XANGLE,XDIR,16,1)
      DIRE=GIRC(ELVANG,XELV,XEDIR,10,1)
      OASPL=60.0*ALOG10(VJWNOZ)+10.0*ALOG10(AREA)-5.0*ALOG10(EJLHW/10.0)
     2 -30.6
      OASPL=OASPL-DIR-DIRE
      DO 10 I=1,24
      SN=F(I)*HDIA/VJWNOZ
      SPEC=GIRC(SN,XSN,XSPEC,18,1)
      SPL(I)=OASPL-SPEC-20.0*ALOG10(STOD)-(STOD/1000.)*ALPHA(I)
      IF(SPL(I).LT.0.0) SPL(I)=0.0
   10 CONTINUE
      CALL DOPLER(SPL)
      DO 20 I=1,24
      SPLL(1,I)=SPL(I)
   20 CONTINUE
      RETURN
      END
```

```
      SUBROUTINE WNGJET(SPLL)
      DIMENSION SPL(24),SPLSH(24)
     1,SPLL(6,24)
     2,THTP(9),OASDIR(9,17),VRAT(5),ARATP(12),FSP(5,12)
      REAL MA,MC,MCF,NPR,K,KA,LOGST(17),LOGS
      COMMON NOPTS,NOPTJ,F(24),ALPHA(24),STOD,ALT,AZMANG,ELVANG,
     2 VAC,DPLUG,DEQUIV,VEQUIV,FLAP1,FLAP2,FLAP3,FLPAG1,FLPAG2,
     3 FLPAG3,TTEQ,HNOZ,WNOZ,VJWNOZ,HWNOZ,WWNOZ,ANGNOZ,ANGWNZ,NRED,
     4 NR1,NR2,NR3,HSLOT,EJL,EJANG,WFF,PRF,DF,TF,TREATF,TREATA,PRT,
     5 DTURB,BLADES,TRPM,PCTP,SA,AR,THICK,NOPTA,BC,SHP,DPRIM,DANIN,
     6 DANOUT,X1,Y1,VTIPT,VJPRIM,VJSEC,TTPRIM,TTSEC,XCN,TTWNOZ,HD
     7 ,ALPHA1,TREATT
      DATA VRAT/0.2,0.4,0.6,0.8,1.0/
      DATA ARATP/0.,.2,.3,.4,.5,.6,.7,.8,1.0,1.2,1.4,1.6/
      DATA ((FSP(I,J),J=1,12),I=1,5)/0.0,.135,.19,.235,.265,.285,.29,
     1 .295,.30,.30,.30,.30,
     2 0.0,.17,.245,.315,.375,.435,.48,.53,.61,.675,.73,.78,
     3 0.0,.23,.325,.41,.475,.535,.585,.63,.71,.765,.82,.86,
     4 0.0,.20,.285,.365,.43,.49,.54,.585,.66,.715,.76,.805,
     5 0.0,.16,.23,.29,.35,.405,.45,.50,.58,.645,.70,.75/
      DATA THTP/0.0,110.,120.,130.,140.,150.,160.,170.,180./
      DATA LOGST/-1.6,-1.4,-1.2,-1.0,-0.8,-0.6,-0.4,-0.2,0.0,
     1 0.2,0.4,0.6,0.8,1.0,1.2,1.4,1.6/
      DATA ((OASDIR(I,J),J=1,17),I=1,9)/34.2,29.6,25.,20.7,17.1,
     1 14.4,12.5,11.3,10.8,11.1,12.,13.4,15.3,17.5,19.8,22.1,24.5,
     2 34.2,29.6,25.,20.7,17.1,14.4,12.5,11.3,10.8,11.1,
     3 12.,13.4,15.3,17.5,19.8,22.1,24.5,
     4 38.1,32.5,26.7,21.5,17.2,14.,11.9,10.8,10.5,11.,12.4,
     5 14.2,16.5,18.8,21.1,23.6,25.9,
     6 35.5,29.6,23.5,17.6,14.1,11.8,10.5,9.9,10.6,12.,14.1,16.5,
     7 19.2,21.6,24.,26.5,28.9,
     8 32.6,26.5,20.1,15.,11.5,9.7,9.4,10.7,
     9 12.8,15.5,18.3,21.1,24.,26.7,29.6,32.4,35.1,
     1 31.5,25.2,18.6,13.6,10.,7.8,9.2,12.1,15.3,
     2 18.6,22.,25.3,28.6,31.9,35.2,38.6,41.9,
     3 30.2,23.8,17.3,12.4,10.6,11.3,14.3,17.9,21.7,
     4 25.6,29.4,33.3,37.2,40.9,44.7,48.5,52.2,
     5 33.5,27.4,21.1,15.6,13.8,15.7,18.3,21.8,26.1,30.4,
     6 34.5,38.8,42.9,47.,51.1,55.2,59.3,
     7 34.7,28.7,22.8,17.7,16.1,18.7,22.1,26.4,31.4,
     8 36.1,40.9,45.6,50.4,55.1,60.,64.8,69.6/
      DO 10 I=1,24
   10 SPLSH(I)=0.0
      R=53.34
      G=32.174
      TSA=519.
      T=TTWNOZ
      U=VJWNOZ
      GAM=1.4
      CA=1116.
      MA=VAC/CA
      TRA=1.+((GAM-1.)/2.)*MA**2
      TTA=TSA*TRA
      RHOA=39.7/TSA
```

```
      NPR=1./(1.-U**2/(2.*G*(GAM/(GAM-1.))*R*T))**(GAM/(GAM-1.))
      RHOJ=(39.7/T)*NPR**((GAM-1.)/GAM)
      THETA=AZMANG+ANGWNZ
      THETAP=THETA*(U/CA)**0.1
      AN=WWNOZ*HWNOZ
      DH=4.*AN/(2.*WWNOZ+2.*HWNOZ)
      DE=SQRT(4.*AN/3.14)
      IF(NOPTS.NE.4) GO TO 13
      DEQUIV=DE
      HD=DH
      VEQUIV=VJWNOZ
      TTEQ=TTWNOZ
   13 CONTINUE
      STF=(T/TTA)**(0.4*(1.+COS(THETAP/57.3)))*(DH/DE)**0.4
      MC=0.62*U/CA
      MCF=30.*ALOG10(1.+MC*((1.+MC**5)**-0.2)*COS(THETA/57.3))
      A=10.*ALOG10(AN*((RHOA/0.0765)**2)*(CA/1116.)**4)
      K=U/CA
      B=10.*(((3.*K**3.5)/(0.6+K**3.5))-1.)*ALOG10(RHOJ/RHOA)
      C=10.*ALOG10((K**7.5)/(1.+0.010*K**4.5))
C
C  CALCULATE OASPL AT 90 DEG FROM EQN #6 OF NASA TMX/1618
C
      KA=134.
      OAS90=KA+A+B+C
      IF(FLAP1.LE.0.0) GO TO 35
      XLP=X1+FLAP1*COS(FLPAG1/57.2957795)+FLAP2*COS(FLPAG2/
     1 57.2957795)+FLAP3*COS(FLPAG3/57.2957795)
      XLP=XLP-X1-2.*DE
      HP=Y1+FLAP1*SIN(FLPAG1/57.2957795)+FLAP2*SIN(FLPAG2/
     2 57.2957795)+FLAP3*SIN(FLPAG3/57.2957795)
      EPS=180.-AZMANG-((ATAN(HP/XLP))*57.2957795)
      RAD=SQRT(XLP*XLP+HP*HP)
      BH=RAD*SIN(EPS/57.2957795)
      SD=SQRT(RAD*RAD-BH*BH)
      OD=STOD-SD
      IF(BH.LE.0.0) GO TO 35
      CALL SHIELD(SPLSH,SD,BH,OD,F,ELVANG)
   35 CONTINUE
      DO 18 J=1,24
      ST=(F(J)*DE/U)*STF
      LOGS=ALOG10(ST)
      DIFF=DTAB2(LOGS,THETAP,LOGST,THTP,17,9,1,1,OASDIR,9,IERR)
      SPL(J)=OAS90-DIFF-MCF-20.*ALOG10(STOD)-ALPHA(J)*(STOD/1000.)
C
C *********    DIFF = OASPL - SPL - MCF
C     REF FIG #5  NASA TMX 71618
C
      IF(FLAP1.GT.0.0) SPL(J)=SPL(J)-SPLSH(J)
   18 IF(SPL(J).LT.0.0) SPL(J)=0.0
      CALL DOPLER(SPL)
      DO 82 J=1,24
   82 SPLL(2,J)=SPL(J)
      RETURN
      END
```

```
      SUBROUTINE IMPING(SPLL)
      DIMENSION SPLL(6,24),SPL(24),SPLOA(9),
     2 PNGDIR(4,14),PNGANG(4),THETAG(14),THEDIR(15),ELVDIR(15)
      REAL MSN(9),MJ,LAM
      COMMON NOPTS,NOPTJ,F(24),ALPHA(24),STOD,ALT,AZMANG,ELVANG,
     2 VAC,DPLUG,DEQUIV,VEQUIV,FLAP1,FLAP2,FLAP3,FLPAG1,FLPAG2,
     3 FLPAG3,TTEQ,HNOZ,WNOZ,VJWNOZ,HWNOZ,WWNOZ,ANGNOZ,ANGWNZ,NRED,
     4 NR1,NR2,NR3,HSLOT,EJL,EJANG,WFF,PRF,DF,TF,TREATF,TREATA,PRT,
     5 DTURB,BLADES,TRPM,PCTP,SA,AR,THICK,NOPTA,BC,SHP,DPRIM,DANIN,
     6 DANOUT,X1,Y1,VTIPT,VJPRIM,VJSEC,TTPRIM,TTSEC,XCN,TTWNOZ,HD
     7 ,ALPHA1,TREATT
      DATA THEDIR/0.,30.,60.,90.,120.,150.,165.,180.,210.,
     2 240.,270.,300.,330.,340.,360./
      DATA ELVDIR/-5.,0.5,1.9,2.2,3.5,10.0,16.0,14.0,4.0,
     2 2.0,0.7,-2.7,-11.0,-11.3,-5./
      DATA MSN/.08,.10,.15,.2,.25,.3,.4,.5,.6/
      DATA SPLOA/-25.4,-22.,-17.,-15.3,-14.9,-15.,-16.2,-17.5,-18.5/
      DATA PNGANG/15.,30.,60.,90./
      DATA THETAG/0.,30.,60.,90.,100.,120.,150.,180.,210.,
     2 240.,270.,300.,330.,360./
      DATA ((PNGDIR(I,J),J=1,14),I=1,4)/-14.,-12.,-10.,-3.,
     2 -2.,-10.,-19.,-23.,-23.,-25.,-25.,-18.,-16.,-14.,
     3 -13.,-11.,-8.,-1.,0.0,-5.,-23.,-25.,-26.,
     4 -25.,-23.,-16.,-14.,-13.,
     5 -6.,-4.,-2.,0.0,0.0,-8.,-20.,-23.,
     6 -24.,-22.,-17.,-12.,-8.,-6.,
     7 0.0,0.0,0.0,0.0,0.0,-7.,-19.,
     8 -23.,-23.,-22.,-18.,-6.,-1.,0.0/
      IF(NOPTS.EQ.4.OR.NOPTS.EQ.5) GO TO 90
      GAM=1.4
      X0=0.0
      R=53.34
      GC=32.2
      T=TTEQ
      U=VEQUIV
      TS=T-((GAM-1.)*U*U)/(2.*GAM*R*GC)
      MJ=U/SQRT(GAM*R*TS*GC)
      IF(VAC.GT.0.1) LAM=U/(VAC)
C  ***********************************************************
C  CALCULATION OF XP , IMPINGEMENT ANGLE ALPHA & IMPINGEMENT AREA
C  ***********************************************************
      IF(NOPTS.EQ.2) GO TO 20
C
C  ******* USB, HYBRID **********************
C
      IF(ALPHA1.LE.0.0) GO TO 90
      ALPH=ALPHA1
      XP=Y1/SIN(ALPHA1/57.3)
      GO TO 26
C  ***********************************************************
C   *******************EBF ********************
C  ***********************************************************
   20 NFLAPS=0
      IF(FLAP1.GT.0.0) NFLAPS=1
```

```
      IF(FLAP2.GT.0.0) NFLAPS=2
      IF(FLAP3.GT.0.0) NFLAPS=3
      IF(NFLAPS.GT.0) AVGFA=(FLPAG1+FLPAG2+FLPAG3)/NFLAPS
      IF(NFLAPS.EQ.0) AVGFA=0.0
      XB=Y1*TAN((90.-AVGFA)/57.3)
      XA=X1+XB
      ZL=FLAP1+FLAP2+FLAP3
      IF(ALPHA1.LT.0.0) GO TO 24
C
C  EBF WITH ALPHA1 GE 0.0***********
C
      IF(ALPHA1.LE.0.0) GO TO 28
      XC=Y1/TAN(ALPHA1/57.3)
      IF(XC.GE.X1) GO TO 28
      XP=Y1/SIN(ALPHA1/57.3)
      ALPH=ALPHA1
      GO TO 26
   28 ALPH=ALPHA1+AVGFA
      PHI=180.-ALPHA1-AVGFA
      XP=SIN(AVGFA/57.3)*XA/SIN(PHI/57.3)
      XH=XP*COS(ALPHA1/57.3)
      XE1=ZL*COS(AVGFA/57.3)+X1
      IF(XH.GE.XE1) GO TO 90
      GO TO 26
   24 CONTINUE
C
C  EBF WITH ALPHA1 LT 0.0 *************
C
      ALPH=AVGFA+ALPHA1
      PHI=180.-AVGFA
      XP=SIN(PHI/57.3)*XA/SIN(ALPH/57.3)
      XH=XP*COS(-ALPHA1/57.3)
      XE1=ZL*COS(AVGFA/57.3)+X1
      IF(XH.GE.XE1) GO TO 90
   26 CONTINUE
      GO TO (12,13,12), NOPTJ
   12 DH=HD
      DE=DEQUIV
      IF(VAC.LT.0.1) DIR=0.089*(XP-X0)/DE
      IF(VAC.GT.0.1) DIR=(0.089*(XP-X0)/DE)/SQRT(1.+(0.2//
     2 SQRT(LAM*(LAM-1.)))*((XP-X0)/DE))
      DI=DIR*DE
      AI=3.14*DI*DI/4.
      GO TO 14
   13 DE=DEQUIV
      DH=HD
      IF(VAC.LT.0.1) HIR=0.109*(XP-X0)/HNOZ
      IF(VAC.GT.0.1) HIR=0.109*((XP-X0)/HNOZ)/(1.+(0.55/SQRT(LAM*
     2 (LAM-1.)))*SQRT((XP-X0)/HNOZ))
      HI=HIR*HNOZ
      AI=WNOZ*HI
      DI=HI
   14 CONTINUE
      A=4.0
```

```
      IF(NOPTJ.EQ.2) A=4./(1.+(8./3.)*(DE/DH-1.))
      VIPR=(1.+((0.15*XP)/(XCN*DE*SQRT(1.+MJ)))**A)**(-1./A)
      VIP=VIPR*U
C
C     CALCULATE OASPL & DIRECTIVITY EFFECTS
C      DIRECTIVITY FIRST CALC'D IN FLYOVER PLANE
C      THEN CORRECTED FOR ELEVATION
C
      OASPL=10.*ALOG10((AI)*(SIN(ALPH/57.3))**2)+80.*ALOG10(VIP)-74.
      IF(NOPTS.EQ.3.OR.NOPTS.EQ.6) THEPNG=360.
     1 -ALPHA1-AZMANG
      IF(NOPTS.EQ.2) THEPNG=AZMANG-ALPHA1
      THTALP=ALPH+THEPNG
      ATHEDB=DTAB2(THEPNG,ALPH,THETAG,PNGANG,14,4,1,1,PNGDIR,4,IERR)
      ELVDB=GIRC(THTALP,THEDIR,ELVDIR,15,2)
      THEDB=ELVDB*COS(ELVANG/57.3)
      OASPL=OASPL+ATHEDB-THEDB
C
C       CALCULATE SPECTRA
C
      DO 17 J=1,24
      SN=F(J)*DI/(VIP*SQRT(SIN(ALPH/57.3)))
      IF(SN.LE.0.08) DEL=37.37*ALOG10(SN)+15.59
      IF(SN.GE.0.6) DEL=-15.38*ALOG10(SN)-22.0
      IF(SN.GT.0.08.AND.SN.LT.0.6) DEL=GIRC(SN,MSN,SPLOA,9,2)
      SPL(J)=OASPL+DEL-20.*ALOG10(STOD)-ALPHA(J)*(STOD/1000.)
   17 IF(SPL(J).LT.0.0) SPL(J)=0.0
      CALL DOPLER(SPL)
      DO 82 J=1,24
   82 SPLL(3,J)=SPL(J)
   90 CONTINUE
      RETURN
      END
```

```
      SUBROUTINE WALJET(SPLL)
      DIMENSION SPLL(6,24),THEDIR(15),ELVDIR(15),
     2 SPL(24),ANGLE(37),DEL(37),OAS90(17)
      REAL LSN,LOGST(17)
      COMMON NOPTS,NOPTJ,F(24),ALPHA(24),STOD,ALT,AZMANG,ELVANG,
     2 VAC,DPLUG,DEQUIV,VEQUIV,FLAP1,FLAP2,FLAP3,FLPAG1,FLPAG2,
     3 FLPAG3,TTEQ,HNOZ,WNOZ,VJWNOZ,HWNOZ,WWNOZ,ANGNOZ,ANGWNZ,NRFD,
     4 NR1,NR2,NR3,HSLOT,EJL,EJANG,WFF,PRF,DF,TF,TREATF,TREATA,PRT,
     5 DTURB,BLADES,TRPM,PCTP,SA,AR,THICK,NOPTA,BC,SHP,DPRIM,DANIN,
     6 DANOUT,X1,Y1,VTIPT,VJPRIM,VJSEC,TTPRIM,TTSEC,XCN,TTWNOZ,HD
     7 ,ALPHA1,TREATT
      DATA LOGST/-1.6,-1.4,-1.2,-1.0,-0.8,-0.6,-0.4,-0.2,
     1 0.0,0.2,0.4,0.6,0.8,1.0,1.2,1.4,1.6/
      DATA OAS90/-32.4,-28.3,-24.4,-20.6,-17.1,-14.4,-12.5,
     1 -11.2,-10.7,-10.7,-11.5,-13.2,-15.5,-18.2,-21.2,-24.3,-27.6/
      DATA ANGLE/0.,10.,20.,30.,40.,50.,60.,70.,80.,90.,100.,110.,
     1 120.,130.,140.,150.,160.,170.,180.,190.,200.,210.,220.,
     2 230.,240.,250.,260.,270.,280.,290.,300.,310.,320.,
     3 330.,340.,350.,360./
      DATA DEL/-6.6,-6.1,-5.4,-4.6,-3.7,-2.7,-1.7,-1.1,-0.4,0.0,
     2 -0.2,-1.1,-1.7,-2.9,-3.9,-4.5,-5.5,-6.3,-6.5,-7.6,-9.9,
     3 -12.9,-17.,-24.4,-33.4,-35.8,-37.,-37.5,-37.2,-36.7,-35.5,
     4 -33.2,-28.,-19.,-13.,-9.,-6.6/
      DATA THEDIR/0.,30.,60.,90.,105.,120.,150.,180.,210.,
     1 240.,270.,280.,300.,330.,360./
      DATA ELVDIR/1.9,2.2,3.5,10.,16.,14.,4.,2.,0.7,
     2 -2.7,-11.,-11.3,-5.,0.5,1.9/
C
C          OAS90 = FUNC(LOGST) SPECTRA SHAPE FOR ENGINE JET NOISE AT
C                     90 DEG FR NOZ AXIS
C
      GAM=1.4
      R=53.34
      GC=32.2
      IF(NOPTS.EQ.4) GO TO 4
      T=TTEQ
      U=VEQUIV
      GO TO 5
    4 T=TTWNOZ
      U=VJWNOZ
    5 TS=T-((GAM-1.)*U*U)/(2.*GAM*R*GC)
      MJ=U/SQRT(GAM*R*TS*GC)
      DE=DEQUIV
      IF(VAC.GT.0.0) LAM=U/VAC
C ******* DETERMINE NO. OF FLAPS & AVER FLAP ANG *******
C
      NFLAPS=0
      IF(FLAP1.GT.0.0) NFLAPS=1
      IF(FLAP2.GT.0.0) NFLAPS=2
      IF(FLAP3.GT.0.0) NFLAPS=3
      IF(NFLAPS.GT.0) AVGFA=(FLPAG1+FLPAG2+FLPAG3)/NFLAPS
      IF(NFLAPS.EQ.0) AVGFA=0.0
      IF(NOPTS.EQ.3.OR.NOPTS.EQ.4.OR.NOPTS.EQ.6) GO TO 60
C  ***********************************************************
```

```
C ***************** EBF COMPUTATIONS *********************
C ****************************************************************
      XB=Y1/TAN(AVGFA/57.3)
      XA=X1+XB
      ZL=FLAP1+FLAP2+FLAP3
      IF(ALPHA1.LT.0.0) GO TO 30
C ******** ALPHA1 GE 0.0 ***********
      IF(ALPHA1.LE.0.0) GO TO 28
      XC=Y1/TAN(ALPHA1/57.3)
      IF(XC.GE.X1) GO TO 28
      XPRIM=ZL+(X1-XC)
      XP=Y1/SIN(ALPHA1/57.3)
      GO TO 32
   28 PHI=180.-AVGFA-ALPHA1
      XP=SIN(AVGFA/57.3)*XA/SIN(PHI/57.3)
      IF(ALPHA1.LE.0.0) XP=XA
      SS=XP*SIN(ALPHA1/57.3)
      P=(Y1-SS)/SIN(AVGFA/57.3)
      XPRIM=ZL-P
      IF(XPRIM.LE.0.0) GO TO 90
      GO TO 32
   30 CONTINUE
C ******** ALPHA1 LT 0.0 *********
      PHI=180.-AVGFA
      GAMMA=AVGFA+ALPHA1
      RR=SIN(-ALPHA1/57.3)*XA/SIN(GAMMA/57.3)
      P=Y1/SIN(AVGFA/57.3)
      XPRIM=ZL-P-RR
      IF(XPRIM.LE.0.0) GO TO 90
      XP=SIN(PHI/57.3)*XA/SIN(GAMMA/57.3)
   32 CONTINUE
      GO TO (12,13,12), NOPTJ
   12 IF(VAC.LE.0.0) DIR=0.089*XP/DE
      IF(VAC.GT.0.0) DIR=(0.089*XP/DE)/SQRT(1.+(0.27/SQRT(LAM*(LAM-1.)
     2 ))*XP/DE)
      DI=DIR*DE
      IF(XPRIM.LE.DI) GO TO 90
      XPRIM=XPRIM-DI
      B=0.33*XPRIM+1.5*DE
      XPDE=XPRIM/DE
      IF(XPDE.LT.0.5) XPDE=0.5
      DELTA=0.42*DE/(XPDE)**0.75
      GO TO 70
   13 IF(VAC.LE.0.0) HIR=0.109*XP/HNOZ
      IF(VAC.GT.0.0) HIR=(0.109*XP/HNOZ)/(1.+(0.55/SQRT(LAM*(LAM-1.)))
     2 *SQRT(XP/HNOZ))
      HI=HIR*HNOZ
      IF(XPRIM.LE.HI) GO TO 90
      XPRIM=XPRIM-HI
      B=0.33*XPRIM+1.5*WNOZ
      XPH=XPRIM/HNOZ
      IF(XPH.LT.0.5) XPH=0.5
      DELTA=0.42*HNOZ/(XPH)**0.75
      GO TO 70
```

```
   60 CONTINUE
C  ******************************************************************
C ************ USB , HYBRID & IBF/BLC COMPUTATIONS **************
C ******************************************************************
C       EBF/USB & IBF/BLC & HYBRID ASSUME SLOT NOZZLES
C
      IF(ALPHA1.GT.0.0) XP=Y1/SIN(ALPHA1/57.3)
      IF(ALPHA1.LT.0.0) GO TO 90
      XW=XP*COS(ALPHA1/57.3)
      IF(ALPHA1.LE.0.0.OR.NOPTS.EQ.4) XW=0.0
      ZL=FLAP1+FLAP2+FLAP3
      THET=2.*AVGFA
      RC=ZL/(THET/57.3)
      RL=X1-XW+ZL
      IF(RL.LE.0.0) GO TO 90
      H=HNOZ
      IF(NOPTS.EQ.4) H=HWNOZ
      W=WNOZ
      IF(NOPTS.EQ.4) W=WWNOZ
      DELTA=H*(0.5*SQRT(RL/H)+8.*(H/RC)**2+0.2*(RC*THET/(H*57.3)))
      DELTA=(H+DELTA)/2.
      XF=ZL*COS(AVGFA/57.3)
      XLS=X1+XF
      B=W
   70 CONTINUE
C   ************ COMPUTE OASPL ***********
C
      IF(NOPTS.EQ.3.OR.NOPTS.EQ.4.OR.NOPTS.EQ.6) OASPL=10.*ALOG10(RL*B
     1 +80.*ALOG10(U)-105.
      IF(NOPTS.EQ.2) OASPL=10.*ALOG10(XPRIM*B)+80.*ALOG10(U)-105.
      PSI1=AZMANG+AVGFA
      IF(NOPTS.EQ.3.OR.NOPTS.EQ.4.OR.NOPTS.EQ.6) PSI1=360.-AZMANG-AVGF
      DIRECT=GIRC(PSI1,ANGLE,DEL,28,1)
      ELVDB=GIRC(PSI1,THEDIR,ELVDIR,15,2)
      THEDB=ELVDB*COS(ELVANG/57.3)
      OASPL=OASPL+DIRECT-THEDB
      DO 81 J=1,24
      LSN=ALOG10(F(J)*DELTA/U)
      SPEC=GIRC(LSN,LOGST,OAS90,17,1)
      SPL(J)=OASPL+SPEC-20.*ALOG10(STOD)-ALPHA(J)*(STOD/1000.)
   81 IF(SPL(J).LT.0.0) SPL(J)=0.0
      CALL DOPLER(SPL)
      DO 82 J=1,24
   82 SPLL(4,J)=SPL(J)
   90 CONTINUE
      RETURN
      END
```

```
      SUBROUTINE WAKE(SPLL)
      DIMENSION SPLL(6,24),VTER(9),XPR(9),
     2 SPL(24),ANGLE(19),VAL1(19),OAS90(17)
      REAL LSN,LOGST(17)
      COMMON NOPTS,NOPTJ,F(24),ALPHA(24),STOD,ALT,AZMANG,ELVANG,
     2 VAC,DPLUG,DEQUIV,VEQUIV,FLAP1,FLAP2,FLAP3,FLPAG1,FLPAG2,
     3 FLPAG3,TTEQ,HNOZ,WNOZ,VJWNOZ,HWNOZ,WWNOZ,ANGNOZ,ANGWNZ,NRFD,
     4 NR1,NR2,NR3,HSLOT,EJL,EJANG,WFF,PRF,DF,TF,TREATF,TREATA,PRT,
     5 DTURB,BLADES,TRPM,PCTP,SA,AR,THICK,NOPTA,BC,SHP,DPRIM,DANIN,
     6 DANOUT,X1,Y1,VTIPT,VJPRIM,VJSEC,TTPRIM,TTSEC,XCN,TTWNOZ,HD
     7 ,ALPHA1,TREATT
      DATA VTER/.91,.91,.9,.89,.85,.8,.75,.68,.62/
      DATA XPR/.5,1.,1.5,2.,2.5,3.,3.5,4.,4.5/
      DATA LOGST/-1.6,-1.4,-1.2,-1.0,-0.8,-0.6,-0.4,-0.2,
     1 0.0,0.2,0.4,0.6,0.8,1.0,1.2,1.4,1.6/
      DATA OAS90/-32.4,-28.3,-24.4,-20.6,-17.1,-14.4,-12.5,
     1 -11.2,-10.7,-10.7,-11.5,-13.2,-15.5,-18.2,-21.2,-24.3,-27.6/
      DATA ANGLE/0.,10.,20.,30.,40.,50.,60.,70.,80.,90.,100.,110.,
     1 120.,130.,140.,150.,160.,170.,180./
      DATA VAL1/-7.,-6.,-5.5,-5.,-4.,-3.5,-2.5,-2.,-1.,0.5,
     1 1.5,3.,4.5,6.,7.,6.,4.5,3.,1./
C
C
      GAM=1.4
      R=53.34
      GC=32.2
      IF(NOPTS.EQ.4) GO TO 3
      T=TTEQ
      U=VEQUIV
      GO TO 4
    3 T=TTWNOZ
      U=VJWNOZ
    4 CONTINUE
      TS=T-((GAM-1.)*U*U)/(2.*GAM*R*GC)
      MJ=U/SQRT(GAM*R*TS*GC)
      IF(NOPTS.EQ.4) GO TO 12
      DE=DEQUIV
      DH=HD
      GO TO 13
   12 AN=WWNOZ*HWNOZ
      DE=SQRT(4.*AN/3.14)
      DH=4.*AN/(2.*WWNOZ+2.*HWNOZ)
   13 CONTINUE
      A=4.0
      IF(NOPTJ.EQ.2) A=4./(1.+(8./3.)*(DE/DH-1.))
C ******* DETERMINE NO. OF FLAPS & AVER FLAP ANG *******
C
      NFLAPS=0
      IF(FLAP1.GT.0.0) NFLAPS=1
      IF(FLAP2.GT.0.0) NFLAPS=2
      IF(FLAP3.GT.0.0) NFLAPS=3
      IF(NFLAPS.GT.0) AVGFA=(FLPAG1+FLPAG2+FLPAG3)/NFLAPS
      IF(NFLAPS.EQ.0) AVGFA=0.0
      IF(NOPTS.EQ.3.OR.NOPTS.EQ.4.OR.NOPTS.EQ.6) GO TO 60
```

```
C  ****************************************************
C ************** EBF COMPUTATIONS ********************************
C ***********************************************************************
      XB=Y1/TAN(AVGFA/57.3)
      XA=X1+XB
      ZL=FLAP1+FLAP2+FLAP3
      IF(ALPHA1.LT.0.0) GO TO 30
C ******** ALPHA1 GE 0.0 ***********
      IF(ALPHA1.LE.0.0) GO TO 28
      XC=Y1/TAN(ALPHA1/57.3)
      IF(XC.GE.X1) GO TO 28
      XPRIM=ZL+(X1-XC)
      XP=Y1/SIN(ALPHA1/57.3)
      GO TO 32
   28 PHI=180.-AVGFA-ALPHA1
      XP=SIN(AVGFA/57.3)*XA/SIN(PHI/57.3)
      IF(ALPHA1.LE.0.0) XP=XA
      SS=XP*SIN(ALPHA1/57.3)
      P=(Y1-SS)/SIN(AVGFA/57.3)
      XPRIM=ZL-P
      IF(XPRIM.LE.0.0) GO TO 90
      GO TO 32
   30 CONTINUE
C ******** ALPHA1 LT 0.0 **********
      PHI=180.-AVGFA
      GAMMA=AVGFA+ALPHA1
      RR=SIN(-ALPHA1/57.3)*XA/SIN(GAMMA/57.3)
      P=Y1/SIN(AVGFA/57.3)
      XPRIM=ZL-P-RR
      IF(XPRIM.LE.0.0) GO TO 90
      XP=SIN(PHI/57.3)*XA/SIN(GAMMA/57.3)
   32 CONTINUE
      VIPR=(1.+((0.15*XP)/(XCN*DE*SQRT(1.+MJ)))**A)**(-1./A)
      VIP=VIPR*U
      XPOD=XPRIM/DE
      VTEVIP=GIRC(XPOD,XPR,VTER,9,1)
      VTE=VTEVIP*VIP
      GO TO (33,34,33), NOPTJ
   33 B=0.33*XPRIM+1.5*DE
      XPDE=XPRIM/DE
      IF(XPDE.LT.0.5) XPDE=0.5
      DELTA=0.42*DE/(XPDE)**0.75
      GO TO 70
   34 B=0.33*XPRIM+1.5*WNOZ
      XPH=XPRIM/HNOZ
      IF(XPH.LT.0.5) XPH=0.5
      DELTA=0.42*HNOZ/(XPH)**0.75
      GO TO 70
   60 CONTINUE
C ***********************************************************
C *********** USB , HYBRID & IBF/BLC COMPUTATIONS **************
C ***********************************************************************
      IF(ALPHA1.GT.0.0) XP=Y1/SIN(ALPHA1/57.3)
      IF(ALPHA1.LT.0.0) GO TO 90
```

```
      XW=XP*COS(ALPHA1/57.3)
      IF(ALPHA1.LE.0.0.OR.NOPTS.EQ.4) XW=0.0
      ZL=FLAP1+FLAP2+FLAP3
      THET=2.*AVGFA
      RC=ZL/(THET/57.3)
      RL=X1-XW+ZL
      IF(RL.LE.0.0) GO TO 90
      W=WNOZ
      IF(NOPTS.EQ.4) W=WWNOZ
      H=HNOZ
      IF(NOPTS.EQ.4) H=HWNOZ
      DELTA=H*(0.5*SQRT(RL/H)+8.*(H/RC)**2+0.2*(RC*THET/(H*57.3)))
      VTE=U
      XF=ZL*COS(AVGFA/57.3)
      XLS=X1+XF
      B=W
   70 CONTINUE
C     ************ COMPUTE OASPL ************
C
      OASPL=10.*ALOG10(DELTA*B)+80.*ALOG10(VTE)-111.0
      DANG=AMAX1(FLPAG1,FLPAG2,FLPAG3)
      PSI1=AZMANG+DANG
      DIRECT=GIRC(PSI1,ANGLE,VAL1,19,1)
      OASPL=OASPL+DIRECT
      DO 81 J=1,24
      LSN=ALOG10(F(J)*DELTA/VTE)
      SPEC=GIRC(LSN,LOGST,OAS90,17,1)
      SPL(J)=OASPL+SPEC-20.*ALOG10(STOD)-ALPHA(J)*(STOD/1000.)
   81 IF(SPL(J).LT.0.0) SPL(J)=0.0
      CALL DOPLER(SPL)
      DO 82 J=1,24
   82 SPLL(5,J)=SPL(J)
   90 CONTINUE
      RETURN
      END
```

```
      SUBROUTINE TRAIL(SPLL)
      DIMENSION SPLL(6,24),VTER(9),XPR(9),STN(16),DEL(16)
     2,SPL(24)
      COMMON NOPTS,NOPTJ,F(24),ALPHA(24),STOD,ALT,AZMANG,ELVANG,
     2 VAC,DPLUG,DEQUIV,VEQUIV,FLAP1,FLAP2,FLAP3,FLPAG1,FLPAG2,
     3 FLPAG3,TTEQ,HNOZ,WNOZ,VJWNOZ,HWNOZ,WWNOZ,ANGNOZ,ANGWNZ,NRED,
     4 NR1,NR2,NR3,HSLOT,EJL,EJANG,WFF,PRF,DF,TF,TREATF,TREATA,PRT,
     5 DTURB,BLADES,TRPM,PCTP,SA,AR,THICK,NOPTA,BC,SHP,DPRIM,DANIN,
     6 DANOUT,X1,Y1,VTIPT,VJPRIM,VJSEC,TTPRIM,TTSEC,XCN,TTWNOZ,HD
     7 ,ALPHA1,TREATT
      DATA VTER/.91,.91,.9,.89,.85,.8,.75,.68,.62/
      DATA XPR/.5,1.,1.5,2.,2.5,3.,3.5,4.,4.5/
      DATA (STN(I),I=1,16)/.6,.7,.8,.9,1.,1.1,1.2,1.3,2.,4.,7.,10.,
     2 20.,40.,60.,80./
      DATA (DEL(I),I=1,16)/-14.3,-12.8,-11.7,-11.2,-11.,-11.1,-11.3,
     2 -11.9,-15.,-20.5,-25.5,-28.8,-35.6,-42.7,-46.9,-50./
C
C
      GAM=1.4
      TURB=0.0
      IF(NOPTS.EQ.3.OR.NOPTS.EQ.4.OR.NOPTS.EQ.6) TURB=(-4.0)
      R=53.34
      GC=32.2
      IF(NOPTS.EQ.4) GO TO 3
      T=TTEQ
      U=VEQUIV
      GO TO 4
    3 T=TTWNOZ
      U=VJWNOZ
    4 CONTINUE
      TS=T-((GAM-1.)*U*U)/(2.*GAM*R*GC)
      MJ=U/SQRT(GAM*R*TS*GC)
      IF(NOPTS.EQ.4) GO TO 12
      DE=DEQUIV
      DH=HD
      GO TO 13
   12 AN=WWNOZ*HWNOZ
      DE=SQRT(4.*AN/3.14)
      DH=4.*AN/(2.*WWNOZ+2.*HWNOZ)
   13 CONTINUE
      A=4.0
      IF(NOPTJ.EQ.2) A=4./(1.+(8./3.)*(DE/DH-1.))
C ******* DETERMINE NO. OF FLAPS & AVER FLAP ANG *******
C
      NFLAPS=0
      IF(FLAP1.GT.0.0) NFLAPS=1
      IF(FLAP2.GT.0.0) NFLAPS=2
      IF(FLAP3.GT.0.0) NFLAPS=3
      IF(NFLAPS.GT.0) AVGFA=(FLPAG1+FLPAG2+FLPAG3)/NFLAPS
      IF(NFLAPS.EQ.0) AVGFA=0.0
      IF(NOPTS.EQ.3.OR.NOPTS.EQ.4.OR.NOPTS.EQ.6) GO TO 60
C  ***********************************************************
C ************** EBF COMPUTATIONS ********************************
C ***********************************************************************
```

```
      XB=Y1/TAN(AVGFA/57.3)
      XA=X1+XB
      ZL=FLAP1+FLAP2+FLAP3
      IF(ALPHA1.LT.0.0) GO TO 30
C ******** ALPHA1 GE 0.0 ***********
      IF(ALPHA1.LE.0.0) GO TO 28
      XC=Y1/TAN(ALPHA1/57.3)
      IF(XC.GE.X1) GO TO 28
      XPRIM=ZL+(X1-XC)
      XP=Y1/SIN(ALPHA1/57.3)
      GO TO 32
   28 PHI=180.-AVGFA-ALPHA1
      XP=SIN(AVGFA/57.3)*XA/SIN(PHI/57.3)
      IF(ALPHA1.LE.0.0) XP=XA
      SS=XP*SIN(ALPHA1/57.3)
      P=(Y1-SS)/SIN(AVGFA/57.3)
      XPRIM=ZL-P
      IF(XPRIM.LE.0.0) GO TO 90
      GO TO 32
   30 CONTINUE
C ******** ALPHA1 LT 0.0 **********
      PHI=180.-AVGFA
      GAMMA=AVGFA+ALPHA1
      RR=SIN(-ALPHA1/57.3)*XA/SIN(GAMMA/57.3)
      P=Y1/SIN(AVGFA/57.3)
      XPRIM=ZL-P-RR
      IF(XPRIM.LE.0.0) GO TO 90
      XP=SIN(PHI/57.3)*XA/SIN(GAMMA/57.3)
   32 CONTINUE
      VIPR=(1.+((0.15*XP)/(XCN*DE*SQRT(1.+MJ)))**A)**(-1./A)
      VIP=VIPR*U
      XPOD=XPRIM/DE
      VTEVIP=GIRC(XPOD,XPR,VTER,9,1)
      VTE=VTEVIP*VIP
      GO TO (33,34,33), NOPTJ
   33 B=0.33*XPRIM+1.5*DE
      XPDE=XPRIM/DE
      IF(XPDE.LT.0.5) XPDE=0.5
      DELTA=0.42*DE/(XPDE)**0.75
      GO TO 70
   34 B=0.33*XPRIM+1.5*WNOZ
      XPH=XPRIM/HNOZ
      IF(XPH.LT.0.5) XPH=0.5
      DELTA=0.42*HNOZ/(XPH)**0.75
      GO TO 70
   60 CONTINUE
C  ***********************************************************
C ****************** USB , HYBRID & IBF/BLC COMPUTATIONS *******
C ***********************************************************
      IF(ALPHA1.GT.0.0) XP=Y1/SIN(ALPHA1/57.3)
      IF(ALPHA1.LT.0.0) GO TO 90
      XW=XP*COS(ALPHA1/57.3)
      IF(ALPHA1.LE.0.0.OR.NOPTS.EQ.4) XW=0.0
      ZL=FLAP1+FLAP2+FLAP3
```

```
      THET=2.*AVGFA
      RC=ZL/(THET/57.3)
      RL=X1-XW+ZL
      IF(RL.LE.0.0) GO TO 90
      W=WNOZ
      IF(NOPTS.EQ.4) W=WWNOZ
      H=HNOZ
      IF(NOPTS.EQ.4) H=HWNOZ
      DELTA=H*(0.5*SQRT(RL/H)+8.*(H/RC)**2+0.2*(RC*THET/(H*57.3)))
      VTE=U
      XF=ZL*COS(AVGFA/57.3)
      XLS=X1+XF
      B=W
   70 CONTINUE
C    ************ COMPUTE OASPL ************
C
      OASPL=50.*ALOG10(VTE)+10.*ALOG10(B*DELTA)-6.+TURB
      IF(NFLAPS.EQ.1) PSI1=(AZMANG+FLPAG1)/57.3
      IF(NFLAPS.EQ.2) PSI1=(AZMANG+FLPAG2)/57.3
      IF(NFLAPS.EQ.3) PSI1=(AZMANG+FLPAG3)/57.3
      DIRECT=(COS(PSI1/2.)**2)*(0.5+0.5*SIN(ELVANG/57.3))
      IF(DIRECT.LE.0.0) OASPL=0.0
      IF(DIRECT.GT.0.0) OASPL=OASPL+10.*ALOG10(DIRFCT)
      IF(OASPL.LT.0.0) OASPL=0.0
      DO 81 J=1,24
      SN=F(J)*DELTA/VTE
      IF(SN.GE.0.6) SPEC=GIRC(SN,STN,DEL,16,1)
      IF(SN.LT.0.6) SPEC=24.67*ALOG10(SN)-8.83
      SPL(J)=OASPL+SPEC-20.*ALOG10(STOD)-ALPHA(J)*(STOD/1000.)
   81 IF(SPL(J).LT.0.0) SPL(J)=0.0
      CALL DOPLER(SPL)
      DO 82 J=1,24
   82 SPLL(6,J)=SPL(J)
   90 CONTINUE
      RETURN
      END
```

```
      SUBROUTINE APU(PNLAPU)
      COMMON NOPTS,NOPTJ,F(24),ALPHA(24),STOD,ALT,AZMANG,ELVANG,
     2 VAC,DPLUG,DEQUIV,VEQUIV,FLAP1,FLAP2,FLAP3,FLPAG1,FLPAG2,
     3 FLPAG3,TTEQ,HNOZ,WNOZ,VJWNOZ,HWNOZ,WWNOZ,ANGNOZ,ANGWNZ,NRED
     4 NR1,NR2,NR3,HSLOT,EJL,EJANG,WFF,PRF,DF,TF,TREATF,TREATA,PRT
     5 DTURB,BLADES,TRPM,PCTP,SA,AR,THICK,NOPTA,BC,SHP,DPRIM,DANIN
     6 DANOUT,X1,Y1,VTIPT,VJPRIM,VJSEC,TTPRIM,TTSEC,XCN,TTWNOZ,HD
     7 ,ALPHA1,TREATT
      IF(NOPTA.EQ.2) GO TO 50
      PNLAPU=103.0+0.11*BC-20.*ALOG10(STOD)
      RETURN
   50 PNLAPU=106.0+0.106*SHP-20.*ALOG10(STOD)
      RETURN
      END
```

```
      SUBROUTINE EGA(EGSPL)
      DIMENSION EGSPL(24),XDIST(19),XANG(4),VAL1(4,19),VAL2(4,19),
     2 VAL3(4,19),VAL4(4,19),VAL5(4,19),VAL6(4,19)
      COMMON NOPTS,NOPTJ,F(24),ALPHA(24),STOD,ALT,AZMANG,ELVANG,
     2 VAC,DPLUG,DEQUIV,VEQUIV,FLAP1,FLAP2,FLAP3,FLPAG1,FLPAG2,
     3 FLPAG3,TTEQ,HNOZ,WNOZ,VJWNOZ,HWNOZ,WWNOZ,ANGNOZ,ANGWNZ,NRED,
     4 NR1,NR2,NR3,HSLOT,EJL,EJANG,WFF,PRF,DF,TF,TREATF,TREATA,PRT,
     5 DTURB,BLADES,TRPM,PCTP,SA,AR,THICK,NOPTA,BC,SHP,DPRIM,DANIN,
     6 DANOUT,X1,Y1,VTIPT,VJPRIM,VJSEC,TTPRIM,TTSEC,XCN,TTWNOZ,HD
     7 ,ALPHA1,TREATT
      DATA XDIST/0.0,100.,200.,300.,400.,500.,600.,700.,800.,900.,
     2 1000.,1250.,1500.,1750.,2000.,2500.,3000.,3500.,4000./
      DATA XANG/0.0,10.0,20.0,30.0/
      DATA ((VAL1(NZ,NX),NX=1,19),NZ=1,4)/ 0.0,0.5,0.8,0.8,0.9,1.0,
     2 1.0,1.2,1.5,1.8,2.0,2.6,3.2,3.8,4.0,4.3,4.6,4.8,5.0,   0.0,0.0,
     3 0.0,0.0,0.0,0.0,0.0,0.0,0.0,0.0,0.0,0.0,0.0,0.1,0.2,0.5,1.0,1.2,
     4 1.8,   0.0,0.0,0.0,0.0,0.1,0.1,0.1,0.2,0.3,0.4,0.5,0.5,0.5,0.5,
     5 0.5,0.5,0.7,0.8,0.9,   0.0,0.0,0.0,0.0,0.0,0.0,0.0,0.0,0.0,0.0,
     6 0.0,0.0,0.0,0.0,0.0,0.0,0.0,0.0,0.0/
      DATA ((VAL2(NZ,NX),NX=1,19),NZ=1,4)/ 0.0,0.7,1.0,1.08,1.34,
     2 2.0,2.0,2.1,2.3,2.8,3.0,4.0,4.6,5.2,6.0,6.8,7.0,7.0,7.0,
     3 0.0,0.0,0.0,0.0,0.0,0.0,0.1,0.2,0.3,0.4,0.5,0.9,1.0,1.1,1.2,1./,
     4 2.0,2.5,3.0,   0.0,0.04,0.08,0.16,0.2,0.2,0.2,0.38,0.48,0.64,
     5 0.76,0.8,0.84,0.88,0.96,1.0,1.22,1.42,1.58,   0.0,0.0,0.0,0.0,
     6 0.0,0.0,0.0,0.0,0.0,0.0,0.0,0.0,0.0,0.0,0.0,0.0,0.0,0.0,0.0/
      DATA ((VAL3(NZ,NX),NX=1,19),NZ=1,4)/ 0.0,0.9,1.2,1.36,1.78,2.3,
     2 2.3,2.8,3.1,3.6,4.0,5.1,6.0,6.9,7.5,8.6,9.0,9.2,9.2,   0.0,0.25,
     3 0.25,0.25,0.33,0.5,0.9,1.0,1.1,1.1,1.2,1.7,1.9,2.0,2.2,2.7,3.0,
     4 3.5,4.0,   0.0,0.1,0.16,0.32,0.4,0.4,0.4,0.56,0.66,0.88,1.02,
     5 1.1,1.18,1.26,1.42,1.5,1.74,2.04,2.26,   0.0,0.0,0.0,0.0,0.0,0.0
     6 ,0.0,0.0,0.0,0.0,0.0,0.0,0.0,0.0,0.0,0.0,0.0,0.0,0.0/
      DATA ((VAL4(NZ,NX),NX=1,19),NZ=1,4)/ 0.0,1.1,1.4,1.64,2.22,3.0,
     2 3.1,3.5,4.0,4.5,5.0,6.3,7.6,8.8,9.8,10.8,11.1,11.2,11.2,   0.0,
     3 0.5,0.5,0.5,0.65,1.0,1.2,1.5,1.8,1.9,2.0,2.4,2.8,3.1,3.3,4.0,4.3
     4 ,5.0,5.5,   0.0,0.12,0.24,0.48,0.6,0.6,0.6,0.74,0.84,1.12,1.28,
     5 1.4,1.52,1.64,1.88,2.0,2.26,2.66,2.94   ,0.0,0.0,0.0,0.0,0.0,0.0
     6 ,0.0,0.0,0.0,0.0,0.0,0.0,0.0,0.0,0.0,0.0,0.0,0.0,0.0/
      DATA ((VAL5(NZ,NX),NX=1,19),NZ=1,4)/ 0.0,1.3,1.6,1.92,2.66,3.2,
     2 3.6,4.2,4.9,5.5,6.0,7.8,9.0,10.2,11.2,12.3,13.0,13.5,13.8,   0.0
     3 ,0.75,0.75,0.75,0.98,1.5,1.9,2.1,2.5,2.8,3.0,3.7,4.0,4.3,4.8,
     4 5.3,6.0,6.5,7.0,   0.0,0.18,0.32,0.64,0.8,0.8,0.8,0.92,1.02,1.36
     5 ,1.54,1.7,1.86,2.02,2.34,2.5,2.78,3.28,3.62,   0.0,0.0,0.0,0.0,
     6 0.0,0.0,0.0,0.0,0.0,0.0,0.0,0.0,0.0,0.0,0.0,0.0,0.0,0.0,0.0/
      DATA ((VAL6(NZ,NX),NX=1,19),NZ=1,4)/ 0.0,1.5,1.8,2.2,3.1,4.0,4.5,
     2 5.1,5.8,6.4,7.0,9.1,10.8,12.0,13.0,14.0,14.8,15.1,15.2,   0.0,
     3 1.0,1.0,1.0,1.3,2.0,2.5,3.0,3.3,3.8,4.1,4.9,5.3,6.1,6.3,7.1,7.9,
     4 8.3,9.0,   0.0,0.2,0.4,0.8,1.0,1.0,1.0,1.1,1.2,1.6,1.8,2.0,2.2,
     5 2.4,2.8,3.0,3.3,3.9,4.3,   0.0,0.0,0.0,0.0,0.0,0.0,0.0,0.0,0.0,
     6 0.0,0.0,0.0,0.0,0.0,0.0,0.0,0.0,0.0,0.0/
      GDIST=SQRT(STOD**2-(ALT-4.0)**2)
      ANGLE=ASIN((ALT-4.0)/STOD)
      UDIST=96.0/SIN(ANGLE)
      DIST=AMIN1(STOD,UDIST)
      DO 10 I=1,24
```

```
   10 EGSPL(I)=0.0
      ANG=ANGLE*57.2957795
      IF(ANG.GT.30.0) GO TO 30
      DO 20 I=1,24
      IF(F(I).LT.75.0) EGSPL(I)=DTAB2(DIST,ANG,XDIST,XANG,19,4,1,1,
     2 VAL1,4,IERR)
      IF(F(I).GT.75.0.AND.F(I).LT.150.0) EGSPL(I)=DTAB2(DIST,ANG,
     2 XDIST,XANG,19,4,1,1,VAL2,4,IERR)
      IF(F(I).GT.150.0.AND.F(I).LT.300.0) EGSPL(I)=DTAB2(DIST,ANG,
     2 XDIST,XANG,19,4,1,1,VAL3,4,IERR)
      IF(F(I).GT.300.0.AND.F(I).LT.600.0) EGSPL(I)=DTAB2(DIST,ANG,
     2 XDIST,XANG,19,4,1,1,VAL4,4,IERR)
      IF(F(I).GT.600.0.AND.F(I).LT.1200.0) EGSPL(I)=DTAB2(DIST,ANG,
     2 XDIST,XANG,19,4,1,1,VAL5,4,IERR)
      IF(F(I).GT.1200.0) EGSPL(I)=DTAB2(DIST,ANG,XDIST,XANG,19,4,
     2 1,1,VAL6,4,IERR)
   20 CONTINUE
   30 RETURN
      END
```

```
      SUBROUTINE GRE(GRSPL)
      DIMENSION GRSPL(24)
      COMMON NOPTS,NOPTJ,F(24),ALPHA(24),STOD,ALT,AZMANG,ELVANG,
     2 VAC,DPLUG,DEQUIV,VEQUIV,FLAP1,FLAP2,FLAP3,FLPAG1,FLPAG2,
     3 FLPAG3,TTEQ,HNOZ,WNOZ,VJWNOZ,HWNOZ,WWNOZ,ANGNOZ,ANGWNZ,NRED,
     4 NR1,NR2,NR3,HSLOT,EJL,EJANG,WFF,PRF,DF,TF,TREATF,TREATA,PRT,
     5 DTURB,BLADES,TRPM,PCTP,SA,AR,THICK,NOPTA,BC,SHP,DPRIM,DANIN,
     6 DANOUT,X1,Y1,VTIPT,VJPRIM,VJSEC,TTPRIM,TTSEC,XCN,TTWNOZ,HD
     7 ,ALPHA1,TREATT
      GDIST=SQRT(STOD**2-(ALT-4.0)**2)
      IF(ELVANG.GT.0.3) PORDO=4.*GDIST/(ALT+4.0)
      IF(ELVANG.LT.0.3) PORDO=GDIST/2.0
      PORDS=GDIST-PORDO
      RD=STOD
      RR=SQRT(4.**2+PORDO**2)+SQRT(ALT**2+PORDS**2)
      IF(ELVANG.GT.89.8.AND.AZMANG.GT.89.8.AND.AZMANG.LT.90.3) RR=RD+8.0
      Z=RR/RD
      DR=RR-RD
      C=1116.0
      AL=0.725707903
      BETA=6.324956092
      DO 10 I=1,24
      XLAMDA=C/F(I)
      AI=AL*DR/XLAMDA
      BI=BETA*DR/XLAMDA
      GRSPL(I)=10.*ALOG10(1.+1./Z**2+((2./Z)*(SIN(AI)/AI)*COS(BI)))
      IF(GRSPL(I).LT.-30.0) GRSPL(I)=-30.0
   10 CONTINUE
      RETURN
      END
```

SHIELD

```
      SUBROUTINE SHIELD(DELSPL,SD,BH,OD,F,ELVANG)
      DIMENSION F(24),DELSPL(24)
      REAL N
C
C     SD = DISTANCE FROM SOURCE TO BARRIER OR WING (FT)
C
C     BH = BARRIER HEIGHT (FT)
C
C     OD = DISTANCE FROM BARRIER TO OBSERVER (FT)
C
C
C   CALCULATE ESTIMATE OF WING SHIELDING EFFECT
C
      CONST=(SD*(SQRT(1.+((BH*BH)/(SD*SD)))-1.)+OD*(SQRT(1.+((BH*BH)/
     2 (OD*OD)))-1.))/567.5
      DO 10 I=1,24
      N=F(I)*CONST
      IF(N.LE.10.0) AE3=10.*ALOG10(N)+10.
      IF(N.GT.10.0) AE3=20.
      DELSPL(I)=AE3*SIN(ELVANG/57.2957795)
      IF(DELSPL(I).LT.0.0) DELSPL(I)=0.0
   10 CONTINUE
      RETURN
      END
```

```
      SUBROUTINE FWDSPD(DELDBF)
      DIMENSION XLSB1(3),XLSB2(3),XLSB3(3),XUSB(3),XAW(2,3),XELV(3),
     2 XFLP(2)
      COMMON NOPTS,NOPTJ,F(24),ALPHA(24),STOD,ALT,AZMANG,ELVANG,
     2 VAC,DPLUG,DEQUIV,VEQUIV,FLAP1,FLAP2,FLAP3,FLPAG1,FLPAG2,
     3 FLPAG3,TTEQ,HNOZ,WNOZ,VJWNOZ,HWNOZ,WWNOZ,ANGNOZ,ANGWNZ,NRED,
     4 NR1,NR2,NR3,HSLOT,EJL,EJANG,WFF,PRF,DF,TF,TREATF,TREATA,PRT,
     5 DTURB,BLADES,TRPM,PCTP,SA,AR,THICK,NOPTA,BC,SHP,DPRIM,DANIN,
     6 DANOUT,X1,Y1,VTIPT,VJPRIM,VJSEC,TTPRIM,TTSEC,XCN,TTWNOZ,HD
     7 ,ALPHA1,TREATT
      DATA XLSB1/1.3,4.2,6.1/
      DATA XLSB2/0.25,3.0,5.05/
      DATA XLSB3/-0.8,1.8,4.0/
      DATA XUSB/0.0,0.9,1.8/
      DATA ((XAW(NZ,NX),NX=1,3),NZ=1,2)/0.0,1.0,1.8,0.0,-1.0,-1.8/
      DATA XELV/0.0,30.0,90.0/
      DATA XFLP/35.0,65.0/
      POWER=0.0
      GO TO (100,200,400,100,300,400),NOPTS
  100 POWER=5.0
      GO TO 500
  200 IF(FLAP1.GT.0.0) POWER=GIRC(ELVANG,XELV,XLSB1,3,1)
      IF(FLAP2.GT.0.0) POWER=GIRC(ELVANG,XELV,XLSB2,3,1)
      IF(FLAP3.GT.0.0) POWER=GIRC(ELVANG,XELV,XLSB3,3,1)
      GO TO 500
  300 POWER=DTAB2(ELVANG,EJANG,XELV,XFLP,3,2,1,1,XAW,2,IERR)
      GO TO 500
  400 POWER=GIRC(ELVANG,XELV,XUSB,3,1)
  500 IF(NOPTS.EQ.4.OR.NOPTS.EQ.5) GO TO 550
      ANGLE=ANGNOZ
      VEL=VEQUIV
      GO TO 560
  550 ANGLE=ANGWNZ
      VEL=VJWNOZ
  560 CONTINUE
      IF(VAC.GE.VEL) GO TO 600
      DELDBF=10.*POWER*ALOG10(1.-VAC*COS(ANGLE/57.2927795)/VEL)
      RETURN
  600 WRITE(6,601)
  601 FORMAT(1H1,5X,'RELATIVE VELOCITY NOT ACCEPTABLE TO SUBROUTINE',
     2 ' FWDSPD',/,1H1)
      RETURN
      END
```

COPY AVAILABLE TO DDC DOES NOT PERMIT FULLY LEGIBLE PRODUCTION


```
      SUBROUTINE DOPLER(SPLS)
      DIMENSION SPLS(24),XSPL(30)
      REAL MAC
      COMMON NOPTS,NOPTJ,F(24),ALPHA(24),STOD,ALT,AZMANG,ELVANG,
     2 VAC,DPLUG,DEQUIV,VEQUIV,FLAP1,FLAP2,FLAP3,FLPAG1,FLPAG2,
     3 FLPAG3,TTEQ,HNOZ,WNOZ,VJWNOZ,HWNOZ,WWNOZ,ANGNOZ,ANGWNZ,NRED,
     4 NR1,NR2,NR3,HSLOT,EJL,EJANG,WHF,PRF,DF,TF,TREATF,TREATA,PRT,
     5 DTURB,BLADES,TRPM,PCTP,SA,AR,THICK,NOPTA,BC,SHP,DPRIM,DANIN,
     6 DANOUT,X1,Y1,VTIPT,VJPRIM,VJSEC,TTPRIM,TTSEC,XCN,TTWNOZ,HD
     7 ,ALPHA1,TREATT
      NSHIFT=0
      DO 10 I=1,24
   10 XSPL(I+3)=SPLS(I)
      DO 20 I=3,1,-1
   20 XSPL(I)=2.*XSPL(I+1)-XSPL(I+2)
      DO 30 I=28,30
   30 XSPL(I)=2.*XSPL(I-1)-XSPL(I-2)
      MAC=VAC/1116.0
      D=1.0/(1.0-MAC*COS(AZMANG/57.2957795))
      IF(D.LT.1.0) GO TO 40
      IF(D.LT.1.122462) GO TO 50
      IF(D.GE.1.122462.AND.D.LT.1.414213) NSHIFT=1
      IF(D.GE.1.414213.AND.D.LT.1.781797) NSHIFT=2
      IF(D.GE.1.781797.AND.D.LT.2.244924) NSHIFT=3
      IF(D.GE.2.244924) GO TO 70
      GO TO 50
   40 IF(D.GT.0.890899) GO TO 50
      IF(D.LE.0.890899.AND.D.GT.0.707107) NSHIFT=-1
      IF(D.LE.0.707107.AND.D.GT.0.561231) NSHIFT=-2
      IF(D.LE.0.561231.AND.D.GT.0.445449) NSHIFT=-3
      IF(D.LE.0.445449) GO TO 70
   50 DO 60 I=4,27
      SPLS(I-3)=XSPL(I+NSHIFT)
   60 CONTINUE
      DO 65 I=1,24
      IF(SPLS(I).LT.0.0) SPLS(I)=0.0
   65 CONTINUE
      RETURN
   70 WRITE(6,601) D
  601 FORMAT(1H1,5X,'THIS VALUE OF D = ',E15.10,' IS NOT ACCEPTABLE',
     2 ' FOR SUBROUTINE DOPLER' ,/,5X,'THEREFORE NO SHIFT WAS USED')
      RETURN
      END
```

```
      SUBROUTINE REDUCE(DELP)
      DIMENSION XPR(9),XHRD(9),XLIN(9),XVEL(9)
      COMMON NOPTS,NOPTJ,F(24),ALPHA(24),STOD,ALT,AZMANG,ELVANG,
     2 VAC,DPLUG,DEQUIV,VEQUIV,FLAP1,FLAP2,FLAP3,FLPAG1,FLPAG2,
     3 FLPAG3,TTEQ,HNOZ,WNOZ,VJWNOZ,HWNOZ,WWNOZ,ANGNOZ,ANGWNZ,NRED,
     4 NR1,NR2,NR3,HSLOT,EJL,EJANG,WFF,PRF,DF,TF,TREATF,TREATA,PRT,
     5 DTURB,BLADES,TRPM,PCTP,SA,AR,THICK,NOPTA,BC,SHP,DPRIM,DANIN,
     6 DANOUT,X1,Y1,VTIPT,VJPRIM,VJSEC,TTPRIM,TTSEC,XCN,TTWNOZ,HD
     7 ,ALPHA1,TREATT
      DATA XPR/1.0,1.5,2.0,2.5,2.6,2.7,2.8,2.9,3.0/
      DATA XHRD/4.0,0.0,-4.5,-9.5,-10.5,-11.0,-11.5,-12.0,-12.3/
      DATA XLIN/0.0,-5.0,-10.0,-15.0,-16.0,-17.0,-18.0,-18.7,-19.5/
      DEL1=0.0
      DEL2=0.0
      DEL3=0.0
      GO TO (900,100,200,900,300,200),NOPTS
  100 IF(NR1.NE.1) GO TO 110
      IF(FLAP1.GT.0.0) S=1.
      IF(FLAP2.GT.0.0) S=2.
      IF(FLAP3.GT.0.0) S=3.
      DEL1=-(803.81/VEQUIV)*(3.0-S)*SIN(ELVANG/57.2957795)
  110 IF(NR2.NE.1) GO TO 120
      DEL2=-(0.5+SIN(ELVANG/57.2957795))
  120 IF(NR3.NE.1) GO TO 900
      DEL3=-(2.0*HSLOT*12.0*SIN(ELVANG/57.2957795))
      GO TO 900
  200 IF(NR2.NE.1) GO TO 210
      DEL2=-2.0*(0.5+SIN(ELVANG/57.2957795))
  210 IF(NR3.NE.1) GO TO 900
      DEL3=-4.0*HSLOT*12.*SIN(ELVANG/57.2957795)
      GO TO 900
  300 DO 310 I=1,9
      XVEL(I)=109.595*SQRT(TTWNOZ*(1.-1./(XPR(I)**.286)))
  310 CONTINUE
  320 IF(NR1.NE.1) GO TO 330
      DEL1=GIRC(VJWNOZ,XVEL,XHRD,9,1)
      GO TO 900
  330 IF(NR2.NE.1) GO TO 900
      DEL2=GIRC(VJWNOZ,XVEL,XLIN,9,1)
  900 DELP=DEL1+DEL2+DEL3
      RETURN
      END
```

```
      SUBROUTINE PNLREV(SPL,PN,NOCT)
      REAL SPL(24),L(5,24),M(4,24),LL(5,8),MM(4,8)
      DATA ((L(I,J),J=1,24),I=1,5)/
     +49.0,44.0,39.0,34.0,30.0,27.0,24.0,21.0,18.0,16.0,16.0,16.0
     1,16.0,16.0,15.0,12.0,9.0,5.0,4.0,5.0,6.0,10.0,17.0,21.0,
     255.0,51.0,46.0,42.0,39.0,36.0,33.0,30.0,27.0,25.0,25.0,25.0,
     325.0,25.0,23.0,21.0,18.0,15.0,14.0,14.0,15.0,17.0,23.0,29.0,
     464.0,60.0,56.0,53.0,51.0,48.0,46.0,44.0,42.0,40.0,40.0,40.0,
     540.0,40.0,38.0,34.0,32.0,30.0,29.0,29.0,30.0,31.0,37.0,41.0,
     691.01,85.88,87.32,79.85,79.76,75.96,73.96,74.91,94.63,100.,100.,
     7100.,100.,100.,100.,100.,100.,100.,100.,100.,100.,100.,44.29,50.72
     8,52.0,51.0,49.0,47.0,46.0,45.0,43.0,42.0,41.0,40.0,40.0,40.0,
     940.0,40.0,38.0,34.0,32.0,30.0,29.0,29.0,30.0,31.0,34.0,37.0/
      DATA((M(I,J),J=1,24),I=1,4)/
     +.07952,.06816,.06816,.05964,10*.053013,.059640,.053013,
     1.053013,.047712,.047712,.053013,.053013,.06816,.07952,.05964,
     2.058098,.058098,.052288,.047534,.043573,.043573,.040221,.037349,
     37*.034859,.040221,.037349,4*.034859,.037349,.037349,.043573,
     4.043478,.040570,.036831,.036831,.035336,.033333,.033333,.032051,
     5.030675,6*.030103,7*.02996,.042285,.042285,15*.030103,9*.02996/
      DATA((LL(I,J),J=1,8),I=1,5)/
     144.0,30.0,21.0,16.0,16.0,9.0,5.0,17.0,
     251.0,39.0,30.0,25.0,25.0,18.0,14.0,23.0,
     360.0,51.0,44.0,40.0,40.0,32.0,29.0,37.0,
     485.88,79.76,74.91,100.,100.,100.,100.,44.29,
     551.0,46.0,42.0,40.0,40.0,32.0,29.0,34.0/
      DATA((MM(I,J),J=1,8),I=1,4)/
     1.068160,6*.053013,.079520,
     2.058098,.043573,.037349,2*.034859,.037349,.034859,.037349,
     3.040570,.035336,.032051,2*.030103,2*.029960,.042285,
     45*.030103,3*.029960/
      IF(NOCT.EQ.2) GO TO 17
C     NOCT=1 OCTAVE BAND INPUT
C     NOCT=2 ONE-THIRD OCTAVE BAND INPUT
      SUM1=0.0
      SUM2=0.0
      DO 26 I=1,8
      IF(SPL(I).GE.LL(1,I)) GO TO 20
      ANOY=0.0
      GO TO 21
   20 IF(SPL(I).GE.LL(2,I)) GO TO 22
      ANOY=.1*10.0**(MM(1,I)*(SPL(I)-LL(1,I)))
      GO TO 21
   22 IF(SPL(I).GE.LL(3,I)) GO TO 23
      ANOY=10.0**(MM(2,I)*(SPL(I)-LL(3,I)))
      GO TO 21
   23 IF(SPL(I).GE.LL(4,I)) GO TO 24
      ANOY=10.0**(MM(3,I)*(SPL(I)-LL(3,I)))
      GO TO 21
   24 IF(SPL(I).GT.150.0) GO TO 25
      ANOY=10.0**(MM(4,I)*(SPL(I)-LL(5,I)))
      GO TO 21
   25 WRITE(6,602)
  602 FORMAT(///,10X,'SPL EXCEEDS 150 DB',///)
```

```
      GO TO 101
   21 IF(ANOY.LE.SUM2) GO TO 26
      SUM2=ANOY
   26 SUM1=SUM1+ANOY
      IF(SUM1.LT.0.01) GO TO 30
      IF(SUM2.LT.0.01) GO TO 30
      IF(SUM2.GT.SUM1) GO TO 30
      PN=40.0+33.22*ALOG10(SUM2+.3*(SUM1-SUM2))
  101 RETURN
   17 SUM1=0.0
      SUM2=0.0
      DO 16 I=1,24
      IF(SPL(I).GE.L(1,I)) GO TO 10
      ANOY=0.0
      GO TO 11
   10 IF(SPL(I).GE.L(2,I)) GO TO 12
      ANOY=.1*10.0**(M(1,I)*(SPL(I)-L(1,I)))
      GO TO 11
   12 IF(SPL(I).GE.L(3,I)) GO TO 13
      ANOY=10.0**(M(2,I)*(SPL(I)-L(3,I)))
      GO TO 11
   13 IF(SPL(I).GE.L(4,I)) GO TO 14
      ANOY=10.0**(M(3,I)*(SPL(I)-L(3,I)))
      GO TO 11
   14 IF(SPL(I).GT.150.) GO TO 15
      ANOY=10.0**(M(4,I)*(SPL(I)-L(5,I)))
      GO TO 11
   15 WRITE(6,601)
  601 FORMAT(///,10X,'SPL EXCEEDS 150 DB',///)
      GO TO 100
   11 IF(ANOY.LE.SUM2) GO TO 16
      SUM2=ANOY
   16 SUM1=SUM1+ANOY
      IF(SUM1.LT.0.01) GO TO 30
      IF(SUM2.LT.0.01) GO TO 30
      IF(SUM2.GT.SUM1) GO TO 30
      PN=40.0+33.22*ALOG10(SUM2+.15*(SUM1-SUM2))
      GO TO 100
   30 PN=0.0
  100 RETURN
      END
```

TONE

```
      SUBROUTINE TONE(SPL,PN,PNLT)
      DIMENSION SPL(24),SS(25),SBAR(25),SPLP(25)
      CMAX=0.0
      SS(3)=0.0
      SPLP(2)=SPL(2)
      SPLP(3)=SPL(3)
      DO 60 I=4,24
      SPLP(I)=SPL(I)
      SS(I)=SPL(I)-SPL(I-1)
      IF(ABS(SS(I)-SS(I-1))-5.0) 60,60,10
   10 IF(SS(I)) 30,30,20
   20 IF(SS(I)-SS(I-1)) 60,60,50
   30 IF(SS(I-1)) 60,60,40
   40 SPLP(I-1)=0.5*(SPL(I-2)+SPL(I))
      GO TO 60
   50 SPLP(I)=0.5*(SPL(I-1)+SPL(I+1))
      IF(I.EQ.24) SPLP(24)=SPL(23)+SS(23)
   60 CONTINUE
      SS(3)=SPLP(4)-SPLP(3)
      DO 80 I=4,24
      SS(I)=SPLP(I)-SPLP(I-1)
   80 CONTINUE
      SS(25)=SS(24)
      DO 90 I=3,23
      SBAR(I)=.3333333*(SS(I)+SS(I+1)+SS(I+2))
   90 CONTINUE
      SPLP(3)=SPL(3)
      DO 100 I=4,24
      SPLP(I)=SPLP(I-1)+SBAR(I-1)
  100 CONTINUE
      DO 150 I=3,24
      F=SPL(I)-SPLP(I)
      IF(F-3.0) 150,120,110
  110 IF(F-20.0) 120,130,130
  120 C=F/6.0
      GO TO 140
  130 C=3.333333
  140 IF(I.GE.11.AND.I.LE.21) C=2.*C
      IF(C.GT.CMAX) CMAX=C
  150 CONTINUE
      PNLT=PN+CMAX
      RETURN
      END
```

```
      FUNCTION GIRC(ARG,X,Y,NX,IC)
C     AITKIN INTERPOLATION
C     ARG=INDEPENDENT ARGUMENT
C     X=INDEPENDENT TABLE
C     Y=DEPENDENT TABLE
C     NX=NUMBER VALUES X TABLE
C     IC=1 FIRST ORDER INTERPOLATION
C     IC=2 SECOND ORDER INTERPOLATION
      DIMENSION X(1),Y(1),XX(4),YY(4),EE(2),FF(2)
      IEND=NX-IC+1
      IF(X(1)-X(2))10,20,20
C     ASCENDING ORDER
   10 DO 15 I=1,IEND
      IF(X(I)-ARG)15,30,30
   15 CONTINUE
   16 IB=NX-IC
      IEX=0
      GO TO 45
   20 DO 25 I=1,IEND
      IF(X(I)-ARG)35,30,25
   25 CONTINUE
      GO TO 16
   30 IF(IC-1)35,35,40
   35 IF(I-1)36,36,37
   36 IB=1
      GO TO 45
   37 IB=I-IC
      GO TO 45
   40 IF(I-2)41,41,42
   41 IEX=1
      GO TO 38
   42 IEX=1
      GO TO 37
   45 DO 51 I=1,4
      XX(I)=X(IB)-ARG
      YY(I)=Y(IB)
   51 IB=IB+1
      DO 61 I=1,2
   61 EE(I)=XX(I+1)-XX(I)
      DO 71 I=1,2
   71 FF(I)=EE(I)+EE(I+1)
      DO 81 I=1,2
      EE(I)=(YY(I)*XX(I+1)-YY(I+1)*XX(I))/EE(I)
      IF(IC-1)100,100,90
   80 CONTINUE
      DO 85 I=1,2
   85 EE(I)=(XX(I+2)*EE(I)-XX(I)*EE(I+1))/FF(I)
      IF(IEX)100,100,95
   95 EE(1)=(EE(1)+EE(2))/2.
  100 GIRC=EE(1)
      RETURN
      END
```

```
      FUNCTION DTAB2 (XX,ZI,X,Z,NX,NZ,KX,KZ,Y,M,IERR)
C     DTAB   DOUBLE INTERPOLATION
C  XX=VALUE TO BE INTERPOLATED X DIRECTION
C  ZI=VALUE TO BE INTERPOLATED Z DIRECTION
C  X= X TABLE
C  Z= Z TABLE
C  NX=NUMBER X VALUES IN TABLE
C  NZ=NUMBER Z VALUES IN TABLE
C  KX=1 IF LINEAR INTERPOLATION X DIRECTION
C     =2 IF CURVILINEAR
C  KZ=1 IF LINEAR INTERPOLATION Z DIRECTION
C     =2 IF CURVILINEAR
C  Y= Y ARRAY
C  M= ROW DIMENSION Y ARRAY
C  IERR=1 SUCCESSFUL RETURN
C     =2 UNSUCCESSFUL RETURN
      DIMENSION X(1),Z(1),Y(1),X2(4),Z2(4),Y2(16),INX(2),IKX(2),
     1ISV(2),IXINT(2)
      ZZ=ZI
      INX(1)=NX
      INX(2)=NZ
      IKX(1)=KX
      IKX(2)=KZ
      DO 200 I=1,2
      IF(INX(I)-2)1000,140,10
   10 IF(I-1)11,11,12
   11 IF(X(1)-X(2))20,1000,30
C     ASCENDING ORDER
   20 DO 21 J=1,NX
      IF(X(J)-XX)21,40,50
   21 CONTINUE
C     VALUE BEYOND END OF TABLE
   22 ISV(I)=INX(I)-IKX(I)
   23 IXINT(I)=IKX(I)
      GO TO 150
   12 IF(Z(1)-Z(2))25,1000,35
   25 DO 26 J=1,NZ
      IF(Z(J)-ZZ)26,40,50
   26 CONTINUE
      GO TO 22
C     DESCENDING ORDER
   30 DO 31 J=1,NX
      IF(X(J)-XX)50,40,31
   31 CONTINUE
      GO TO 22
   35 DO 36 J=1,NZ
      IF(Z(J)-ZZ) 50,40,36
   36 CONTINUE
      GO TO 22
C     VALUE EQUAL VALUE IN TABLE
   40 IXINT(I)=0
      ISV(I)=J
      GO TO 150
   50 IF(J-1)60,60,70
```

```
      FUNCTION DTA82 (XX,ZI,X,Z,NX,NZ,KX,KZ,Y,M,IERR)
C     DTA8   DOUBLE INTERPOLATION
C  XX=VALUE TO BE INTERPOLATED X DIRECTION
C  ZI=VALUE TO BE INTERPOLATED Z DIRECTION
C  X= X TABLE
C  Z= Z TABLE
C  NX=NUMBER X VALUES IN TABLE
C  NZ=NUMBER Z VALUES IN TABLE
C  KX=1 IF LINEAR INTERPOLATION X DIRECTION
C     =2 IF CURVILINEAR
C  KZ=1 IF LINEAR INTERPOLATION Z DIRECTION
C     =2 IF CURVILINEAR
C  Y= Y ARRAY
C  M= ROW DIMENSION Y ARRAY
C  IERR=1 SUCCESSFUL RETURN
C     =2 UNSUCCESSFUL RETURN
      DIMENSION X(1),Z(1),Y(1),X2(4),Z2(4),Y2(16),INX(2),IKX(2),
     1ISV(2),IXINT(2)
      ZZ=ZI
      INX(1)=NX
      INX(2)=NZ
      IKX(1)=KX
      IKX(2)=KZ
      DO 200 I=1,2
      IF(INX(I)-2)1000,140,10
   10 IF(I-1)11,11,12
   11 IF(X(1)-X(2))20,1000,30
C     ASCENDING ORDER
   20 DO 21 J=1,NX
      IF(X(J)-XX)21,40,50
   21 CONTINUE
C     VALUE BEYOND END OF TABLE
   22 ISV(I)=INX(I)-IKX(I)
   23 IXINT(I)=IKX(I)
      GO TO 150
   12 IF(Z(1)-Z(2))25,1000,25
   25 DO 26 J=1,NZ
      IF(Z(J)-ZZ)26,40,50
   26 CONTINUE
      GO TO 22
C     DESCENDING ORDER
   30 DO 31 J=1,NX
      IF(X(J)-XX)50,40,31
   31 CONTINUE
      GO TO 22
   35 DO 36 J=1,NZ
       IF(Z(J)-ZZ) 50,40,36
   36 CONTINUE
      GO TO 22
C     VALUE EQUAL VALUE IN TABLE
   40 IXINT(I)=0
      ISV(I)=0
      GO TO 150
   50 IF(J-1)60,60,70
```

```
      GO TO 225
400   DTAB2 =Y2(1)
      IERR=1
      RETURN
1000  IERR=2
      DTAB2 =0.
      RETURN
      END
```

COPY AVAILABLE TO DDC DOES NOT
PERMIT FULLY LEGIBLE PRODUCTION

C. BASELINE AIRCRAFT NOISE PREDICTIONS

The following pages contain the inputs and outputs from the prediction for the seven baseline high-lift aircraft.

The predictions were made using an aircraft velocity of 80 knots and 0 knots, to show a comparison between in-flight and static results.

DATA FOR VT (STATIC)

```
 1     BASELINE VECTORED THRUST AIRCRAFT
 2      1     3     4
 3 500.        4.0         90.         0.0         8.0
 4     10 50.        2000.
 5      0     1     1     1     1     0     0     0     0     0     0     1
 6 -40.        3.43        3.43
 7 3.43        2.74        0.0         20.         40.         0.0
 8      3
 9 0.0         2.5854      700.        1629.       40.
10 2.5854      5.2624      685.        602.
11 873.6       1.3         6.3         602.        17.5        18.
12 1.105       1400.       2.4936      60.         17400.      59.         0.
13      2 200.
14      0
```

BASELINE VECTORED THRUST AIRCRAFT

AIRCRAFT VELOCITY = .0 KNOTS
SIDELINE DISTANCE = 500.0 FEET

ALTITUDE (FT)	DISTANCE ALONG FLIGHT PATH (FT)	ELEVATION ANGLE (DEG)	AZIMUTHAL ANGLE (DEG)	SOURCE TO OBSERVER DISTANCE (FT)	MAXIMUM PNL (PNDB)	MAXIMUM PNLT (PNDB)
4.0	20[illegible].0	.0	90.0	500.0	100.6	102.8
54.0	235[illegible].8	5.7	90.0	502.5	99.5	101.9
104.0	271[illegible].5	11.3	90.0	509.0	99.6	101.5
154.0	3067.3	16.7	80.0	530.1	99.8	101.2
204.0	3423.1	21.8	70.0	573.1	98.6	100.6
254.0	3778.8	26.5	90.0	559.0	100.3	101.9
304.0	4134.6	31.0	90.0	583.1	99.0	102.1
354.0	4490.4	35.0	90.0	610.3	99.5	100.9
404.0	4846.1	38.7	90.0	640.3	99.0	99.7
454.0	5201.9	42.0	90.0	672.7	98.6	99.8

*** MAXIMUM NOISE ***

ALTITUDE (FT)	DISTANCE ALONG FLIGHT PATH (FT)	ELEVATION ANGLE (DEG)	AZIMUTHAL ANGLE (DEG)	SOURCE TO OBSERVER DISTANCE (FT)	MAXIMUM PNL (PNDB)	MAXIMUM PNLT (PNDB)
4.0	20[illegible]	.0	90.0	50[illegible].0	100.6	102.8

DATA FOR VT (INFLIGHT)

```
 1    BASELINE VECTORED THRUST AIRCRAFT
 2      1    3    4
 3 500.       4.0        90.        80.        8.0
 4     10 50.       2000.
 5      1    1    1    1    1    0    0    0    0    0    0    1
 6 -40.       3.43       3.43
 7 3.43       2.74       0.0        20.        40.        0.0
 8      3
 9 0.0        2.5854     700.       1629.      40.
10 2.5854     5.2624     685.       602.
11 2492.06    6.5128     1.367
12 873.6      1.3        6.3        602.       17.5       18.
13 1.105      1400.      2.4936     60.        1740.      59.        0.
14      2 200.
15      0
```

BASELINE VECTORED THRUST AIRCRAFT

AIRCRAFT VELOCITY = 80.0 KNOTS
SIDELINE DISTANCE = 500.0 FEET

ALTITUDE (FT)	DISTANCE ALONG FLIGHT PATH (FT)	ELEVATION ANGLE (DEG)	AZIMUTHAL ANGLE (DEG)	SOURCE TO OBSERVER DISTANCE (FT)	MAXIMUM PNL (PNDB)	MAXIMUM PNLT (PNDB)
4.0	20[illegible]	.0	90.0	500.0	97.4	99.6
54.0	2357.8	5.7	90.0	502.5	96.4	98.8
104.0	2711.5	11.3	90.0	509.0	96.5	98.4
154.0	3067.3	15.7	80.0	530.1	96.7	98.1
204.0	3423.1	21.8	70.0	573.1	95.6	97.7
254.0	3778.8	26.0	90.0	559.0	97.2	98.7
304.0	4134.6	31.0	90.0	583.1	96.8	99.0
354.0	4490.4	35.0	90.0	610.3	96.4	97.8
404.0	4846.1	38.7	90.0	640.3	95.9	96.6
454.0	5201.9	42.0	90.0	672.7	95.5	96.7

** MAXIMUM NOISE **

ALTITUDE (FT)	DISTANCE ALONG FLIGHT PATH (FT)	ELEVATION ANGLE (DEG)	AZIMUTHAL ANGLE (DEG)	SOURCE TO OBSERVER DISTANCE (FT)	MAXIMUM PNL (PNDB)	MAXIMUM PNLT (PNDB)
4.0	20[illegible]	.0	90.0	50[illegible]	97.4	99.6

DATA FOR EBF (STATIC)

```
 1    BASELINE EBF AIRCRAFT
 2     2    3    4
 3 500.       4.0        90.        0.0        8.0
 4    10 50.0      2000.0
 5     0    1    1    1    1    0    0    1    1    1    1    1
 6 7.0        12.4583    3.9106
 7 3.0416     1.9666     1.6833     12.        20.        25.
 8     3
 9 0.0        1.7625     700.       1529.      -7.0
10 1.7625     4.8388     650.       596.
11 778.       1.25       5.9        596.       17.5       18.0
12 1.105      1400.      2.3352     60.        1740.      59.        0.
13     2 200.
14     0
```

BASELINE EBF AIRCRAFT

AIRCRAFT VELOCITY = .0 KNOTS
SIDELINE DISTANCE = 500.0 FEET

ALTITUDE (FT)	DISTANCE ALONG FLIGHT PATH (FT)	ELEVATION ANGLE (DEG)	AZIMUTHAL ANGLE (DEG)	SOURCE TO OBSERVER DISTANCE (FT)	MAXIMUM PNL (PNDB)	MAXIMUM PNLT (PNDB)
4.0	20[illegible].0	.0	90.0	500.0	96.9	99.0
54.0	2355.8	5.7	100.0	510.2	96.4	98.7
104.0	2711.5	11.3	100.0	517.8	96.3	97.8
154.0	3067.3	16.7	110.0	55[illegible].5	96.7	98.8
204.0	3423.1	21.8	110.0	573.1	96.9	98.8
254.0	3778.8	26.5	110.0	594.9	96.7	99.1
304.0	4134.6	31.0	90.0	583.1	96.8	99.0
354.0	4490.4	35.0	110.0	649.5	96.4	98.6
404.0	4846.1	38.7	60.0	739.4	95.2	97.5
454.0	5201.9	42.0	1[illegible]	683.1	96.0	97.1

** MAXIMUM NOISE **

ALTITUDE (FT)	DISTANCE ALONG FLIGHT PATH (FT)	ELEVATION ANGLE (DEG)	AZIMUTHAL ANGLE (DEG)	SOURCE TO OBSERVER DISTANCE (FT)	MAXIMUM PNL (PNDB)	MAXIMUM PNLT (PNDB)
254.0	37[illegible]8.[illegible]	2[illegible]	1[illegible]	594.9	96.7	99.1

DATA FOR EBF (INFLIGHT)

```
 1    BASELINE EBF AIRCRAFT
 2     2    3    4
 3 500.       4.0        90.        80.        8.0
 4    10 50.0      2000.0
 5     1    1    1    1    1    0    0    1    1    1    1    1
 6 7.0        12.4583    3.9106
 7 3.0416     1.9666     1.6833     12.        20.        25.
 8     3
 9 0.0        1.7625     700.       1529.      -7.0
10 1.7625     4.8388     650.       556.
11 1445.89    6.4765     1.367
12 778.       1.25       5.9        556.       17.5       18.0
13 1.105      1400.      2.3352     60.        17400.     59.        0.0
14     2 200.
15     0
```

BASELINE FBF AIRCRAFT

AIRCRAFT VELOCITY = 80.0 KNOTS
SIDELINE DISTANCE = 500.0 FEET

ALTITUDE (FT)	DISTANCE ALONG FLIGHT PATH (FT)	ELEVATION ANGLE (DEG)	AZIMUTHAL ANGLE (DEG)	SOURCE TO OBSERVER DISTANCE (FT)	MAXIMUM PNL (PNDB)	MAXIMUM PNLT (PNDB)
4.0	20[illegible]	.0	90.0	501.0	96.5	98.6
54.0	2355.8	5.7	100.0	519.2	95.6	97.8
104.0	2711.5	11.5	90.0	509.9	94.0	96.8
154.0	3067.3	16.7	110.0	55[illegible].5	94.9	96.9
204.0	3423.1	21.8	110.0	573.1	94.8	96.8
254.0	3778.8	26.5	110.0	594.9	94.5	96.8
304.0	4134.5	31.0	90.0	583.1	94.7	96.9
354.0	4490.4	35.0	70.0	649.5	94.1	96.4
404.0	4846.1	38.7	60.0	739.4	93.2	95.5
454.0	5201.9	42.0	90.0	672.7	93.6	94.7

* MAXIMUM NOISE *

ALTITUDE (FT)	DISTANCE ALONG FLIGHT PATH (FT)	ELEVATION ANGLE (DEG)	AZIMUTHAL ANGLE (DEG)	SOURCE TO OBSERVER DISTANCE (FT)	MAXIMUM PNL (PNDB)	MAXIMUM PNLT (PNDB)
4.0	20[illegible]	.0	90.0	50[illegible]	96.5	98.6

DATA FOR USB (STATIC)

```
 1    BASELINE USB AIRCRAFT
 2      3     3     4
 3 500.       4.0        90.        0.0        8.0
 4     10 50.0      2000.0
 5      0     1     1     1     1     0     0     1     1     1     1     1
 6 0.0        5.33       0.9
 7 6.25       0.0        0.0        25.        0.0        0.0
 8      2
 9 1.80       7.255      717.       662.       0.0
10 575.       1.3        5.0        602.       17.5       18.0
11 1.105      1400.      1.9789     60.0       17400.     59.        0.0
12      2 200.
13      0
```

BASELINE USB AIRCRAFT

AIRCRAFT VELOCITY = .0 KNOTS
SIDELINE DISTANCE = 500.0 FEET

ALTITUDE (FT)	DISTANCE ALONG FLIGHT PATH (FT)	ELEVATION ANGLE (DEG)	AZIMUTHAL ANGLE (DEG)	SOURCE TO OBSERVER DISTANCE (FT)	MAXIMUM PNL (PNDB)	MAXIMUM PNLT (PNDB)
4.0	2000.0	.0	100.0	507.7	98.6	100.3
54.0	2355.8	5.7	100.0	510.2	97.4	99.6
104.0	2711.5	11.3	100.0	517.8	97.1	98.7
154.0	3067.3	16.7	110.0	555.5	98.1	100.3
204.0	3423.1	21.8	110.0	573.1	98.2	100.0
254.0	3778.8	26.6	110.0	594.9	97.9	100.4
304.0	4134.6	31.0	100.0	592.1	97.4	99.4
354.0	4490.4	35.0	110.0	649.5	97.4	99.7
404.0	4846.1	38.7	120.0	739.4	96.3	98.6
454.0	5201.9	42.0	100.0	683.1	96.3	97.5

**** MAXIMUM NOISE ****

ALTITUDE (FT)	DISTANCE ALONG FLIGHT PATH (FT)	ELEVATION ANGLE (DEG)	AZIMUTHAL ANGLE (DEG)	SOURCE TO OBSERVER DISTANCE (FT)	MAXIMUM PNL (PNDB)	MAXIMUM PNLT (PNDB)
254.0	3778.8	26.6	110.0	594.9	97.9	100.4

DATA FOR USB (INFLIGHT)

```
 1    BASELINE USB AIRCRAFT
 2      3     3     4
 3 500.       4.0        90.        80.        8.0
 4     10 50.0      2000.0
 5      1     1     1     1     1     0     0     1     1     1     1     1
 6 0.0        5.33       0.9
 7 6.25       0.0        0.0        25.        0.0        0.0
 8      2
 9 1.80       7.255      717.       662.       0.0
10 970.0      6.4552     1.367
11 575.       1.3        5.0        602.       17.5       58.0
12 1.105      1400.      1.9789     60.0       17400.     59.        0.0
13      2 200.
14      0
```

BASELINE USB AIRCRAFT

AIRCRAFT VELOCITY = 80.0 KNOTS
SIDELINE DISTANCE = 500.0 FEET

ALTITUDE (FT)	DISTANCE ALONG FLIGHT PATH (FT)	ELEVATION ANGLE (DEG)	AZIMUTHAL ANGLE (DEG)	SOURCE TO OBSERVER DISTANCE (FT)	MAXIMUM PNL (PNDB)	MAXIMUM PNLT (PNDB)
4.0	2000.0	.0	90.0	500.0	97.8	99.9
54.0	2355.8	5.7	100.0	510.2	96.9	99.2
104.0	2711.5	11.3	100.0	517.8	96.5	98.1
154.0	3067.3	16.7	110.0	555.5	97.3	99.6
204.0	3423.1	21.8	110.0	573.1	97.4	99.2
254.0	3778.8	26.6	110.0	594.9	97.0	99.4
304.0	4134.6	31.0	100.0	592.1	96.5	98.5
354.0	4490.4	35.0	110.0	649.5	96.4	98.6
404.0	4846.1	38.7	120.0	739.4	95.1	97.3
454.0	5201.9	42.0	100.0	683.1	95.3	96.4

**** MAXIMUM NOISE ****

ALTITUDE (FT)	DISTANCE ALONG FLIGHT PATH (FT)	ELEVATION ANGLE (DEG)	AZIMUTHAL ANGLE (DEG)	SOURCE TO OBSERVER DISTANCE (FT)	MAXIMUM PNL (PNDB)	MAXIMUM PNLT (PNDB)
4.0	2000.0	.0	90.0	500.0	97.8	99.9

DATA FOR IBF/BLC (STATIC)

```
 1     BASELINE IBF/BLC AIRCRAFT
 2      4     3     4
 3 500.        4.0         90.         0.0         8.0
 4     10 50.0      2000.0
 5      0     1     1     1     1     0     1     0     1     1     1     1
 6 0.0         0.0         0.5
 7 2.3333      1.5583      1.2916      12.0        20.0        25.
 8      3
 9 0.0         1.8333      700.        1629.       0.0
10 1.8333      3.9458      720.        602.
11 0.0833      15.0        685.        0.0         602.
12 544.        1.3         5.68        602.        17.5        18.
13 1.105       1400.       2.2480      60.         1740.       59.         0.0
14      2 200.
15      0
```

BASELINE IBF/HLC AIRCRAFT

AIRCRAFT VELOCITY = [illegible].0 KNOTS
SIDELINE DISTANCE = 50[illegible].0 FEET

ALTITUDE (FT)	DISTANCE ALONG FLIGHT PATH (FT)	ELEVATION ANGLE (DEG)	AZIMUTHAL ANGLE (DEG)	SOURCE TO OBSERVER DISTANCE (FT)	MAXIMUM PNL (PNDB)	MAXIMUM PNLT (PNDB)
4.0	20[illegible]	[illegible].0	10[illegible]	507.[illegible]	98.9	100.7
54.0	23[illegible].8	5.7	10[illegible]	510.2	98.2	100.5
104.0	271[illegible].5	1[illegible].3	90.0	509.[illegible]	98.3	100.2
154.0	3057.[illegible]	16.7	1[illegible].0	55[illegible]	99.3	101.5
204.0	3423.1	21.8	1[illegible].0	573.1	99.3	101.2
254.0	3778.8	26.[illegible]	110.0	594.9	99.1	101.5
304.0	4134.6	31.0	90.0	583.1	98.6	100.9
354.0	4490.4	35.9	110.0	649.5	98.6	101.0
404.0	4846.1	38.7	120.0	739.4	97.6	99.9
454.0	5201.9	42.0	10[illegible]	683.1	97.7	98.9

** MAXIMUM NOISE *

ALTITUDE (FT)	DISTANCE ALONG FLIGHT PATH (FT)	ELEVATION ANGLE (DEG)	AZIMUTHAL ANGLE (DEG)	SOURCE TO OBSERVER DISTANCE (FT)	MAXIMUM PNL (PNDB)	MAXIMUM PNLT (PNDB)
254.0	37[illegible]	26.	1[illegible]	594.[illegible]	99.1	101.5

COPY AVAILABLE TO DDC DOES NOT PERMIT FULLY LEGIBLE PRODUCTION

DATA FOR IBF/BLC (INFLIGHT)

```
 1    BASELINE IBF/BLC AIRCRAFT
 2     4    3    4
 3 500.       4.0        90.        80.        8.0
 4    10 50.0      2000.0
 5     1    1    1    1    1    0    1    0    1    1    1    1
 6 0.0        0.0        0.5
 7 2.3333     1.5583     1.2916     12.0       20.0       25.
 8     3
 9 0.0        1.8333     700.       1629.      0.0
10 1.8333     3.9958     720.       602.
11 0.0833     15.0       685.       0.0        602.
12 1410.26    6.5039     1.367
13 544.       1.3        5.68       602.       17.5       18.
14 1.105      1400.      2.2480     60.        17400.     59.        0.
15     2 200.
16     0
```

BASELINE UBF/BLC AIRCRAFT

AIRCRAFT VELOCITY = 80.0 KNOTS
SIDELINE DISTANCE = 500.0 FEET

ALTITUDE (FT)	DISTANCE ALONG FLIGHT PATH (FT)	ELEVATION ANGLE (DEG)	AZIMUTHAL ANGLE (DEG)	SOURCE TO OBSERVER DISTANCE (FT)	MAXIMUM PNL (PNDB)	MAXIMUM PNLT (PNDB)
4.0	2011.0	.0	100.0	507.7	95.1	96.8
54.0	2355.8	5.7	100.0	510.2	94.5	96.8
104.0	2711.5	11.3	120.0	588.8	94.4	96.5
154.0	3067.3	16.7	110.0	550.5	95.4	97.6
204.0	3423.1	21.8	110.0	573.1	95.5	97.4
254.0	3778.9	26.5	110.0	594.9	95.4	97.7
304.0	4134.6	31.0	90.0	583.1	94.6	96.9
354.0	4490.4	35.0	110.0	649.5	94.8	97.1
404.0	4846.1	38.7	120.0	739.4	93.8	96.1
454.0	5201.9	42.0	100.0	683.1	93.7	94.9

* MAXIMUM NOISE **

ALTITUDE (FT)	DISTANCE ALONG FLIGHT PATH (FT)	ELEVATION ANGLE (DEG)	AZIMUTHAL ANGLE (DEG)	SOURCE TO OBSERVER DISTANCE (FT)	MAXIMUM PNL (PNDB)	MAXIMUM PNLT (PNDB)
254.0	3778.9	26.5	110.0	594.9	95.4	97.7

DATA FOR IBF/JF (STATIC)

```
 1    BASELINE IBF/JF AIRCRAFT
 2      4     3     4
 3 500.        4.0         90.         0.1         8.0
 4     10 50.0       2000.0
 5      0     1     1     1     1     0     1     0     0     0     0     1
 6 0.0         0.0         0.0
 7 0.0         0.0         0.0         0.1         0.0         0.0         0.0
 8      3
 9 0.0         2.2397      700.        1527.       0.0
10 2.2397      4.1058      718.        602.
11 0.196       17.4083     675.        40.         602.
12 511.        1.3         5.44        602.        17.5        18.
13 1.105       1400.       2.1530      60.         1740.       59.         0.0
14      2 200.
15      0
```

BASELINE IBF/JF AIRCRAFT

AIRCRAFT VELOCITY = .0 KNOTS
SIDELINE DISTANCE = 500.0 FEET

ALTITUDE (FT)	DISTANCE ALONG FLIGHT PATH (FT)	ELEVATION ANGLE (DEG)	AZIMUTHAL ANGLE (DEG)	SOURCE TO OBSERVER DISTANCE (FT)	MAXIMUM PNL (PNDB)	MAXIMUM PNLT (PNDB)
4.0	2000.0	.0	100.0	507.7	95.6	97.3
54.0	2350.8	5.7	100.0	510.2	94.8	97.1
104.0	2711.5	11.3	120.0	583.8	95.0	97.1
154.0	3067.3	16.7	110.0	555.5	95.9	98.1
204.0	3423.1	21.8	120.0	621.8	95.8	98.0
254.0	3778.8	26.6	110.0	594.9	95.7	98.1
304.0	4134.6	31.0	120.0	673.3	95.4	97.1
354.0	4490.4	35.0	110.0	649.5	95.1	97.3
404.0	4846.1	38.7	120.0	739.4	94.5	96.8
454.0	5201.9	42.0	120.0	776.7	94.1	95.3

*** MAXIMUM NOISE ***

ALTITUDE (FT)	DISTANCE ALONG FLIGHT PATH (FT)	ELEVATION ANGLE (DEG)	AZIMUTHAL ANGLE (DEG)	SOURCE TO OBSERVER DISTANCE (FT)	MAXIMUM PNL (PNDB)	MAXIMUM PNLT (PNDB)
154.0	3067.3	16.7	110.0	[illegible]	95.9	98.1

DATA FOR IBF/JF (INFLIGHT)

```
 1     BASELINE IBF/JF AIRCRAFT
 2      4     3     4
 3 500.       4.0        90.        80         8.0
 4     10 50.0      2000.0
 5      1     1     1     1     1     0     1     0     0     0     0     1
 6 0.0        0.0        0.0
 7 0.0        0.0        0.0        0.0        0.0        0.0        0.0
 8      3
 9 0.0        2.2397     700.       1527.      0.0
10 2.2397     4.1058     718.       602.
11 0.196      17.4083    675.       40.        602.
12 1265.41    6.4857     1.367
13 511.       1.5        5.44       602.       17.5       18.
14 1.105      1400.      2.1530     60.        17400.     59.        0.
15      2 200.
16      0
```

BASELINE IBF/JF AIRCRAFT

AIRCRAFT VELOCITY = 80.0 KNOTS
SIDELINE DISTANCE = 500.0 FEET

ALTITUDE (FT)	DISTANCE ALONG FLIGHT PATH (FT)	ELEVATION ANGLE (DEG)	AZIMUTHAL ANGLE (DEG)	SOURCE TO OBSERVER DISTANCE (FT)	MAXIMUM PNL (PNDB)	MAXIMUM PNLT (PNDB)
4.0	200[illegible].0	.0	100.0	507.7	92.4	94.1
54.0	2355.8	5.7	100.0	510.2	91.9	94.1
104.0	2711.5	11.3	120.0	588.8	92.0	94.0
154.0	3067.3	16.7	110.0	555.5	92.8	95.1
204.0	3423.1	21.8	120.0	621.8	92.5	94.7
254.0	3778.8	26.6	110.0	594.9	92.6	94.9
304.0	4134.6	31.0	100.0	592.1	91.9	93.8
354.0	4490.4	35.0	110.0	649.5	91.9	94.2
404.0	4846.1	38.7	120.0	739.4	91.3	93.5
454.0	5201.9	42.0	120.0	776.7	90.8	91.9

***** MAXIMUM NOISE *****

ALTITUDE (FT)	DISTANCE ALONG FLIGHT PATH (FT)	ELEVATION ANGLE (DEG)	AZIMUTHAL ANGLE (DEG)	SOURCE TO OBSERVER DISTANCE (FT)	MAXIMUM PNL (PNDB)	MAXIMUM PNLT (PNDB)
154.0	3067.3	16.7	110.0	55[illegible]	92.8	95.1

DATA FOR AW-2S (STATIC)

```
 1    BASELINE AW-2S AIRCRAFT
 2      5    3    4
 3 500.      4.0       90.       0.0       8.0
 4    10 50.0     2000.0
 5      0    1    0    1    1    1    0    0    0    0    0    1
 6 0.0       0.0       0.0
 7 0.0       0.0       0.0       0.0       0.0       0.0
 8      1
 9 0.0       2.2426    774.      1411.     0.0
10 0.9166    15.       1400.     3.4166    20.
11 187.      3.0       3.08      747.      17.5      150.
12      2 200.
13      0
```

BASELINE AW-2S AIRCRAFT

AIRCRAFT VELOCITY = .0 KNOTS
SIDELINE DISTANCE = 500.0 FEET

ALTITUDE (FT)	DISTANCE ALONG FLIGHT PATH (FT)	ELEVATION ANGLE (DEG)	AZIMUTHAL ANGLE (DEG)	SOURCE TO OBSERVER DISTANCE (FT)	MAXIMUM PNL (PNDB)	MAXIMUM PNLT (PNDB)
4.0	2000.0	.0	110.0	532.1	125.0	125.0
54.0	2355.8	5.7	110.0	534.7	124.0	125.8
104.0	2711.5	11.3	120.0	588.8	123.1	125.0
154.0	3067.3	16.7	110.0	555.5	125.1	127.4
204.0	3423.1	21.8	110.0	573.1	125.8	127.8
254.0	3778.8	26.6	110.0	594.9	126.1	128.5
304.0	4134.6	31.0	120.0	673.3	125.6	127.3
354.0	4490.4	35.0	110.0	649.5	125.8	128.0
404.0	4846.1	38.7	120.0	739.4	125.0	127.2
454.0	5201.9	42.0	120.0	776.7	124.7	125.9

***** MAXIMUM NOISE *****

ALTITUDE (FT)	DISTANCE ALONG FLIGHT PATH (FT)	ELEVATION ANGLE (DEG)	AZIMUTHAL ANGLE (DEG)	SOURCE TO OBSERVER DISTANCE (FT)	MAXIMUM PNL (PNDB)	MAXIMUM PNLT (PNDB)
254.0	3778.8	26.6	110.0	594.9	126.1	128.5

DATA FOR AW-2S (INFLIGHT)

```
 1     BASELINE AW-2S AIRCRAFT
 2      5     3     4
 3 500.       4.0        90.        80.        8.0
 4     10 50.0      2000.0
 5      1     1     0     1     1     1     0     0     0     0     0     1
 6 0.0        0.0        0.0
 7 0.0        0.0        0.0        0.0        0.0        0.0
 8      1
 9 0.0        2.2426     774.       1411.      0.0
10 0.9166     15.        1400.      3.4166     20.
11 1139.54    6.2773     1.367
12 187.       3.0        3.08       747.       17.5       150.
13      2 200.
14      0
```

BASELINE AW-2S AIRCRAFT

AIRCRAFT VELOCITY = 80.0 KNOTS
SIDELINE DISTANCE = 500.0 FEET

ALTITUDE (FT)	DISTANCE ALONG FLIGHT PATH (FT)	ELEVATION ANGLE (DEG)	AZIMUTHAL ANGLE (DEG)	SOURCE TO OBSERVER DISTANCE (FT)	MAXIMUM PNL (PNDB)	MAXIMUM PNLT (PNDB)
4.0	2000.0	.0	110.0	532.1	125.0	125.0
54.0	2355.8	5.7	110.0	534.7	123.8	125.7
104.0	2711.5	11.3	120.0	588.8	122.7	124.6
154.0	3067.3	16.7	110.0	555.5	124.7	126.9
204.0	3423.1	21.8	110.0	573.1	125.2	127.1
254.0	3778.8	26.6	110.0	594.9	125.3	127.7
304.0	4134.6	31.0	120.0	673.3	124.7	126.5
354.0	4490.4	35.0	110.0	649.5	124.9	127.1
404.0	4846.1	38.7	120.0	739.4	124.0	126.3
454.0	5201.9	42.0	120.0	776.7	123.7	124.9

***** MAXIMUM NOISE *****

ALTITUDE (FT)	DISTANCE ALONG FLIGHT PATH (FT)	ELEVATION ANGLE (DEG)	AZIMUTHAL ANGLE (DEG)	SOURCE TO OBSERVER DISTANCE (FT)	MAXIMUM PNL (PNDB)	MAXIMUM PNLT (PNDB)
254.0	3778.8	26.6	110.0	594.9	125.3	127.7

DATA FOR HYBRID (STATIC)

```
 1    BASELINE HYBRID AIRCRAFT
 2      6    3    4
 3 500.       4.0        90.        0.0        8.0
 4     10 50.0      2000.0
 5      0    1    1    1    1    0    1    1    1    1    1    1
 6 12.        8.6162     0.6710
 7 5.5815     0.0        0.0        30.        0.0        0.0
 8      2
 9 1.3206     8.54       600.       565.       12.
10 0.0456     17.3086    640.       0.0        565.
11 214.       1.255      6.0999     519.       17.5       18.0
12 1.105      1400.      2.8974     60.        17400.     59.        0.0
13      2 200.
14      0
```

BASELINE HYBRID AIRCRAFT

AIRCRAFT VELOCITY = .0 KNOTS
SIDELINE DISTANCE = 500.0 FEET

ALTITUDE (FT)	DISTANCE ALONG FLIGHT PATH (FT)	ELEVATION ANGLE (DEG)	AZIMUTHAL ANGLE (DEG)	SOURCE TO OBSERVER DISTANCE (FT)	MAXIMUM PNL (PNDB)	MAXIMUM PNLT (PNDB)
4.0	2000.0	.0	90.0	500.0	93.5	95.6
54.0	2355.8	5.7	100.0	510.2	92.7	94.9
104.0	2711.5	11.3	100.0	517.8	92.2	93.8
154.0	3067.3	16.7	110.0	555.5	92.8	94.9
204.0	3 23.1	21.8	110.0	573.1	92.7	94.6
254.0	3778.8	26.6	110.0	594.9	92.3	94.7
304.0	4134.6	31.0	90.0	583.1	92.0	94.2
354.0	4490.4	35.0	110.0	649.5	91.8	94.0
404.0	4846.1	38.7	60.0	739.4	90.7	93.0
454.0	5201.9	42.0	90.0	672.7	91.0	92.2

***** MAXIMUM NOISE *****

ALTITUDE (FT)	DISTANCE ALONG FLIGHT PATH (FT)	ELEVATION ANGLE (DEG)	AZIMUTHAL ANGLE (DEG)	SOURCE TO OBSERVER DISTANCE (FT)	MAXIMUM PNL (PNDB)	MAXIMUM PNLT (PNDB)
4.0	2000.0	.0	90.0	500.0	93.5	95.6

DATA FOR HYBRID (INFLIGHT)

```
 1    BASELINE HYBRID AIRCRAFT
 2      6    3    4
 3 500.       4.0        90.        80.        8.0
 4    10 50.0      2000.0
 5      1    1    1    1    1    0    1    1    1    1    1    1
 6 12.        8.6162     0.6710
 7 5.5815     0.0        0.0        30.        0.0        0.0
 8      2
 9 1.3206     8.54       600.       565.       12.
10 0.0456     17.3086    640.       0.0        565.
11 2304.      6.72       1.367
12 214.       1.255      6.0999     519.       17.5       18.0
13 1.105      1400.      2.8974     60.        17400.     59.        0.0
14      2 200.
15      0
```

BASELINE HYBRID AIRCRAFT

AIRCRAFT VELOCITY = 80.0 KNOTS
SIDELINE DISTANCE = 500.0 FEET

ALTITUDE (FT)	DISTANCE ALONG FLIGHT PATH (FT)	ELEVATION ANGLE (DEG)	AZIMUTHAL ANGLE (DEG)	SOURCE TO OBSERVER DISTANCE (FT)	MAXIMUM PNL (PNDB)	MAXIMUM PNLT (PNDB)
4.0	2000.0	.0	90.0	500.0	93.3	95.4
54.0	2355.8	5.7	100.0	510.2	92.5	94.7
104.0	2711.5	11.3	90.0	509.9	91.5	93.4
154.0	3067.3	16.7	110.0	555.5	92.2	94.3
204.0	3423.1	21.8	110.0	573.1	92.1	93.9
254.0	3778.8	26.6	110.0	594.9	91.6	94.0
304.0	4134.6	31.0	90.0	583.1	91.2	93.4
354.0	4490.4	35.0	110.0	649.5	90.9	93.1
404.0	4846.1	38.7	60.0	739.4	89.7	92.0
454.0	5201.9	42.0	90.0	672.7	90.1	91.3

***** MAXIMUM NOISE *****

ALTITUDE (FT)	DISTANCE ALONG FLIGHT PATH (FT)	ELEVATION ANGLE (DEG)	AZIMUTHAL ANGLE (DEG)	SOURCE TO OBSERVER DISTANCE (FT)	MAXIMUM PNL (PNDB)	MAXIMUM PNLT (PNDB)
4.0	2000.0	.0	90.0	500.0	93.3	95.4

D. HAND-CALCULATION PROCEDURE

The following pages describe a simplified procedure to calculate the V/STOL aircraft noise manually.

A method is described to estimate the noise levels of V/STOL aircraft without the use of a computer. The analytical model discussed in sections 2 and 3 is used with a few modifications. These modifications simplify the procedure to enable the hand calculations with little sacrifice in accuracy. The general procedure used in calculating the noise levels is shown in Figure A-1.

The noise source components which contribute to the radiated sound for any propulsive-lift concept of V/STOL aircraft are selected from Figure 2-5. Using the flight path geometry given in Figure 1-22 or 2-3, the contribution from each of the sources to the radiated noise is computed. The details of calculating the one-third octave spectra, PNL, and PNLT, using the geometrical and operational variables, is discussed in this Appendix.

INTERNALLY GENERATED ENGINE NOISE

Fan/Compressor: The unsuppressed OASPL is calculated using equation (2) with $K = 127$ and Figure 1-3. The spectral distribution is determined from Figure 1-4. The effect of noise suppression by duct treatment is determined by adding a reduction in SPL (ΔdB) to the unsuppressed radiated noise.

Turbine: Equation (3) and Figure 1-5 are used to estimate the OASPL. For a turbine with more than one stage, PR_{stage} is assumed to be the same as overall total to static pressure ratio of the turbine, and A_T is turbine exit area. The spectral distribution is computed with the use of Figure 1-6. The effect of duct treatment is estimated as described under Fan/Compressor.

Excess (Core and Tailpipe): Excess noise which includes core and tailpipe noise is calculated using equation (4) with $K = -70$. The percent ratio of fluctuating thrust to steady-state thrust, ε, is assumed to be 10. Figure 1-7 is used to estimate the spectral distribution.

JET MIXING NOISE

Equation (5) with $K = 134$ is used to compute the OASPL at azimuthal angle, $\theta = 90°$ for circular and slot nozzle jets. Equations (7) and (9) are used to calculate the OASPL for plug and co-axial nozzle jets, respectively. In these equations, C_a/C_{ISA} and ρ_a/ρ_{ISA} are assumed to be unity. In the case of the VT

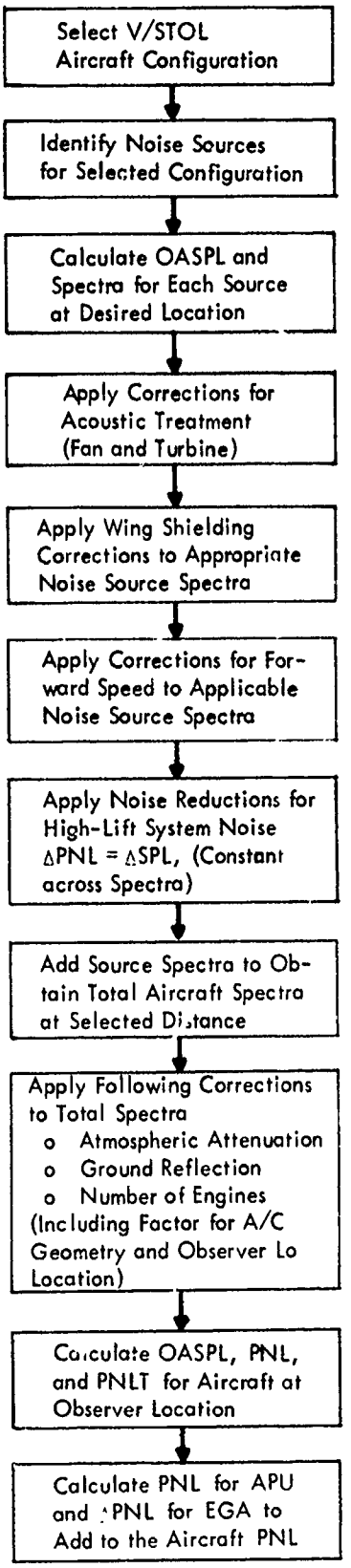

Figure A-1. Noise Prediction by Hand Calculation Procedure

concept, 3 dB are added to the OASPL to account for the additional noise generated by the turning vanes.

Generally the temperature and convection effects are small. Thus, equation (8) with $T_J/T_a = 1$ is used to calculate the Strouhal number. However for co-axial jets, the Strouhal number should be modified using the equation on page 1-22 and Figure 1-9. The curve in Figure 1-8 for $0° \leq \theta' \leq 110°$ is used to evaluate the spectral distribution.

The effect of aircraft motion on jet noise is calculated either using equation (26) or Figure 1-25. The estimated reduction in SPL (ΔdB) is added to the static jet noise spectra. The Doppler frequency shift due to motion of source with respect to an observer is neglected.

LIFT-AUGMENTATION NOISE

Impingement: Equation (10) with $K = -74$ and Figure 1-11 are used to compute OASPL. The directivity as a function of elevation angle is given as $A\cos\phi$, where A is determined from Figure 1-11(b). V_{IP} is assumed to be the same as jet velocity, V_J. A_I is calculated using equation (12) or (13). The spectral distribution is obtained from Figure 1-12.

Wall Jet: Wall jet noise contributes primarily in the case of USB, IBF/BLC, and Hybrid. The OASPL is calculated using equation (14) with $K = -105$, and Figure 1-13. In the equation, b is taken as the width of the nozzle and ℓ is the distance between the nozzle exit or impingement point and the flap trailing edge. V_m is the same as the jet velocity, V_J. The directivity as a function of elevation angle, is given as $A\cos\phi$, where A can be obtained from Figure 1-11b with $\alpha = 0$. With δ as the average value between the nozzle height, h, and the δ_{te} calculated from equation (17), Figure 1-14 is used to determine the spectral distribution.

Trailing Edge: Equation (15) is used to determine OASPL at $\theta = 90°$. For EBF, the constant, K, is assumed to be -6; V_{te} is determined from Figure 1-16 with $V_I = V_J$; the jet thickness and width (δ_{te} and w) are calculated using equations on top of page 1-37. For all the other configurations, the K is taken as -10,

because the distance between the turbulence and the edge is farther compared with EBF; V_{te} is assumed to be the same as V_J; w is the same as the width of the nozzle; and δ_{te} is determined from equation (17). The spectral distribution is evaluated from Figure 1-15.

Trailing-Edge Wake: The OASPL is determined using equation (18) with K = -111 and Figure 1-18. The spectral distribution is calculated as given under jet mixing noise with the definition of Strouhal number as $S = f\delta_{te}/V_{te}$.

Wing Nozzle Jet: The jet noise from the wing nozzle for the case of IBF/JF is calculated using the same procedure as discussed for jet noise. For the other configurations, the wing nozzle jet noise is neglected.

Augmentor Wing: The OASPL is calculated using equation (19) with K = -30.6 and Figure 1-19. The spectral distribution is determined from Figure 1-20.

The effect of aircraft motion for the total high-lift system is calculated using equations (27) and (28). Equation (27) is used for EBF, USB, IBF/BLC, AW, and Hybrid; equation (28) is used for IBF/JF and VT. The value of the exponent K in these equations is determined from Table I (page 1-60). The Doppler frequency shift is neglected.

NON-PROPULSIVE NOISE

Airframe: Equation (21) is used to calculate OASPL for airframe aerodynamic noise. The spectral distribution is determined from Figure 1-21.

Auxiliary Power Unit (APU): Contribution of APU noise to community is generally small. However, for comparison, the maximum PNL from APU is estimated using equation (22).

NOISE REDUCTION FOR HIGH-LIFT SYSTEMS

Maximum noise reduction by trailing edge treatment and trailing edge blowing for EBF and USB configurations is given by the equations on page 1-71. The expressions given for USB can be used for the Hybrid configuration also. By

reducing the number of flap segments in the case of the EBF, the noise could be reduced. This effect is calculated using the equation on page 1-73.

In the case of AW, the noise reductions by the use of a multi-element nozzle with a hard-wall or acoustically treated ejector is determined from Figure 1-33.

The reduction in noise levels (ΔPNL) are applied by reducing the sound pressure levels by ΔPNL across the spectra.

PROPAGATION AND OTHER PHENOMENA

Number of Engines: For multi-engine aircraft, the increase in noise is estimated by,

$$\Delta dB = 10 \log(N) \qquad \text{where } N = \text{number of engines.}$$

The fuselage shielding is determined using the expression,

$$\Delta dB = -2 \cos\phi, \qquad \text{where } \phi = \text{elevation angle.}$$

The other propagation effects are given below.

Wing Shielding: For the USB and Hybrid, the internally generated engine and jet noise are shielded from the community by the wing/flap. The shielding effect for these sources is calculated by using the equation on page 1-68. Internally generated engine noise sources are assumed to be at the center of the nozzle exit, and the jet noise source is at two equivalent nozzle diameters along the jet axis, downstream of the nozzle exit.

Atmospheric Attenuation: Atmospheric attenuation for one-third octave bands is given by the equation on page 1-49 and Figure 1-23. Ground reflection effects are calculated using equation (29) or Figure 1-28.

Extra Ground Attenuation: Extra ground attenuation is estimated as ΔPNL from Figure 1-30. This reduction in noise level is added to the total aircraft noise at the observer location.

SUBJECTIVE NOISE CALCULATIONS

Perceived noise levels (PNL) are calculated for one-third octave band SPL's using the procedures of SAE ARP 865A. Tone corrected PNL (PNLT) are calculated as described in FAR 36, Appendix B.